NEOTECTONICS OF THE NORTH FRONTAL FAULT SYSTEM OF THE SAN BERNARDINO MOUNTAINS, SOUTHERN CALIFORNIA: CAJON PASS TO LUCERNE VALLEY

Thesis by

Kristian Erik Meisling

In Partial Fulfillment of the Requirements

for the Degree of

Doctor of Philosophy

California Institute of Technology

Pasadena, California

1984

(Submitted July 22, 1983)

To my father

ACKNOWLEDGMENTS

I would like to acknowledge the many people who gave me assistance, advice, and encouragement during the course of my thesis work at Caltech. First and foremost, I am greatly indebted to Clarence R. Allen for his valued advice and steadfast support.

Special thanks to Ray Weldon for his companionship, enthusiasm, and insightful criticism of my work. Many of the ideas contained in this thesis were developed as the direct result of dialogue with Ray, and our cooperation has expanded my horizons immensely.

My thesis topic was suggested to me by Ron Shreve, to whom I owe a special debt of gratitude. I also wish to thank the many colleagues who joined me in numerous discussions and field trips, particularly Peter Sadler for his unflagging interest in my work, and his willingness to sit down and talk for hours on end about everything from outcrops to regional problems. A very special thanks to John Foster who willingly joined me in the field and provided moral support by phone, and to Dick Crook for contributing many valuable ideas, and lending his perspective during our many discussions. Many thanks to Joe Kirschvink for advice, tutelage, and unbridled enthusiasm during the course of my paleomagnetic work. Lee Silver provided many insights into southern California regional geology, and followed my progress with great interest.

I gratefully acknowledge support for my thesis work by the U. S. Geological Survey Contract No. 14-08-0001-19754, California Department of Water Resources Agreement No. B-53653, and the Caltech Division of Geological and Planetary Sciences. I would like specifically to thank Doug Morton, Fred Miller and John Matti of the U.S.G.S., Jack Marlette of the California DWR, and Chuck Orvis of the U. S. Army Corps of Engineers for providing

airphoto coverage of the study area, and for encouraging me in my endeavors.

I am grateful to Clarence Allen, Joe Kirschvink, and Dick Crook for their detailed reading and criticism of the manuscript.

I especially appreciate the efforts of Jan Mayne and Kathi Kronenfeld who drafted my map and made it possible for me to meet my deadline.

I would also like to express heartfelt gratitude to all the members of the Division staff, especially Dee Page, Virginia Gilliam, Ann Hutton, and Roberta Eager, who ushered me through the paperwork and protocol related to the U.S.G.S. contract.

Finally, a special thanks to my parents, Torben and Gladys Meisling, for encouraging me and seeing me through the completion of my studies.

ABSTRACT

The north frontal fault system of the San Bernardino Mountains is made up of a number of disparate structural elements, each of which accommodates range-front deformation in a manner dictated by its geometry. A two-stage history of late Cenozoic structural development is proposed for the northwestern San Bernardino Mountains: the range was first uplifted on low-angle structures and later modified by high-angle faulting. Evidence for Pliocene onset of deformation and uplift in the westernmost San Bernardino Mountains is found in the provenance and character of the associated sediments.

Thrusting uplifted the northern range front during a pulse of deformation spanning late Pliocene through middle Pleistocene time. Uplift in the westernmost San Bernardino Mountains was accomplished contemporaneously by tilting, warping, and arching. Nature and timing of deformation are consistent with the hypothesized formation of a transpressional welt across the San Andreas fault, which may have affected both the San Bernardino and San Gabriel Mountains.

High-angle faulting replaced thrusting and warping as the dominant style of deformation in the northwestern San Bernardino Mountains beginning in middle to late Pleistocene time. Pleistocene left-lateral faulting in the westernmost San Bernardino Mountains has accomplished north-south crustal shortening by squeezing the San Bernardino Mountains block eastward. Northwest-trending right-lateral faults, characteristic of the Mojave block prior to range-front uplift, have reasserted and incorporated themselves in the complex zone of range-front deformation. Local extension resulting in minor graben formation, appears to have been associated with lateral motion on the north frontal fault zone in Fifteenmile Valley (Sky Hi Ranch fault zone) and the Cleghorn fault zone.

Arcuate patterns of faulting in the western San Bernardino Mountains can be explained in terms of the pattern of faulting predicted for secondary faults near the end of a strike-slip fault. In this case the "end effect" would be produced by a change in slip rate on the San Andreas fault in Cajon Pass, possibly related to motion on the San Jacinto fault. All faulting in the study area is interpreted as the product of compression across the San Andreas fault.

A weathered erosion surface was developed on the crystalline terrane over most of the area in response to humid conditions during the late Miocene(?), at which time the region was characterized by an upland surface of subdued relief. This weathered erosion surface is a useful index to structural deformation in the northwestern San Bernardino Mountains.

Late Cenozoic stratigraphy constrains the timing of deformation and uplift in the northwestern San Bernardino Mountains. The late Miocene to Pliocene(?) Crowder Formation was deposited by drainages carrying distinctive volcanic and metamorphic clasts from the Victorville area southward, across the site of the western San Bernardino Mountains. The late Miocene beds of the Punchbowl Formation are faulted against the lower Crowder Formation, but are overlain by the upper Crowder Formation. The Punchbowl and Crowder Formations share the same age and paleocurrent direction, yet differ markedly in sediment character and provenance. The relationship between these two units remains an unsolved stratigraphic problem, which seemingly requires substantial lateral structural translation

The middle to late Pliocene onset of deformation and uplift is recorded in the stratigraphic sequence by the appearance of fine-grained sediments, new clast lithologies, and northerly paleocurrent directions. The volcanogenic eastern facies of the Crowder(?) Formation is believed to be a syn-

tectonic deposit indicative of ponding that accompanied the reversal in drainage direction brought on by incipient uplift of the western San Bernardino Mountains. The fine grained, lacustrine character of the Harold Formation can be interpreted in the same way; the base of the Harold Formation is <2.75 my old on the basis of paleomagnetic constraints. The Old Woman Sandstone in Lucerne Valley records an abrupt change from fine-grained sediments indicative of incipient uplift to coarse, angular debris signalling the emergence of the range front as a topographic element. The influx of range-front debris is estimated to have occurred <2.5 my ago. Several small, deformed patches of fine-grained sediment in Arrastre Canyon appear to be of similar origin.

The Quaternary stratigraphy of the western San Bernardino is dominated by the Harold Formation, Shoemaker Gravel and Older Alluvium, which underlie the Victorville Fan. These units were shed northeast off the San Gabriel and western San Bernardino Mountains, and record their uplift. The Harold Formation contains the earliest appearance of San Gabriel Mountains crystalline basement lithology within the stratigraphy of the Mojave block. The Victorville Fan sequence is believed to be time-transgressive, reflecting the northwestward movement of the San Gabriel Mountains crystalline terrane along the San Andreas fault.

The Older Alluvium capping the Shoemaker Gravel in Cajon Pass records the Brunhes/Matuyama polarity reversal of 730,000 y B.P. The Older Alluvium can be divided into dissected and undissected facies believed to predate and postdate the polarity transition respectively. This crude chronology can be extended to sediments on the flanks of the Ord Mountains that define a late Pleistocene drainage system tributary to the ancestral Mojave River. The Pleistocene units contain evidence of progressive growth and integration of

drainage in the Western San Bernardino Mountains in response to uplift during Pleistocene time.

Detailed geologic mapping of the northwestern San Bernardino Mountains permits slip rates and offsets to be calculated for important range-front faults. The Cleghorn fault has a cumulative left-lateral offset of 3.5 to 4.0 kilometers, and a slip rate of about 3.0 mm/yr. The Sky Hi Ranch fault zone has a late Pleistocene right-lateral offset of approximately 0.5 kilometers, with a slip-rate on the order of 1 mm/yr. The faults along the west flank of the Ord Mountains have a vertical slip-rate of less than 1 mm/yr.

The Cleghorn fault is classified as "active", under the criteria set forth by the State of California in the Alquist-Priolo Act of 1972, and is considered capable of a M_s 6.8 earthquake. Parts of the north frontal fault system on the west flank of the Ord Mountains and the Sky Hi Ranch fault zone are classified as "potentially active", in the terminology of the Alquist-Priolo Act, and are thought to be capable of a M_s 6.6 to 6.8 event. The Tunnel Ridge lineament and Arrastre Canyon Narrows fault zones are considered tentatively active, and should be examined in detail prior to development of adjoining areas. Clearly, the San Andreas fault poses the greatest seismic hazard to the communities in the study area.

TABLE OF CONTENTS

PLATES

FIGURES (page)

TABLES (page)

CHAPTER I

INTRODUCTION

1.1 MOTIVATION

The north frontal fault system of the San Bernardino Mountains forms the boundary between the Transverse Ranges and Mojave structural provinces. While numerous thrust faults characterize the late Cenozoic structure of the Transverse Ranges west of the San Andreas fault, thrusts are rare east of the San Andreas fault. By far the largest late Cenozoic thrust system in the eastern Transverse Ranges lies along the north front of the San Bernardino Mountains. What is the nature, origin and deformation history of this unique structural element? What implications does it have for tectonic models of southern California.

The San Bernardino Mountains represent one of the most prominent topographic features in southern California, serving as the source for both the Mojave and Santa Ana rivers. They are capped by a subdued, relict surface which is abruptly truncated along the precipitous margins of the range. Fresh scarps cutting Quaternary alluvial fan deposits, and bold relief testify to the youthfulness of the northern range front. When did uplift of the San Bernardino Mountains occur? How is uplift reflected in the stratigraphic record? What was the nature of the deformation responsible for uplift, and is it still going on today?

Published estimates of uplift rates for the San Bernardino Mountains vary by two orders of magnitude, leaving a disconcertingly wide range of possible recurrence intervals for frontal faulting. A moderate earthquake on the north frontal fault system would result not only in property damage to the neighboring desert communities, but in possible disruption of railway lines and aqueducts supplying the metropolitan areas to the west and south.

What is the earthquake potential of the north frontal fault system?

This thesis project grew out of the need to address these and other important questions. It focuses on developing a working chronology for the neotectonic evolution of range front between Cajon Pass and Lucerne Valley, and on assessing the seismic hazard posed by the north frontal fault system.

1.2 PREVIOUS WORK

This section presents a brief summary of previous work pertinent to the study area. A detailed discussion of the specific contributions of each author is included in the body of the text, where it will be most relevant. No attempt is made herein to review the vast quantity of work that has been done on the problems of the Transverse Ranges province as a whole. For a comprehensive review of work done in the province, see Baird et al. (1974).

1.2.1 The Transverse Ranges

The San Bernardino Mountains are part of the Transverse Ranges physiographic and structural province, named for its oblique orientation relative to the dominant northwest-trending structural grain in southern California (Figure 1-1). They constitute the western end of the eastern Transverse Ranges, and are sometimes grouped with the San Gabriel Mountains and referred to as the central Transverse Ranges. The Transverse Ranges have been an enigmatic problem in the development of a coherent tectonic model for southern California. Their Cenozoic structure lies athwart the regional tectonic grain, yet they do not appear offset more than 100 kilometer along the San Andreas fault. Geologists have advanced a variety of models for the structural evolution of the Transverse Ranges province and its relation to the San Andreas fault.

Many workers believe that the Transverse Ranges divide the San Andreas

Figure 1-1. The Transverse Ranges province (stippled area) as related to principal faults in southern California. Its structurally discordant trend has existed at least since the Miocene (Jahns, 1973) and perhaps the Cretaceous (Baird et al., 1974). The San Andreas fault has accumulated several hundred kilometers of right slip since the Miocene (Baird et al., 1974), yet the Transverse Ranges province does not appear to bo offset more than 100 kilometers. Identified cities are Bakersfield (B), El Centro (EC), Los Angeles (LA), Needles (N), San Bernardino (SB), San Diego (SD), and Santa Barbara (SBA). Compiled mainly from the geologic map of California (Olaf P. Jenkins edition), California Division of Mines and Geology. (figure from Jahns, 1973)

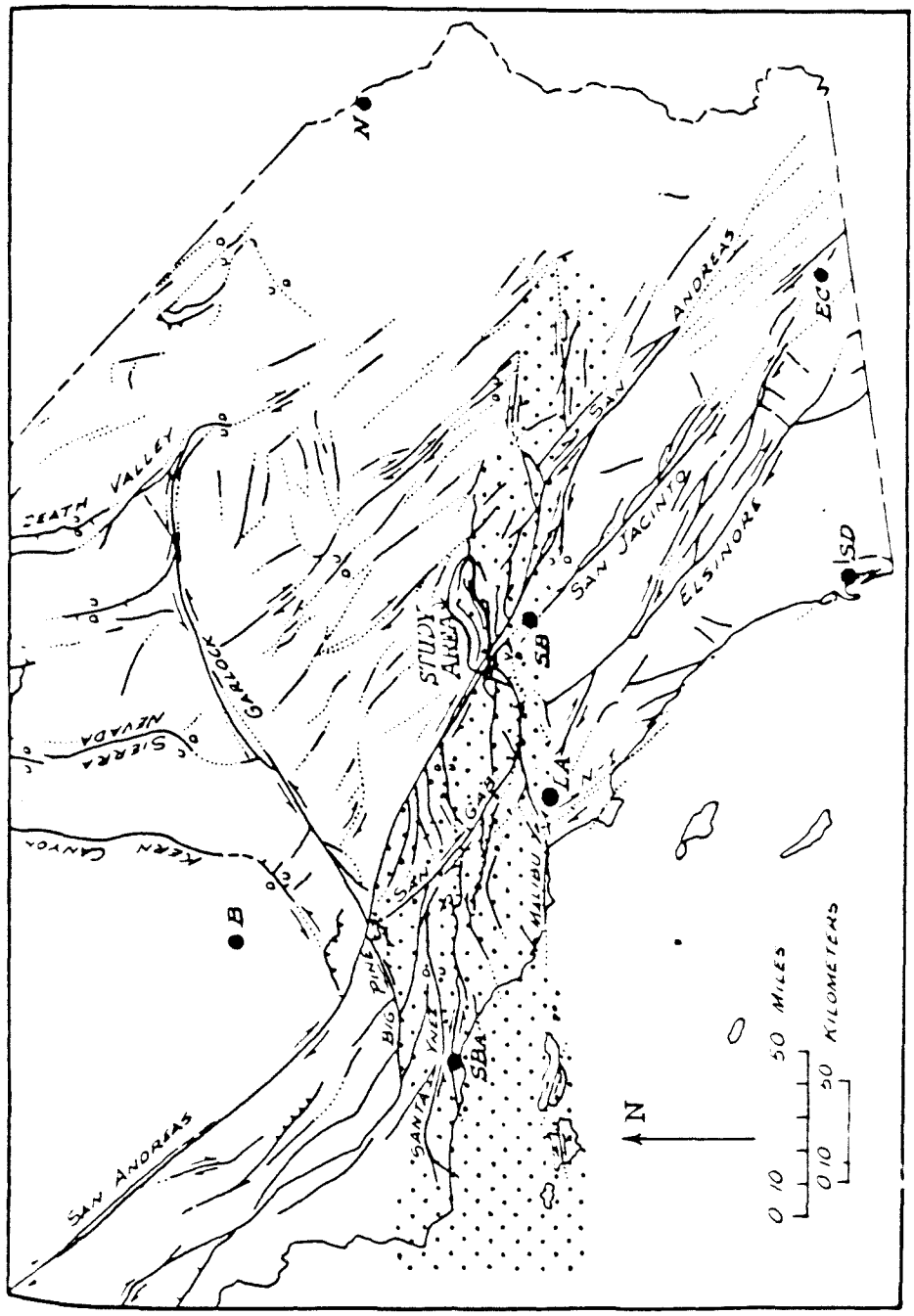
N
EC
SD
SB
LA
B
SBa
DEATH VALLEY
GARLOCK
SIERRA NEVADA
KERN CANYON
SAN ANDREAS
SAN ANDREAS
SAN JACINTO
ELSINORE
STUDY AREA
SANTA YNEZ
BIG PINE
SAN GABRIEL
MALIBU
N
0 10 50 MILES
0 10 50 KILOMETERS

fault into two parts with different movement histories (Baird et al., 1974). Some invoke large components of upward relief and thrusting in the Transverse Ranges to alleviate strain accumulation resulting from different slip-rates on the San Andreas north and south of the province. If such a relationship exists between Transverse Ranges structure and the San Andreas fault, it should be most evident at their junction.

Antipodal symmetry displayed by the frontal fault systems of the San Bernardino and San Gabriel Mountains has led to the hypothesis that the entire Transverse Ranges province may have been rotated up to 55° about a central axis (Baird et al., 1974). If so, very large horizontal displacements might be expected on the principal range-bounding structures. Based on the work of Woodford and Harriss (1928), Baird et al. (1974) favor at most two to three kilometers of horizontal crustal shortening across the north frontal fault system of the San Bernardino Mountains. Recent paleomagnetic data from the western Transverse Ranges tend to support rotations, but of smaller blocks in a regional right-lateral shear couple (Kamerling and Luyendyk, 1979). Such rotations, if they exist, should be reflected in the sedimentary rocks and structural geometries of the San Bernardino Mountains.

Hadley and Kanamori (1977) advance a radically different explanation for the structure of the Transverse Ranges, in which the plate boundary in the upper mantle is offset from the San Andreas fault in the region of the central Transverse Ranges (Section 6.4.1.4). Enhanced coupling across an low-angle discontinuity beneath the San Bernardino Mountains might have resulted in buckling of the crust to produce the Transverse Ranges. In this model, the northern margin of the Transverse Ranges east of the San Andreas fault should propagate northward and eastward with time.

Clearly these models have conflicting implications for the nature and history of deformation along the north frontal fault system of the San Bernardino Mountains. Field data contained in this thesis offer a test for the various consequences predicted by the above models.

1.2.2 The North Frontal Fault System of the San Bernardino Mountains

The physiographic San Bernardino Mountains extend east from Cajon Pass to Morongo and Yucca Valleys, and south from Summit, Apple, Fifteenmile, Lucerne and Johnson Valleys to the San Bernardino plain and Banning Pass (Figure 1-2). They are structurally bounded by the north frontal, San Andreas, and Pinto Mountain fault zones.

The geomorphic discordance between the extensive upland erosion surface and steep northern escarpment of the San Bernardino Mountains was first recognized by Mendenhall (1905) as evidence of the extreme youthfulness of the range. Vaughan (1922) made the original reconnaissance mapping study of the central San Bernardino Mountains, which included insights into the origin of the range front. Noble (1932, 1953, 1954a, 1954b) contributed greatly to the understanding of Cajon Pass area through his reconnaissance studies of the San Andreas fault zone. Local studies along the northern range front by Woodford and Harriss (1928), Gillou (1953), and Richmond (1960) were primarily concerned with with pre-Tertiary rocks and structures, yet they noted much evidence of late Cenozoic faulting and deformation. In mapping the Blackhawk landslide, Shreve (1959, 1968) showed than an extensive and useful late Tertiary and Quaternary stratigraphy exists on the range front.

Pre-batholithic metasedimentary rocks have been studied and mapped by numerous workers, including Coffman (1980), Brown (1979), and Ely (1982) in the Ord Mountains, Hollenbaugh (1970) in the Furnace Canyon area, Brown (1982) in the White Mountains, and Cameron (1981) in the Delamar Mountain

Figure 1-2. Index figure showing the principal faults, and physiographic features of the northwestern San Bernardino Mountains study area. Structural features in bold letters: SPF = Squaw Peak Fault; CF = Cleghorn Fault; SAFZ = San Andreas Fault Zone; WCF = Waterman Canyon Fault; PCF = Powell Canyon Fault; CSFS = Cedar Springs Fault System; NF = Notch Fault; SC = Seeley Creek Fault; GVF = Grass Valley Fault; SVFS = Summit Valley Fault System; TRL = Tunnel Ridge Lineament; OMF = Ord Mountains Fault Zone; BRF = Bowen Ranch Fault; ACN = Arrastre Canyon Narrows Fault Zone; LCF = Lovelace Canyon Fault; SHR = Sky Hi Ranch Fault Zone; WMT = White Mountain Thrust System; HF = Helendale Fault. Physiographic features in fine letters: CP = Cajon Pass; SV = Summit Valley; CR = Cleghorn Ridge; PR = Pilot Rock Ridge; P = Pinnacles; DC = Deep Creek; OM = Ord Mountains; JF = Juniper Flats; OR = Ocotillo Ridge; MRI = Milpas Ridge; MR = Marianas Rancho; FMV = Fifteenmile Valley; WM = White Mountain; LV = Lucerne Valley

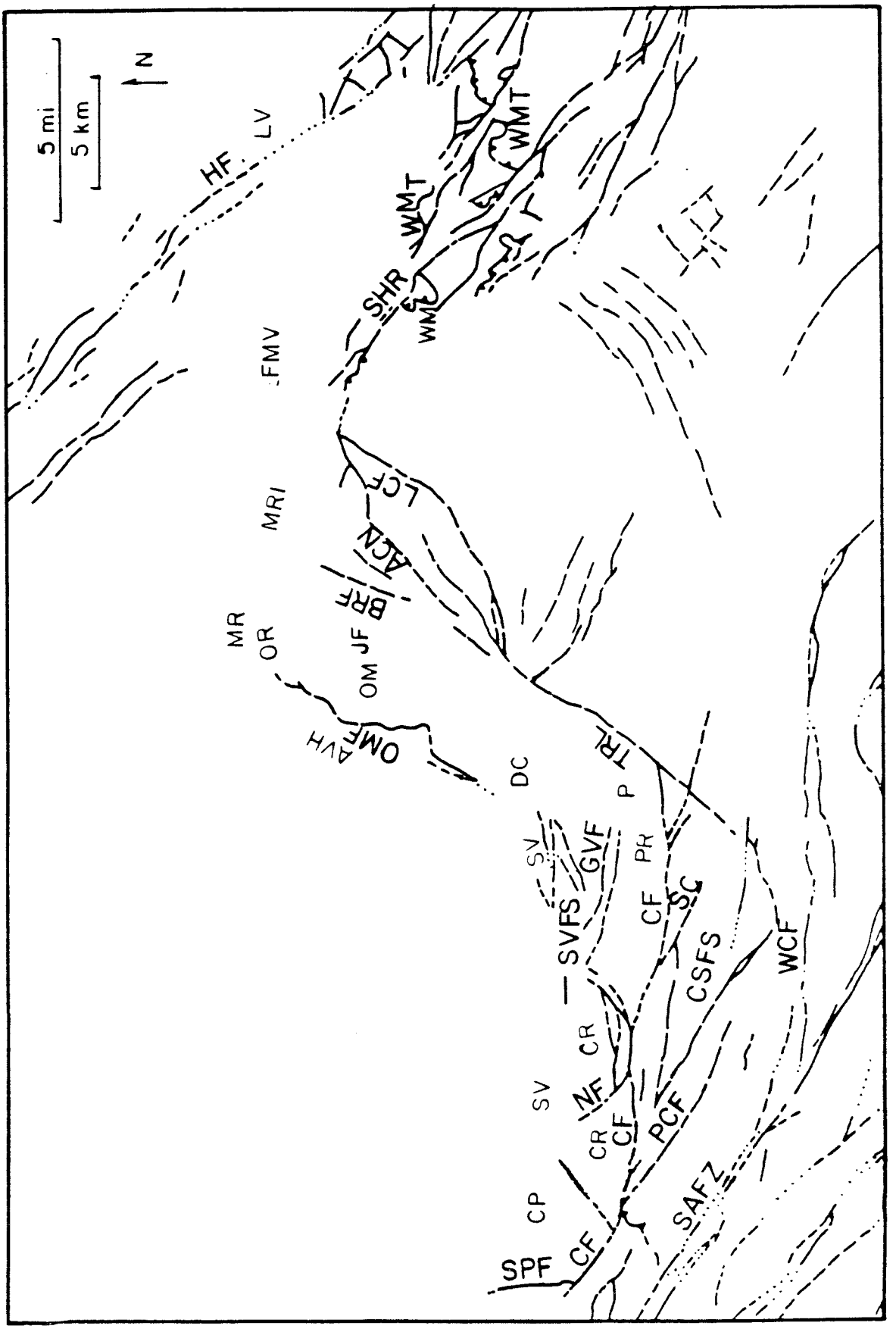
5 mi
5 km
N
HF
LV
FMV
SHR
WMT
WMT
WMT
MRI
LCF
ACN
BRF
MR
OR
OM
JF
OMFAVH
DC
TR
P
SV
GVF
SVFS
PR
CF
SC
CSFS
WCF
SV
CR
NF
CR
CF
PCF
CP
SAFZ
SPF
CF

area. Studies of batholithic rocks include work by MacColl (1964) in the Rattlesnake Mountain pluton, Smith (1982) in the White Mountain area, and C. F. Miller (1977) in the Fawnskin Monzonite. Geochronologic data for batholithic rocks in the San Bernardino Mountains are summarized by Miller and Morton (1975, 1980), and Smith (1982).

Although the physiography of the relict erosion surface that caps the San Bernardino Mountains was discussed in detail by Vaughan (1922), the origin of its characteristic boulder mantle was first studied by Blackwelder (1925), and then Oberlander (1972), who developed a model for its origin in the study area. Sadler and Reeder (1983) have proposed drainage reconstructions based on the distribution of gravels preserved on the relict surface.

Dibblee (1964, 1965, 1967, 1974) mapped the entire range-front study area at a scale of 1:62,000 and presented arguments for late Quaternary uplift in the San Bernardino Mountains (Dibblee, 1975). The general geology of the range front between the Ord and Bighorn Mountains was recently mapped in reconnaissance by Fred Miller of the U.S. Geological Survey. Miller (in preparation) made a strip-map of the zone of active faulting at a scale of 1:48,000 in order to clarify the relationships between the northwest-trending strike-slip Mojave block faults and the east-trending frontal fault system. Sadler (1981, 1982) has mapped extensively along the range front, as well as within the range, under contract to the California Division of Mines and geology in preparation for publication of the upcoming revised San Bernardino 1 x 2° State map sheet. Weldon et al. (1981), Meisling and Weldon (1982a,b), and Weldon and Meisling (1982) mapped and studied the neotectonics of the westernmost San Bernardino Mountains. Woodburne and Golz (1972) and Foster (1980) mapped the area between Cajon Pass and Valyermo, erecting a detailed

stratigraphy for the Punchbowl and Crowder Formations.

Detailed site studies were prepared in connection with the Mojave River Dam by the U.S. Army Corps of Engineers (1982), and the Cedar Springs Dam by the California Department of Water Resources (1968a,b).

Woodburne and Golz (1972), Repenning (1982) and Reynolds (pers. comm.) have done much paleontological work in the Punchbowl, Crowder, and Harold Formations, while May and Repenning (1982) and May and Sadler (1981) have made a similar contribution in the Old Woman Sandstone. Sadler (1982) has brought together data on late Cenozoic deposits around the margin of the San Bernardino Mountains. Weldon and Naeser (pers. comm.) have dated tuffs in the eastern Crowder Formation.

1.2.3 Uplift Rates for the San Bernardino Mountains

There exists in the literature an unacceptably high uncertainty of almost two orders of magnitude in the proposed uplift rate of the San Bernardino Mountains. Shreve (1959) concluded that uplift of the range began in late Pliocene(?) with deposition of the Old Woman Sandstone; recent discoveries of a late Pliocene fauna places the deposition of this formation at 2.0 to 3.2 my (May and Repenning, 1982). This yields an approximate uplift rate for the 1000-meter northern escarpment of about 0.3 mm/yr (1000 m/ 3 my). Based on the elevation of Wisconsin-age snowlines inferred from glacial sediments in the San Bernardino Mountains, Morton and Herd (1980) suggest that between 18,000 and 10,000 y B.P. the uplift rate was between 18 and 36 mm/yr. Recent geophysical modeling of crustal strain rates in southern California predicts 19 mm/yr uplift along the north frontal fault system (Bird, 1980). At a minimum rate of 0.3 mm/yr, uplift would have taken 3 my; at the maximum proposed rate of 36 mm/yr, the entire northern escarpment could have been created in less than 30,000 years.

1.3 STUDY GOALS

The primary goals of this thesis study, as stated at its inception, were: (1) to establish a better constrained uplift history for the San Bernardino Mountains, (2) to elucidate the nature and modes of deformation acting on the northern range-front, (3) to estimate Holocene rates of deformation along the range front, and (4) to estimate, if possible, earthquake recurrence intervals and vertical/lateral offsets for the north frontal fault system.

1.4 THE PRESENT STUDY

This dissertation is an integration of my field work with the work of others to present an overview of the neotectonic evolution of the northwestern range front of the San Bernardino Mountains. The work was carried out under the direction of Clarence R. Allen, and funded under the Earthquake Hazards Reduction Program of the U. S. Geological Survey, contract # 14-08-0001-19754. Preliminary work in the Silverwood Lake area was funded under California Department of Water Resources Agreement #B-53653.

A primary contribution of this thesis is a 1:24,000 scale map of the north frontal fault system between Cajon Pass and Lucerne Valley (Plates 1A and 1B). This mapping covers about 150 square miles and has incorporated detailed mapping by Weldon et al. (1981), Foster (1980), Sadler (1981), Coffman (1980), and MacColl (1964), where available, in an effort to present as complete a picture of range-front geology as possible (Figure 1-3). The study emphasizes a five-mile-wide zone of range-front faulting and deformation.

Work in the westernmost San Bernardino Mountains was done in close cooperation with Ray Weldon. Many of the ideas presented in this thesis are his, and I have made a concerted effort to identify them as such.

Figure 1-3. Boundaries of map area. The names of U.S.G.S. 7-1/2 minute quadrangle sheets are shown. Areas compiled from the work of others are defined and sources identified. The diagram shows the limits of Plates 1A and 1B in heavy lines.

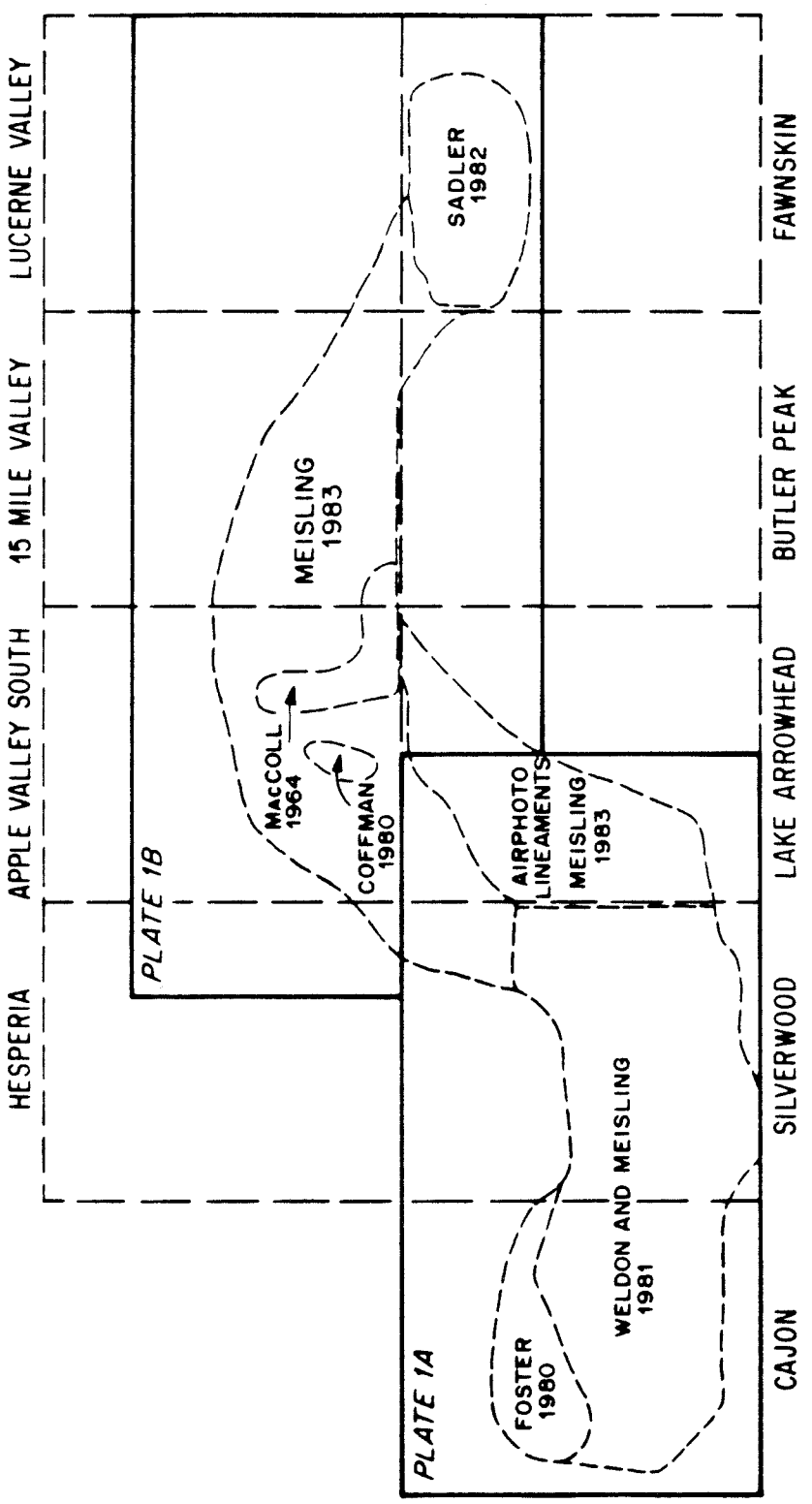
HESPERIA
APPLE VALLEY SOUTH
15 MILE VALLEY
LUCERNE VALLEY
SILVERWOOD
LAKE ARROWHEAD
BUTLER PEAK
FAWNSKIN
CAJON
PLATE 1B
PLATE 1A
SADLER 1982
MEISLING 1983
MACCOLL 1964
COFFMAN 1980
AIRPHOTO LINEAMENTS
MEISLING 1983
WELDON AND MEISLING 1981
FOSTER 1980

The dissertation is organized into eight chapters. Chapter II, "Stratigraphy", integrates and supplements existing work to present an overview of the rock record in the study area, from pre-batholithic rocks to the Pleistocene Victorville Fan Complex. Chapter III, "Geomorphology", discusses the relict erosion surface, terraces, alluvial fans, and the drainage evolution of the Mojave River in the study area. Chapter IV, "Paleomagnetism", presents the data and results of magnetostratigraphic work on the sediments of the Harold Formation, Shoemaker Gravel, Older Alluvium and their correlatives. Chapter V, "Structure", discusses each fault in the study area individually, citing detailed evidence for the geometry, geomorphology, character, displacement and age. Chapter VI, "Tectonic Evolution", reviews the constraints on uplift history presented in Chapters II through V, and develops a working chronology of tectonic events along the northern range front. Chapter VI also discusses the nature and modes of deformation, their relationship to each other, and possible models for their origin. Chapter VII, "Seismic Risk", discusses the evidence for activity, cumulative offset, slip-rate, and earthquake hazard posed by the each major fault or fault system in the study area. The closing chapter, Chapter VIII "Summary and Conclusions" offers a brief overview of the major results of the thesis.

CHAPTER II

STRATIGRAPHY

2.1 INTRODUCTION

An understanding of the character, expression, origin and distribution of rocks in the study area is fundamental to the interpretation of structure, regional neotectonics and seismic risk. This chapter describes the stratigraphic record along the northern front of the San Bernardino Mountains from Cajon Pass to Lucerne Valley. Much of the work described herein was done by others. The object of this chapter is not to erect a definitive stratigraphy for the range-front area, but to integrate and supplement existing work to provide an overview of the rock record along the range front.

Crystalline rocks were studied primarily as local sources of clasts and sediment; detailed analysis of the crystalline rocks is beyond the scope of this study. Early Tertiary rocks are absent throughout most of the San Bernardino Mountains. Miocene and Pliocene sediments are present in Cajon Pass, Summit Valley, and Lucerne Valley, but missing elsewhere along the northern range front. In fact, the range front between Deep Creek and Lucerne Valley lacks any stratigraphic record between late Cretaceous and middle Pleistocene time. The incompleteness of the stratigraphic record makes interpretation of geologic history difficult. In order to establish a sequence of depositional and structural events, it is necessary to take a broader view of local stratigraphy as the product of its regional tectonic context.

This chapter is divided into three sections: Crystalline Basement, Tertiary Sediments and Quaternary Sediments. Late Quaternary alluvial fans and terraces are discussed with geomorphic surfaces, drainage evolution

and soils in Chapter III, "Geomorphology and Alluvial Stratigraphy".

The superscripted numbers in the text refer to the localities listed in Appendix B and correspond to the circled numbers on Plates 1A and 1B.

2.2 CRYSTALLINE BASEMENT

Crystalline rocks were studied in order to (1) identify faults and folds, (2) delimit clast source areas, and (3) provide uniform regional coverage at a reconnaissance level.

Batholithic intrusive rocks of Cretaceous age are the dominant crystalline lithology in the San Bernardino Mountains and western Mojave Desert (Figures 2-1 and 2-2; Plates 1A and 1B). Roof pendants, composed primarily of slightly metamorphosed Precambrian to Carboniferous sedimentary rocks of the Cordilleran miogeocline, contain mafic intrusive bodies of probable early Mesozoic age that predate emplacement of the main batholithic mass. Distinctive intrusive and metamorphic lithologies of the San Gabriel Mountains crystalline basement terrane occur only southwest of the San Andreas fault, but are briefly discussed since their appearance as clasts in Pleistocene gravels within the study area is tectonically significant.

2.2.1 Pre-Batholithic Intrusive Rocks

Pre-batholithic intrusive rocks occur throughout the range-front study area and tend to be more mafic than rocks of the batholithic suite (Figure 2-3; Plates 1A and 1B). Small inclusions of hornblende-diorite to hornblendite are commonly found in association with batholithic rocks in the western San Bernardino Mountains[1]. Gabbro and hornblende-diorite at White Mountain (D. K. Smith, 1982; H. Brown, 1982b) and quartz-syenite sheets[2] in the Ord Mountains are spatially confined to metasedimentary roof pendants which are cut by rocks of batholithic affinity. A large

Figure 2-1. Diagramatic sketch of generalized rock units of the northwestern San Bernardino Mountains (modified from Dibblee, 1967).

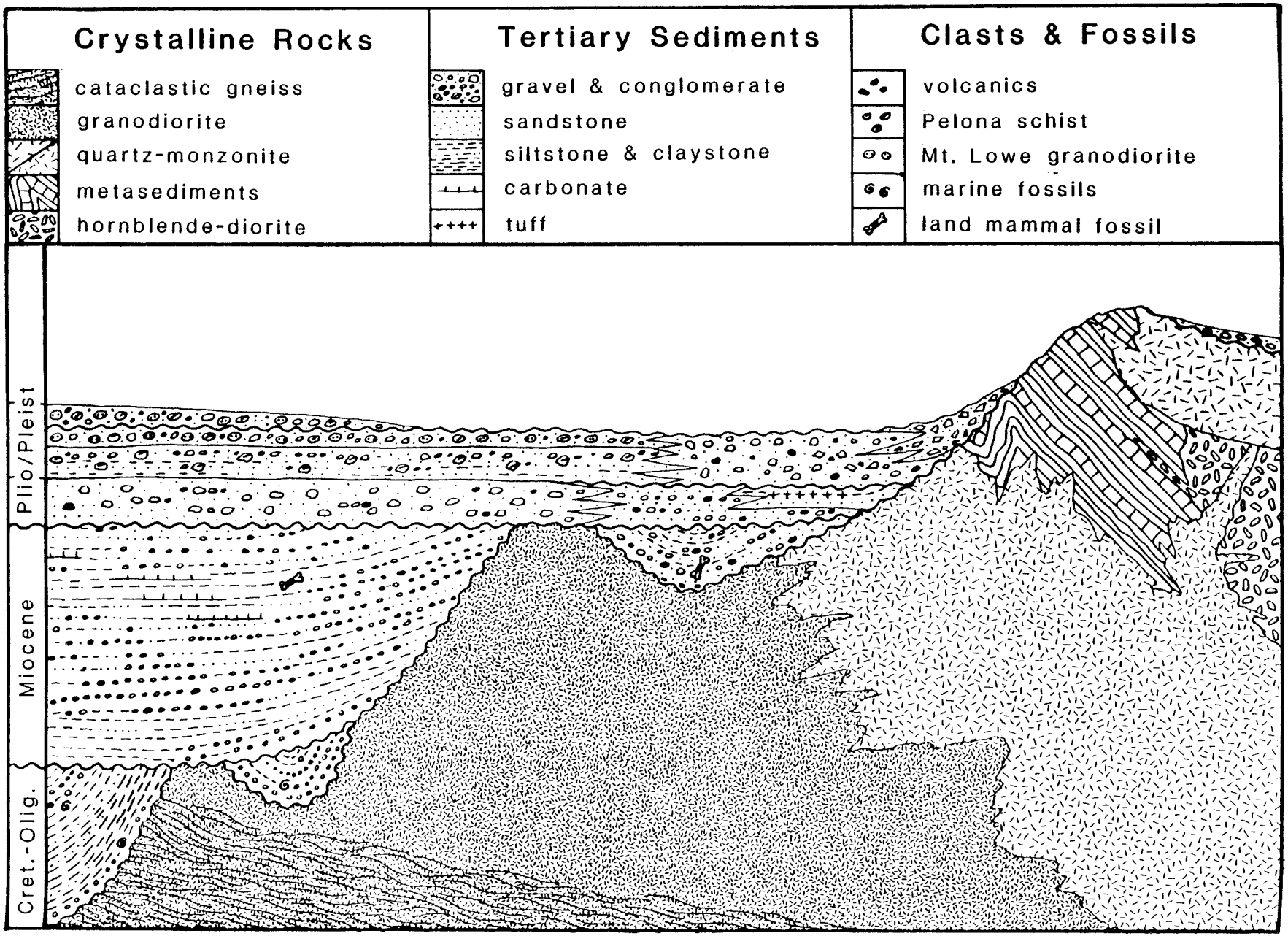
Crystalline Rocks
cataclastic gneiss
granodiorite
quartz-monzonite
metasediments
hornblende-diorite
Tertiary Sediments
gravel & conglomerate
sandstone
siltstone & claystone
carbonate
tuff
Clasts & Fossils
volcanics
Pelona schist
Mt. Lowe granodiorite
marine fossils
land mammal fossil
Plio/Pleist
Miocene
Cret.-Olig.

Figure 2-2a. Explanation of patterns for map of generalized geology (Figure 1b). The rock units are described in detail in the text and in the explanation for Plates 1A ans 1B.

Explanation

Quaternary Rocks


Older Alluvium, undissected


Older Alluvium, dissected


Harold Fm. & Shoemaker Gravel

Tertiary Sedimentary Rocks


Old Woman Sandstone


Crowder Formation


Santa Ana Sandstone


Punchbowl Formation


San Francisquito Formation

Batholithic Intrusive Rocks


biotite quartz monzonite


granodiorite


granite

Metasedimentary Rocks


carbonate


phyllite


quartzite


Pelona schist

Pre-batholithic Intrusive Rocks


hornblende diorite


hornblende quartz monzonite

Figure 2-2b. Generalized geologic map of the western San Bernardino Mountains area (from Jennings, 1983). See Figure 1a for explanation of map patterns. See Plates 1A and 1B for detailed geology. LV = Lucerne Valley; AV = Apple Valley; V = Victorville.

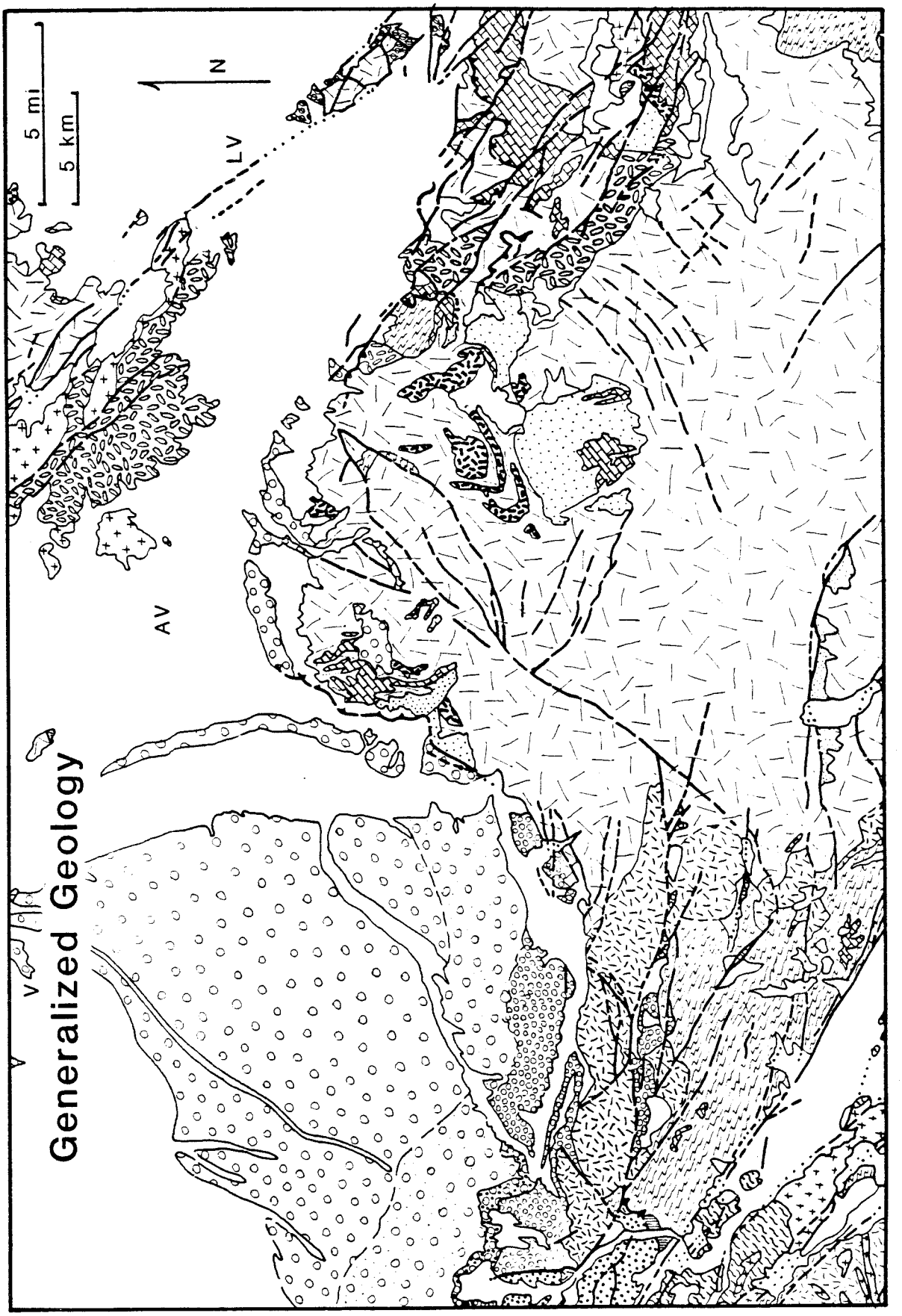
Generalized Geology
5 mi
5 km
N
LV
AV

Figure 2-3. Generalized map of the western San Bernardino Mountains showing the distribution of pre-batholithic igneous rocks (after Jennings, 1983). AV = Apple Valley; LV = Lucerne Valley; SAFZ = San Andreas fault zone; V = Victorville; GM = Granite Mountains; FM = Fawnskin Monzonite.

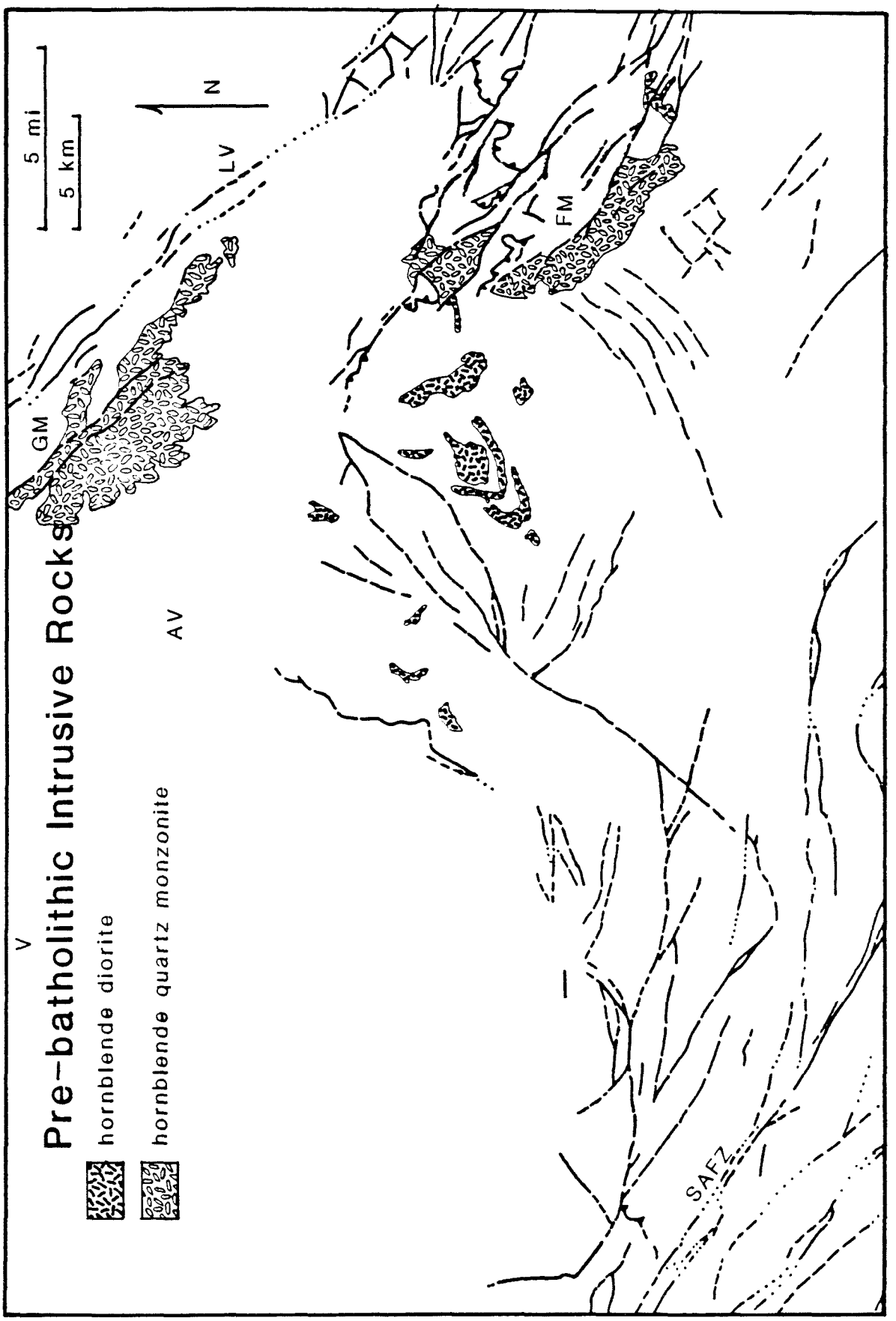
Pre-batholithic Intrusive Rocks
hornblende diorite
hornblende quartz monzonite
5 mi
5 km
N
GM
AV
LV
FM
SAFZ

hornblende-diorite[3] body intruding quartzo-feldspathic metasediments northeast of Deep Creek Dam is intruded by fine-grained biotite-quartz-monzonite of batholithic affinity. At the south end of Milpas Road, another large hornblende-diorite mass[4] is truncated and injected by porphyritic biotite-quartz-monzonite of the Rattlesnake Mountain pluton. These mafic rocks clearly predate intrusion of the main batholithic mass. They may represent early phases of the protracted Cretaceous intrusive event, or, as Smith (1982) suggests, an earlier Triassic(?) intrusive event.

A major body of foliated hornblende quartz monzonite[5] to hornblende monzonite intrudes the metasediments at White Mountain, and is in turn intruded by biotite quartz monzonite of the Cretaceous batholith (Figure 2-3; Plate 1B). This body, called the Fawnskin Monzonite by Cameron (1981), is described in the White Mountain area by Smith (1982), and was mapped by Richmond (1960), Dibblee (1964), and C. Miller (1977) between Delamar Mountain and White Mountain. Smith (1982) summarizes published evidence for the age of the Fawnskin Monzonite (Armstrong and Suppe, 1973; C. Miller, 1977; F. Miller and Morton, 1980) leading to an Ar^{39}/Ar^{40} age estimate of 229 my (Cameron, 1981) when adjusted for argon loss due to emplacement of the Cretaceous batholith.

Weldon et al. (1981) report several isolated outcrops of pre-batholithic intrusive rocks of unknown affinity in the western San Bernardino Mountains south of Cajon Pass. A few small masses of quartz-garnet-mica-rich rocks occur at the top of Cajon Mountain. A body of distinctive "clotted" hornblende-granodiorite is reportedly in structural contact with batholithic rocks on the south flank of the western San Bernardino Mountains (Weldon, 1982, pers. comm.). Ages and protoliths for these rocks are not known.

2.2.2 Pre-batholithic Metasedimentary Rocks

Most of the Ord Mountains are underlain by a sequence of low-grade metasedimentary rocks (Figure 2-4; Plates 1A and 1B) consisting of interbedded marble, schist, phyllite, calc-silicate, and quartzite (R. L. Coffman, 1980) of Cordilleran miogeoclinal affinity (Dibblee, 1967). Although the bedding initially appears homoclinal, abundant evidence of isoclinal folding suggests that the 600-meter-thick section has been tectonically thickened. The section, in order of decreasing abundance, consists of dolomitic marble[6], phyllite with interbedded marble[7], hornfelsic calc-silicate[8], and quartzite[9]. Maximum metamorphic grade is lower hornfels facies (R. L. Coffman, 1980), as demonstrated by the preservation of fine laminations in stromatolites.

The Ord Mountains carbonates have been assigned to the Paleozoic Era (Dibblee, 1967) on the basis of crinoid stems reportedly found in "granite-injected limestone" beds by Noble (1932). Unfortunately, Noble's crinoid stems are lost, as is the location of his collection site. A well-preserved stromatolite[10], collected in slope rubble derived from the dolomitic marbles in the Ord Mountains by Marion Ely II and K. E. Meisling, has been provisionally identified by Stanton Awramick (1982, pers. comm.) as conophyta, a stromatolite of distinctive conical morphology known only from the late Precambrian. Howard Brown (1982a) has independently suggested a lithologic correlation between the Ord Mountains section and Cordilleran miogeoclinal rocks of the Death Valley sequence, specifically the Sterling (quartzites), Johnny, Wood Canyon (phyllites), Bonanza King (dolomites) and Carrara (calcsilicates) Formations (H. Brown, 1982, pers. comm.). Thus, the Ord Mountains carbonates appear to be late Precambrian to early Cambrian in age (M. Ely, 1982).

Figure 2-4. Generalized map of the western San Bernardino Mountains showing the distribution of metasedimentary rocks (after Jennings, 1983). AV = Apple Valley; LV = Lucerne Valley; SAFZ = San Andreas fault zone; V = Victorville; OM = Ord Mountains pendant; WM = White Mountains pendant; FC = Furnace Canyon pendant; DM = Delamar Mountain pendant

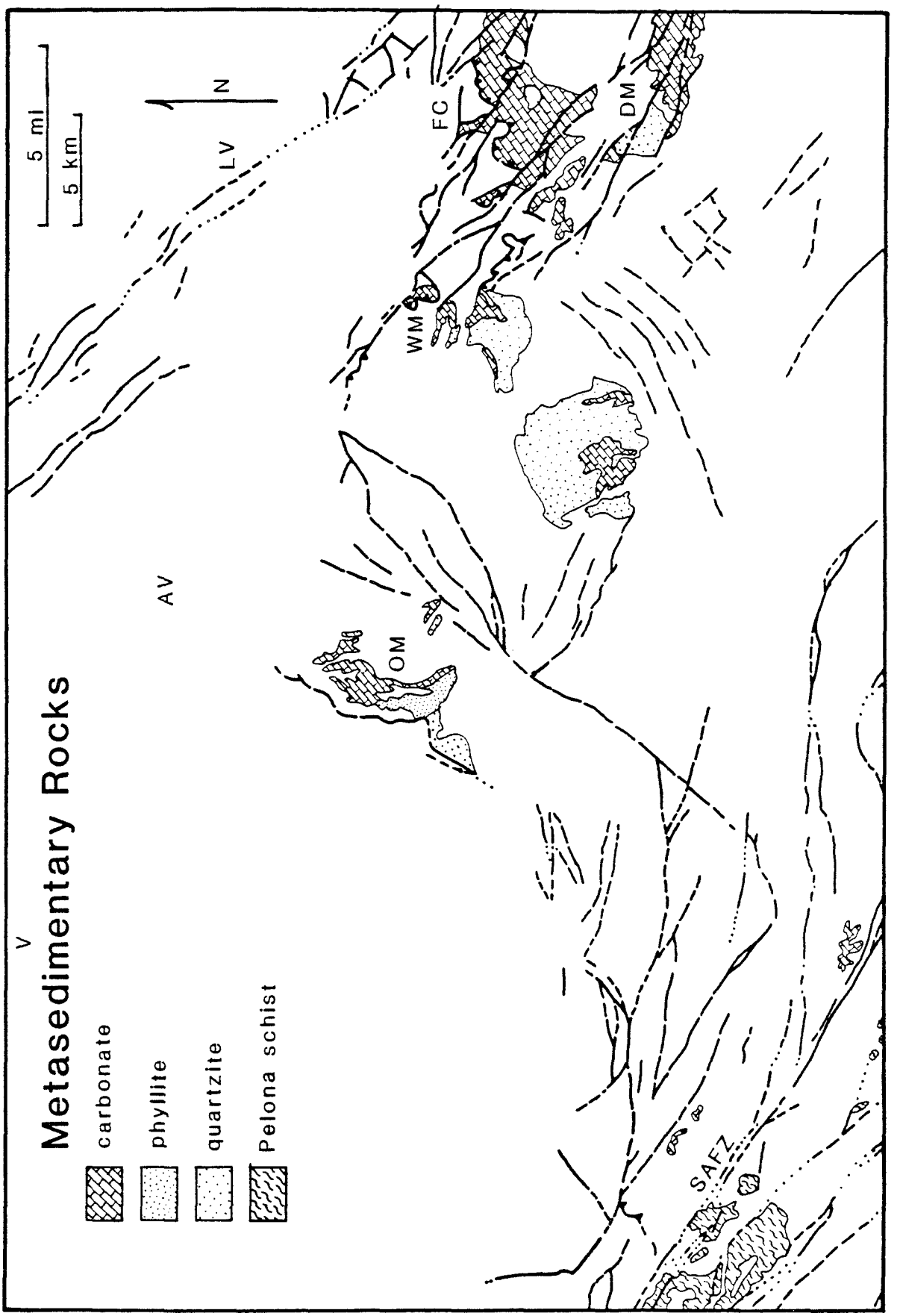
Metasedimentary Rocks
carbonate
phyllite
quartzite
Pelona schist
5 mi
5 km
N
V
AV
LV
OM
WM
FC
DM
SAFZ

Metasediments of distinctly higher grade occur just northeast of Deep Creek Dam (Figure 2-4; Plate 1A). These strata were referred by Dibblee (1966) to the Saragossa Quartzite of Vaughan (1922) based on lithologic similarity to the localities in the San Bernardino Mountains to the east. The Ord Mountains section consists of coarse-grained white quartzite[11], pelitic granofels[12], and biotite-sillimanite gneiss[13], in order of decreasing abundance. The presence of sillimanite indicates significantly higher metamorphic grade than the Ord Mountains carbonate section (R. E. Powell, 1982, pers. comm.). Lithology and grade of these rocks suggest correlation with the Joshua-Tree terrane of Powell (1981), and/or the Chicopee Canyon Formation of Richmond (1960).

The higher grade, quartzo-feldspathic sequence is in steep contact with the phyllites of the lower-grade carbonate sequence north of the SCE power-line road. A quarter-kilometer-wide zone of deformed phyllonite[14] separates the two sections, indicating that the contact is tectonic in origin (Section 5.6).

White Mountain is underlain by a complexly deformed metasedimentary roof pendant (Figure 2-4; Plate 1B) composed mainly of marble and color-banded quartzite, with minor calc-silicate (Smith, 1982; H. Brown, 1982, pers. comm.). Brown correlates the bulk of the marbles at White Mountain with the Furnace Formation (Vaughan, 1922; Richmond, 1960) and the Dawn, Anchor, and Bullion Members of the Mississippian Monte Cristo Limestone (H. Brown, 1982, pers. comm.). He has suggested that tectonic slices of marble at White Mountain may be correlative with the Muav Limestone and Banded Mountain Member of the Cambrian Bonanza King Formation, calc-silicates with the Carrara Formation, and quartzites with the Sterling Formation of the Death Valley sequence. The quartzites have been referred to Chicopee

Canyon Formation at Delamar Mountain by Sadler (1981) and Smith (1982). The White Mountain section has been metamorphosed to albite-epidote-hornfels grade (Smith, 1982).

The Furnace Canyon pendant (Figure 2-4; Plate 1B) is composed of more than 9700 feet of dolomitic, arenaceous and siliceous limestones that constitute the Furnace formation of Mississippian and Pennsylvanian age (Vaughan, 1922; Richmond, 1960; Hollenbaugh, 1970). The Furnace Formation is correlated with the Carboniferous section in the Inyo Mountains by Hollenbaugh (1970), and has been metamorphosed to low- to middle-hornfels grade (Richmond, 1960). Skarns are common in the contact zones with the surrounding plutonic rocks (Richmond, 1960). Marbles of the Furnace Formation are being mined for high-grade limestone and for use in portland cement.

2.2.3 Batholithic Rocks

The crystalline basement underlying the western San Bernardino Mountains is predominantly hornblende-biotite-granodiorite[15] and biotite-quartz-monzonite[16] (Figure 2-5; Plates 1A and 1B). The quartz-monzonite is medium- to coarse-grained, equigranular, and commonly contains K-spar phenocrysts. The granodiorite tends to be finer grained and more mafic, with hornblende as well as biotite in abundance. The granodiorite contains accessory sphene and locally becomes dioritic in composition (Weldon et al., 1981). The quartz-monzonite is much less resistant to weathering than is the granodiorite, disintegrating readily to form grus. There is no consistent cross-cutting age relationship between the quartz-monzonite and the granodiorite. The contact zone is locally gradational with abundant evidence of assimilation, lit-par-lit injection, dike formation and syn-plutonic deformation. Granodiorite is the dominant rock type west of Silverwood Lake, and

Figure 2-5. Generalized map of the western San Bernardino Mountains showing the distribution of batholithic intrusive rocks (after Jennings, 1983). AV = Apple Valley; LV = Lucerne Valley; SAFZ = San Andreas fault zone; V = Victorville.

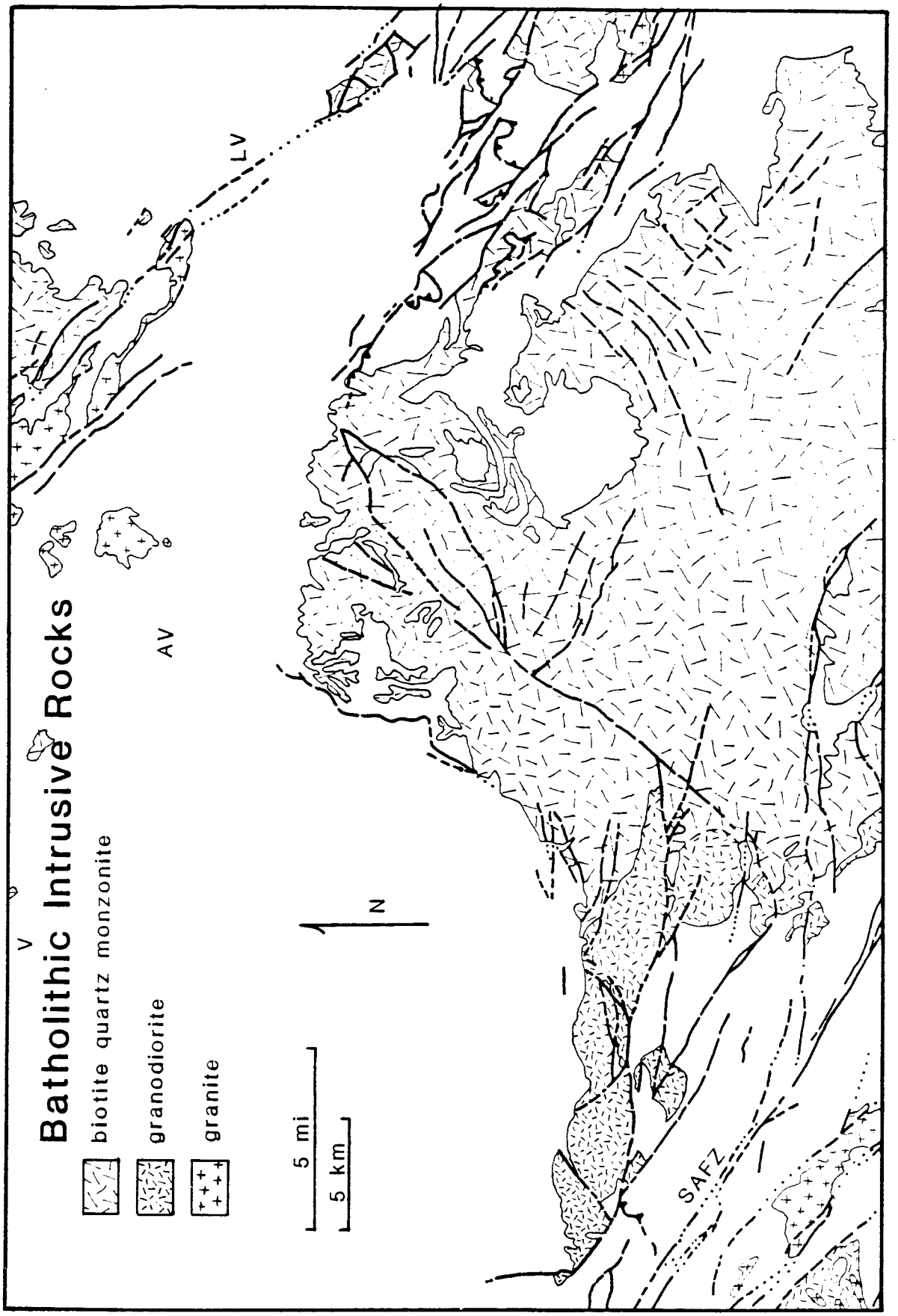
Batholithic Intrusive Rocks
biotite quartz monzonite
granodiorite
granite
5 mi
5 km
N
LV
AV
V
SAFZ

quartz-monzonite is more common to the east. To the south, these rocks grade into, or intrude, fine-grained hornblende diorite to hornblendite (Weldon et al., 1981).

The batholithic rocks in the western San Bernardino Mountains contain many small pendants and inclusions of marble, calc-silicate, quartzite and garnet-mica-schist, inferred to have been derived from a miogeoclinal sedimentary protolith. Although volumetrically minor, they prove useful in delineating structure within the batholithic rocks. Pendants of white marble, along with minor amounts of calc-silicate and quartzite, are generally recrystallized and surrounded by garnet-diopside skarns. Associated with these bodies are quartz-rich dikes containing large, well-formed hornblende crystals, but no biotite. These dikes are unlike the K-spar and mica pegmatites typically associated with the batholithic intrusives and suggest partial assimilation of the pendants by the intruding body. Several of the skarns have metallic mineralization, and at least one body is being mined for precious metals[17] (J. L. Coulson, 1981, pers. comm.).

All of the above lithologies are cut by a variety of late-stage dikes ranging from coarse-grained K-spar-quartz-biotite pegmatites to fine-grained aplites. Abundant small epidote veins[18] cut everything, including pegmatites, and are commonly associated with reddish oxidation halos suggesting a hydrothermal origin.

It is possible that the entire batholithic suite of hornblendite, granodiorite, quartz-monzonite, pegmatite and epidote veins may have been produced by one protracted intrusive event. The compositional variation could be due to either fractionation or partial assimilation of a more mafic pre-batholithic terrane (Weldon et al., 1981).

The intrusive rocks of the western San Bernardino Mountains are litho-

logically similar to the Mesozoic intrusive suite of the Mojave Desert (Dibblee, 1967, 1975; R. E. Powell, 1982, pers. comm.). K-Ar ages for batholithic rocks in the San Bernardino Mountains range from 55 to 122 my and reflect a protracted regional cooling history, rather than the timing of emplacement for individual plutons (Miller and Morton, 1975, 1980). Published K-Ar dates for plutonic rocks in the study area are shown on Plates 1A and 1B.

Batholithic rocks in the Pinnacles and Ord Mountains are dominantly biotite- and hornblende-quartz-monzonite (Miller and Morton, 1980; R. L. Coffman, 1980), displaying a wide variety of textures that reflect a complex history of intrusion and interaction with metasedimentary host rocks. These rocks have been mapped only in a reconnaissance fashion (Dibblee, 1966), and a detailed analysis of them is beyond the scope of this study.

Porphyritic biotite-quartz-monzonite of the late-Cretaceous Rattlesnake Mountain pluton[19], widely exposed between the Ord Mountains and Lovelace Canyon, has been studied in detail by MacColl (1964). MacColl showed the Rattlesnake Mountain pluton to be a tongue-shaped body consisting of several lobes emplaced from the southeast to northwest. Septa of hornblende-diorite commonly define the contacts between adjacent lobes of the pluton, and planar schlieren throughout the body permit detailed analysis of internal geometry and emplacement history (MacColl, 1964). Except for a modest increase in mafic content at its margin, the Rattlesnake Mountain pluton is remarkably uniform in texture and mineralogy.

2.2.4 Cataclastic Rocks

At deeper structural levels in the western San Bernardino Mountains, all of the crystalline basement rocks have a strong cataclastic foliation[28] superimposed on them. In general, this foliation is subhorizontal; in detail

the fabric is chaotic with abundant evidence of folding, slip and disruption on many scales. Although some mineral segregation appears to be associated with shearing, most of the color and textural banding in these rocks probably reflects dragging of dikes, inclusions and other heterogeneities parallel to the foliation. The degree of cataclasis increases gradually with depth, and batholithic intrusive lithologies can commonly be traced continuously into their compositionally identical gneissic equivalents[20]. It is therefore doubtful that these gneissic rocks are Precambrian in age (Dibblee, 1975; Jenkins, 1969).

"Granulite" (cataclastic gneiss) and "alaskite" (quartz-feldspar rock) occur at the margins of the Rattlesnake Mountain pluton where it intrudes the biotite-quartz-monzonite of the main batholith[21] (MacColl, 1964).

2.2.5 The San Gabriel Mountains Terrane

Crystalline basement in the San Gabriel Mountains southwest of the San Andreas fault includes several distinctive lithologies not found within the basement rocks of the San Bernardino Mountains. The appearance of two of these lithologies, the Pelona Schist and Lowe Granodiorite, within the Pleistocene sediments of the Cajon Pass area, provides important clues to the uplift of the San Gabriel Mountains and timing of related tectonic events. The key basement rocks of the San Gabriel Mountains are summarized by Ehlig (1975) as follows:

> "A highly varied basement terrane containing unusual rock types is exposed within the San Gabriel Mountains south of the San Andreas fault. Precambrian rocks in the western part of the range and adjoining Soledad Basin include from oldest to youngest: (1) amphibolite facies gneiss and amphibolite; (2) distinctive augen-gneiss derived from granite; (3) distinctive granulite-facies Mendenhall Gneiss formed from older granitic and gneissic rocks and subsequently largely retrograded to amphibolite-facies ; and (4) highly distinctive anorthosite, syenite and Gabbro(sic). Permo-Triassic Lowe Granodiorite forms a large differentiated pluton within the northwestern and central parts of the range. It has four facies, each with a characteristic mineralogy and

texture. The above formations are intruded by Mesozoic and older(?) basic dikes which are metamorphosed to amphibolite. Late Mesozoic granitic rocks form extensive plutons in the central and southern parts of the range."

"The above formations form the upper plate of the late Mesozoic-early Cenozoic Vincent thrust fault; Mesozoic(?) Pelona Schist forms the lower plate. The Vincent thrust and Pelona Schist are exposed in the northeastern San Gabriel Mountains and in Sierra Pelona, and(sic) anti-form north of the Soledad Basin. The thrust is marked by a thick zone of cataclastic rocks partially retrograded to greenschist-facies. The Pelona Schist is derived from interbedded graywacke, siltstone, shale, basic volcanics and minor chert and limestone which were prograded to greenschist-facies synchronously with the movement on the Vincent thrust."

2.3 TERTIARY SEDIMENTARY ROCKS

The late-Cenozoic stratigraphy along the northern range front is the primary key to the history, nature and modes of uplift of the San Bernardino Mountains (Figures 2-1, 2-2 and 2-6). The early Tertiary stratigraphic record is absent in most of the study area, being present only in limited exposures along the San Andreas fault in the Cajon Pass area. Middle- to late-Miocene time is represented by the Punchbowl Formation in Cajon Valley and the lower Crowder Formation in fault-bounded wedges throughout the western San Bernardino Mountains. Pliocene units, including the upper Crowder Formation in Summit Valley and the Old Woman Sandstone in Lucerne Valley, record an abrupt change in clast provenance and drainage regime that signals the incipient uplift of San Bernardino Mountains. Pleistocene deposits are the products of rapid uplift of the San Bernardino Mountains along the north frontal fault system and the appearance of the San Gabriel Mountains as a profound topographic high and dominant source of sediment across the San Andreas fault to the southwest.

2.3.1 Early Tertiary Sediments

2.3.1.1 The San Francisquito(?) Formation

Dibblee (1967) refers a 400-foot-thick (~130-meter-thick) section

Figure 2-6. Generalized map of the western San Bernardino Mountains showing the distribution of Tertiary sedimentary rocks (after Jennings, 1983). AV = Apple Valley; LV = Lucerne Valley; SAFZ = San Andreas fault zone; V = Victorville.

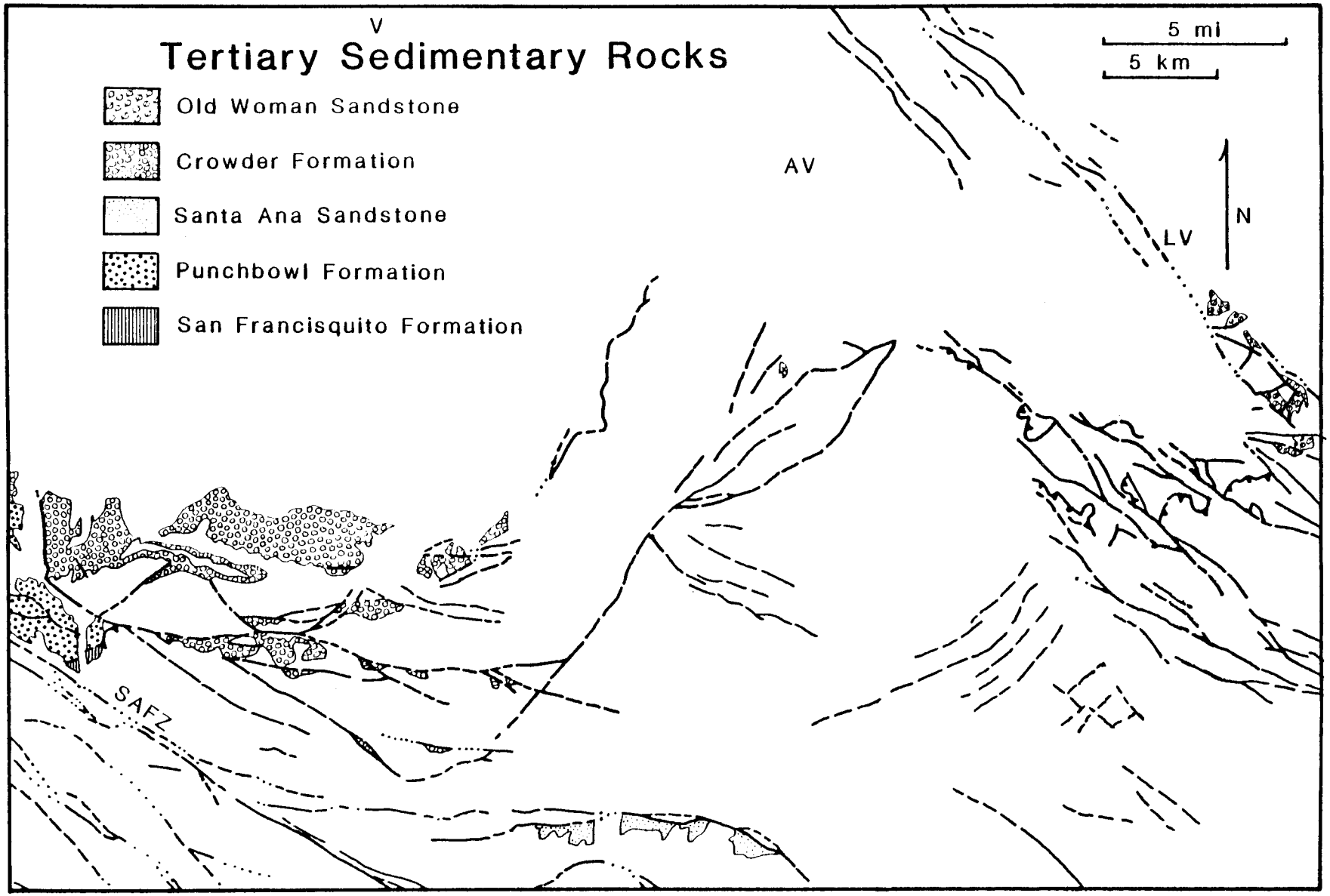
Tertiary Sedimentary Rocks
Old Woman Sandstone
Crowder Formation
Santa Ana Sandstone
Punchbowl Formation
San Francisquito Formation
V
AV
LV
N
5 mi
5 km
SAFZ

of coarse arkosic marine conglomerates, sandstones and siltstones that rest on plutonic and gneissic basement in Cajon Valley to the San Francisquito(?) Formation[22] (Figures 2-1 and 2-6; Plate 1A). This assignment is questioned by Woodburne and Golz (1972), who point out that the limited exposures in Cajon Pass are coarser and the clasts more angular than the type San Francisquito Formation in the Devil's Punchbowl. The San Francisquito is considered to be Paleocene and Eocene(?) in the type area (Woodburne and Golz, 1972). A Plesiosaur has recently been discovered in San Francisquito(?) Formation in Cajon Pass[31] (R. E. Reynolds, 1982, pers. comm.), indicating a late Cretaceous or Eocene age for this section. The San Francisquito(?) Formation in Cajon Valley is unconformably overlain by the Punchbowl Formation (Woodburne and Golz, 1972).

2.3.1.2 The Vaqueros(?) Formation

About 500 feet (~260 meters) of marine clastic deposits, assigned to the Vaqueros(?) Formation by Dibblee (1967), unconformably overlie the gneissic bedrock of Lone Pine Ridge and are unconformably overlain by the Punchbowl Formation (Woodburne and Golz, 1972). Marine invertebrate fossils indicate an age of early Miocene for these beds (Woodring, 1942; Woodburne and Golz, 1972). The Vaqueros(?) Formation is the youngest marine unit in the Cajon Valley area.

2.3.2 The Punchbowl Formation (Cajon Beds)

Over 8000 ft (~2660 meters) of nonmarine conglomerate and conlomeratic sandstone, widely exposed in the Cajon Pass area (Figures 2-1 and 2-6; Plate 1A), have been assigned an age of late Hemingfordian [middle Miocene] to Barstovian [late Miocene] based on mammalian fossils (Woodburne and Golz, 1972; see Figure 2-7). Although these strata (known informally as

Figure 2-7. Correlation between North American Land Mammal Ages and European epochs for the late Cenozoic (from Woodburne and Golz, 1972).

North American Land Mammal Age		European Epoch
Rancholabrean		PLEISTOCENE
Irvingtonian		
Blancan		
	late	
Hemphillian	middle	PLIOCENE
Clarendonian	early	
Barstovian	late	MIOCENE
Hemingfordian	middle	

the "Cajon Beds") have been referred to the Punchbowl Formation by Noble (1954) and Dibblee (1967), Woodburne and Golz (1972) argue that they are of sufficiently different lithology, fossil age and geologic history to be considered a separate unit. In addition to abundant granodiorite clasts, the Punchbowl Formation contains porphyritic volcanic clasts that suggest derivation from the Sidewinder Volcanic Series to the northeast, near Victorville (Robinson and Woodburne, 1971; Woodburne and Golz, 1972). The Punchbowl Formation is unconformably overlain by the Crowder Formation (Woodburne and Golz, 1972; Foster, 1980).

2.3.3 The Crowder Formation

The Crowder Formation, widely exposed between Summit Valley and Valyermo (Figures 2-1 and 2-6; Plate 1A) averages 980 meters in thickness and consists of poorly sorted nonmarine lithic arkose and arkosic wacke with interdigitated sand and gravel lenses (Dibblee, 1967; Foster, 1980). It is fluvial in character, with lenticular beds that commonly display internal low-angle, trough cross-stratification and cobble imbrication (Foster, 1980). Distinctive clast lithologies and paleocurrent indicators are consistent with derivation from the Victorville area to the northeast (Foster, 1980). The Crowder Formation in Cajon Pass can be divided into at least five units based on grain-size and lithology (Foster, 1980; Woodburne and Golz, 1972). Volcanogenic sediments exposed at the east end of Summit Valley are correlated with the upper part of the Crowder Formation (Figure 2-8).

2.3.3.1 The Lower Crowder Formation

The lower Crowder Formation is divided into Units 1 to 4 by Foster (1980). He describes Unit 1^{23} of the Crowder Formation as a quartzo-felds-

Figure 2-8. Proposed correlation of the Crowder Formation between Cajon Pass and Deep Creek (modified from Meisling and Weldon, 1982). Cajon Pass stratigraphic section after Foster (1980).

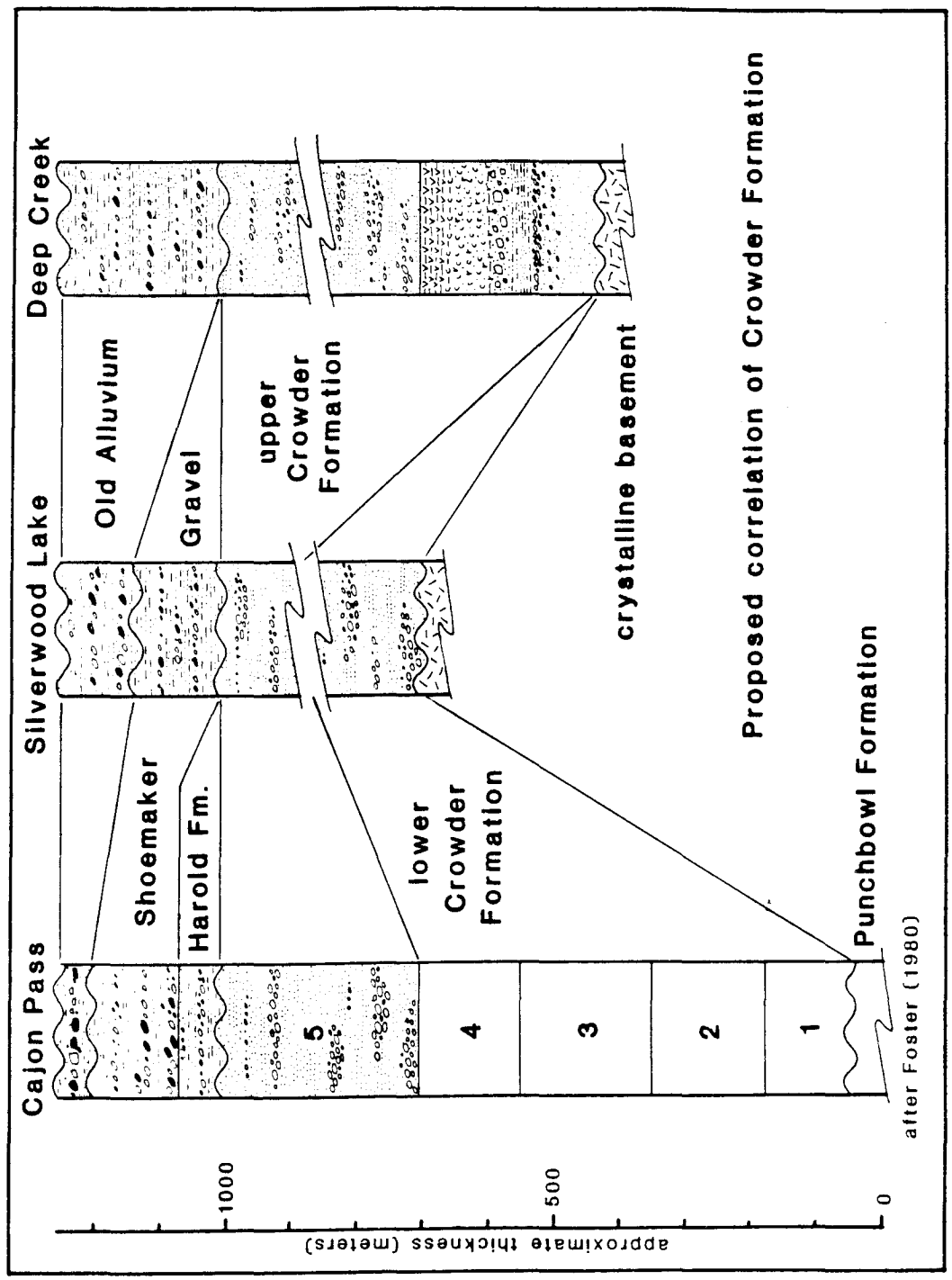
Cajon Pass
Silverwood Lake
Deep Creek
Shoemaker
Harold Fm.
Old Alluvium
Gravel
upper Crowder Formation
lower Crowder Formation
crystalline basement
Punchbowl Formation
5
4
3
2
1
1000
500
0
approximate thickness (meters)
Proposed correlation of Crowder Formation
after Foster (1980)

pathic arkose composed of poorly sorted coarse sand in fining-up sequences with conglomerate lenses and locally derived basal granodiorite boulders. Unit 2[24] is a finer grained quartzo-feldspathic arkosic wacke made up of poorly sorted sandy silt and clay with some thick sand beds. An apparent disconformity separates Units 2 and 3 (Foster, 1983, pers. comm.). Unit 3[25], like Unit 1, is a very coarse to granular arkosic sand with cobble- to boulder-conglomerate lenses and clay-capped fining-up sequences. Unit 4[26] resembles Unit 2, being an arkosic wacke composed of sandy mudstone, siltstone and conglomerate. Exposures of the lower Crowder Formation are largely confined to Crowder Canyon.

Paleocurrents in the lower Crowder Formation indicate southwestward flow, across the site of the San Andreas fault (Foster, 1980). Composition and rounding of clasts in these units indicate derivation from exposures of the Oro Grande Formation, Fairview Valley Formation and Sidewinder Volcanic Series near Victorville, with minimal contribution from the local basement (Woodburne and Golz, 1972; Foster, 1980).

Limited down-dip exposure and complex deformational history of the lower Crowder Formation make detailed reconstruction of the Crowder basin geometry difficult. Down-faulted patches of lithic arkose and conglomerate that occur throughout the western San Bernardino Mountains are correlated with the lower Crowder Formation in Cajon Valley on grounds of lithology and deformational style. They provide evidence that the Crowder Formation once overlay much of the mountains south and east of Cajon Pass. In the easternmost exposures of the Crowder Formation, basal beds usually overlie several meters of grus[27], rarely being deposited directly on bedrock[28]. This suggests that the Crowder Formation was deposited on a surface of low relief that occupied the present site of the western San Bernardino Mountains.

Fossil evidence indicates an age of middle to late Miocene for the lower Crowder Formation. R. E. Reynolds (1982, pers. comm.) of the San Bernardino County Museum has extracted a mammalian faunal assemblage[29] from Units 1 and 2 of the Crowder Formation near Squaw Peak which yields an age of late-Hemingfordian to Barstovian (middle to late Miocene; ~15 my; see Figure 2-7). Based on some of this material, C. A. Repenning (1982) favored an age of Barstovian to early Clarendonian (late Miocene to early Pliocene; ~10 my) for Units 1 and 2 of the lower Crowder Formation. Woodburne and Golz (1972) also cite fossil evidence for a middle to late Miocene age for the lower Crowder Formation, but dismiss this age as impossible on stratigraphic grounds. They argue that since the Crowder unconformably overlies late Miocene beds of the Punchbowl Formation, it must be post-late-Miocene in age. A paleomagnetic study, aimed at resolving the uncertainty in these age assignments, is now under way (J. L. Kirschvink, 1983, pers. comm.).

2.3.3.2 The Upper Crowder Formation

Unit 5 of Foster (1980), which constitutes the upper Crowder Formation, is divided into a western and an eastern facies. The western facies, which is composed of conglomeratic litharenite and arkosic wacke, grades into the eastern facies, consisting of poorly-sorted lithic arkose with interdigitated sand and gravel lenses, just west of Cajon Pass. The upper Crowder Formation is continuously exposed from Valyermo to Summit Valley.

The upper Crowder Formation differs from the lower Crowder Formation in both clast composition and paleocurrent direction. Its clast suite contains an abundance of gneiss, granodiorite and quartz diorite not found in the lower units, as well as clasts of Victorville provenance (Foster, 1980). Paleocurrents in the upper Crowder Formation indicate northeasterly flow

directions in the western facies and mixed directions in the eastern facies (Foster, 1980).

A reasonable case can be made for upper Crowder Formation being a time-transgressive unit. The Crowder Formation was originally considered part of the Harold Formation by Noble (1954b), since it grades conformably up into deposits of the Harold Formation along the inface bluffs near Valyermo (Woodburne and Golz, 1972). The Harold Formation and Shoemaker gravel are, by their very nature, time-transgressive units (Section 4.1.3). Since the western facies of the upper Crowder Formation resembles the Harold Formation with respect to areal distribution, paleocurrent direction and degree of deformation, it may also be time-transgressive. This hypothesis could easily be tested using magnetostratigraphic techniques.

In Cajon Valley, the upper Crowder Formation unconformably overlies the Punchbowl Formation and is unconformably overlain by the Harold Formation. The Cajon Valley beds of the Punchbowl Formation are assigned an age of Hemingfordian to Barstovian (middle to late Miocene; ~15 my) based on mammalian fossils (Woodburne and Golz, 1972). Fossil evidence suggests a middle to late Pleistocene age for the type Harold Formation (Noble, 1953; Repenning, 1982). Paleomagnetic studies show the Harold formation at Cajon Pass to be of reversed polarity (Section 4.4, Chapter IV), and therefore older than 730,000 y B.P. The history of the Victorville Fan complex (Section 2.4, Chapter II) supports an age of middle Pleistocene for the Harold Formation. The age of the upper Crowder Formation can only be firmly constrained between about 15 and 2.75 my. Foster (1980) argues for an age of about 2 to 4 my for the Crowder Formation, based on its greater structural and stratigraphic affinity with the Harold Formation than with the Punchbowl Formation.

2.3.3.3 The Volcanogenic Eastern Facies of the Crowder Formation

At the east end of Summit Valley, 150 meters of heretofore undescribed interbedded tuffs and volcanogenic siltstones[30], sandstones[31], and swelling claystones[32] interfinger[33] with the eastern facies of the upper Crowder Formation (Figure 2-8). The upper Crowder Formation cannot be traced beyond the east end of Summit Valley, probably due to burial by later deposits of the Victorville Fan complex. Although the thickness of volcanogenic material in Summit Valley suggests a nearby source, no obvious volcanic source exists.

Zircons, separated from several silicic tuff beds[34] within the volcanogenic section by Ray Weldon, have been dated by fission-track methods, yielding a radiometric age of 3.8 ± 0.4 my B.P. (C. F. Naeser, 1982, writ. comm.). This age is in close agreement with Foster's (1980) age estimate for the Crowder Formation of 2 to 4 my and is consistent with a proposed history of rapid late Pliocene uplift in the western San Bernardino Mountains (Weldon et al., 1981; Meisling and Weldon, 1982).

Coarse-grained beds in the volcanogenic sequence contain an abundance of quartz-monzonite and quartzite clasts[35], indicating local derivation from the San Bernardino Mountains to the south and east. No Crowder Formation has been found in the Pinnacles and Ord Mountains to the east and northeast, supporting the interpretation that these areas were topographic highs at the time of upper Crowder deposition. The fine-grained beds are thinly laminated and lacustrine in character, which suggests that drainage was locally dammed, in marked contrast to the broad unconfined fluvial plain of the type Crowder Formation to the east. The volcanogenic sediments are highly deformed and bedding is locally vertical[36]. Based on these observations, the volcanogenic eastern facies of the Crowder Formation is interpreted as a synorogenic

deposit, reflecting a change in drainage direction in response to incipient uplift of the western San Bernardino Mountains. The tuff date for the volcanogenic eastern facies of the upper Crowder Formation is consistent with Foster's age estimate of 2 to 4 my and with the proposed history of rapid late Pliocene uplift in the western San Bernardino Mountains (Weldon et al., 1981; Meisling and Weldon, 1982).

2.3.4 Miocene Gravel Veneers

Quartzite gravel veneers are reported sporadically throughout the San Bernardino Mountains (Sadler, 1983). Sadler presents evidence to show that extensive gravel veneers once capped much of the erosion surface on top of the San Bernardino Mountains. As a consequence, uplift of the San Bernardino Mountains must have produced a sudden pulse of second-cycle quartzite clasts in the deposits skirting the range (Sadler, 1983). This greatly complicates fault-offset determinations based on clast-source studies (Sadler, 1983). The veneers appear to be deformed with the Miocene erosion surface atop the San Bernardino Mountains, and are therefore roughly contemporaneous with the Crowder Formation. Sadler (1983) concludes that quartzite cobbles now found in the Crowder Formation may have been transported westward from Sugarloaf Mountain in the San Bernardino Mountains, rather than south from the area around Victorville as suggested by Foster (1980).

2.3.5 The Old Woman Sandstone

The late Pliocene Old Woman Sandstone of Shreve (1959, 1968) is exposed south and east of Lucerne Valley (Figure 2-6) and consists predominantly of conglomeratic arkose and mudstone. It contains a sudden change in clast composition and character near its top, reflecting incipient uplift of the central San Bernardino Mountains (Sadler, 1981, 1982). The Old Woman Sand-

stone can be divided into a central, western and eastern facies (Sadler, 1982; Richmond, 1960; Vaughan, 1922), distinguished on the basis of lithology. Vertebrate faunal assemblages from two localities within the Old Woman Sandstone indicate an age of 2.0 to 3.0 my (late Blancan) or late Pliocene (May and Repenning, 1982; see Figure 2-7).

The central facies of the Old Woman Sandstone consists of over 800 feet (~260 meters) of conglomeratic arkose containing clasts of basalt and other volcanics, but no marbles (Shreve, 1959; Sadler, 1982). It overlies a deeply weathered erosion surface developed on gneissic bedrock, and is overthrust by crystalline rocks in Blackhawk Canyon (Shreve, 1959). The central facies becomes finer upward, fines and thins northward, and contains north-dipping crossbedding (Shreve, 1959). These observations suggest an alluvial fan depositional environment (Shreve, 1959). Sadler (1981) assigns monolithologic marble breccias that overlie the fine-grained beds of the Old Woman Sandstone to the unit, rather than to the range-front fanglomerates (c.f. Shreve, 1959). He believes that this change in clast character and composition records the initiation of uplift along the range-front thrusts (Sadler, 1982). Fauna from the central facies suggest a late Blancan age of 2.0 to 3.2 my (May and Repenning, 1982). The strata from which these fossils were collected lie below the monolithologic breccias, and therefore predate the uplift of the San Bernardino Mountains.

In the western facies of the Old Woman Sandstone (Dibblee, 1966, 1967; Richmond, 1960), basal beds correlated with the central facies are succeeded by clays, silts, concretionary sandstones, and carbonates (Sadler, 1982). These deposits[36] resemble the small exposure of fine-grained, paleomagnetically reversed, sediments along the Bowen Ranch Road at Rock Springs Road[37], which appear to predate major relief in that area. May and

Repenning (1982) report a late Pliocene vertebrate fauna 2.5 to 3.0 my in age (late Blancan), suggesting that the western and central facies of the Old Woman Sandstone are roughly correlative.

South of Old Woman Springs, deposits originally described by Vaughan as "older desert deposits" have been included in the Old Woman Sandstone by Shreve (1959) and are called the eastern facies by Sadler (1981, 1982). The lower part of the eastern facies does not contain San Bernardino Mountains clast lithologies. The upper conglomeratic beds contain abundant rounded clasts of quartzite interpreted by Sadler (1982) as having been reworked from Miocene gravels that once overlay large areas of the San Bernardino Mountains, and whose stripping signals the inception of uplift. No fossils have been found in the eastern facies of the Old Woman Sandstone.

2.4 QUATERNARY SEDIMENTS

Quaternary sediments throughout the northwestern San Bernardino Mountains signal a fundamental change in drainage régime that occurred in early Pleistocene time. The Harold Formation, Shoemaker Gravel and Older Alluvium, informally known as the Victorville Fan complex, contain the first appearance of distinctive clasts of San Gabriel Mountains crystalline basement lithologies (Noble, 1954b) in the stratigraphy of the western San Bernardino Mountains (Figures 2-1 and 2-9; Plate 1A).

Clasts lithologies, areal distribution, and paleocurrent indicators all suggest that the Harold Formation and Shoemaker Gravel are time-transgressive units (Section 4.1.3, Chapter IV). Each represents a trail of sediment shed across the San Andreas fault opposite distinctive crystalline basement terranes within the San Gabriel Mountains as they moved northwest past the Cajon Valley deposition site along the San Andreas fault. The upper Crowder Formation bears a strong resemblance to the Harold Formation and Shoemaker

Figure 2-9. Generalized map of the western San Bernardino Mountains showing the distribution of early and middle Quaternary rocks (after Jennings, 1983). Only the deposits of the Victorville fan and associated units are shown in this diagram. Late Quaternary alluvial fans and terraces are discussed in Chapter III. AV = Apple Valley; LV = Lucerne Valley; SAFZ = San Andreas fault zone.

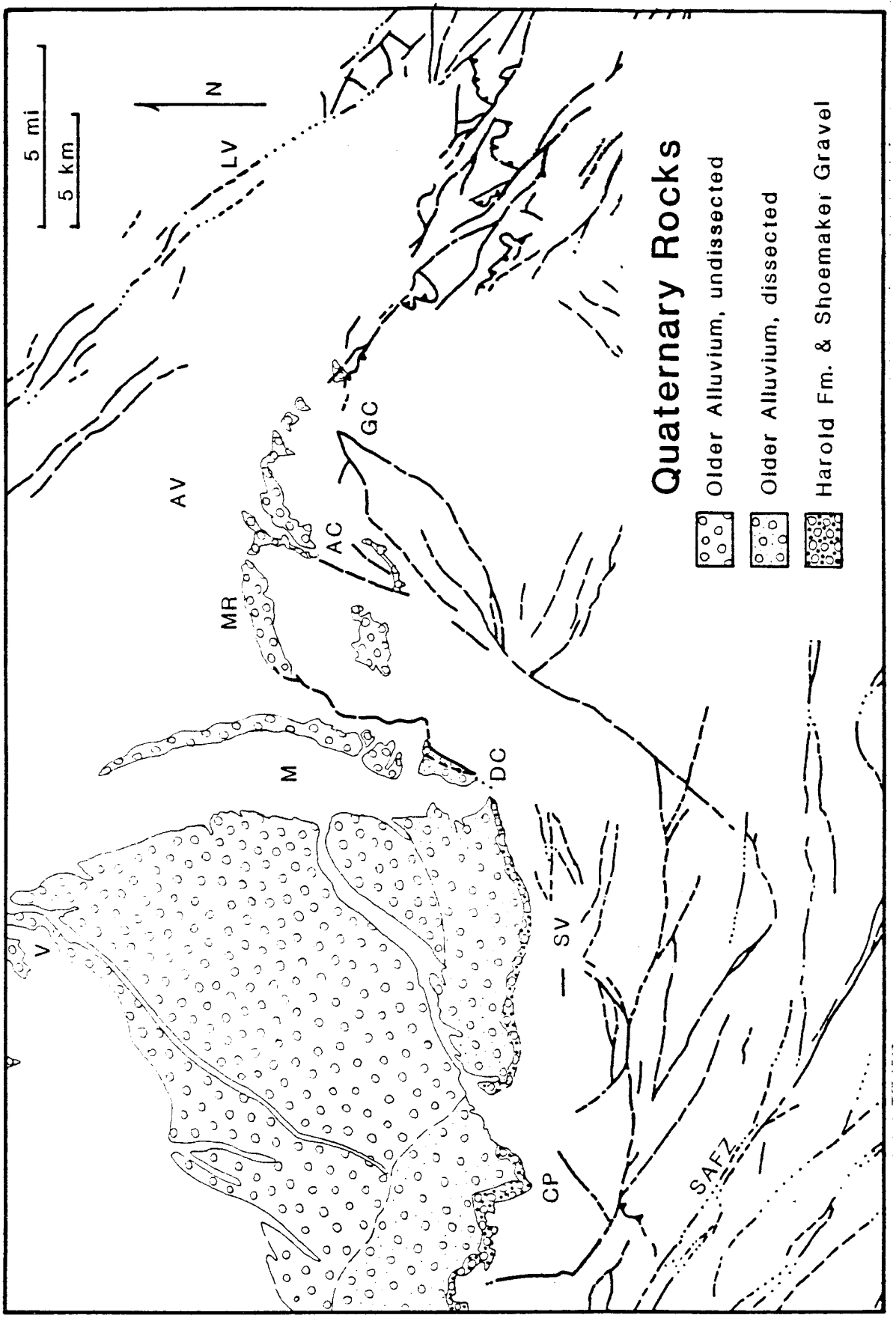
5 mi
5 km
N
LV
AV
MR
AC
GC
M
DC
V
SV
CP
SAFZ
A
Quaternary Rocks
Older Alluvium, undissected
Older Alluvium, dissected
Harold Fm. & Shoemaker Gravel

Gravel and may have been deposited in a similar fashion. Quaternary deposits along the northern front of the San Bernardino Mountains also manifest a dramatic change in character with the sudden appearance of poorly-sorted angular fanglomerates and the introduction of new clast lithologies.

2.4.1 The Harold Formation

Deposits referred to the Harold Formation by Noble (1954a) unconformably overlie the Crowder Formation in Cajon Pass (Figures 2-1 and 2-9; Plate 1A). The Harold Formation in Cajon Pass is laterally continuous with deposits on the northwest side of the San Andreas fault near Littlerock (Foster, 1980), considered by Noble (1953, 1954a) to be correlative with Harold Formation exposed across the San Andreas fault in the Devil's Punchbowl area. The Harold Formation in the Devil's Punchbowl is, in turn, referred to the type locality of the Harold Formation in the Pearland quadrangle, near Lancaster (Noble, 1954b, 1953).

The Harold Formation in Cajon Pass[38] consists of 76 meters of arkosic wacke to fine-grained arkose and lithic arkose pebbly sandstone (Foster, 1980) that unconformably overlie the eastern facies of the upper Crowder Formation. The Harold Formation grades upward into the Shoemaker Gravel[39]. Although the Harold Formation appears to pinch out just east of Cajon Pass, paleomagnetic studies (Section 4.3.3, Chapter IV) suggest that sediments derived from the western San Bernardino Mountains and exposed along the inface bluffs in Summit Valley may be lateral facies equivalents.

At Littlerock, the Harold Formation is about 200 feet in thickness, consisting of sandy siltstone and occasional arkosic sand beds with gravel lenses which increase in frequency near the conformable contact with the overlying Shoemaker Gravel (Noble, 1954a). The upper Crowder Formation is gradationally conformable with Harold Formation, the latter being

distinguished primarily on the basis of its greater conglomerate content and Pelona Schist clasts (Woodburne and Golz, 1972). Cobble imbrications in both the Crowder Formation and Shoemaker Gravel indicate northeastward flow (Noble, 1954b; Woodburne and Golz, 1972).

The Harold Formation contains the first appearance of Pelona schist clasts in the sediments of Mojave Desert (Noble, 1954b). The Pelona schist is a distinctive lithology characteristic of the San Gabriel Mountains igneous-metamorphic complex, and its appearance in the Harold Formation signals the arrival of the San Gabriel terrane as the dominant source of detritus in the Cajon Valley area. A reversal in drainage flow from southwestward to northeastward reflects the emergence of the San Gabriel Mountains as a prominent topographic high.

The type Harold Formation in the Pearland quadrangle was thought to be of Rancholabrean age (late Pleistocene; <450,000 y B.P.) based on fossil mammals (Noble, 1953). Recent work on microvertebrates indicates that the uppermost beds of the Harold Formation at Barrel Springs (U. C. Riverside Fossil Locality RV-7618; sec 18, R11W T5N), near Lancaster, are late Irvingtonian (middle to late Pleistocene; 0.7 to 1.2 my B.P.; see Figure 2-7) in age. A late Pleistocene age is inferred for the Harold Formation in the Devil's Punchbowl area based on stratigraphic extrapolations from the type area and local geologic history (Noble, 1954b). The Harold Formation in Cajon Valley and along the northeast side of the San Andreas fault is considered lithologically correlative with the Harold Formation in the Devil's Punchbowl area, and therefore late Pleistocene. Late Miocene fossils found in the basal Harold Formation in Cajon Pass by C. L. Gazin (Noble, 1932) are considered reworked (Noble, 1954b). No other fossils are known from the Harold Formation northeast of the San Andreas fault.

The upper 50 meters of the Harold Formation in Cajon Pass is paleomagnetically reversed (Section 4.3.1, Chapter IV), and therefore older than 730,000 y B.P. At least 88 meters of the overlying Shoemaker Gravels and an unknown thickness of Older Alluvium is also reversed (Section 4.3.2, Chapter IV), indicating that the Harold Formation is almost certainly mid-Pleistocene or older.

2.4.2 The Shoemaker Gravel

Deposits considered equivalent to the type Shoemaker Gravel in the Devil's Punchbowl by Noble (1954a) conformably overlie the Harold Formation in Cajon Pass[40] (Figures 2-1 and 2-9; Plate 1A). The beds are exposed along the inface bluffs from Cajon Pass to Valyermo, consisting of poorly sorted lithic arkose composed of conglomeratic sand and sandy conglomerate (Foster, 1980). The Shoemaker Gravel is distinguished from the underlying Harold Formation by a greater abundance of coarse conglomerate and the presence of clasts of Lowe Granodiorite (Noble, 1954b). The unit attains a maximum thickness of about 120 meters in Cajon Valley, thinning to the west and pinching out just east of Cajon Pass (Foster, 1980). As with the Harold Formation, the Shoemaker Gravel may undergo a facies change east of Cajon Pass and be equivalent in age to deposits exposed in Summit Valley that are paleomagnetically reversed.

The age of the Shoemaker Gravel, though not well known, is almost certainly middle to late Pleistocene. Dibblee reports late Pleistocene fossils in deposits near Victorville that are considered correlative with the Shoemaker Gravel (Dibblee, 1967). Paleomagnetic studies show the Shoemaker Gravel to be reversed in Cajon Pass, and therefore older than 730,000 y B.P. (Section 4.4, Chapter IV). The Brunhes/Matuyama polarity reversal occurs in the overlying Older Alluvium, which is separated from the Shoemaker Gravel

by a local angular unconformity and a deeply weathered soil horizon displaying normal paleomagnetic polarity (Section 4.3.2, Chapter IV). Thus the Shoemaker Gravel was probably deposited in the middle to late Pleistocene, prior to the Brunhes/Matuyama polarity reversal 730,000 y B.P. The areal distribution of the Shoemaker Gravel parallels the underlying Harold Formation, suggesting that the locus of deposition migrated northwest with time.

2.4.3 The Older Alluvium

The term Older Alluvium has been used by Noble (1953, 1954a) and others (Dibblee, 1967; Woodburne and Golz, 1972; Foster, 1980) to describe reddish, weathered alluvial deposits of probable late Pleistocene age. For the purposes of this study, the term Older Alluvium is restricted to the deposits that unconformably overlie the Shoemaker Gravel and underlie the abandoned geomorphic surfaces of the Victorville Fan (Figures 2-1 and 2-9; Plates 1A and 1B).

At least 10-15 meters of Older Alluvium unconformably overlies the Shoemaker Gravel in Cajon Pass[41] (Foster, 1980). It is composed of poorly sorted lithic arkose with cobble-conglomerates containing a distinctive suite of Pelona Schist clasts that are characteristic of the eastern San Gabriel Mountains (Foster, 1980). The unit is interpreted as a bajada, or alluvial apron, shed off the north flank of the San Gabriel Mountains (Noble, 1954b). It can be followed along the inface bluffs to the northwest at least as far as Valyermo. The Older Alluvium has been isolated from its source area by erosion in the Cajon Valley amphitheater and along the San Andreas fault.

The Older Alluvium that underlies the surface of the Victorville Fan can be divided into an older and a younger unit based on degree of dissection

(Figure 2-9; Dibblee, 1965, 1967; Jennings, 1983). Dissected Older Alluvium underlies the topographic head of the Victorville Fan in a broad strip trending parallel to the inface bluffs in Cajon Pass, and along its southern shoulder between Summit Valley and Oro Grande Wash. Undissected Older Alluvium forms a large fan-shaped body north of Oro Grande wash which underlies most of the town of Hesperia. Paleomagnetic work suggests that the dissected Older Alluvium is older than 730,000 y B.P., while the undissected Older Alluvium is younger (Section 4.4.1, Chapter IV).

2.4.4 The Ord River Gravels

Extensive exposures of fluvial sand and gravel that occur north of the Deep Creek Dam and east of the Mojave River are informally named the Ord River Gravel. On the basis of clast lithologies, the Ord River Gravel is divided into the Deep Creek and Summit Valley facies, correlative with the dissected and undissected parts of the Older Alluvium respectively (Figure 2-9; Plates 1A and 1B).

The Deep Creek facies of the Ord River Gravel only occurs south of Piedmont Road. It is best viewed in exposures along the Southern California Edison powerline road, where it interfingers with, and is overlain by, basal fanglomerates of the oldest alluvial fans on the west flank of the Ord Mountains[42]. The Deep Creek facies consists of poorly sorted conglomeratic arkose with rounded clasts of gneiss, quartz-monzonite and occasional volcanic porphyries, which is consistent with derivation from the Deep Creek drainage basin. Neither Pelona Schist nor Sidewinder volcanics were found among the clast suite. Reversed paleomagnetic polarity (Section 4.4.3, Chapter IV) indicates an age of middle to late Pleistocene. The Deep Creek facies beds are elevated above the Summit Valley facies deposits.

The Summit Valley facies of the Ord River Gravel[43] is a conglomeratic

arkose, containing well-rounded clasts of Sidewinder Volcanic Series, Fairview Valley Formation and fine-grained granitoids of Victorville affinity in addition to quartz-monzonites, quartzites and calc-silicates of local derivation. It does not contain clasts of Pelona Schist. The clasts suite is interpreted as the product of stripping of the Crowder Formation from the western San Bernardino Mountains during uplift. The Summit Valley facies of the Ord River Gravel underlies a well-graded geomorphic surface throughout the Apple Valley Highlands and Mariannas Rancho areas in an obvious continuation of the undissected Older Alluvium west of the Mojave River in Hesperia.

The Ord River Gravel is interpreted as having been deposited by a major drainage system peripheral to the Victorville Fan that was fed by streams flowing north out of the western San Bernardino Mountains and west out of the Ord Mountains and Deep Creek drainage basins. Deposition of the Deep Creek facies occurred prior to the existence of Summit Valley, and was probably contemporaneous with deposition of the Shoemaker Gravel and/or dissected Older Alluvium of the Victorville Fan complex. The integration of drainage in the western San Bernardino Mountains created an ancestral Summit Valley, causing Deep Creek to incise and abandon its old course. Deposition of the Summit Valley facies of the Ord River Gravel followed the uplift of the western San Bernardino Mountains and resultant stripping of the Crowder Formation from the late Tertiary erosion surface. The lack of Pelona Schist clasts requires that deposition occurred prior to the appearance of Pelona-bearing units in Summit Valley.

A prominent linear ridge in the Marianas Rancho of Apple Valley[44], hereafter referred to as "Ocotillo Ridge", is underlain by river sands and gravel very similar in character to the Ord River Gravel. The Ocotillo Ridge deposits (Figure 2-9), however, contain distinctive clasts of syenite,

basalt and volcanic agglomerates[45] not found to the southwest. The Ocotillo Ridge deposits appear to be continuous with the Ord River Gravel, perhaps representing a west-flowing tributary drainage fed by streams along the north flank of the San Bernardino Mountains to the east. As the Ocotillo Ridge deposits are followed eastward, the clasts become dominated by quartz-monzonitic lithologies, indicating that the Arrastre Canyon fan was active during the deposition of this unit. The age, history and geometry of these fluvial sand and gravel units are critical, since their deposition precedes the last phase of deformation along the flanks of the Ord Mountains.

Fluvial sand and gravel exposed along a prominant east-west trending linear ridge just south of the AT&SF tracks at Milpas Road[46], hereafter referred to as "Milpas Ridge" (Figure 2-9), can be traced almost continuously from the Ocotillo Ridge deposits in the Marianas Rancho to the west. These well-sorted arkosic sands contain occasional well-rounded cobbles of quartz-monzonite, leucocratic porphyry, calc-silicate and quartzite[47] derived from the Arrastre Canyon drainage basin. They contrast sharply with overlying debris-flow and alluvial fan deposits[48] containing angular clasts and large boulders derived from the immediate range-front area, indicating proximity to source. The Milpas Ridge deposits constitute the bulk of the material exposed in the walls of Arrastre Canyon, and thus probably underlie most of the Milpas and Marianas Rancho area at a shallow depth. The Milpas and Ocotillo Ridge deposits, along with possibly correlative gravels at Juniper Flats, define a mid-Pleistocene(?) drainage system that was tributary to the ancestral Mojave River and fed by the Arrastre Canyon basin.

Deposits similar in structural and stratigraphic context are found just southwest of Sky High Ranch[49] and south of the AT&SF tracks at Grapevine Canyon wash[50]. These eastern exposures appear to have been derived from

an ancestral Grapevine Canyon which drains part of the upland erosion surface east of the Arrastre Canyon basin. These sediments are tentatively correlated with the Milpas Ridge deposits based on their maturity and deformational style.

2.4.5 Late Quaternary Alluvial Fans and Terraces

Late Pleistocene and Holocene alluvial fans and terrace deposits that underlie relatively continuous geomorphic surfaces were grouped into map units on the basis of geomorphic, rather than stratigraphic, criteria. Widely varying sediment composition and discontinuous nature of these alluvial deposits make lithologic correlation difficult. Graded surfaces, however, commonly persist well beyond the limits of alluvial deposition, providing a basis for correlation of alluvial units over large areas. Since geomorphic surfaces play a key role in the definition of late Quaternary alluvial units, these units are discussed in the Chapter III, "Geomorphology and Alluvial Stratigraphy".

2.5 SUMMARY AND CONCLUSIONS

Pre-batholithic metasedimentary rocks of Cordilleran miogeoclinal affinity are exposed in three highly deformed roof pendants in the Ord Mountains, White Mountain and Furnace Canyon areas. Stromatolites found in the hornfels-grade carbonate sequence of the Ord Mountains pendant are provisionally assigned to the late pre-Cambrian genus conophyta, supporting proposed stratigraphic correlation of these rocks with the late Precambrian section in Death Valley, California. The Ord Mountains carbonate section is in tectonic contact with a higher grade quartzo-feldspathic sequence of unknown age and affinity. The metasedimentary sequence at White Mountain is lithologically correlated with the Carboniferous section of the Furnace

Canyon pendant, tentatively correlated with rocks of similar age in the Inyo Mountains. Carbonates that occur as isolated inclusions in the western San Bernardino Mountains are of probable Cordilleran miogeoclinal affinity.

Pre-batholithic intrusives are preserved in close association with metasedimentary pendants. A large hornblende quartz-monzonite east of Grapevine Canyon is Triassic in age. Widespread mafic rocks, including gabbro, hornblende diorite and hornblendite, may be early intrusive phases of the Cretaceous batholith. Sheets of distinctive quartz-syenite in the Ord Mountains pendant postdate miogeoclinal rocks and predate batholithic intrusion. Isolated exposures of unusual crystalline rocks in the westernmost San Bernardino Mountains are of unknown origin.

Marine sediments of early Tertiary age, exposed in the study region only in the Cajon Pass area, are lithologically correlated with the San Francisquito and Vaqueros Formations. A Plesiosaur, found in the San Francisquito(?) Formation in Cajon Pass, indicates a Cretaceous or early Eocene age. The Vaqueros(?) Formation in Cajon Valley is thought to be early Miocene in age.

The Miocene continental deposits of the Punchbowl and Crowder Formations, exposed in Cajon Pass and the western San Bernardino Mountains, were deposited by southwest-flowing streams that carried clasts of quartzite and volcanics from the Victorville area. They lack any significant contribution of clasts from the western San Bernardino Mountains. The Punchbowl and Crowder Formations present an interesting stratigraphic problem. The middle to late Miocene Punchbowl Formation appears to be unconformably overlain by the upper beds of the middle to late Miocene Crowder Formation. A volcanogenic eastern facies of the upper Crowder Formation has been dated at 3.8 ±0.4 my, suggesting that the upper Crowder Formation may be Pliocene and

may unconformably overlie the lower Crowder Formation as well as the Punchbowl Formation. While this inference is strongly supported by similarities between the upper Crowder Formation and the overlying Pleistocene Harold Formation, it has yet to be demonstrated in Cajon Pass. Magnetostratigraphic methods are ideally suited to delineating such a relationship, and efforts are currently under way to do so.

Middle to late Pleistocene deposits in Cajon Pass referred to the Harold Formation and Shoemaker Gravel differ dramatically from underlying Crowder and Punchbowl Formations in both provenance and depositional environment. These units contain the first clasts of San Gabriel Mountains crystalline basement terrane to appear in the study region, and display northeasterly paleocurrent indicators. The Harold Formation and Shoemaker Gravel contain the first clasts of San Gabriel Mountains crystalline basement terrane to appear in the Cajon Pass region, signaling the emergence of the San Gabriel terrane as the dominant sediment source. Furthermore, paleocurrents in the Pleistocene units reflect a reversal of drainage direction from southwesterly flow in the late Miocene to northeasterly flow in the mid-Pleistocene. The Harold Formation and Shoemaker Gravel are interpreted as time-transgressive units, representing a trail of sediment shed across the San Andreas fault opposite distinctive crystalline basement terranes within the San Gabriel Mountains as they moved northwest past the Cajon Valley deposition site along the fault zone. Sediments in Summit Valley derived from the western San Bernardino Mountains are thought to be possible facies equivalents of the Harold Formation and Shoemaker Gravel.

A veneer of Older Alluvium capping the Shoemaker Gravel in Cajon Pass records the Brunhes/Matuyama polarity reversal of 730,000 y B.P. This Older Alluvium can be divided into dissected and undissected facies which

appear to predate and postdate the polarity transition respectively. This crude chronology can be extended to sediments on the flanks of the Ord Mountains that define a late Pleistocene drainage system tributary to the ancestral Mojave River. The Pleistocene units contain evidence of progressive growth and integration of drainage in the western San Bernardino Mountains in reponse to uplift during Pleistocene time.

The late Tertiary stratigraphy in the Cajon Pass area is the product of major lateral displacement on the San Andreas fault and reflects constantly changing source terranes and depositional conditions. Sediments along the northwestern front of the San Bernardino Mountains record the uplift of the San Bernardino Mountains with the sudden appearance of clasts of locally derived basement lithologies. The uplift of the San Bernardino Mountains along the northern range front roughly coincides with the arrival of the San Gabriel Mountains in the Cajon Pass region.

CHAPTER III

GEOMORPHOLOGY

3.1 INTRODUCTION

3.1.1 Purpose

A major goal of this study was to investigate the nature and modes of deformation along the northern range front of the San Bernardino Mountains, and geomorphic surfaces were very useful as an index to structural deformation. In many parts of the study area lacking sedimentary cover, an understanding of landforms was critical in evaluating fault offsets, warping and tilting.

Another important objective of this study was to develop a history of uplift for the San Bernardino Mountains along the northern range front. The only stratigraphy available in many parts of the area consists of Pleistocene alluvial fan and terrace units. These units, by their very nature, are recognized and correlated mainly on the basis of their geomorphic form rather than their lithology or geometry. Thus, an understanding of the nature and history of alluvial geomorphic surfaces was necessary before their form and distribution could be applied to the study of deformation.

3.1.2 Scope

This chapter is divided into four sections: Weathered Miocene(?) Erosion Surface; Late Quaternary Terraces; Late Quaternary Alluvial Fans; Drainage Evolution. Superscripted numbers refer to Appendix B and Plates 1A and 1B.

A deeply weathered erosion surface is widely developed on the crystalline basement of the San Bernardino Mountains. The evidence suggests that this relict and buried surface was developed during the late Miocene, at a time when conditions were more humid than today. The present site of the San Bernardino Mountains was then occupied by a gently rolling lowland

mantled by residual and colluvial soils and dissected by streams. The ancient surface has since been uplifted and, in many areas, stripped of soil cover. Surprisingly, it has survived largely intact throughout most of the study area. Where present, the sub-horizontal weathering horizon is useful in defining the nature and amount of deformation within the crystalline rocks. The late Miocene surface was an indispensable aid in reconstructing the neotectonic history of the study area.

Terrace surfaces and associated terrace gravels in Cajon Pass and along the Mojave River reveal a complex history of drainage evolution. Although variable lithology and poor exposures hamper correlation, certain distinctive clast lithologies within the terrace deposits can be used to document several important events in the drainage evolution of the area.

Headward expansion of the West Fork of the Mojave River into the western San Bernardino Mountains occurred during the middle to late Pleistocene, as revealed by the surfaces and distinctive alluvial clasts of the terrace deposits. The Mojave River briefly captured part of the San Andreas fault zone in Cajon Pass, prior to the Cajon Pass drainage area being taken over by Cajon Creek. The Mojave River now receives virtually all of its runoff from its headwaters in the western and central San Bernardino Mountains.

East of the Mojave River, the physiography of the northern range front is characterized by small drainage basins and alluvial fans. These fans coalesce to form a broad bajada, which drains to Rabbit and Lucerne dry lakes. Drainage on the northern range front is not integrated. The alluvial fans on the range front are the direct result of uplift and deformation along the range-front fault system. In this chapter, alluvial fans are discussed in general geomorphic terms. Their geomorphic relationship to structural features is discussed in detail in Chapter V, "Structure", along

with the faults responsible for uplift.

3.2 MIOCENE WEATHERING SURFACE

A deeply weathered erosion surface is developed on the crystalline bedrock throughout the northwestern San Bernardino Mountains (Figure 3-1; Plates 1A and 1B). This surface is essentially continuous with the extensive late-Tertiary erosion surface developed atop the central and eastern San Bernardino Mountains. It provides a much needed time-stratigraphic reference horizon for delineating structural deformation in the basement rocks in the absence of late Cenozoic sedimentary cover.

3.2.1 Previous Work

Mendenhall (1905) identified the subdued upland plateau of the San Bernardino Mountains as an old relict surface, noting that it contrasts sharply with the steep youthful margins of the range. Vaughan (1922) described the physiography of the old geomorphic surface in considerable detail, proposing three ancient cycles of erosion and weathering to explain differences in the character of the surface across the range. Oberlander (1972) accounted for such differences with one ancient cycle of deep weathering under humid conditions, which gave rise to a single weathering profile that includes all of the surface characteristics observed by Vaughan (1922).

Noble (1932, 1954b) recognized the potential usefulness of the relict surface as an index to structural deformation in the western San Bernardino Mountains. The erosion surface in this part of the range is warped into a broad asymmetric northwest-trending arch (Noble, 1932), the flanks of which are sliced into a series of fault-bounded blocks (Figure 3-1; Dibblee, 1975). The surface has been removed where range front faulting and uplift have accelerated erosion; in the absence of faulting, the ancient surface ramps

Figure 3-1. Geomorphology of the San Bernardino Mountains and its relation to major faulting (figure from Dibblee, 1975). Random hatchures show the distribution of the late Miocene weathered erosion surface described by Oberlander (1972). It is present throughout most of the study area, as well as in the neighboring ranges to the north and south. It is faulted by the north frontal fault system, the Cleghorn fault, and numerous other faults in the northwestern San Bernardino Mountains. The erosion surface provides a datum which records post late Miocene deformation within the crystalline terrane. Dibblee's "new erosion surface of high relief" refers to areas where erosion has been rejuvenated in response to faulting, resulting in fresh bedrock, steep V-shaped canyons, and small drainage basins.

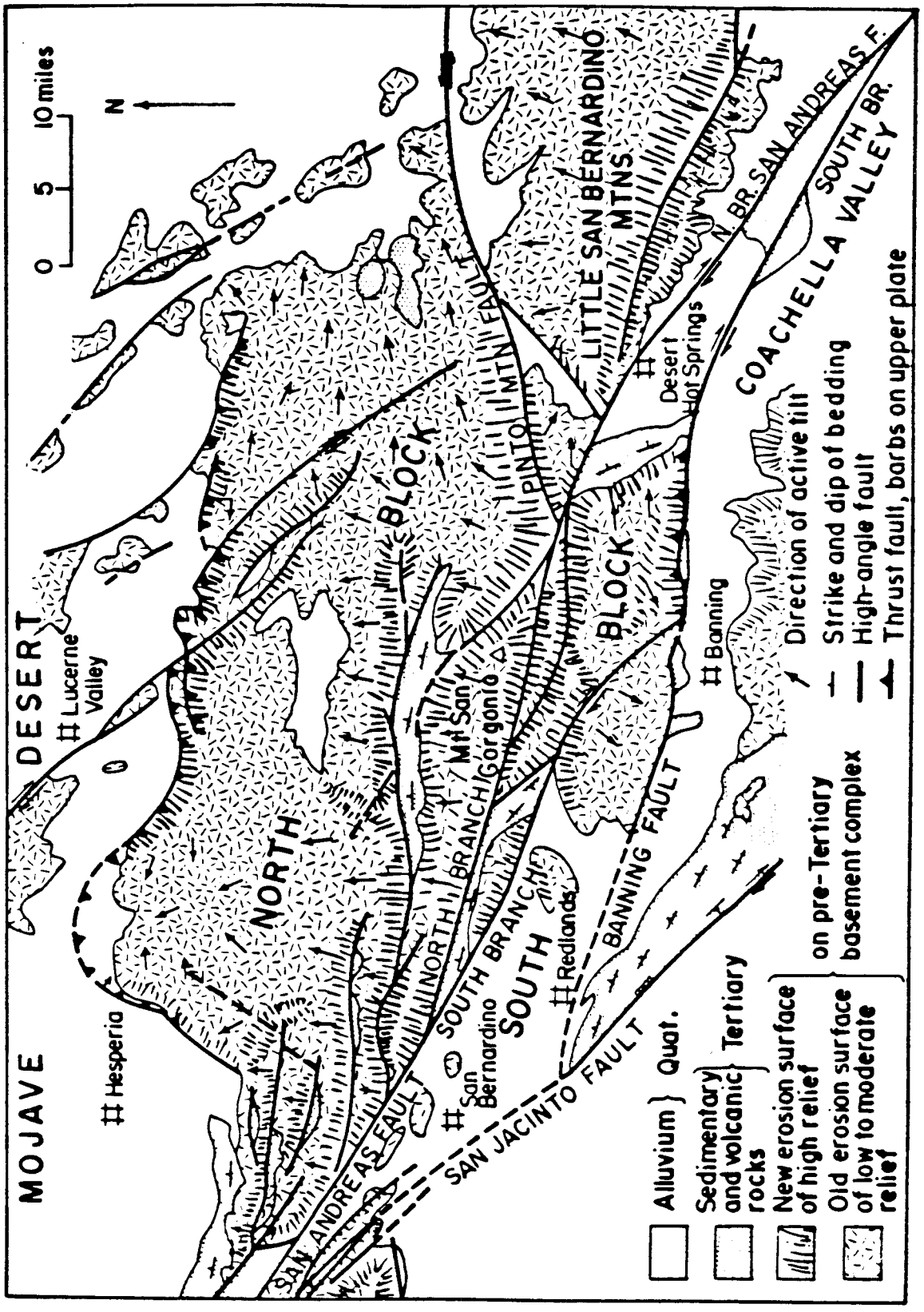
MOJAVE DESERT
NORTH BLOCK
SOUTH BLOCK
Hesperia
Lucerne Valley
San Bernardino
Redlands
Mt San Gorgonio
Banning
Desert Hot Springs
PINTO MTN FAULT
LITTLE SAN BERNARDINO MTNS
COACHELLA VALLEY
SOUTH BR.
N. BR. SAN ANDREAS F.
SAN ANDREAS FAULT
NORTH BRANCH
SOUTH BRANCH
BANNING FAULT
SAN JACINTO FAULT
0 5 10 miles
N
Alluvium } Quat.
Sedimentary and volcanic rocks } Tertiary
New erosion surface of high relief
Old erosion surface of low to moderate relief
on pre-Tertiary basement complex
Direction of active tilt
Strike and dip of bedding
High-angle fault
Thrust fault, barbs on upper plate

down to the desert floor (Dibblee, 1975). Its either case, its widespread preservation is a testament to the recency of faulting and uplift in the San Bernardino Mountains.

3.2.2 Character and Origin

The relict weathering surface is developed on crystalline basement throughout the northwestern San Bernardino Mountains. It is especially well expressed east of Silverwood Lake[51], where fresh bedrock is commonly overlain by a 10-30 m thick zone of well-rounded residual boulders in a matrix of grus and partly disintegrated bedrock. Locally, this weathered zone grades into several tens of meters of reworked grus containing occasional angular fragments of locally-derived bedrock[52]. The grus and weathered bedrock have been stripped from the erosion surface over much of the western San Bernardino Mountains, leaving characteristic piles of residual boulders on an irregular surface of partly decomposed bedrock.

These piles of residual boulders represent corestones (Figure 3-2) isolated by deep chemical weathering that attacked the bedrock along its joint system (Blackwelder, 1925; Davis, 1938; Oberlander, 1972). Such boulder mantles are commonly found throughout the Mojave Desert, indicating that the conditions for their formation were once widespread (Oberlander, 1972). Davis (1938) considered the production of residual boulders to be an ongoing process, with a new crop of boulders always developing in the subsurface to replace the extant ones as they disintegrate. Oberlander (1972) argued that the boulder-mantled slopes of the Mojave Desert represent a transitional landform developed during the removal of the products of a major episode of deep weathering that occurred during the late Miocene.

On the eastern flank of the Ord Mountains, resistant knobs of biotite-quartz-monzonite protrude above subdued exposures of metasedimentary car-

Figure 3-2. Development of granitic boulders by subsoil weathering. (figure from Davis, 1938). Residual boulders are the corestones that are left when chemical break-down of granitic rock into grus progresses along joint fractures. Such a process has been observed to be taking place in the subsurface in humid regions today (Oberlander, 1972), and is inferred to have taken place under similar conditions in the Mojave Desert during the middle to late Miocene. Deep weathering is not occurring in the Mojave Desert today, and no residual boulders are being produced in the subsoil to replace the boulders that are widely observed on granitic surfaces (Oberlander, 1972). Oberlander concludes that the boulder-covered granitic landforms in the Mojave Desert (and the San Bernardino Mountains) are a transitional stage of the surface; when the boulders are removed by erosion the surface will have a smooth appearance.

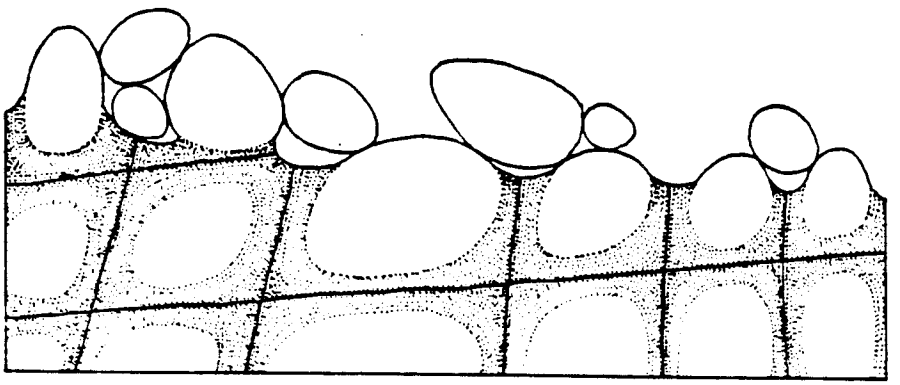

bonates (R. L. Coffman, 1980). This appears consistent with formation of the weathering surface at a time when wetter climatic conditions prevailed (Oberlander, 1972), favoring solution weathering of marble over mechanical disintegration of plutonic rocks. The present-day semi-arid climate favors mechanical breakdown of quartz-monzonite and preservation of carbonates.

The Crowder Formation once widely overlay the bedrock weathering surface throughout the western San Bernardino Mountains (Weldon et al., 1981), as evidenced by numerous remnants[53], usually protected from erosion by faulting. Southeast of Silverwood Lake, the Crowder Formation is usually deposited on grus overlying bedrock, suggesting that there was little relief on the weathering surface at the time of Crowder deposition (Meisling and Weldon, 1982). There appears to have been some relief near Cajon Pass resulting in the deposition of the basal Crowder Formation directly on granodiorite basement in the absence of a basal layer of grus (Foster, 1980). Locally, the basal Crowder Formation cut channels into the weathering surface, exposing fresh bedrock and locally-derived basal conglomerate[28].

The abundant evidence of subdued positive relief, deep weathering and limited erosion suggests that the San Bernardino Mountains crystalline terrane may have had the form of a "desert dome", as described by Davis (1938), prior to the onset of uplift in the Pliocene.

3.2.3 Stratigraphic Significance

The weathering surface provides a valuable datum for delineating post-late-Miocene structural deformation in the crystalline basement of the northwestern San Bernardino Mountains (Figure 3-1; Dibblee, 1975; Noble, 1932, 1954b). Although the stripped weathering surface is irregular in detail, its gross aspect is surprisingly continuous and flat where not affected by range-front deformation. Vertical offset of the surface by late-Tertiary

faulting commonly exposes fresh bedrock on the upthrown side, creating a resistant fault scarp. Even minor displacements which might be difficult to see on the ground are clearly expressed as lineaments on aerial photographs. In the vicinity of Silverwood Lake, the surface is tilted northward and warped into asymmetric folds (Meisling and Weldon, 1982). Once its significance is appreciated, the weathering horizon permits the three-dimensional geometry of tilting, warping, folding and faulting to be examined in detail (Section 5.10).

3.2.4 Distribution

The weathering surface can be traced almost continuously from Cajon Pass to White Mountain across the northwestern San Bernardino Mountains (Figure 3-1). In Cajon Pass a prominent erosion surface reportedly lies between the middle to late Miocene Cajon Formation from the middle Miocene to Pliocene(?) Crowder Formation (Woodburne and Golz, 1972; Foster, 1980). This surface may be correlative with the weathering surface underlying the Crowder Formation in Cajon Pass and throughout the western San Bernardino Mountains (Meisling and Weldon, 1982).

A deeply weathered surface in the Pinnacles[54] and Ord Mountains[55] appears to be a straightforward continuation of the surface capping the western San Bernardino Mountains. It is best expressed where underlain by biotite-quartz-monzonite, exhibiting the characteristic rounded residual boulders in a matrix of grus and disintegrating bedrock. Here, as in the Silverwood Lake area, the grus and weathered bedrock have been largely stripped from the surface.

The surface in the Ord Mountains appears to continue eastward across Juniper Flats and the broad Arrastre Canyon basin, underlain by the porphyritic biotite-quartz-monzonite of the Rattlesnake Mountain Pluton.

Concordant ridge-crests are in places capped with mature Miocene(?) gravels[56] that antedate mountain uplift, suggesting continuity of the surface. The Arrastre Canyon basin seems to be structurally controlled by dip-slip motion on several northeast-trending faults that form a broad graben in the surface (Section 5.7).

East of Grapevine Canyon the weathering surface described by Oberlander (1972) is well expressed on the more resistant hornblende-quartz-monzonite and metasediments of White Mountain. The surface at White Mountain is part of the extensive relict surface, described by Vaughan (1922) and Sadler and Reeder (1983), that can be traced across the central and eastern San Bernardino Mountains. The Old Woman Sandstone is reportedly deposited on this deeply weathered erosion surface near Old Woman Springs (Shreve, 1968).

3.2.5 Age and Continuity

Many lines of evidence suggest that the weathered erosional surface is late Miocene in age. Oberlander (1972) proposes a late Tertiary age for the relict surface, since it is overlain by basalts radiometrically dated at 8.2 ± 0.5 my in the eastern San Bernardino Mountains and 8.9 ± 0.9 my old lavas in the Fry Mountains. Sadler and Reeder (1983) document the widespread occurrence of patches of rounded-quartzite gravels on the ancient erosion surface which are locally interbedded with late Miocene basalts near Pipes Wash at the east end of the San Bernardino Mountains. In Cajon Pass, the erosion surface is overlain by the middle to late Miocene basal beds of the Crowder Formation (Foster, 1980; Reynolds, 1982, pers. comm.). Most of the structure that postdates the erosion surface in the western San Bernardino Mountains is demonstrably Pliocene or older (Meisling and Weldon, 1982).

The consistency of character of the weathering surface in the northwestern San Bernardino Mountains suggests that it remains largely intact

between Silverwood Lake and White Mountain. The tectonic stability and length of time required to produce the deep weathering profile described by Oberlander (1972) argues against the elements of the surface being of widely different age. The late Miocene gravel veneers offer evidence that most of the deeply weathered upland surfaces in the San Bernardino Mountains are indeed roughly contemporaneous (Sadler and Reeder, 1983). The possibility that the observed surface is a composite of several weathering horizons of different ages (Vaughan, 1922) seems highly unlikely, but cannot be ruled out.

3.2.6 Summary

All of the above evidence suggests that the weathered erosion surface was developed over a widespread area in response humid conditions during middle to late Miocene time. At that time the present site of the San Bernardino Mountains was occupied by an upland surface of subdued relief. This surface was relatively flat, and serves as a useful datum that helps delineate the geometry and magnitude of deformation in the crystalline rocks in the absence of any other suitable datum.

3.3 LATE QUATERNARY TERRACES

Late-Pleistocene and Holocene terrace surfaces are present along the Mojave River and in Cajon Pass (Figure 3-3). They can be either erosional or depositional in origin. Such surfaces are preserved when they become isolated from ongoing erosion and alluviation by incision. The age of a surface is defined as the time since it was abandoned as a site of erosion, transportion or deposition.

Erosional surfaces can be underlain by either terrace gravels or bedrock pediments. The terrace gravels are of highly variable lithology,

Figure 3-3. Generalized map of the western San Bernardino Mountains showing the distribution of late Quaternary fans and terraces and the location of the Mojave River (after Jennings, 1983). AV = Apple Valley; LV = Lucerne Valley; SAFZ = San Andreas fault zone; V = Victorville.

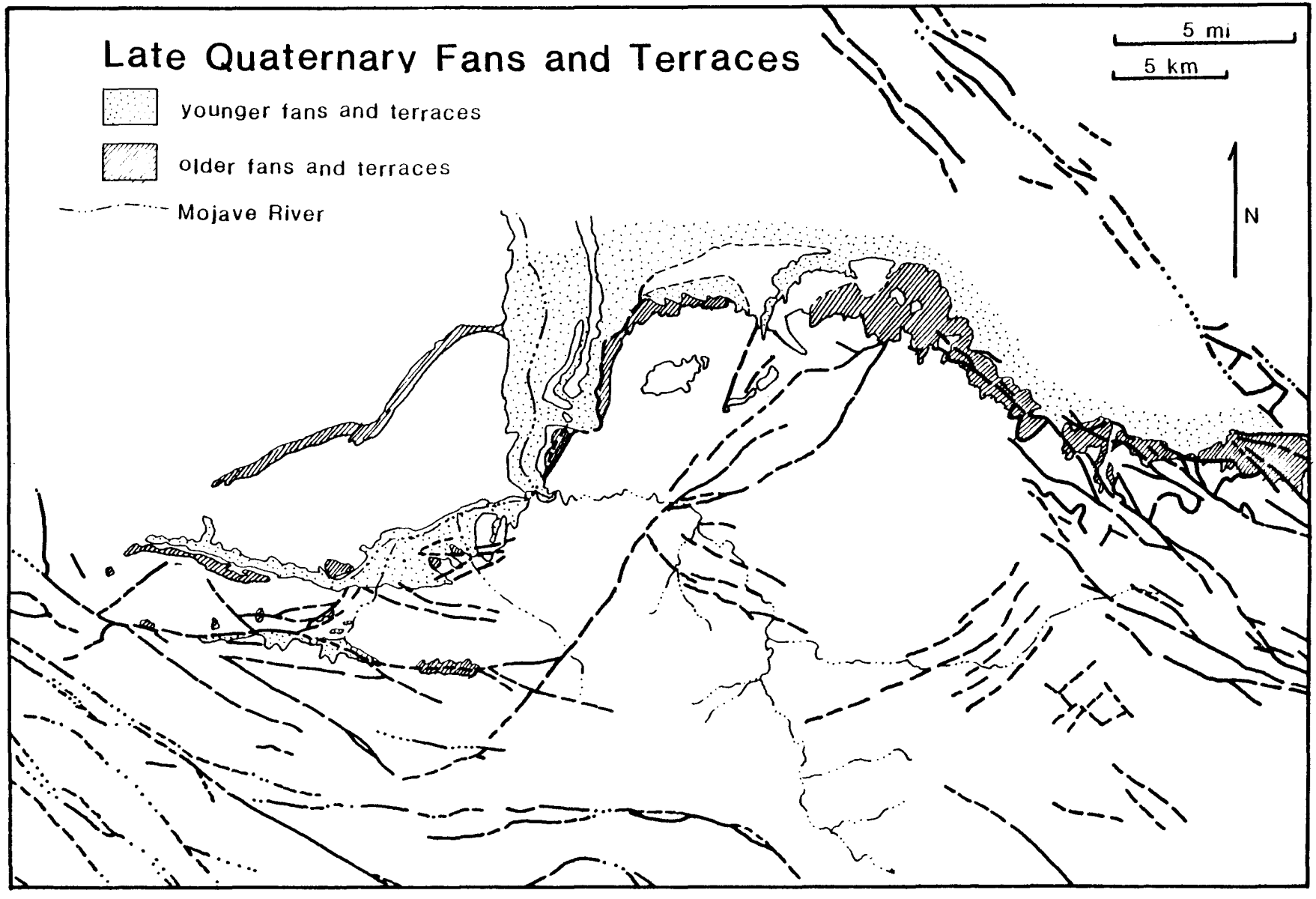
Late Quaternary Fans and Terraces
younger fans and terraces
older fans and terraces
Mojave River
5 mi
5 km
N

reflecting differences in the source drainages of the alluvial material. Certain distinctive clast lithologies found in these deposits have important implications for both tectonic and drainage reconstruction.

The limited preservation and poor exposure of alluvial deposits in many areas, however, make it necessary to erect an alluvial chronology based on geomorphic surfaces rather than lithology or internal geometry of alluvial units. In some critical localities erosional surfaces underlain by bedrock are useful in establishing continuity of the graded surfaces.

3.3.1 Cajon Pass

The drainage in Cajon Pass has experienced more than 500 meters of incision since the oldest mapped terrace was abandoned (Meisling and Weldon, 1982). High incision rates permit the resolution of five major terrace levels that postdate the incision of the Victorville Fan (Figure 3-4; Weldon et al., 1981; Weldon and Meisling, 1982a; Weldon and Sieh, in preparation). The ideas in Sections 3.3.1, 3.3.2, and 3.3.3 are largely due to R. Weldon.

The oldest and highest graded surface in Cajon Pass (Qte) was formed by a drainage system that included part of the San Andreas fault zone and the north-sloping face of the San Gabriel Mountains, passing through Summit Valley to join the ancestral Mojave River. Remnants of this surface, locally underlain by weathered terrace gravels containing clasts of Pelona Schist, are preserved in Cleghorn Canyon and along the San Andreas fault zone southeast of Cajon Pass (Plate 1A).

The age of the Qte surface can be roughly constrained by offset and slip-rate on the San Andreas fault. About 10 km of right-lateral motion on the San Andreas fault must be restored before the San Gabriel Mountains are in a position to topographically confine, and shed material into, the Qte drainage system. Weldon and Sieh (in preparation) made a best estimate of

Figure 3-4. Correlation of terrace levels in the Cajon Pass and Mojave River drainages (from Meisling and Weldon, 1982). Five graded terrace levels can be recognized in Cajon Pass, due to high incision rates and climatic conditions conducive to terrace formation. Only two graded terrace levels can be recognized in the Mojave River drainage, due to lower incision rates and conditions less conducive to terrace formation. Age estimates are approximate, and correlation is based on relative height, preservation, and degree of weathering. Qt2 is essentially continuous with Qte; Qtl is thought to be equivalent to Qtd and Qtc. These age estimates have been somewhat refined: Qte and Qt2 are now thought to be ~400,000 y old; Qtd and Qtl are thought to be ~ 53,000 to ~57,000 y old, based on approximate offset of geomorphic surfaces and best estimate of slip rate on the San Andreas fault.

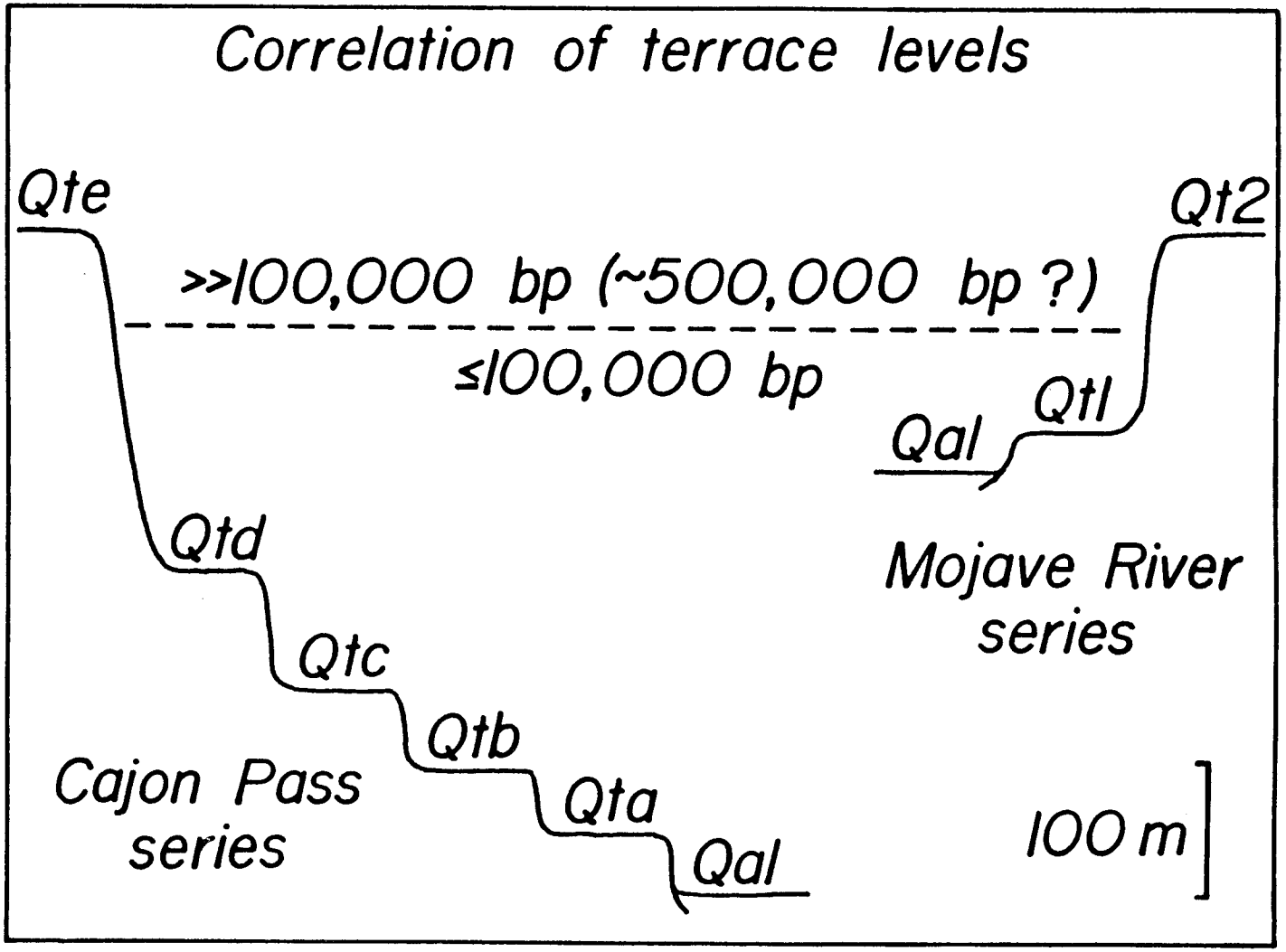
Correlation of terrace levels
Qte
Qt2
>>100,000 bp (~500,000 bp ?)
≤100,000 bp
Qtl
Qal
Qtd
Mojave River series
Qtc
Qtb
Cajon Pass series
Qta
Qal
100 m

the Holocene slip rate for the San Andreas fault in Cajon Pass of 24.5 mm/yr (c.f. 20 to 25 mm/yr: Weldon and Sieh, 1980). Assuming a uniform slip rate on the San Andreas fault of 24.5 mm/yr for the late Pleistocene and ~10 km of offset for Qte, the surface must be ~400,000 years old (c.f. ~500,000 y B.P.: Meisling and Weldon, 1982). Despite the uncertainty in this age estimate, it probably cannot be off by more than a factor of two without requiring an unreasonably fast or slow slip-rate for the San Andreas fault (Meisling and Weldon, 1982). Furthermore, the geometry and topographic position of the Qte surface clearly require that it postdate the Older Alluvium in Cajon Pass, part of which cannot be older than 730,000 y B.P. (see Section 4.4.2, Chapter IV).

The next three lower surfaces in the Cajon Pass sequence (Qtd, Qtc and Qtb; Figure 3-4; Plate 1A) were graded to the level of a drainage system that exited southward to the San Bernardino plain. This drainage system evolved as the result of headward erosion of Cajon Creek and ultimately excavated Cajon Valley and Crowder Canyon. The surfaces Qtd, Qtc and Qtb, which are quite close to each other in elevation, immediately precede and postdate the incision of the inner gorge of Cajon Creek. This gorge is offset about 1.3 to 1.4 km along the San Andreas fault (Weldon and Sieh, in preparation; c.f. 2.0 km: Weldon et al, 1981). At a slip-rate of 24.5 mm/yr, the base of terrace Qtd is estimated to be 53,000 to 57,000 years old (Weldon and Sieh, in preparation).

3.3.2 Cleghorn Valley and Miller Canyon

In marked contrast to the dramatic relief in Cajon Pass and Cleghorn Canyon, Cleghorn Valley has been incised only 100 meters since the formation of the highest graded surfaces, and Miller Canyon has been cut down only several tens of meters. Only two terrace levels can be readily distinguished

in Cleghorn Valley and Miller Canyon (Figure 3-5; Meisling and Weldon, 1982).

Terrace surfaces in Cleghorn Valley and Miller Canyon, are best expressed where underlain by the easily eroded Crowder Formation. In Miller Canyon, where there is little Crowder Formation, surfaces are represented by erosional pediments and the irregular tops of alluvial fan and colluvial mantle deposits. Nevertheless, terraces can be crudely correlated by their soil development and relative heights above the current drainage (Figure 3-5).

The highest pediment surfaces in Cleghorn Valley (Qt2) appear to be continuous with the Qte surface in Cleghorn Canyon and Cajon Pass. Remnants of the Qt2 surface are preserved on Cleghorn Ridge and in an abandoned stream course just west of Silverwood Lake[56] . Since Cleghorn Valley and Miller Canyon joined each other at Silverwood Lake and were both part of the Mojave River system, it is reasonable to correlate high surfaces in Miller Canyon with Qt2 in Cleghorn Valley. Similarly well-developed soil profiles on Qt2 in both Miller Canyon and Cleghorn Valley support this correlation.

The lower terrace surfaces (Qt1) in Cleghorn Valley and Miller Canyon are largely confined to areas along the Mojave River underlain by Crowder Formation and where major tributaries such as Houston Creek and Sawpit Canyon join the valley (Plate 1A). The Qt1 surface is much more continuous than Qt2, and several remnants[57] suggest that it drained via the gap now occupied by Silverwood Lake. The Qt1 surface is tentatively correlated with Qtc and Qtd in Cajon Pass based on degree of soil development and relative height above the present drainage.

3.3.3 Summit Valley

Despite the extensive preservation of terrace surfaces and deposits in Summit Valley, there are only two major terrace levels that can be readily

Figure 3-5. Generalized cross-sections of graded terrace levels and depositional relationships along different segments of the Mojave River. Dark line is drainage pattern of the headwaters of the Mojave River: LM = lower Mojave River; DC = Deep Creek; ESV = east Summit Valley; GV = Grass Valley; WSV = west Summit Valley; SL = Silverwood Lake; CV = Cleghorn Valley; MC = Miller Canyon. See Plates 1A and 1B for detailed geology. Cross-sections: random hachure = gr = crystalline basement; light stipple = Tc = Crowder Formation; dark stipple = Qv = Victorville Fan deposits; white = Quaternary terrace fill; vertical lines = Qal = active alluvium; vertical divisions on sections are 100 feet (30.5 m); horizontal scale is compressed. Terrace relationships for each segment of the Mojave River are discussed in the text.

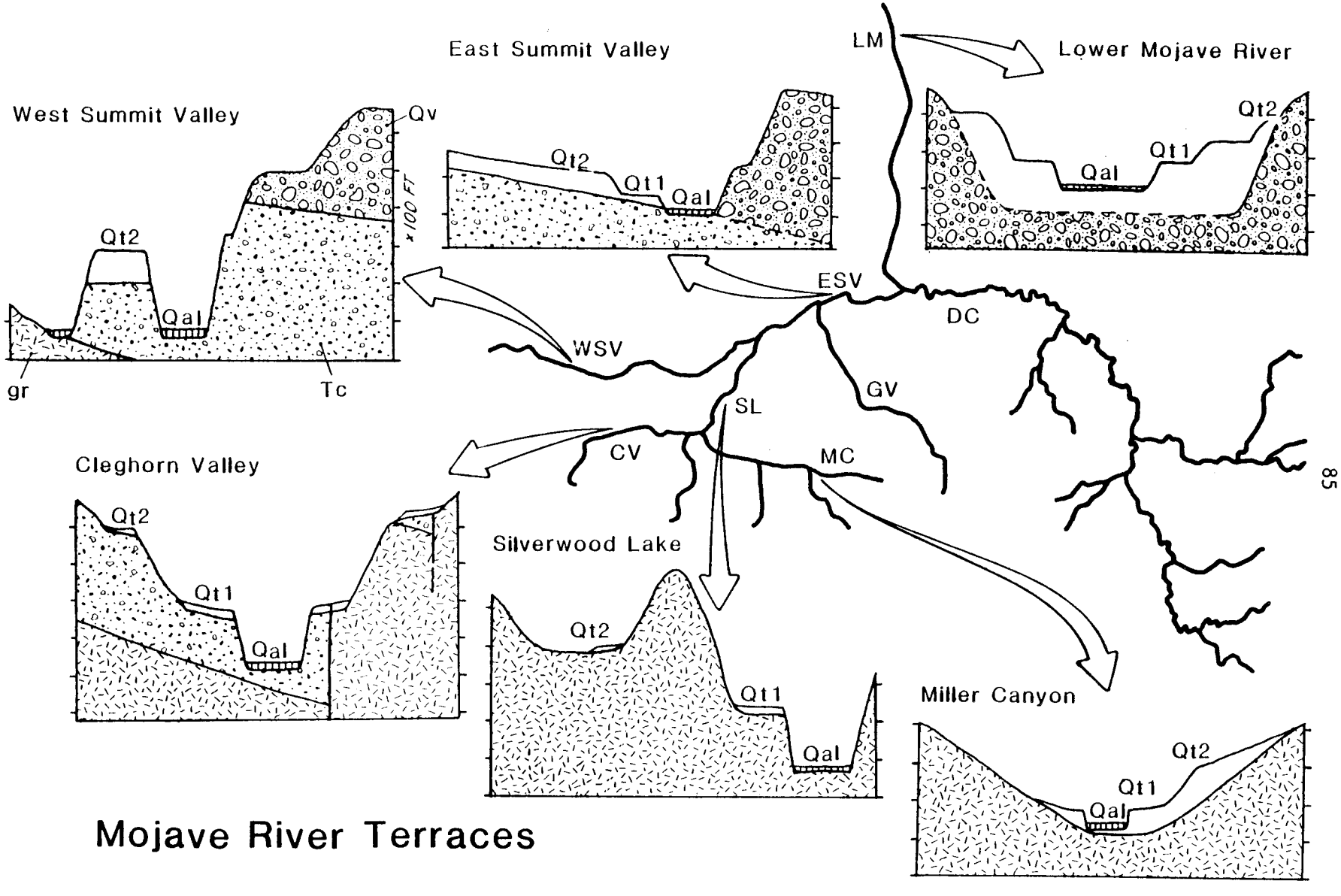

Mojave River Terraces

distinguished (Figure 3-4; Plate 1A).

The highest terrace level in Summit Valley (Qt2) is extensively preserved on terrace gravels at the west end of Summit Valley[58]. The Qt2 surface and underlying terrace gravels lie within the Summit Valley incision, well below the level of the Older Alluvium on top of the Victorville Fan (Figure 3-5). The Qt2 terrace gravels contain abundant clasts of Pelona Schist, indicating that they were derived from the San Gabriel Mountains via the Cajon Pass drainage area. Furthermore, the Qt2 surface is very nearly continuous with remnants of the Qte surface in Cajon Pass (Plate 1A). Hence, the Qt2 surface and deposits in west Summit Valley are considered part of the Qte drainage system and ~400,000 years old. A deep soil profile, developed on the terrace deposits that underlie Qt2 in Summit Valley, is consistent with an age of ~400,000 y B.P. (Weldon and McFadden, 1982, pers. comm.).

Isolated patches of terrace gravel between Cedar Springs Dam and Grass Valley[59] indicate that Qt2 extended into east Summit Valley. The gravels contain clasts of Pelona Schist, indicating that they were derived from the Cajon Pass area and delivered via west Summit Valley. The degree of soil formation on the isolated terraces, as well as their height above the present stream level, suggests that they were once continuous with each other and with Qt2 in west Summit Valley. They are therefore estimated to be ~400,000 years old. Evidence of a terrace surface at the Qt2 level is visible in the bluffs[60] of the Mojave River a mile west of Mojave River Dam. The west dike of the Mojave River Dam rests on a sill, cut in the sediments of the Victorville Fan, that was approximately at the Qt2 level.

A lower graded terrace (Qt1) is present throughout most of Summit Valley. It is best expressed near Mojave River Dam[61] where it clearly

lies below the level of the sill under the west dike of the Mojave River Dam. It must therefore postdate the abandonment of the gap occupied by the western sill in favor of the eastern bedrock gap now occupied by the Mojave River Dam proper. The Qt1 terrace deposits contain Pelona Schist, which is interpreted as having been derived from the erosion of the Qt2 deposits. The Qt1 terrace surface is considered ~57,000 years in age based on similarity in soil development with Qt1 in Cleghorn Valley and Qtc/Qtd in Cajon Pass.

3.3.4 The Mojave River North of Deep Creek

A flight of terraces surfaces along the Mojave River north of Mojave River Dam (Figure 3-5) can be correlated with the Summit Valley terrace sequence. The Mojave River terrace deposits contain the earliest appearance of Pelona Schist clasts north of Mojave River Dam, and lie within the incision made by the ancestral Mojave River into the Summit Valley facies of the Ord River Gravel. They interfinger with monolithologic alluvial fan-gravels shed off the western flank of the Ord Mountains[62], indicating a competition between local alluvial fan building and deposition by the Mojave River. On the east bank of the Mojave River the terrace surfaces abandoned due to incision are buried by advancing alluvial fan gravels[63]. The height of the Pelona-bearing deposits is consistent with Qt2 in Summit Valley, suggesting an age of ~400,000 y B.P.

Two lower terrace surfaces are preserved along the east bank of the Mojave River[64]. Following incision and abandonment, the tread and riser of each terrace was buried by advancing alluvial fan gravels, giving rise to a linear buttress unconformity[65]. No stratigraphic evidence was found to establish more than one episode of alluviation north of Mojave River Dam, yet the lower terrace surfaces lie beneath the level of the sill under the

west dike of the Mojave River Dam and must be correlative with Qtl in Summit Valley.

3.4 LATE QUATERNARY ALLUVIAL FANS

While fluvial terraces are developed in the westernmost San Bernardino Mountains, alluvial fans are characteristic of the range front further east. A nested series of Pleistocene and Holocene alluvial fans mantle the west flank of the Ord Mountains, interfingering with and overlying the Ord River Gravel. The steepest and highest fan surfaces appear to be graded to the level of the Ord River Gravel and Older Alluvium in Victorville Fan across the Mojave River to the west. The fans are made up of clasts of igneous and metamorphic rock derived from the adjacent mountain front. Similar nested fan sequences are characteristic of the northern range front in Fifteenmile and Lucerne Valleys.

3.4.1 Miller Canyon

A series of weathered and incised alluvial fans (Qt2) occurs on the north side of Miller Canyon where debris was shed across the Cleghorn fault from the steep south-facing slope of Pilot Rock ridge[66] (Figure 3-6). They are preserved only on the slope between the Cleghorn fault and Miller Creek; where Miller Creek runs along the fault zone, the fans are not present. The fans have a deep clay-rich soil developed on them. Constituent clasts are rotten and do not reflect the lithologies now exposed in the drainage basins upstream. The fans are interpreted as a depositional response to left-lateral motion on the Cleghorn fault, which has had the effect of lowering the base-level for these small drainages, resulting in fan depostion on the downstream side of the fault. These fans have been laterally displaced from their source drainages (Section 7.4.2).

Figure 3-6. Alluvial fan/terraces (Qt2) along the Cleghorn fault in Miller Canyon (from Meisling and Weldon, 1982). Alluvial fans and terraces deposited on the south flank of Pilot Rock ridge can be reconstructed by matching their height, areal distribution and drainage geometry across the Cleghorn fault. These alluvial fans are the product of steep topography created by motion on the Cleghorn fault. The lower parts of these fans are graded to the Qt2 level in Miller Canyon. See Plate 1A for detailed geology.

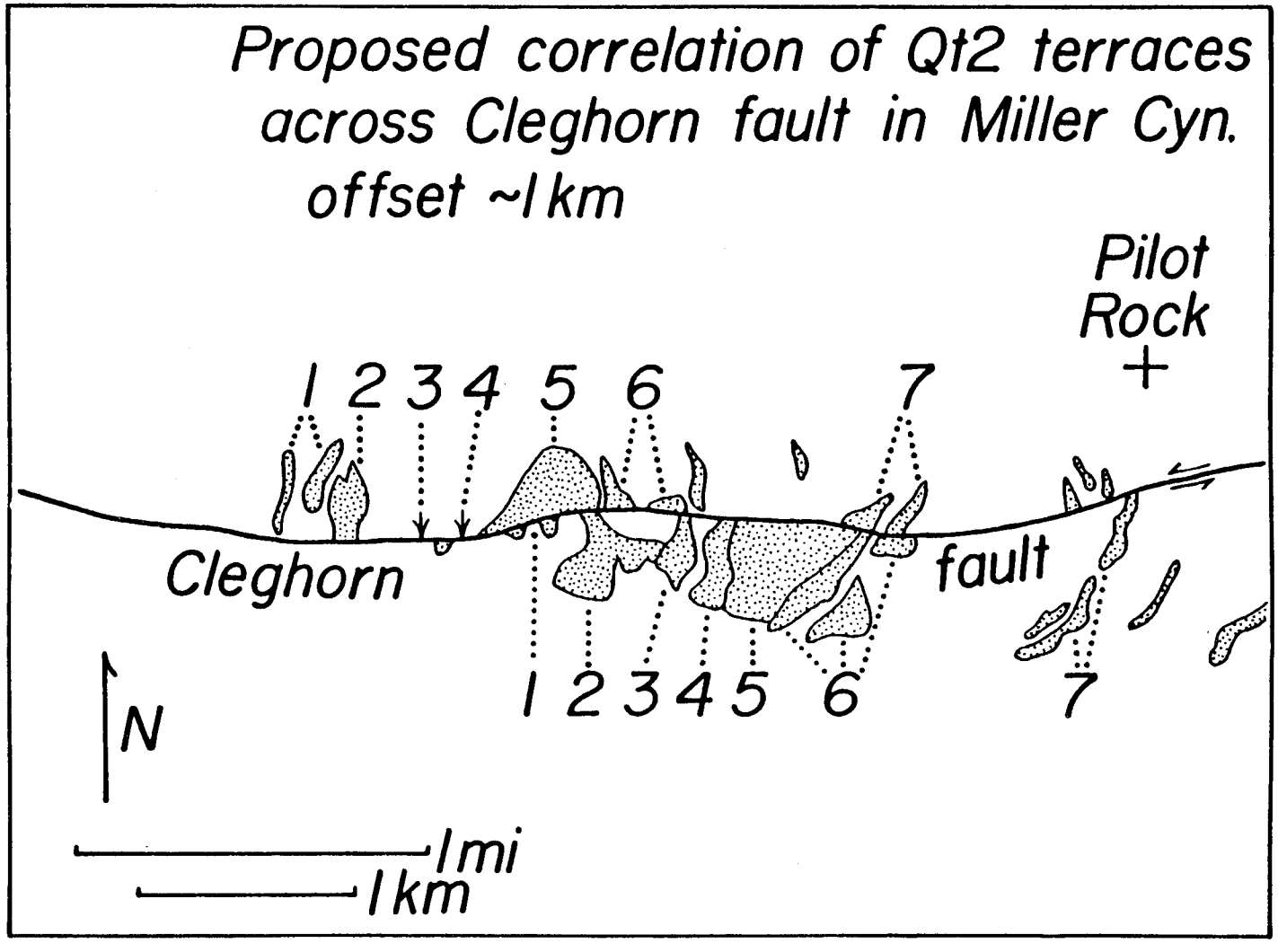
Proposed correlation of Qt2 terraces
across Cleghorn fault in Miller Cyn.
offset ~1 km
Pilot
Rock
1 2 3 4 5 6 7
Cleghorn
fault
1 2 3 4 5 6 7
N
1mi
1km

Graded terrace surfaces on Pilot Rock ridge upstream of the Cleghorn fault[67] are considered correlative with the alluvial fans based on soils and drainage reconstructions. The Qt2 terraces are steep with large differences in height between adjacent surfaces, suggesting that the drainage basins upstream of the fans were small and precipitous. The Qt2 fans and terrace in Miller Canyon are important since they demonstrably overlie older reverse faults and are offset by the Cleghorn fault (Section 7.3.2).

The Qt1 surface in Miller Canyon is fairly continuous and moderately planar. Although it lacks the alluvial fan morphology, the surface does rise at the mouth of tributary canyons to form a hybrid fan/terrace surface[68].

3.4.2 Cleghorn Valley and Cleghorn Canyon

Conditions in Cleghorn Valley and Cleghorn Canyon have not been conducive to the formation and preservation of alluvial fans. Cleghorn Valley is widely underlain by the easily eroded Crowder Formation, which seems to favor the formation of graded terraces rather than alluvial fans. In Cleghorn Canyon, which is now graded to the Cajon Pass drainage, incision has occurred so rapidly that there has been virtually no preservation of alluvial deposits whatsoever.

3.4.3 Summit Valley

Alluvial fan-shaped pediments have formed in east Summit Valley where major drainages exit narrow bedrock canyons of the western San Bernardino Mountains onto the graded valley floor. A broad fan is developed at the mouth of Grass Valley. A fan-shaped erosional pediment, capped by alluvium, is developed at the foot of the unnamed canyon just west of Grass Valley [69]. The drainage area upstream of this feature seems too small to be its only

source, suggesting that the canyon may have once carried Grass Valley Creek (Section 5.3.3). No other alluvial fan deposits of any size are developed in Summit Valley.

3.4.4 The Ord Mountains

3.4.4.1 The West Flank

A nested series of Pleistocene and Holocene alluvial fans mantle the west flank of the Ord Mountains, interfingering with and overlying the Ord River Gravel (Figure 3-7). The steepest and highest fan surfaces appear to be graded to the level of the Ord River Gravel and Older Alluvium in Victorville Fan across the Mojave River to the west. The fans are made up of clasts of igneous and metamorphic rock derived from the adjacent mountain front.

South of the Deep Creek power-line road, highly weathered alluvial fans (Qt2) graded to the approximate level of the Victorville Fan surface west of the Mojave River are deeply dissected[70]. These fans contain angular clasts of quartzite, granofels and biotite gneiss, derived from the metamorphic terrane immediately above them, in a matrix of clay and lithic fragments. The fanglomerates interfinger with and overlie fluvial gravels of the Deep Creek facies of the Ord River Gravel in exposures along the Deep Creek power-line road[42]. The angular metamorphic clasts of the fanglomerate constrast sharply with the well-rounded quartz-monzonitic and gneissic clasts of the underlying Ord River Gravel. A deep clay-rich soil has developed on the fan surface, reflecting its older age, and perhaps a greater availability of soil-forming elements in the metamorphic detritus. This soil is normal in polarity while the underlying Ord River Gravel has reversed polarity (Section 4.3.5), suggesting that they may both have been deposited around the time of the Brunhes/Matuyama polarity reversal, 730,000 y B.P. Based on these

Figure 3-7. Alluvial fans on the west flank of the Ord Mountains. In this airphoto, N is up and the scale is 1:16,000 (or 1 inch = ~1400 feet) It shows (a) the relict erosion surface atop Ord Mountains, (b) narrow, youthful, V-shaped canyons, (c) Qf2 = Older segmented alluvial fans composed of monolithologic limestone fanglomerate, (d) steep-walled gullies formed in response to faulting, (e) Holocene(?) alluvial fans at the mouth of gullies where they cross fault scarp, (f) fault scarp and (g) Ord River Gravel. Alluvial fans mantle lower slope of mountains and continue up several major canyons. They appear to have been formed in response to uplift along a steep, receding mountain front.

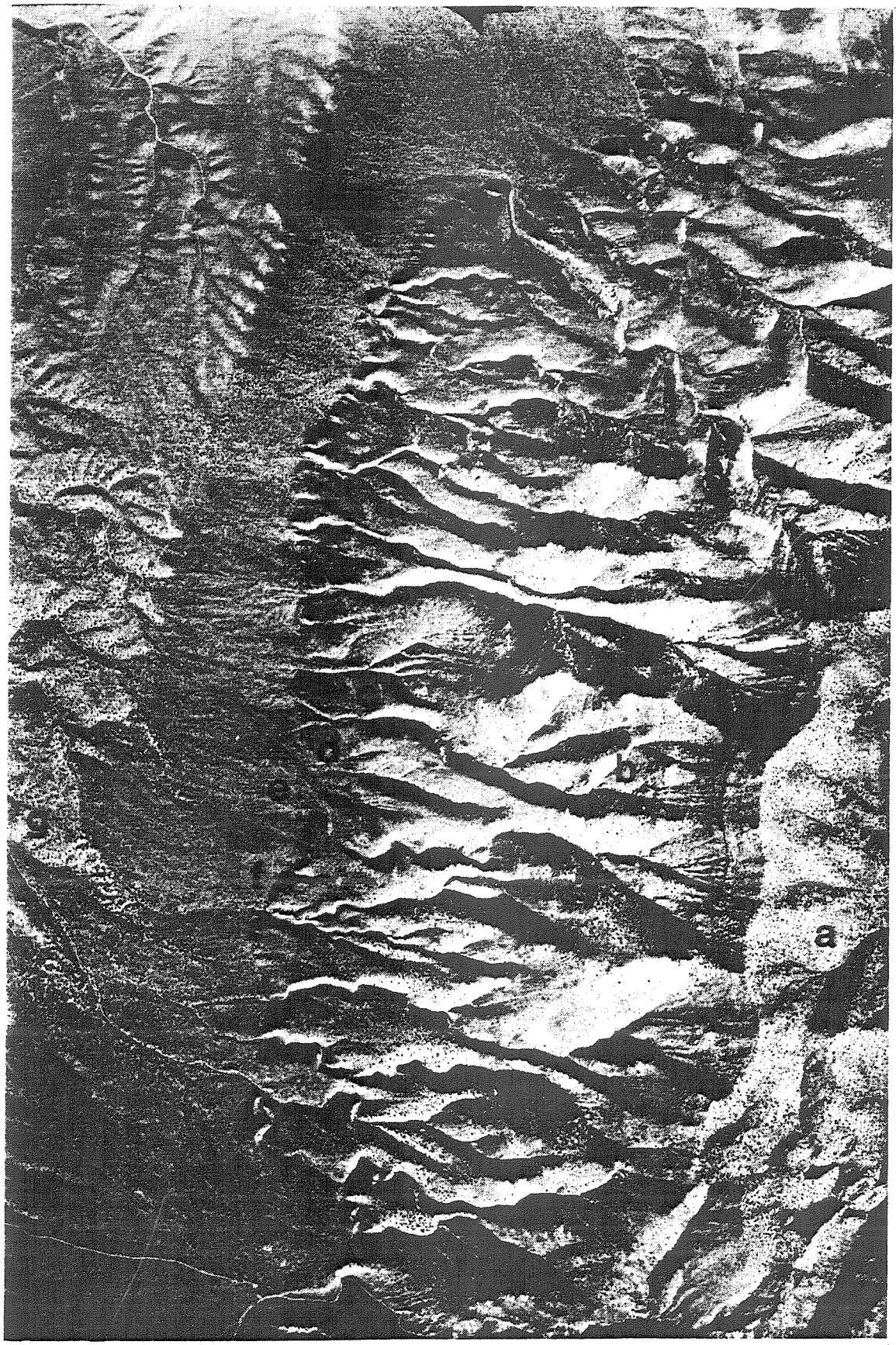
a
b

observations, the high alluvial fans south of the Deep Creek power-line road are correlated with the dissected Older Alluvium of the Victorville Fan.

North of the Deep Creek power-line road, alluvial fan deposits cover most of the lower slope of the Ord Mountains (Figure 3-7). The deposits consist of monolithologic limestone fanglomerate with occasional quartz-monzonite and quartz-syenite clasts in a well-indurated matrix of lithic fragments[71]. The contact between the fans and the bedrock is commonly marked by an angular breccia with a carbonate matrix[72], interpreted as a cemented talus deposits, suggesting that a steep mountain front prevailed at the time of fan deposition. Finger-shaped remnants of fanglomerate can be followed far up several narrow canyons[73], indicating that drainages were confined to small steep-walled canyons cut in the bedrock of a rugged, youthful mountain front. The gravels disgorged from these narrow canyons building their fans onto a linear mountain front. The contacts between fan deposits and bedrock are steep buttress unconformities without any trace of an intervening shear zone[74]. These observations suggest that the Ord Mountains fans are the product of a rapid pulse of erosion, perhaps in response to climatic change or rapid uplift, which buried the steep west flank of the Ord Mountains immediately following its creation.

Bull (1964) showed that segmented alluvial fan morphology can be a useful tool for deciphering tectonic history. Three segments are evident in most fans, with segments nearest the range front being the oldest. Fan surfaces are extremely steep, indicating that tilting or warping may have accompanied uplift and faulting along the range front (Section 5.10). Clasts in each fan are derived from the drainage basin immediately upstream, with no evidence of significant lateral offset.

The incision of steep-walled gullies[75] in the fan surfaces was

initiated by faulting at the toe of the coalesced fan surface. The faulting created an impressive scarp (Section 5.5.1.2) and resulted in the propagation of these gullies upstream from the topographic disturbance. Although the gullies appear youthful, they are cut into fanglomerate composed of thoroughly cemented carbonate clasts that may have an erosional resistance approaching that of bedrock. Where the gullies exit the scarp face, small alluvial fans are being deposited. The size of these fans suggests that they were produced by erosion of the fanglomerate during excavation of the gullies. These small fans are actively building, with little or no soil developed on them, indicating Holocene age.

3.4.4.2 The North Flank

The north flank of the Ord Mountains is somewhat more sinuous and embayed than the west flank. Nevertheless, the late Miocene(?) erosion surface in the Juniper Flats area is abruptly incised at the north flank of the Ord Mountains[76] by steep, V-shaped canyons that are relatively free of alluvial fill. The ancient erosion surface descends to the east, and the base of the mountain front rises to the east as it approaches the topographic head of the Arrastre Canyon fan. Hence, range front relief decreases to the east along the north flank of the Ord Mountains, where canyons become more subdued[77] with rounded, mature ridge crests. These features indicate that faulting responsible for the uplift of the Ord Mountains died out to the east. They may also suggest an eastward tilting of the mountain block.

Flat, concordant ridge crests on the north flank of the Ord Mountains[78] may be remnants of a sloping pediment surface that would postdate the late Miocene weathering surface, but predate most of the range front uplift. These pediment remnants support the conclusion that the Ord Mountains were a positive feature prior to the onset of frontal faulting and uplift.

3.4.5 The Northern Range Front East of Arrastre Canyon

The range front east of Arrastre Canyon is characterized by alluvial fan deposits, developed at the foot of each range-front drainage basin, that coalesce to form a bajada that descends to the level of Rabbit Dry Lake (Plate 1B). Three generations of alluvial fan deposits can be recognized in almost every major drainage. The surfaces of these fans are generally composed of three segments, decreasing in age away from the mountain front. These remnants have deep soil profiles developed on them and are commonly deformed along fault traces. In these respects, the fans east of Arrastre Canyon resemble the fans on the west flank of the Ord Mountains.

The highest and oldest fan deposits (Qf3) are preserved as remnants[79]. The Qf3 surface is deeply incised[80], and drainage confined to a fan-head trench[81]. The slopes of the older surfaces are commonly oversteepened[82], suggesting that tilting or warping has accompanied faulting along the range front. They have a deeper soil developed on them than the younger fan Qt2.

The lower and younger fan deposits (Qf2) are more continuously preserved than Qf3, having the geomorphic form of alluvial fans. They are commonly incised[83], with the youngest and lowest fan surface (Qf1) developed where the fan-head trench merges with the fan surface.

The (Qt3) and (Qt2) fan deposits are both cut and deformed by range-front faults (Section 5.8). The Qt3 deposits are everywhere cut by the range-front thrust faults. The Qt2 deposits overlie some low-angle faults while being clearly cut by others. It appears that some of the low-angle fault planes have been reactivated simultaneuosly with movement on the younger high-angle fault system. In some areas this deformation has been so complex that it is difficult to reconstruct the original geomorphic

configuration of the alluvial fan deposits.

The older fan deposits (Qt3) have been displaced by the lateral movement on the high-angle fault system to form shutter ridges. This has resulted in the lateral diversion of local drainages. Evidence that the younger fans are cut by high-angle faults can be seen in the form of linear trains of boulders that cross the fan surface transverse to drainage. Crystalline basement lithologies vary along the range front, with the result that each drainage basin contributes a unique suite of clasts to its fans. Clasts within the younger fans gravels (Qt2) are consistent with their being derived from the drainage basin presently upstream of the adjacent fan. This observation suggests about a half a kilometer of lateral slip along the high-angle rangefront fault system (Section 7.4.2). The tectonic geomorphology of the alluvial fans along the range front east of Arrastre Canyon is discussed in conjunction with range-front structure in Chapter V, "Structure".

The character of alluvial fans and their drainage basins changes east of Grapevine Canyon, reflecting the change in bedrock lithology of the mountain front from Rattlesnake Mountain Pluton to Fawnskin Monzonite and Metamorphic rocks. Drainage basins along the range front are smaller and steeper. The relief along the range front must be largely the product of thrust faulting, since the alluvial fans extend progressively farther up the canyons to the east, where thrusting is the dominant form of faulting. The steeper range front is also the result of high-angle faulting that has modified the topographic relief originally resulting from thrust faulting.

The fact that each major drainage east of High Road has three levels of alluvial surfaces suggests that the surfaces may record regional tectonic or climatic events. If climatic in origin, these episodes may correlate with

the pulses of fan building in the Ord Mountains and Silverwood Lake areas.

The sizes of drainage basins giving rise to alluvial fans are a major factor in their character. Although it may not be reasonable to compare drainage basins of different sizes, the progressive increase in size of drainage basins east from Arrastre Canyon suggests that uplift may have occurred in the Lucerne Valley area first.

3.5 DRAINAGE EVOLUTION

The drainage evolution of the northwestern San Bernardino Mountains reflects modification of relief by tectonic processes. Alluvial fan and terrace deposits permit a history of drainage evolution to be erected for the late Pleistocene. Age constraints on some of the alluvial units allow reasonable estimates to be made for the timing of events in the alluvial chronology. Although reasonably consistent, the proposed history is far from complete and would benefit from future detailed study.

3.5.1 Cajon Pass

The drainage divide between streams flowing to the Pacific Ocean and streams flowing to closed basins within the Mojave Desert presently lies along the crest of the inface bluffs in Cajon Pass. The drainage history of the Cajon Pass area reflects the migration of this major divide back and forth across the area in response to erosion along and motion on the San Andreas fault. The late-Pleistocene movement of the San Gabriel Mountains along the San Andreas fault resulted in a switch from the Mojave Desert to the Pacific Ocean base-level with the headward migration of Cajon Creek.

In the early Pleistocene, drainage in the Cajon Pass area was dominated by the topographic influence of the San Gabriel Mountains, which drained north and east to form the growing Victorville Fan. During the deposition

of the middle-Pleistocene Harold Formation, drainages along the north side of the rising San Gabriel and western San Bernardino Mountains fed alluvial fans at the foot of the mountains which coalesced to form broad bajadas (Figure 8a). Drainage may have been to closed dry lakes, such as is the case in Fifteenmile Valley today. As the San Gabriel Mountains rose and moved northwestward along the San Andreas Fault, drainages sampled successively more southerly terranes within the San Gabriel Mountains crystalline complex. The alluvial apron grew and deposition of the coarser Shoemaker Gravel took place. Drainage basins were probably larger than during deposition of the Harold Formation and may have run along the fault for miles, confined by the rift zone topography, before disgorging onto the bajada. As the bajada expanded, a large master fan began to emerge, fed by the north flank of the western San Bernardino Mountains as well as the northeast flank of the San Gabriel Mountains (Figure 3-8b). Drainages probably joined the flow from Deep Creek to form the ancestral Mojave River. Finally, the Older Alluvium was deposited in large fan-shaped lobes that emanated from sources in the eastern San Gabriel Mountains and joined the ancestral Mojave River which carried material away to the north (Figure 3-8b).

As the San Gabriel Mountains continued to move to the northwest, base-level in the Cajon Pass area fell, fan-head incision occurred, and the surface of the Older Alluvium was abandoned (Figure 3-8c). Antelope Valley was the largest fan-head incision, and it is incised into the undissected Older Alluvium and was fed by headwaters in Cajon Pass (Figure 3-8c). Summit Valley later captured these headwaters (Figure 3-8d) as evidenced by the sudden appearance of the Pelona-Schist-bearing Summit Valley alluvial fill and the the fact that the two drainages join at Cajon Pass proper. The Qte deposits represent the last evidence of northward drainage in the Cajon Pass

Figure 3-8. Middle to Late Pleistocene drainage evolution of the West Fork of the Mojave River. Each diagram is the same map view with pseudo-perspective physiography. North is up, circle is 30 km across. Diagrams progress forward in time from (a) to (e). On each circle: 1 = San Andreas Fault; 2 = Cajon Pass; 3 = Victorville Fan; 4 = lower Mojave River; 5 = Ord Mountains; 6 = Deep Creek; 7 = Pinnacles; 8 = western San Bernardino Mountains; 9 = San Gabriel Mountains. The proposed drainage evolution is as follows: (a) >730,000 y B.P.: The Mojave River began as the "Ord River" drainage that skirted the Victorville Fan and was probably fed by Deep Creek. The Deep Creek Facies of the Ord River Gravel was deposited. The western San Bernardino Mountains were uplifted, but still mantled by Crowder Formation. The dissected Older Alluvium was deposited in the form of a bajada flanking the San Gabriel and San Bernardino Mountains. (b) ~730,000 y B.P.: The mouth of Deep Creek moves west as integrated drainage develops in the western San Bernardino Mountains. The Crowder formation is stripped from the range laying bare the underlying relict surface. The undissected Older Alluvium and Summit Valley facies of the Ord River Gravel are deposited from sources in the San Gabriels and San Bernardino Mountains respectively. (c) ~500,000 y B.P.?: The Mojave River advances into Cleghorn Valley and Miller Canyon; Summit Valley approaches Cajon Pass. Drainage on the Victorville Fan becomes entrenched in Antelope Valley. (d) ~400,000 y B.P.: Drainage in Cajon Pass is captured by Summit Valley; Qt2 is deposited. (e) ~60,000 y B.P.: Headward erosion of Cajon Creek into Cajon Pass reclaims the area from the Mojave River drainage; Qt1 is deposited. (e) is essentially the configuration of the West Fork of the Mojave River today (see Figure 3-5).

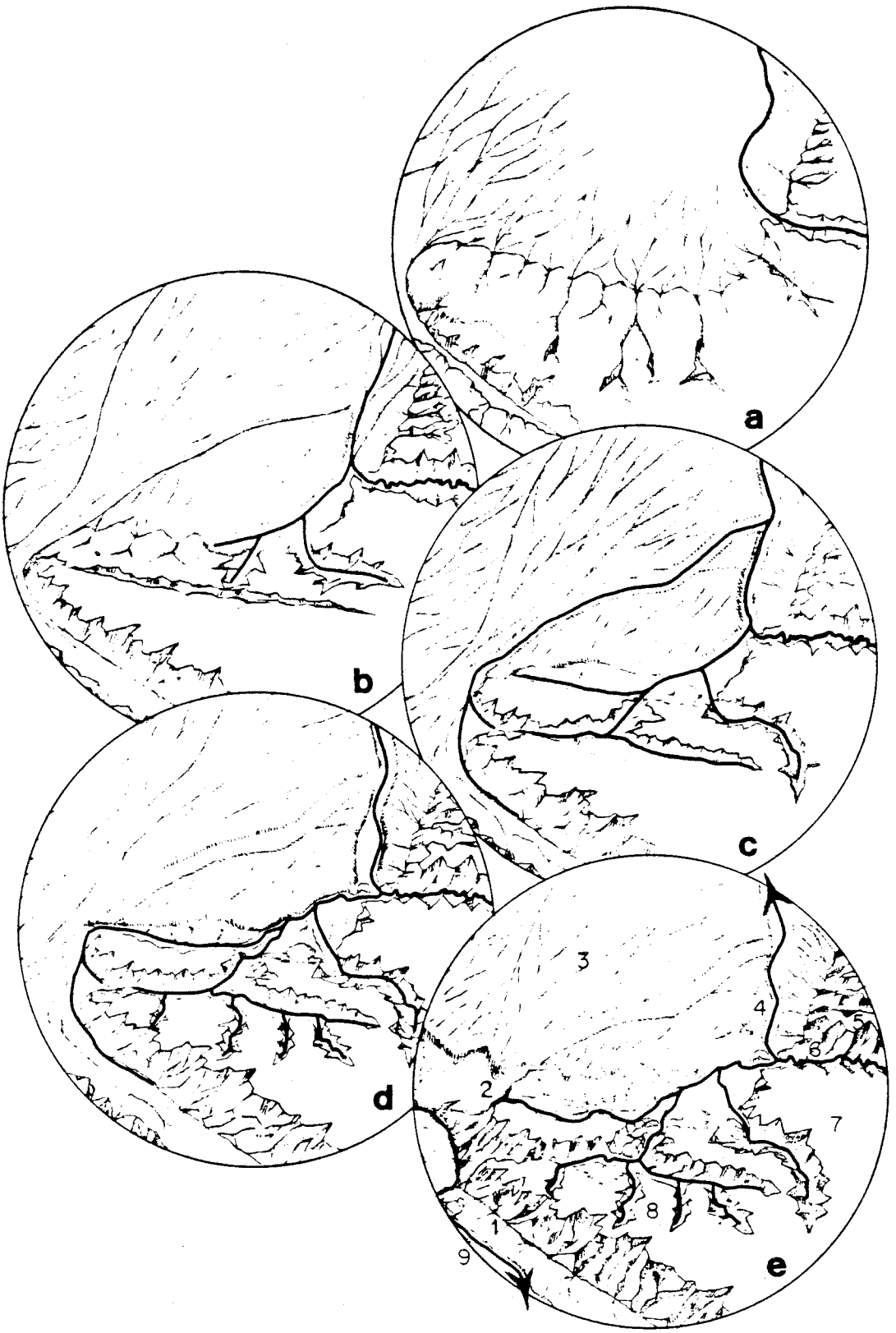
a
b
c
d
e
1
2
3
4
5
6
7
8
9

areas prior to the reversal of direction and change in base-level that accompanied the capture (Figure 3-8e) of the area by Cajon Creek.

The detailed evolution of drainage in Cajon Pass following the incision of Cajon Creek (Figure 3-8e; Weldon, 1982, pers. comm.; Weldon and Sieh, in preparation) is briefly summarized below, insofar as it bears on the drainage evolution of the adjacent Mojave River basin. The earliest evidence of southward drainage is seen in the Qtd graded surface (Plate 1A), which predates the incision of the inner gorge of Cajon Creek and is estimated to be between 53,000 and 57,000 y B.P. in age on the basis of offset and slip rate on the San Andreas fault (see Section 3.3.1, Chapter III). Following the incision of the inner gorge, the deposition of Qtc, Qtb and Qta occurred (Plate 1A).

3.5.2 The Mojave River

The Mojave River underwent headward erosion and incision in the late Pleistocene, strongly controled by the structures responsible for the uplift of the western San Bernardino Mountains (Figure 3-8). Headward growth of the Mojave River began with the cessation of deposition on the Victorville Fan. Deposits along the Mojave River from Cajon Pass to the Ord Mountains reflect a sequence of events whereby the Mojave River basin grew by the addition of Deep Creek, Cleghorn Valley, Miller Canyon, and Summit Valley, each contributing a distinctive suite of clasts.

The upper Mojave River grew out of the Ord River, which skirted the margin of the Victorville Fan during its final stages of activity (Figure 3-8a). During deposition of the dissected Older Alluvium (>730,000 y B.P.) an ancestral Deep Creek flowed northwest out of the San Bernardino Mountains in approximately its present location. It deposited the Deep Creek facies of the Ord River Gravel, which contains no clast contribution from the

western San Bernardino Mountains. Deep Creek flowed north, confined by the alluvial mantles shed off the western San Bernardino and Ord Mountains. The ancestral Deep Creek was joined by runoff from the Victorville Fan. In all probability an ancient Arrastre Canyon also joined the Deep Creek drainage north of the Ord Mountains, since there is evidence that Arrastre Canyon existed as a drainage basin prior to the uplift of the San Bernardino Mountains.

Continued uplift of the Ord Mountains caused the Deep Creek drainage to shift west and incise near the Deep Creek Dam (Figure 3-8b). This westward shift and incision coincided with the development of Summit Valley as sheet-flood on the southern shoulder of the Victorville Fan began to integrate, creating a drainage in the western San Bernardinos. At this time the western San Bernardino Mountains, at this time, were blanketed by Crowder Formation, which became incised and was stripped off and deposited as the Summit Valley facies of the Ord River Gravel. The Summit Valley facies contains clasts from the Deep Creek drainage and Crowder clasts from the western San Bernardino drainage area, but no Pelona Schist.

Headward erosion continued on the Mojave River, especially along the bedrock/sediment contact in Summit Valley (Figure 3-8c), until it reached the Cajon Pass basin which had heretofore been draining through the fan-head incision of Antelope Valley (Figure 3-8c,d). Drainage capture occurred, and the Pelona-Schist-bearing gravels were deposited in Summit Valley and along the Mojave River (Figure 3-8d). Aggradation proceeded in the Mojave drainage until the drainage reversal occurred in Cajon Pass, recapturing the area to the Pacific drainage basin by headward erosion of Cajon Creek (Figure 3-8e). The supply of material was cut off from Summit Valley.

3.6 CONCLUSIONS

The salient results of the geomorphic investigations in the northwestern San Bernardino Mountains are as follows:

(1) A weathered erosion surface was developed on the crystalline terrane over most of the area in response to humid conditions during the late Miocene, at which time the region was characterized by an upland surface of subdued relief.

(2) This weathered erosion surface is a useful index to structural deformation in the study area.

(3) Late Quaternary graded terrace deposits, present in Cajon Pass and along the Mojave River, can be correlated based on geomorphic criteria.

(4) These terraces reveal a complex history of drainage evolution involving headward expansion of the Mojave River leading to the brief capture of the Cajon Pass drainage area prior to the development of Cajon Creek.

(5) Alluvial fans were formed on the west flank of the Ord Mountains and along the northern range front east of the Mojave River in direct response to uplift on the north frontal fault system.

CHAPTER IV

PALEOMAGNETISM

4.1 INTRODUCTION

4.1.1 Purpose

The goal of this paleomagnetic study was to place limits on the ages of Pleistocene deposits in the study area in order to constrain the slip rate and recency of faulting for the north frontal fault system of the San Bernardino Mountains. These age limits also serve to provide a time framework for the interpretation of Pleistocene drainage evolution and depositional history which record the uplift of the western San Bernardino Mountains.

4.1.2 Scope

The sampling effort was focused on the Harold Formation, Shoemaker Gravel and Older Alluvium, known collectively as the "Victorville Fan" complex (Figure 4-1). These units span the critical time period during which the uplift of the western San Bernardino Mountains took place. A sequence of paleomagnetic samples was collected from each of four stratigraphic sections within the Victorville Fan complex in an effort to determine whether or not the sediments were deposited prior to the Brunhes/Matuyama polarity reversal at 730,000 years B.P. Sample coverage was expanded along the range front between Deep Creek and Arrastre Canyon through a limited number of key sample localities.

4.1.3 Age Constraints

The uppermost Harold Formation has been provisionally assigned an age of 0.7 to 1.2 my B.P. (late Irvingtonian) by C. A. Repenning (1982), based on the land mammal assemblage at the U. C. Riverside Barrel Springs locality (RV-7618 & RV-7617) near Lancaster. R. E. Reynolds (pers. comm., 1982) has

Figure 4-1. Generalized index map of the Victorville Fan complex and vicinity, western Mojave Desert, southern California, showing location of paleomagnetic sampling localities. The Pleistocene Victorville Fan complex (VF) was derived from crystalline basement source areas in the San Gabriel Mountains (SGM), western San Bernardino Mountains (WSBM) and San Bernardino Mountains (SBM). The San Gabriel Mountains are bounded on the northeast side by the San Andreas fault zone (SAFZ), which also defines the southwestern limit of the western San Bernardino Mountains. The north frontal fault system (NFFS) defines the northern boundary of the SBM, deforming and cutting sediments of the Victorville Fan complex in the Marianas Rancho (MR) and Apple Valley Highlands (AH), north and west of the Ord Mountains (OM) respectively. Deep incision in the Cajon Pass area (CP) exposes the sediments of the Victorville Fan complex [the Harold Formation and Shoemaker Gravel (stippled), Dissected Older Alluvium (textured grey), and Older Alluvium (grey)] along the inface bluffs (IB). The WSBM and SBM are drained by the Mojave River (M), via Summit Valley (SV), Deep Creek (DC) and Arrastre Canyon (AC). The southeastern part of the Victorville Fan is drained by Oro Grande Wash (OGW), an antecedent drainage. The towns of Hesperia (H), Apple Valley (AV) and Victorville (V) are included for reference. Paleomagnetic sampling localities [cross-hairs = section locality; heavy point = key sample locality] include the Harold Formation/Power-line Road Site (HPL), Shoemaker Gravel/Power-line Road Site (SPL), Mojave River Forks Site (MRF), Ord River Gravel/Deep Creek Sites (ORD), Ord River Gravel/Marianas Rancho Sites (ORM), Hesperia/Reynolds Fossil Locality Site (HRF), Arrastre Canyon Fan Site (ACF), Rock Springs Road Site (RSR), and Bowen Ranch Road Site (BRR). [Figure modified after State Geologic Map, San Bernardino 2° Sheet (Jennings, 1983, in preparation)]

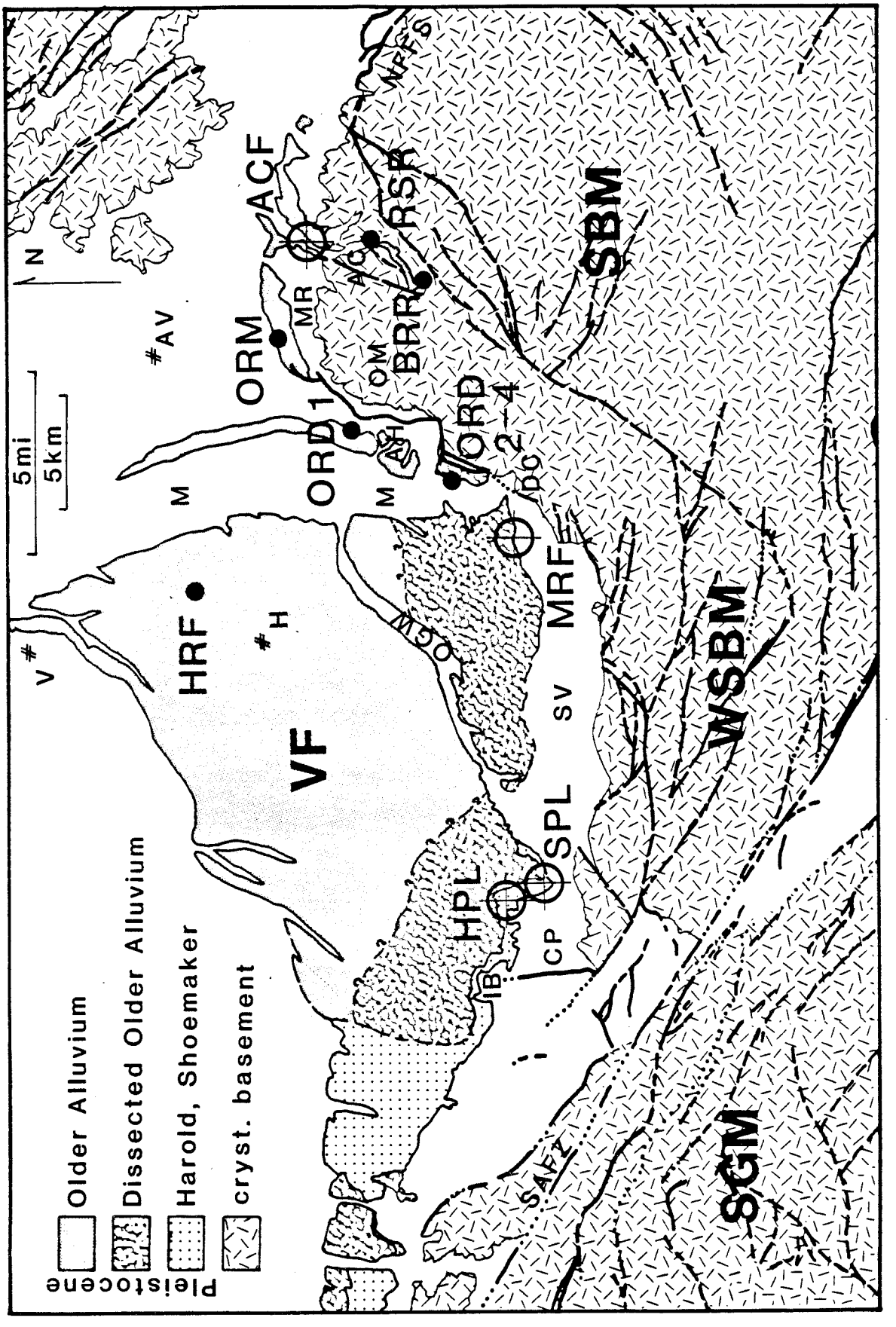
Pleistocene
Older Alluvium
Dissected Older Alluvium
Harold, Shoemaker
cryst. basement
5mi
5km
N
V
HRF
H
VF
M
AV
ORM
ACF
MR
OM
BRR
RSR
WFS
ORD 1
ORD 2-4
OGM
MRF
SV
SPL
CP
HPL
IB
SAFZ
WSBM
SBM
SGM

tentatively assigned lacustrine beds of the upper Older Alluvium in Hesperia an age of 0.7 to 0.45 my B.P. (late Irvingtonian) based on fossils at the San Bernardino County Museum Bear Valley Road Redevelopment locality (1.114.8 to 1.114.20). A profound angular unconformity separates the Victorville Fan sediments exposed in the bluffs of the Mojave River west of Deep Creek dam from underlying volcanogenic eastern facies of the Crowder(?) Formation, dated radiometrically at 3.8 0.4 my B.P. (R. J. Weldon and C. F. Naeser, pers. comm., 1982). These age constraints support the conclusion that deposition of the Victorville Fan complex began during the Matuyama polarity epoch (2.48 to 0.73 my B.P.) and continued into the Brunhes polarity epoch (0.73 my B.P. to present; see Mankinen and Dalrymple, 1979). The unconsolidated nature of the Harold Formation, Shoemaker Gravel and Older Alluvium, and the preservation of fine depositional features on the upper geomorphic surface of the Older Alluvium, support this conclusion.

Some tectonic control also exists to constrain the age of the Victorville Fan deposits. Victorville Fan sediments in the Mojave River bluffs in Summit Valley contain the earliest evidence of clasts shed north from the western San Bernardino Mountains following the onset of uplift. The inception of uplift in the western San Bernardino Mountains is thought to have been roughly contemporaneous with early uplift along thrust faults in the north-central San Bernardino Mountains (Meisling and Weldon, 1982). The latter event is reflected in the clast composition of the Old Woman Sandstone (Sadler, 1982), which May and Sadler (1982) assigned an age of 2.0 to 3.2 my B.P. (late Blancan).

In Cajon Pass, the Harold Formation contains the earliest reported clasts of Pelona Schist and other unique lithologies derived exclusively from the San Gabriel Mountains crystalline basement terrane (Foster, 1980),

brought into the area by strike-slip movement on the San Andreas fault (Weldon, pers. comm., 1982). The Holocene slip-rate on the San Andreas fault has been measured at 2.5 cm/yr in Cajon Pass (Weldon and Sieh, 1981). Assuming a constant slip-rate of 2.5 cm/yr for the Pleistocene, 2.0 my ago the San Gabriel terrane was 50 km southeast of its present position along the San Andreas fault, well south of the site of deposition of the Harold Formation in Cajon Pass. Thus, the San Gabriel source terrane was not available for the deposition of the Harold Formation prior to about 2.0 my ago.

In the discussion that follows, it is assumed that the Victorville Fan is Pleistocene in age, and that samples displaying reversed polarity were deposited before the Brunhes/Matuyama polarity boundary, 730,000 years B.P. The magnetic behavior of reversed samples shows that primary polarity survives in most samples and permits the sequence of consistently normal samples to be interpreted as younger than the Brunhes/Matuyama polarity transition. All age assignments are in complete agreement with depositional sequence as deduced from detailed geological and geomorphological field mapping.

4.2 METHODS

Some of the soft-sediment sampling techniques were developed for this study following the suggestions of D. R. Van Alstine (pers. comm., 1980). They yield surprisingly consistent results for the unconsolidated fluvial and alluvial sands and silts examined, and permit a large number of samples to be taken quickly and efficiently.

4.2.1 Sampling Techniques

Oriented sediment samples were collected in both cylindrical quartz-

glass tubes [1.0 in. diameter x 1.0 in. long, closed at one end] and plastic boxes [1.0 in^2 x 0.75 in., with lid]. Tubes and boxes were demagnetized in an alternating-field (AF) demagnetizer before sampling, and the tubes were heated to 650° C prior to use to anneal them and break flawed ones.

Samples were taken by placing a quartz-glass tube or plastic box against the outcrop face and gently pressing it over a pedestal of sediment as it was being carved with a brass, bronze or non-magnetic stainless steel scribe. Water was applied during carving to hold loose lithologies together and make hard units penetrable.

The samples were oriented by drawing a horizontal reference line on the closed end of each container, with barbs indicating the down-dip direction. The attitude of the closed end of the sample tube or box was then measured with a Brunton compass using a right-handed convention in which the strike line azimuth points to the sampler's right and the dip azimuth is measured 90° from it in a clockwise sense. Measured in this way, sample orientations in unconsolidated sediments are considered accurate to within 10°, as evidenced by reproducibility of results from two samples taken from the same horizon (see sample RSR-1,2, Figure 4-7).

The samples were given a three-letter site-code and numbered in stratigraphic sequence. Each sampled horizon was marked with a stake bearing the site code and sample number(s).

The tubes were covered with Parafilm®, and lids were placed on the boxes to minimize disturbance during transport to the laboratory. Due to their coarse, sandy composition, many samples were prone to disaggregation. This problem was minimized by adding a little dilute sodium silicate solution (water glass) to the sample tubes in the laboratory, thereby cementing the loose grains.

4.2.2 Sample Demagnetization

All sample demagnetization was carried in the field-free space of Caltech's magnetically shielded laboratory. Natural remanent magnetism (NRM) was measured for each sample. Most samples collected in quartz-glass tubes were demagnetized thermally by step-wise heating in a non-inductively wound oven and cooled to room temperature in zero-field. Several tube samples were lost when their tubes broke at high temperature due to expansion of the sample and/or flaws in the glass tube. Samples in plastic boxes were chemically demagnetized by soaking them in dithionite solution under vacuum (Kirschvink, 1981; Mehra and Jackson, 1958). Some box samples were disturbed when they liquefied or flipped over while immersed in the solution.

4.2.3 Sample Measurement

The sediment samples were measured on a two-axis superconducting SQUID magnetometer built by Superconducting Technology Inc. of Mountain View, California. The high sensitivity and fast response time of this type of magnetometer makes it possible to measure a large number of relatively weak samples in a short time. Since the instrument does not require spinning or vibrating of the sample during measurement, the risk of disturbing delicate unconsolidated sediment samples is reduced. Goree and Fuller (1976) provide a discussion of the operating principles, configuration and applications of the instrument.

After each demagnetization step, the remanent moment of each sample was measured with it in eight different orientations, permitting a variety of consistency checks on the reliability and homogeneity of the moment.

4.2.4 Data Analysis

The effect of progressive demagnetization for each sample was monitored

by plotting the remanent vector direction on an equal-area stereographic projection both before and after the stratigraphic tilt correction. (Figure 4-2a).

Progressive demagnetization data are also plotted on a modified Zijderveld, or Roy-Park, diagram in which two useful projections of the paleomagnetic vector are combined (Zijderveld, 1967; Roy and Park, 1974; Figure 4-2b). For open points, the x-axis is the radial component of the vector in the horizontal plane (horizontal intensity) and the y-axis is the vertical component of the vector (vertical intensity: positive above the x-axis, and negative below). Solid points are the projection of the paleomagnetic vector on the horizontal plane, with the positive x-axis pointing east and the positive y-axis pointing north; this projection plane is simply a horizontal slice through the equator of the equal area projection. In both of these projections, the length of the vector is proportional to its intensity.

In a systematic effort to explore for evidence of rotations, least-squares lines were fit to groups of points in the demagnetization path interpreted as stable components of magnetization (Kirschvink, 1980). Vector mean directions were then calculated for groups of normal and reversed least-squares lines (Fisher, 1953) in the HPL, SPL, MRF and ACF sample series.

Equal-area and vector projections of the progressive demagnetization data for each sample are presented in Appendix A, and are summarized in Tables 4-1 to 4-5.

4.3 DISCUSSION OF DATA

4.3.1 Harold Formation: Power-Line Road Section (HPL)

Samples HPL 1 to 39 were collected along the power-line road that lies north of Highway 138 in sec 17, 19 & 20, R5W T3N (Figure 4-1; Plate 1A;

Figure 4-2. Example of equal-area stereographic projection and Roy-Park plot of demagnetization data. (a) Top: Equal-area stereographic projection showing the direction of the paleomagnetic vector during progressive thermal demagnetization of sample MRF-1. Open points plot in the upper hemisphere; solid points plot in the lower hemisphere. "NRM" is the natural remanent magnetic vector prior to demagnetization, which is the sum of a stable reversed paleomagnetic vector and a less stable normal vector overprint due to the present local magnetic field (PLF). As the normal overprint is removed by progressive thermal demagnetization, the vector sum tracks across the plot to a reversed direction. The vector remains at this ancient declination and inclination during further heating, decreasing only in intensity. When the blocking temperature of the minerals carrying the ancient field direction is exceeded, the vector drifts randomly across the plot. (b) Bottom: Zijderveld diagram as modified by Roy and Park (1974) for MRF-1 in which two useful projections of the paleomagnetic vector are combined. For open points, the x-axis is the radial component of the vector in the horizontal plane (horizontal intensity) and the y-axis is the vertical component of the vector (vertical intensity: positive above the x-axis, and negative below); this projection plane is a vertical slice through both upper and lower hemispheres of the plot that passes through each point when plotted. Solid points are the projection of the paleomagnetic vector on the horizontal plane, with the positive x-axis pointing east and the positive y-axis pointing north; this projection plane is simply a horizontal slice through the equator of the plot. The plot for MRF-1 clearly shows that a strong normal component is removed after heating to the 200° demag step, leaving a remanent paleomagnetic vector of reversed polarity which decreases in intensity and is constant in direction with stepwise heating.

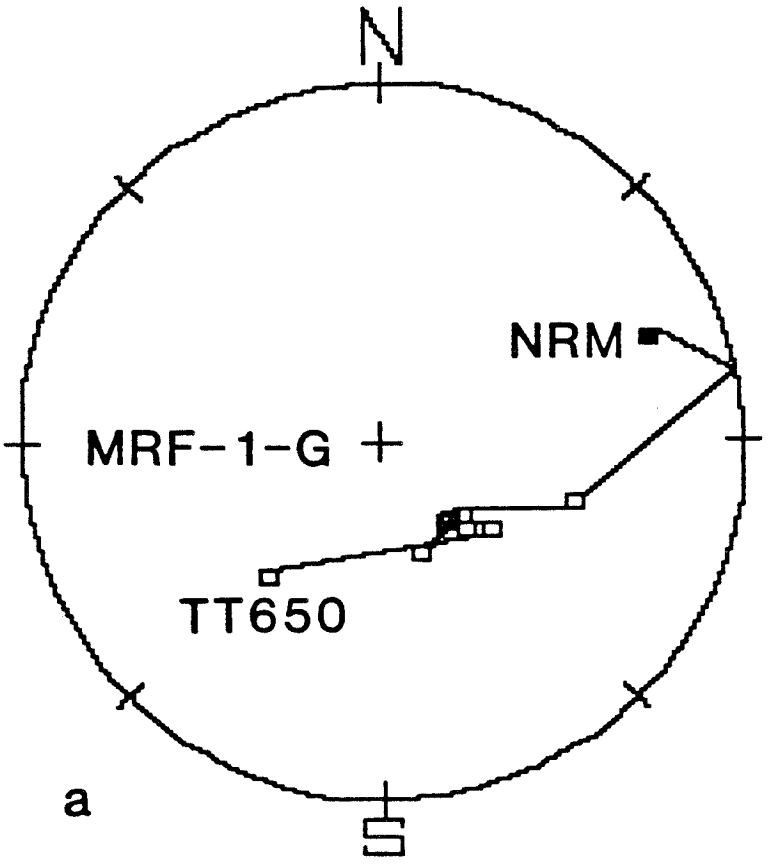
N
NRM
MRF-1-G
TT650
a
S

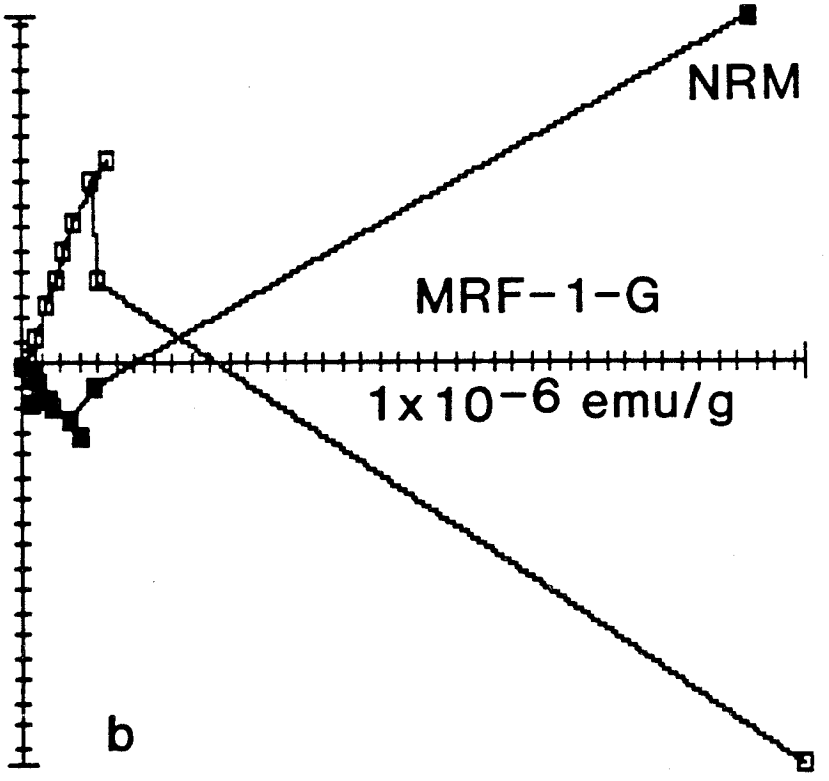
NRM
MRF-1-G
1x10-6 emu/g
b

Table 4-1; Appendix A). The sampled section includes part of the Harold Formation (HPL 1-29), the Shoemaker Gravel (HPL 30-37) and the Older Alluvium (HPL 38, 39) of Dibblee (1965, 1967) as mapped by John Foster (1980). The Shoemaker Gravel lies gradationally above the Harold Formation and is distinguished by its coarse grain-size and alluvial character (Foster, 1980). A marked angular unconformity separates the Older Alluvium from the Shoemaker Gravel at the HPL site.

Eighteen samples were collected in plastic boxes and twenty-one in quartz-glass tubes. Natural remnant magnetism (NRM) was measured for each of the 39 samples. Box samples were chemically demagnetized and measured after 14, 39, and 80 hours in the citrate/bicarbonate buffered Na-dithionite solution. Tube samples were demagnetized thermally and measured after heating to 100, 150, 200, 250, 300, 350, 425, 500, 550, 600, and 650° Centigrade.

Both thermally and chemically demagnetized samples from the Harold Formation (HPL 1-29) and lower Shoemaker Gravels (HPL 32-33) display predominantly reversed polarity (Table 4-1). The lower part of the sampled section in the Harold Formation is clearly reversed (HPL 1-17; Figure 4-3a). Many of these samples showed reversed NRM's (HPL 1,2,4-9,12-15; Figure 4-3b). Near the top of the Harold Formation, HPL 24, 25 and 26 appear to be tracking toward reversed polarity (Figure 4-4). Within the Shoemaker Gravels, HPL 33 clearly tracks toward reversed polarity, and sample 34 may be tracking toward reversed polarity (Figure 4-4). Therefore, the Brunhes/Matuyama polarity reversal must have occurred after sample 33 was laid down, and normal-polarity samples lying stratigraphically below HPL 33 probably bear a later overprint.

Both chemical and thermal demagnetization result in a good clustering

Table 4-1. Data for progressive thermal and chemical demagnetization of HPL sample series.

Sample Number	Cum. Strat. Int.(m)	Fm*	Texture	demag type	Primary Component		Secondary Component		Notes†
					Polarity	Stability T(°C);C(h)	Polarity	Stability T(°C);C(h)	
HPL-1	0.0	H	silt-f.sand	Therm	Reversed	600-650	Normal	100-150	skewed 20-30° clockwise
HPL-2	0.0	H	silt-f.sand	Chem	Reversed	>80	None	---	skewed 10-20° clockwise
HPL-3	1.5	H	f.sand-gran	Therm	Reversed	500-550	Normal	100-150	tracks toward reversed; some disaggregation
HPL-4	6.0	H	silt-f.sand	Therm	Reversed	>650	Normal	100-150	skewed 20° clockwise; tube broke at 650° C
HPL-5	6.0	H	silt-f.sand	Chem	Reversed	>80	None	---	skewed 10° clockwise
HPL-6	10.5	H	silt-f.sand	Therm	Reversed	>650	Normal	100-150	skewed 20° clockwise?; some disaggregation
HPL-7	10.5	H	silt-f.sand	Chem	Reversed	>80	None	---	skewed 10° clockwise?
HPL-8	13.0	H	cl-v.f.sand	Therm	Reversed	600-650	Normal	NRM-100	not skewed;sample shrank
HPL-9	13.0	H	cl-v.f.sand	Chem	Reversed	>80	None	---	not skewed
HPL-10	17.0	H	v.f.-f.sand	Chem	Reversed	>80	Normal	14-39	tracks toward reversed
HPL-11	17.0	H	v.f.-f.sand	Therm	Reversed	550-600	Normal	150-200	tracks toward reversed
HPL-12	18.5	H	silt-f.sand	Therm	Reversed	>650	Normal	100-150	skewed 10° clockwise?
HPL-13	18.5	H	silt-f.sand	Chem	Reversed	>80	Normal	NRM-14	not skewed
HPL-14	23.0	H	f.-med.sand	Chem	Reversed	>80	Normal	NRM-14	not skewed
HPL-15	23.0	H	f.-med sand	Therm	Reversed	>650	Normal	100-150	skewed 10-45° clockwise

*H=Harold Fm; S=Shoemaker Gravels; O=Old Alluvium †PLF=present local field

Table 4-1(cont.). Data for progressive thermal and chemical demagnetization of HPL sample series.

Sample Number	Cum. Strat. Int.(m)	Fm*	Texture	demag type	Primary Component Polarity	Primary Component Stability T(°C);C(h)	Secondary Component Polarity	Secondary Component Stability T(°C);C(h)	Notes†
HPL-16	26.5	H	f.-med sand	Therm	Reversed?	500-550	Normal	500-550	tracks toward reversed 600° spurious.
HPL-17	26.5	H	f.-med sand	Chem	Reversed?	>80	Normal	>80	tracks toward reversed
HPL-18	31.0	H	f.-med sand	Chem	Normal	>80	None	---	PLF
HPL-19	31.0	H	f.-med sand	Therm	Normal	500-550	Normal	100-150	skewed 50-60° clockwise tracks from PLF
HPL-20	35.5	H	silt-f.sand	Chem	Reversed?	>80	Normal	>80	tracks toward reversed
HPL-21	35.5	H	silt-f.sand	Therm	Reversed?	200-250	Normal	(?)	tracks toward reversed uninterpretable >200°
HPL-22	39.5	H	f-crs.sand	Therm	Reversed?	600-650	Normal	600-650	tracks toward reversed skew 45°cl.;250° spur
HPL-23	39.5	H	f-crs.sand	Chem	Normal	39-80	None?	---	skewed 30° clockwise
HPL-24	45.0	H	vf.sand	Chem	Reversed?	>80	Normal	>80	tracks toward reversed
HPL-25	45.0	H	vf.sand	Therm	Reversed	>650	Normal	600-650	tracks to reversed; 250° step spurious
HPL-26	48.5	H	cly-crs.sand	Chem	Reversed	>80	Normal	NRM-14	tracks to reversed; skewed 80° c.clockwise
HPL-27	48.5	H	cly-crs.sand	Therm	Reversed	500-550	Normal	100-150	tracks to reversed; skewed 60-80° c.clock
HPL-28	58.0	S	vf-f.sand	Therm	Reversed?	550-600	Normal	300-350	tracks toward reversed; normal skewed 45° cl.
HPL-29	58.0	S	vf-f.sand	Chem	Normal	49-80	None	---	skewed 45° clockwise
HPL-30	60.0	S	f-med sand	Chem	---	---	---	---	too strong to measure

*H=Harold Fm; S=Shoemaker Gravels; O=Old Alluvium †PLF=present local field

Table 4-1(cont.). Data for progressive thermal and chemical demagnetization of HPL sample series.

Sample Number	Cum. Strat. Int.(m)	Fm*	Texture	demag type	Primary Component		Secondary Component		Notes†
					Polarity	Stability T(°C);C(h)	Polarity	Stability T(°C);C(h)	
HPL-31	60.0	S	f-med sand	Therm	---	---	---	---	too strong to measure
HPL-32	74.0	S	vf sand	Chem	Normal	>80	Normal	NRM-14	skewed 45° clockwise
HPL-33	74.0	S	vf sand	Therm	Reversed	550-600	Normal	500-550	tracks to reversed
HPL-34	104.0	S	paleosol	Therm	Reversed?	550-600	---	---	tracks toward reversed?
HPL-35	104.0	S	paleosol	Therm	Normal	550-600	None	---	PLF; 650° spurious?
HPL-36	138.0	S	paleosol	Therm	Normal	550-600	None	---	PLF; 650° spurious?
HPL-37	138.0	S	paleosol	Chem	Normal	49-80	None	---	skewed 10-30° clock.
HPL-38	140.0	O	silt-vf.sand	Chem	Normal	49-80	None	---	skewed 10-30° clock. PLF
HPL-39	140.0	O	silt-vf.sand	Therm	Normal	600-650	None	---	not skewed; 650 rev? PLF

*H=Harold Fm; S=Shoemaker Gravels; O=Old Alluvium †PLF=present local field

Figure 4-3. Summary diagram of HPL and SPL data. (a) Tilt-corrected plot of least-squares lines fit to groups of points describing stable reversed remanence directions for HPL 1-17. These data have a mean declination (X) of 173° and inclination of -51°. (b) Tilt-corrected plot of natural remanent magnetism (NRM) for HPL 1-17. Many of the samples possess reversed NRMs, reflecting the strength and stability of their reversed primary magnetism. (c) Tilt-corrected plot of HPL 1-17 after heating to 650° C. Some samples have reversed remanence that is stable to >650° C. The directions for these stable samples suggest 20° or more of clockwise rotation. (d) Geographic plot of least-squares lines for HPL 35, 36, 37, 38 and 39. The vector mean (+) has a declination of 11° and an inclination of 59°, parallel to the present local field. There is no rotation apparent in these data. (e) Geographic plot of least-squares lines for all HPL samples displaying stable normal remanence. The vector mean (+) has a declination of 30° and an inclination of 58°. The scatter in these data includes the present local field direction, but seem to be displaced in declination about 20° in a clockwise sense. (a) Tilt-corrected plot of least-squares fit lines for all SPL samples with stable reversed remanence (SPL 1,2,5,6,8,10,11,14). Note the wide scatter in the data, which lies along the path followed by samples as they track toward reversed with heating. Many samples are not reaching the primary reversed direction before becoming unstable. The vector mean direction (X) has a declination of 184° and inclination of -21°. (b) Tilt-corrected plot of least-squares fit lines for all SPL samples with stable normal remanence (SPL 1-12,16-19). Scatter in the suggest incomplete separation of over-printed normal and primary reversed components, as in (a). The vector mean direction (+) has a declination of 21° and inclination of 57°.

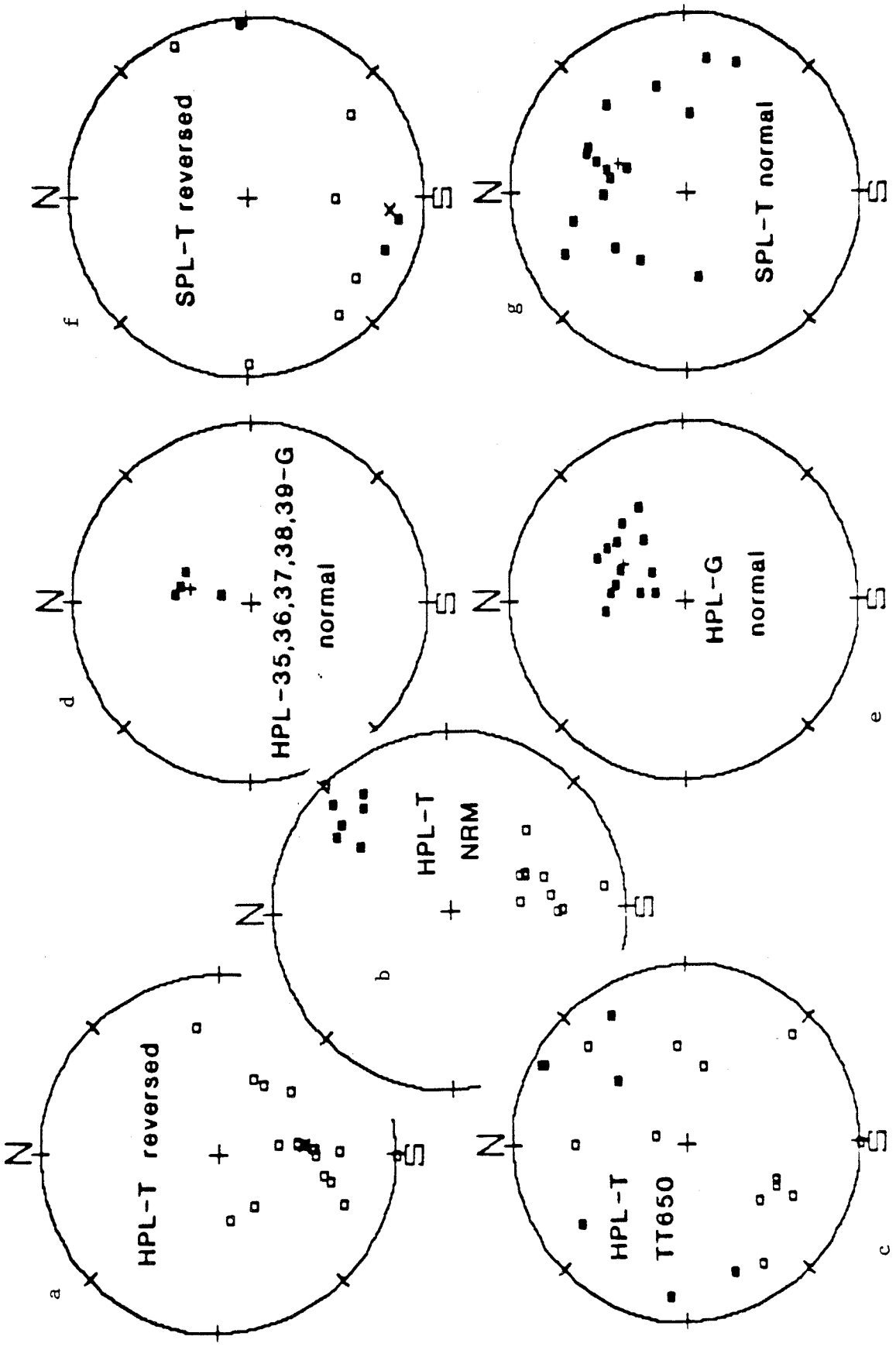
HPL-T reversed
N
S
a
HPL-T
NRM
b
HPL-T
TT650
c
HPL-35,36,37,38,39-G
normal
d
HPL-G
normal
e
SPL-T reversed
f
SPL-T normal
g

Figure 4-4. Summary diagram of HPL data. Many samples in the upper part of the Harold Formation track from normal toward reversed directions with both thermal and chemical progressive demagnetization. Sample HPL-24 was chemically demagnetized and moves from normal polarity in the direction of reversed as the less stable components of magnetism are stripped off. Thermal demagnetization of HPL-25 produces a demagnetization path similar to HPL-24, but the normal overprint is effectively removed to reveal a reversed primary remanence. The 250° demagnetization step is spurious. It is difficult to be sure that the 650° step is not simply random behavior of the sample after removal of all remanence. For sample HPL-26, chemical demagnetization strips a normal component from a two-component NRM direction, and the resultant vector moves in the direction of reversed polarity. The lower and middle parts of the Shoemaker Gravel at the HPL site are reversed. Samples HPL-33 and 34 display behavior similar to HPL 24, 25 and 26. Sample HPL 33 taken from the lower Shoemaker Gravel, tracks systematically toward a reversed direction with increased heating, finally reaching a true reversed remanence before becoming unstable at 550-600° C. There can be little doubt that this sample possesses a stable reversed polarity component. Sample HPL 34 was taken from a paleosol in the middle of the Shoemaker Gravel section and displays similar behavior to HPL-33 with progressive thermal demagnetization. HPL-34 does not lose its over-printed normal component before its reversed component becomes unstable at 550-600°.

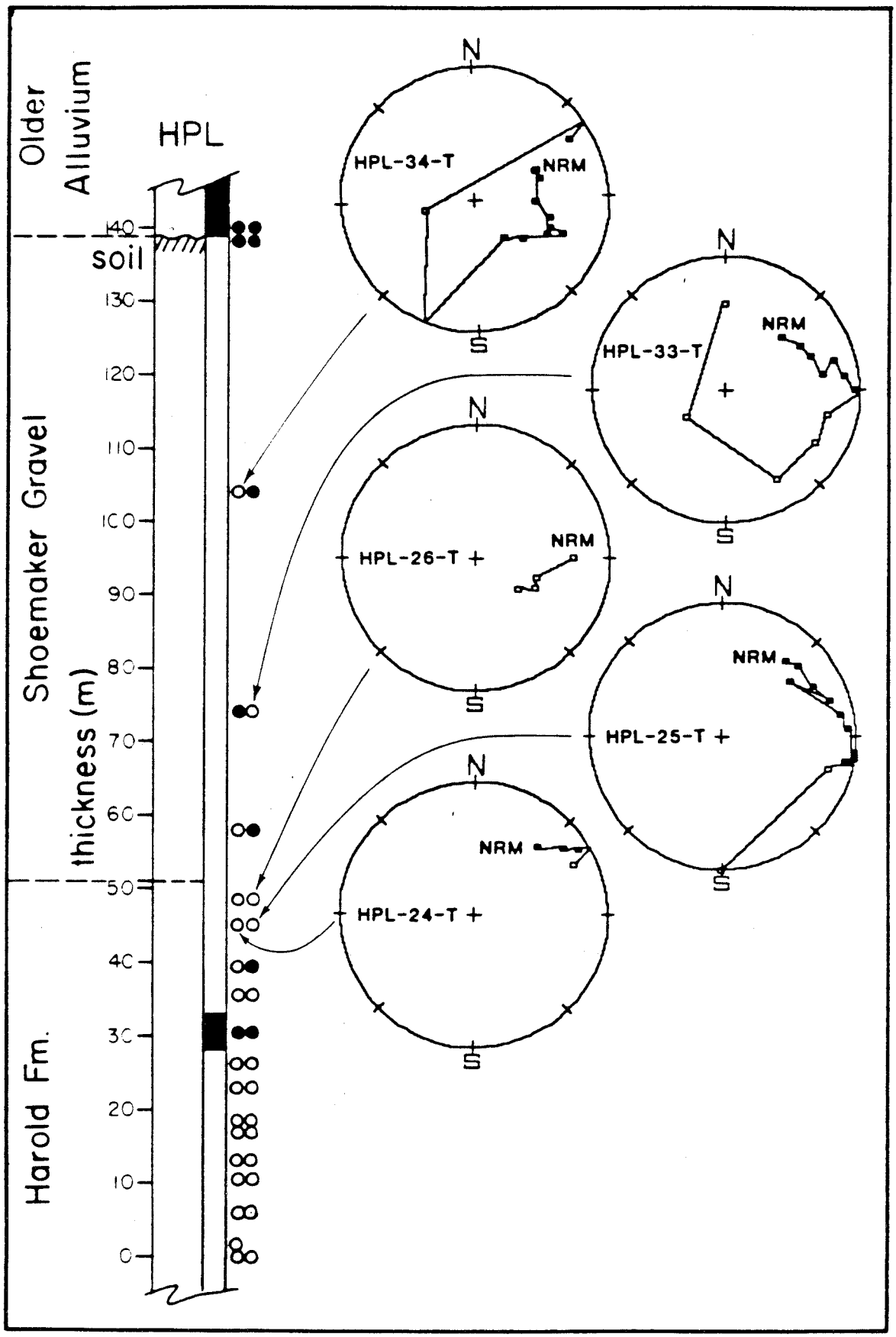
Older Alluvium
HPL
soil
Shoemaker Gravel
thickness (m)
Harold Fm.
140
130
120
110
100
90
80
70
60
50
40
30
20
10
0
N
S
HPL-34-T
NRM
HPL-33-T
NRM
HPL-26-T +
NRM
HPL-25-T +
NRM
HPL-24-T +
NRM

of normal vectors for samples from the Older Alluvium and upper Shoemaker Gravels (HPL 35-39; Figure 4-3d). These samples, which include both buried paleosols and unweathered sediment, raise the possibility that the Brunhes/Matuyama polarity transition occurred during deposition of the Shoemaker Gravel.

The declination directions of samples exhibiting normal polarity (HPL 19,22,28,29,32,35-37) are consistently displaced from magnetic north in a clockwise sense (Figure 4-3e). This displacement is clearly not present in samples from the upper Shoemaker Gravel and Older Alluvium (HPL 38,39; Figure 4-3d). There is also some suggestion that reversed samples in the Harold Formation have been displaced 20° in a clockwise sense, since after the 650° demag step the vectors tend to cluster around an azimuth of 200° (HPL 1,2, 4-7,12) rather than 180° (Figure 4-3c). Unavoidable field orientation errors and physical disturbance due to handling of these unconsolidated sediments introduce some uncertainty as to the magnitude and sense of this displacement. It is also possible that the observed variations in azimuth record virtual geomagnetic pole positions rather than time-averaged directions.

4.3.2 Shoemaker Gravel: Power-Line Road Section (SPL)

In an effort to locate the Brunhes/Matuyama polarity transition more accurately, samples SPL 1 to 19 were collected along the power-line road that lies north of the AT&SF railroad tracks in sec 20, R5W T3N (Figure 4-1; Plate 1A; Table 4.2; Appendix A). They include part of the Shoemaker Gravel (SPL 1-13) and Older Alluvium (SPL 14-19). An unconformity separates the two units at this locality (Foster, 1980).

All samples were retrieved in quartz-glass tubes and progressively thermally demagnetized in 10 steps up to 650° C. Despite the addition of

sodium silicate, several samples fell apart during heating (SPL 4,7,8, 9,14,15).

Two samples in the SPL section are clearly reversed (SPL 1,5; Figure 4-5) and five track toward reversed (SPL 2,3,6,13,17; e.g. Figure 4-5; Table 4.2). SPL-5 is a textbook example of a reversely magnetized sample with a normal, present local field overprint (PLF; declination ~15°, inclination ~60°). Sample SPL-17 lies within the Older Alluvium as mapped by Foster (1980) and clearly tracks to a reversed polarity. Three samples that disaggregated yield consistently uninterpretable results (SPL 4,9,15; Appendix A).

Two samples in the SPL section are clearly of normal polarity (SPL 7,18; Figure 4-5). SPL-7 possesses a stable present local field (PLF) component. During progressive demagnetization of SPL-18 a normal (PLF) component is removed to reveal a more stable normal remanence that is displaced 45° in a clockwise sense (Figure 4-5). The stable, displaced normal direction shown by SPL 18 may represent a primary normal component. The unsystematic behavior of five other samples (SPL 8,10,10.5,11,19) suggest a combination of reversed remanence and normal overprint (Appendix A), neither of which is stable to high temperature.

The Brunhes/Matuyama polarity reversal certainly lies above SPL 5. The most reasonable interpretation of the data at SPL seems to be that the Brunhes/Matuyama polarity transition is above SPL-17, possibly below SPL-18. The possibility that the entire SPL section is reversed cannot be ruled out.

There are suggestions of both clockwise (SPL 1,12,17) and counter-clockwise (SPL 2,6,10.5,11,13,18) displacements of the SPL sample declinations, measuring between 25 and 75° (Figure 4-3f,g).

Table 4-2. Data for progressive thermal demagnetization of SPL sample series.

Sample Number	Cum. Strat. Int.(m)	Fm*	Texture	demag type	Primary Component Polarity	Primary Component Stability T(°C)	Secondary Component Polarity	Secondary Component Stability T(°C)	Notes†
SPL-1	0.0	S	clay-gran	Therm	Reversed	550-600	Normal	200-300	skewed 35° c.clockwise sample coherent;no 650
SPL-2	35.0	S	f.-med sand	Therm	Reversed	550-600	Normal	200-300	skewed 25° clockwise sample coherent
SPL-3	41.0	S	med-crs sand	Therm	Reversed?	>600	Normal	550-600	tracks toward reversed some disaggregation
SPL-4	45.5	S	f.sand-gran	Therm	Ambiguous	(?)	Normal	200-300	tracks toward reversed serious disaggregation
SPL-5	51.5	S	silt-f.sand	Therm	Reversed	>650	Normal	100-200	not skewed sample coherent
SPL-6	52.5	S	med-crs sand	Therm	Reversed?	>550	Normal	300-400	skewed 45° clockwise some disag;no 600,650
SPL-7	56.0	S	f.-med sand	Therm	Normal	>650	Normal	300-350	PLF; some disag; 600 spurious
SPL-8	61.5	S	f.sand-gran	Therm	Reversed	600-650	Normal	350-400	tracks toward reversed? some disag;400 spur.
SPL-9	64.0	S	m.sand-gran	Therm	Normal?	600-650	Normal	(?)	PLF; serious disaggregation
SPL-10	67.0	S	clay-gran	Therm	Reversed?	550-600	Normal	350-400	tracks toward reversed? coherent sample
SPL-10.5	69.0	S	f.-med sand	Therm	Reversed	600-650	Normal	550-600	tracks to reversed some disag
SPL-11	75.5	S	f.-med sand	Therm	Ambiguous	(?)	Normal	200-300	uninterpretable coherent sample
SPL-12	78.0	S	f-v.crs sand	Therm	Reversed	550-600	Normal	100-200	skewed 55° c.clockwise some disag
SPL-13	81.0	S	f.-crs sand	Therm	Reversed	>650	Normal	200-300	skewed 10-35° clockwise coh. sample;550 spur.
SPL-14	83.0	O	f.-med sand	Therm	Reversed	550-600	None	---	reversed w/bedding cor. serious disaggregation

*H=Harold Fm; S=Shoemaker Gravels; O=Old Alluvium †PLF=present local field

Table 4-2. Data for progressive thermal demagnetization of SPL sample series.

Sample Number	Cum. Strat. Int.(m)	Fm*	Texture	demag type	Primary Component Polarity	Primary Component Stability T(°C)	Secondary Component Polarity	Secondary Component Stability T(°C)	Notes†
SPL-15	86.0	O	vf.sand-gran	Therm	Ambiguous	(?)	Normal?	>650	uninterp;550,650 spur. serious disaggregation
SPL-16	93.0	O	paleosol	Therm	Reversed?	600-650	Normal	550-600	tracks to reversed coherent sample
SPL-17	98.0	O	f.-crs sand	Therm	Reversed	>650	Normal	550-600	tracks to reversed some disaggregation
SPL-18	103.0	O	f.-crs sand	Therm	Normal	600-650	Normal	300-350	PLF tracks skewed normal
SPL-19	106.0	O	m-v.crs sand	Therm	Normal	550-600	Normal	100-200	normal w/bedding cor.

*H=Harold Fm; S=Shoemaker Gravels; O=Old Alluvium †PLF=present local field

Figure 4-5. Summary diagram of SPL data. The lower part of the Shoemaker Gravel section at the SPL site is clearly reversed. Sample SPL-1 tracks across the plot from a two-component direction to a reversed position before becoming unstable at 600-650° C. SPL-5 displays a single, very stable reversed direction from NRM through 550° C. The linearity of the points in the demagnetization path indicate that a single reversed component is present. A weak present local field overprint is removed at 100°, as evidenced by the "hook" at the beginning of the Ray-Park plot demagnetization path. Many samples within the upper Shoemaker Gravel and Older Alluvium at the SPL site track to reversed, indicating that the entire Shoemaker Gravel section, and possibly the Older Alluvium, has primary reversed polarity. Sample SPL-3 tracks to reversed with removal of a skewed normal overprint. The 650° step is considered questionable. SPL-6 clearly tracks from a present local field direction to a skewed reversed direction with stepwise heating. The behavior of SPL-17, which is in the Older Alluvium as mapped by Foster (1980), is similar to SPL-3 and 6; the sample systematically tracks toward reversed. SPL-17 probably never completely reaches the true direction of its reversed remanence component, however. Some samples from the SPL section display stable normal directions. For SPL-7 and 18, a case can be made for normal overprinting of primary reversed directions. Normal remanence for SPL-7 is stable to 350° C at which point the vector begins to track across the plot. The sample becomes unstable at 550-600° C. The track between 350 and 550° C could be due to a reversed component that disappeared at the same temperature as a normal overprint. The polarity of SPL-18 is stable and normal up to 600° C. The 650° C step can be interpreted as random noise after complete demagnetization of sample. The plot is not linear, suggesting that at least two normal components of magnetization are present.

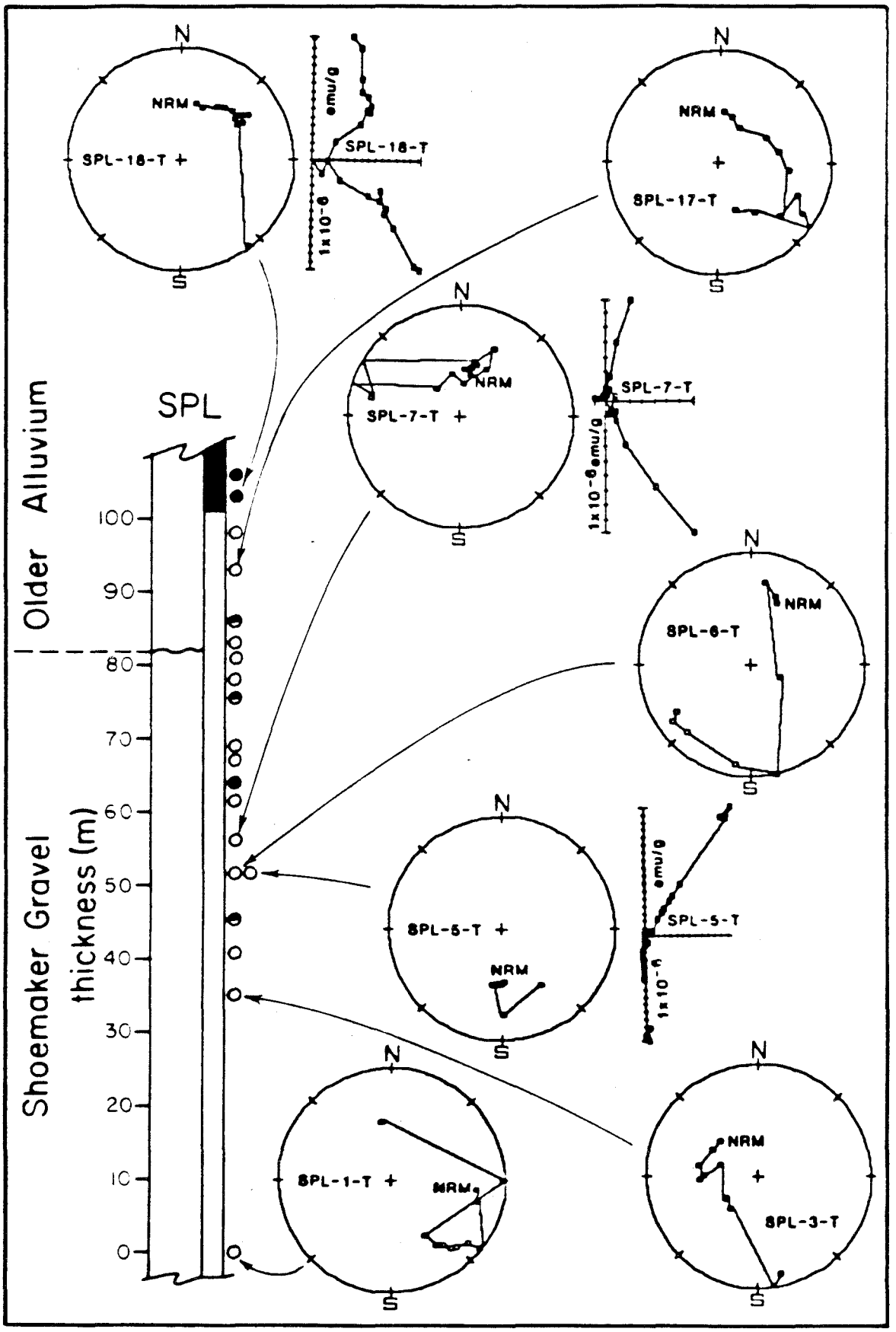
SPL
Older Alluvium
Shoemaker Gravel
thickness (m)
100
90
80
70
60
50
40
30
20
10
0
N
S
NRM
SPL-18-T +
SPL-18-T
emu/g
1x10-6
SPL-17-T
SPL-7-T +
SPL-7-T
1x10-6emu/g
SPL-6-T
SPL-5-T +
SPL-5-T
SPL-1-T +
SPL-3-T

4.3.3 Mojave River Forks Section (MRF)

In order to extend the time constraints established in Cajon Pass to the range front of the San Bernardino Mountains, ten samples were collected from the bluffs along the Mojave River due east of the Deep Creek flood control dam in sec 14, R4W T3N (MRF 1-10; Figure 4-1; Table 4-3; Appendix A). Although the MRF section is clearly part of the Victorville Fan complex, it was derived from the western San Bernardino Mountains, as evidenced by clast lithologies and antecedent drainage patterns. It may be a facies equivalent of the Shoemaker Gravel in Cajon Pass, although this is difficult to demonstrate.

Procedures for treatment and measurement of the MRF samples were identical to those employed at the SPL site, except that the 450° C thermal demagnetization step was omitted. Sample disaggregation was not a serious problem in the MRF sample series.

The majority of samples from the MRF section unquestionably displays reversed polarity (MRF 1-4,6-8; Figure 4-6). MRF 5, 9 and 10 appear to be tracking toward a reversed direction (Figure 4-6). The Brunhes/ Matuyama polarity reversal is certainly above MRF 8, and may lie below MRF 10; MRF 10 may be overprinted, and the entire section may actually be reversed.

Three of the MRF sample series show a 35-50° clockwise displacement in declination (MRF 4,6,7), two appear unrotated (MRF 2,8) and two suggest 35° of counterclockwise displacement (MRF 1,3; Figure 4-6). The vector mean of least-squares directions for normal and reversed components suggests a 20-30° clockwise displacement.

4.3.4 Arrastre Canyon Fan Section (ACF)

Eight samples were collected from the Arrastre Canyon Fan in sec 19,

Table 4-3. Data for progressive thermal demagnetization of MRF sample series.

Sample Number	Cum. Strat. Int.(m)	Fm*	Texture	demag type	Primary Component Polarity	Primary Component Stability T(°C)	Secondary Component Polarity	Secondary Component Stability T(°C)	Notes†
MRF-1	0.0	S?	vf-crs sand	Therm	Reversed	600-650	Normal	100-200	Skewed 35° c. clockwise
MRF-2	3.0	S?	vf-f.sand	Therm	Reversed	550-600	Normal	100-200	not skewed
MRF-3	6.0	S?	vf-f.sand	Therm	Reversed	550-600	Normal	100-200	skewed 35° c. clockwise
MRF-4	13.5	S?	silt-vf.sand	Therm	Reversed	>650	Normal	NRM-100	skewed 35-50° clockwise
MRF-5	23.5	S?	vf-med.sand	Therm	Reversed?	300-400	Normal	200-300	skewed 80° c. clockwise
MRF-6	33.5	S?	vf-crs.sand	Therm	Reversed	550-600	Normal	200-300	skewed 45° clockwise (100° step spurious)
MRF-7	44.5	S?	cl-silt	Therm	Reversed?	450-500	Normal	200-300	skewed 50° clockwise
MRF-8	54.5	S?	med-crs.sand	Therm	Reversed	550-600	Normal	200-300	skewed 15° c. clockwise
MRF-9	63.5	S?	vf-med.sand	Therm	Reversed?	450-500	Normal	300-400	tracks toward reversed
MRF-10	70.5	O?	paleosol	Therm	Normal?	600-650	Normal	100-200	may go reversed at 650°

*H=Harold Fm; S=Shoemaker Gravels; O=Old Alluvium †PLF=present local field

Figure 4-6. Summary diagram of MRF data. Least-squares lines fit to the data for each sample from the MRF series show that this section is clearly reversed. Both primary reversed directions and normal overprint directions appear to be skewed 20-30° in a clockwise sense. Geographic plot of least-squares fit lines for all MRF samples displaying stable reversed directions (MRF 1-4,6-8), indicates that the MRF sample series is clearly reversed. The vector mean direction (X) has a declination of 199° and inclination of -56°, suggesting a clockwise displacement of 20°. The limited number of data points, however, preclude any firm conclusion about the possibility of rotations. In a geographic plot of least-squares fit lines for all MRF samples displaying stable normal directions (MRF 1-5,7-9), the vector mean (+) has a declination of 35° and an inclination of 51°, indicating a clockwise skewing of directions. More data would be required to make a definitive conclusion regarding the significance of this displacement of the mean direction. Some samples in the MRF series display questionable primary polarity. The data are interpreted as consistent with primary reversed magnetization with secondary normal overprinting. Sample MRF-5 tracks toward reversed up to 300° as normal component is stripped off, but magnetism becomes unstable at 400° suggesting that the primary component disappeared before the later overprint was removed. MRF-9 behaves similarly, becoming unstable at 400° after tracking in a direction that suggests the combination of a primary reversed component and a normal overprint. Sample MRF-10 can be interpreted as having primary normal remanence. Although the 650° demag step reveals a possible stable reversed direction, this direction may simply represent random drift of the remnant vector. More samples from the upper part of the MRF section would be required to confirm the normal polarity of this part of the MRF section.

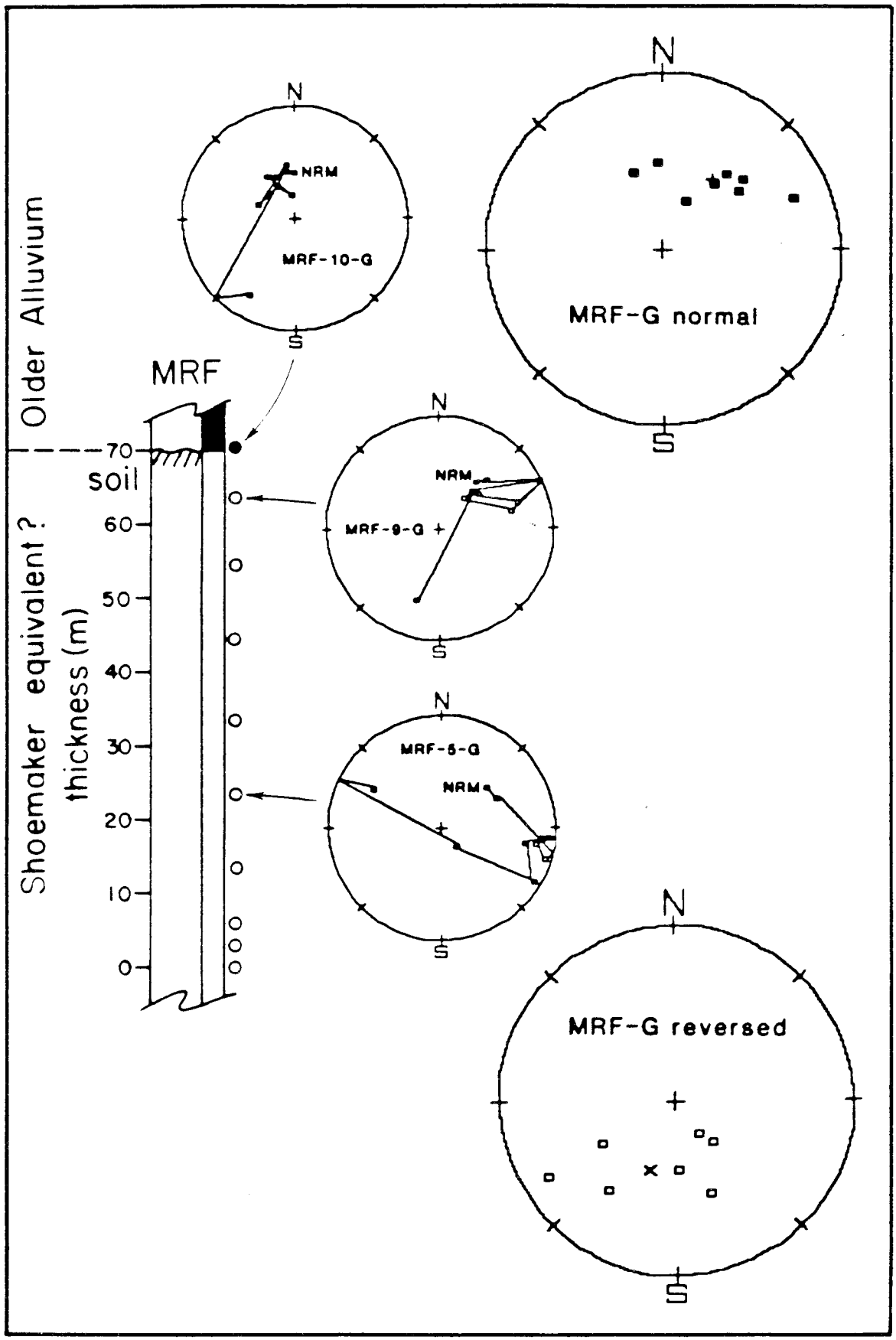
Older Alluvium
Shoemaker equivalent?
thickness (m)
MRF
soil
70
60
50
40
30
20
10
0
N
S
NRM
MRF-10-G
MRF-9-G
MRF-5-G
MRF-G normal
MRF-G reversed

R2W T4N, where a 15-meter-thick section of fine sands is exposed in the fan-head trench (Figure 4-1; Plate 1B; Table 4.4; Appendix A). The Arrastre Canyon Fan deposits are continuous with the Ord River Gravel in the Marianas area.

The entire ACF section possesses a stable normal remanence (Figure 4-7), and there is no suggestion of a reversed remanence at 650° C (Figure 4-7). It seems reasonable to conclude that the entire Arrastre Canyon Fan section was deposited after the Brunhes/Matuyama polarity transition.

4.3.5 Other Sites: (ORD, HRF, ORM, RSR, BRR)

Thirteen samples were taken from localities where complete sections could not be sampled due to poor exposure (ORD 1-4,HRF 1-2,ORM 1-4,RSR 1-2, BRR 1; Figure 4-1; Plate 1B; Table 4-4 & 4.5; Appendix A). They are discussed from west to east along the range front, starting near Deep Creek.

4.3.5.1 Ord River Gravel (ORD)

Four samples were taken from the Ord River deposits and correlative Old Fan gravels along the western flank of the Ord Mountains (ORD 1-4; Table 4-5; Appendix A). Fluvial sands and rounded gravels of the Ord River deposits interfinger with, and underlie, the fanglomerate of the Old Fan gravel; a deep soil is developed on both deposits. Based on lithologic similarities, drainage reconstructions and geomorphic criteria, Ord River and Old Fan deposits are considered correlative with each other and contemporaneous with the Victorville Fan sediments exposed across the Mojave River to the west.

The ORD samples were collected, treated and measured in the same manner as for the SPL site.

ORD 1 was retrieved from a soil zone exposed in a roadcut in sec 32, R3W T4N in the Apple Valley Highlands area. It displays a very stable normal

Table 4-4. Data for progressive thermal demagnetization of ACF, RSR and BRR sample series.

Sample Number	Cum. Strat. Int.(m)	Fm*	Texture	demag type	Primary Component Polarity	Primary Component Stability T(°C)	Secondary Component Polarity	Secondary Component Stability T(°C)	Notes†
ACF-1	---	A	f.sand-gran	Therm	Normal	600-650	None	---	skewed 35-85° clockwise
ACF-2	0.0	A	vf-crs.sand	Therm	Normal	550-600	Normal	450-500?	not skewed PLF overprint
ACF-3	1.0	A	f.sand-gran	Therm	Normal	500-550	Normal	300-400?	not skewed PLF overprint
ACF-4	4.0	A	f-crs.sand	Therm	Normal	500-550	Normal	300-400?	not skewed PLF overprint
ACF-5	9.0	A	vf-f.sand	Therm	Normal	550-600	None	---	skewed <10° clockwise PLF?
ACF-6	10.0	A	vf-f.sand	Therm	Normal	600-650	None	---	skewed <10° clockwise PLF?
ACF-7	12.0	A	vf=f.sand	Therm	Normal	600-650	None	---	skewed <10° clockwise PLF?
ACF-8	13.5	A	paleosol	Therm	Normal	550-600	None	---	not skewed PLF!
RSR-1	0.0	?	vf-f.sand	Therm	Reversed	600-650	Normal	100-200	skewed 10° c. clockwise
RSR-2	5.0	?	clay-silt	Therm	Reversed	>650	Normal	100-200	not skewed
BRR-1	---	A	paleosol	Therm	Normal	550-600	None	---	skewed 35° c. clockwise

*A=Arrastre Cyn Fan

†PLF=present local field

Figure 4-7. Summary diagram of samples from the Arrastre Canyon Fan Deposits. Samples from the ACF site show this section to be unquestionably normal. There is no suggestion of reversed remanence, even after high temperature demagnetization. Geographic least-squares fit lines for all ACF samples displaying stable normal directions (ACF 1-8) show a tight clustering of normal directions which coincides with the present local field direction, the vector mean direction (+) has a declination of 7° and an inclination of 54°. After heating to 650°C, none of the samples are really suggestive of a primary reversed component. The vector mean (+) declination is 17° and inclination is 35°, still roughly the present local normal field direction. The samples at the RSR site are clearly reversed. RSR-1 displays primary reversed remanence, starting with the NRM measurement. A normal component of magnetism is removed by 200° C as seen in the "hook" on the Ray-Park plot demagnetization path. Linearity of points on the Ray-Park diagram supports a single component of reverse polarity magnetization. Clustering of points is excellent, and the direction of RSR-1 is in close agreement with the direction for RSR-2 below. The results for RSR-2 are even better than for RSR-1. The removal of the normal overprint is accomplished by 200° C. A remarkably linear demagnetization path characterizes the plot for RSR-2; there is clearly one component of primary reversed magnetization. Sample BRR-1 is of normal polarity, but has a shallow inclination. No bedding correction was attempted for BRR-1 since bedding is difficult to measure at the site. Deformation of the sediments is likely, since the site is near a fault. The linearity of the demagnetization path for BRR-1 on the Roy-Park plot is evidence of a single normal remanence direction of probably primary nature.

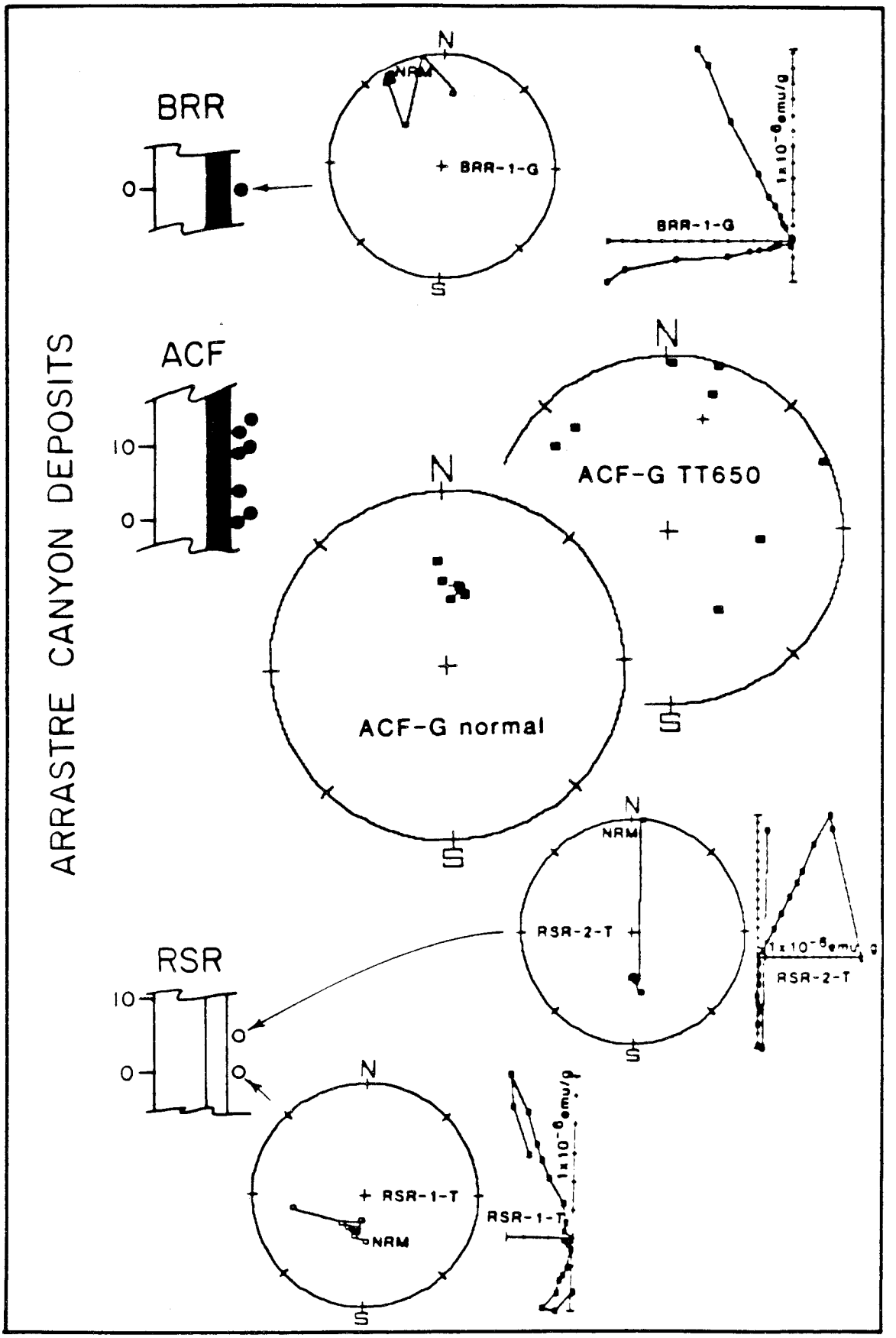
ARRASTRE CANYON DEPOSITS
BRR
0
N
NRM
+ BRR-1-G
S
1x10⁻⁶emu/g
BRR-1-G
ACF
10
0
N
ACF-G TT650
S
N
ACF-G normal
S
RSR
10
0
N
NRM
RSR-2-T
S
1x10⁻⁶emu/g
RSR-2-T
N
+ RSR-1-T
NRM
S
1x10⁻⁶emu/g
RSR-1-T

Table 4-5. Data for progressive thermal demagnetization of ORM, HRF, and ORD sample series.

Sample Number	Cum. Strat. Int.(m)	Fm*	Texture	demag type	Primary Component Polarity	Primary Component Stability T(°C)	Secondary Component Polarity	Secondary Component Stability T(°C)	Notes†
ORM-1	---	OR	vf-med,sand	Therm	Normal	>650	None	---	skewed 10° clockwise PLF
ORM-2	---	OR	f-crs sand	Therm	Normal	550-600	None	---	skewed 35° clockwise post-tilt overprint
ORM-3	---	OR	slt-crs.sand	Therm	Normal	>650	Normal	100-200	pre-tilt normal with PLF overprint
ORM-4	---	OR	slt-crs.sand	Therm	Normal	>650	Normal	100-200	pre-tilt normal with PLF overprint
HRF-1	---	O	vf-f.sand	Therm	Normal	500-550	None	---	skewed 60-70° clockwise
HRF-2	---	O	cly-med.sand	Therm	Normal	>650	None	---	not skewed; 500° spur.
ORD-1	---	OR	m-vcrs.sand	Therm	Normal?	600-650	Normal	100-200	skewed 45-65° c. clock.
ORD-2	---	S?	slt-vf.sand	Therm	Reversed	600-650	Normal	300-400	tracks to reversed PLF overprint
ORD-3	---	S?	paleosol	Therm	Normal	600-650	None	---	skewed 30° clockwise
ORD-4	---	S?	m-crs.sand	Therm	Reversed?	550-600	Normal	300-400	tracks toward reversed PLF overprint

*OR=Ord River; S=Shoemaker Gravels; O=Old Alluvium †PLF=present local field

remanence, skewed 50-60° in a counter-clockwise sense (Figure 4-8).

ORD 3 is a sample of the soil developed on the surface of the Old Fan deposits. It similarly shows a stable normal direction (Figure 4-8). ORD 2 and 4 were taken from the Ord River sands that interfinger with the Old Fan deposits in roadcut exposures along the power-line road that lies east of Deep Creek Road in sec 7, R3W T3N. ORD 2 and 4 both track toward reversed polarity (Figure 4-8). The Brunhes/Matuyama polarity reversal must have occurred after deposition of the sampled Ord River deposits, but prior to development of the soil on both the Old Fan and Ord River deposits.

4.3.5.2 Hesperia: Reynolds Fossil-Locality (HRF)

Two samples were taken in the Victorville Fan sediments just east of Hesperia Road in sec 27, R4W T5N at San Bernardino County vertebrate paleontological localities 1.114.17 (HRF 1) and 1.114.11 (HRF 2; Table 4-5; Appendix A-5). The sediments at these localities are greenish-gray lacustrine(?) silts and have been provisionally assigned to the late Blancan or Irvingtonian land mammal age (R. E. Reynolds, pers. comm., 1982). Demagnetization was carried out following the procedures used for the MRF samples.

Both HRF 1 and 2 display stable normal remanence (Figure 4-8). The declination in HRF 1 is skewed 75° in a clockwise sense; HRF 1 is not skewed. There is no suggestion or reversed remanence in either HRF 1 or 2.

4.3.5.3 Ocotillo Ridge: Marianas Rancho (ORM)

ORM 1-4 were collected in exposures along Ocotillo ridge (sec 15&22, R3W T4N) of the Ocotillo Ridge deposits, a facies of the Ord River deposits on the north flank of the Ord Mountains (Table 4-5; Appendix A). Demagnetization of the ORM samples followed the same procedure as for the ORD samples.

When bedding is restored, all of the ORM samples display stable normal

Figure 4-8. Summary diagram of Ord River Gravel data. Samples from the HRF locality are of normal polarity, with no suggestion of primary reversed remanence. HRF-1 is clearly normal and stable to 500° C, although the declination direction is skewed 75° in a clockwise direction. HRF-2 displays a stable normal direction that is roughly the present local field direction. The 550° step is spurious. The linear alignment of points on the Roy-Park plot suggest a single component of normal magnetization. The ORD series were taken from three diffent units at two localities described in detail in Section 4.3.5.1. ORD 1 has a stable normal remanence that is skewed 50-60° in a counter-clockwise sense and is clearly of primary normal polarity. ORD 2 tracks to a reversed direction, albeit with shallow positive inclination. The dip of bedding is not known and has not been taken into account. A clearly normal remanence in ORD 3 is stable to 600°, with no hint of a primary reversed component. Sample ORD 4 tracks toward reversed from the present local field direction, becoming unstable at 600°. The ORM sample series were taken in the uppermost unit of the Ord River Gravel along the anticline that underlies Ocotillo Ridge. Thus, the coincidence of the directions for these units on the tilt-corrected equal-area plot constitutes a crude fold test, establishing the primary nature of their normal magnetism. ORM-1 is unquestionably normal and shows the present local field. Sample ORM-2 has a normal declination, but its inclination is very shallow, perhaps due to an error in bedding attitude. ORM-3 was taken, along with ORM-4, in the debris-flow unit of the Ocotillo Ridge trench. The two samples together constitute a test of the accuracy of the sampling techniques. The beds at the trench dip 55° northwestward. Their general agreement with the results for ORM 1 and 2 constitute a crude fold test for primary normal remanence.

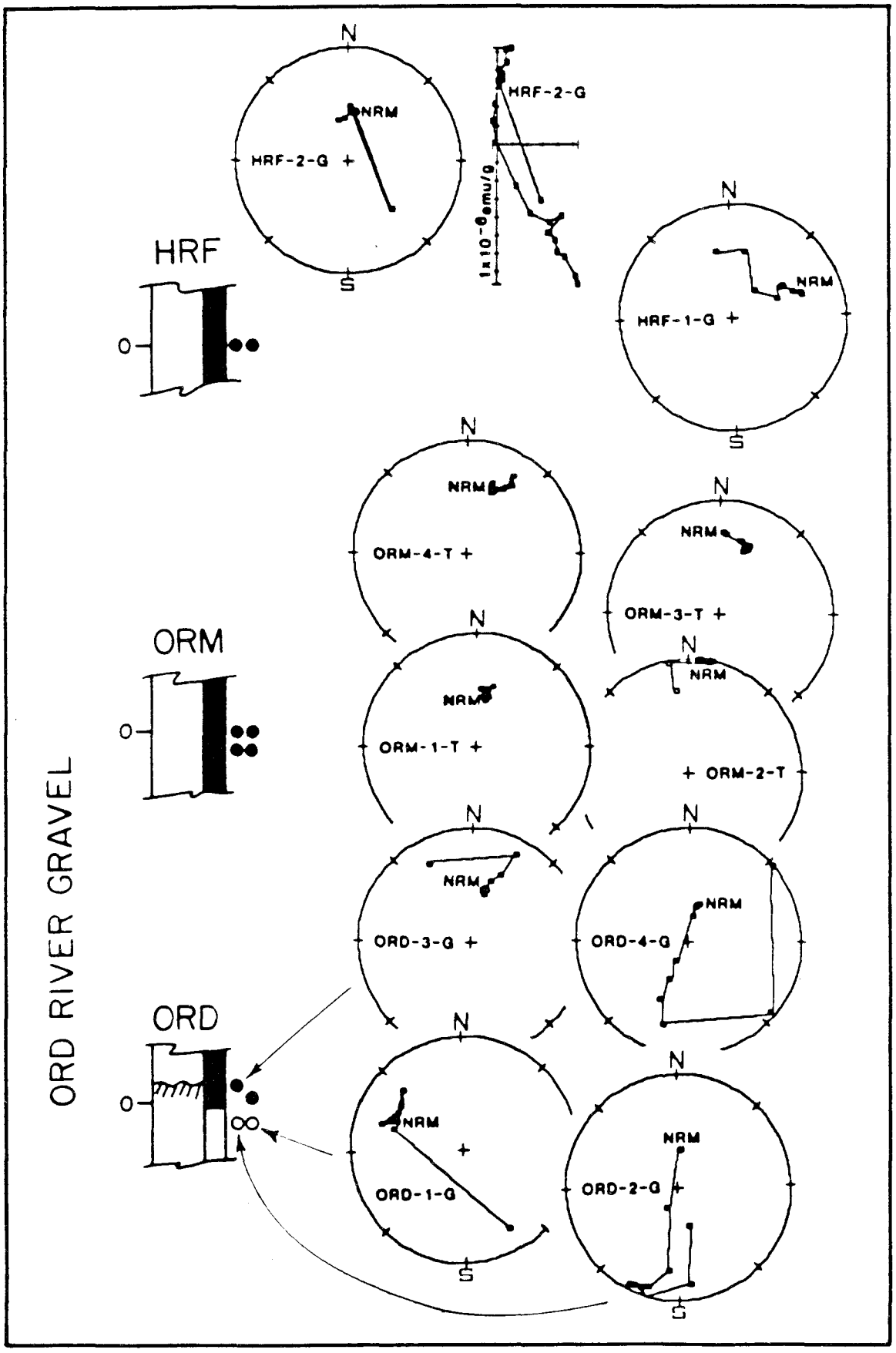
ORD RIVER GRAVEL
HRF
ORM
ORD
N
S
NRM
HRF-2-G +
HRF-2-G
1x10⁻⁶emu/g
HRF-1-G +
ORM-4-T +
ORM-3-T +
ORM-1-T +
ORM-2-T
ORD-3-G +
ORD-4-G
ORD-1-G
ORD-2-G

directions (Figure 4-8). ORM 1 and 2 are from the soil zone that caps Ocotillo ridge; ORM 3 and 4 are duplicate samples from the debris-flow deposit exposed in the Ocotillo Ridge trench. Declination directions are skewed 10 to 30° in a clockwise sense. Both Ocotillo Ridge deposits and soil are younger than the Brunhes/Matuyama reversal.

4.3.5.4 Rock Springs Road Deposits (RSR)

Two samples were taken from fine-grained deposits exposed along the Bowen Ranch Road at Rock Springs in sec 30, R2W T4N (RSR 1,2; Table 4-4; Appendix A). This deposit underlies the terrace gravels of Arrastre Canyon with angular unconformity. Demagnetization was carried out according to the procedure described for the ORD samples.

Both RSR 1 and 2 are unquestionably of reversed polarity. Tilt-corrected directions for RSR 1 are skewed 15° clockwise; RSR 2 is not skewed (Figure 4-7).

4.3.5.5 Bowen Ranch Road (BRR)

A single sample (BRR 1) was retrieved from the faulted terrace gravels along the Bowen Ranch Road in sec 1, R3W T3N (Table 4-4; Appendix A-4). The sample was taken in a roadcut through a weathered exposure adjacent to a fault.

Thermal demagnetization yielded a clearly normal polarity for BRR 1 (Figure 4-7). Although a strong present local field overprint cannot be ruled out, it is skewed 35° in a counter-clockwise sense, suggesting that the normal polarity is due to early magnetization.

4.4 INTERPRETATION OF DATA

4.4.1 The Brunhes/Matuyama Polarity Reversal in Cajon Pass

The paleomagnetic data clearly show that a large part of the Victorville Fan complex in Cajon Pass and Summit Valley was deposited during the Matuyama polarity epoch (Figure 4-9). The HPL data indicate that the upper 50 meters of the Harold Formation (HPL 1-27) and lower 25 meters of the Shoemaker Gravel (HPL 28-33) are reversed (Table 4-1), and hence predate the Brunhes/Matuyama polarity reversal, 730,000 y B.P. Results from the SPL site confirm that the upper 80 meters of the Shoemaker Gravel is reversed and suggest that part of the Older Alluvium may also lie beneath the polarity boundary.

The data are suggestive but inconclusive as to which stratigraphic interval in Cajon Pass, if any, contains the Brunhes/Matuyama polarity transition. Samples HPL 34-37 were taken from two paleosols in the upper 35 meters of the Shoemaker Gravel and possess a stable normal remanence. Although these data point to the conclusion that deposition of the upper Shoemaker Gravel postdated the polarity reversal, post-depositional overprinting is impossible to rule out. HPL 34 can be interpreted as tracking toward reversed polarity, and since HPL 35 was taken from the same horizon, it may be overprinted. HPL 36 and 37 are from the paleosol that unconformably underlies the Older Alluvium and postdates the deposition of the Shoemaker Gravel by an unknown period of time. Thus, the entire section of Shoemaker Gravel at the HPL site may be reversed. This conclusion is corroborated by the predominantly reversed polarity of samples from the Shoemaker Gravel at the nearby SPL site.

Stable normal directions obtained from unweathered sands at the base of the Older Alluvium (HPL 38 & 39) suggest that the polarity reversal may lie at the unconformity with the Shoemaker Gravel. Part of the Older Alluvium

Figure 4-9. Diagram summarizing the evidence for tectonic rotation in the studied sediments. There are not enough data to make any definitive judgment as to the existence of tectonic rotations. There is some suggestion of clockwise displacements in declination, especially in the normal vectors, which may be the result of secular variation of the magnetic field in the recent past.

(a) Tilt-corrected EQPLOT of least-squares fit lines for both normal and reversed samples of the HPL sample series. The vector mean for the reversed directions (X) is MD=173° MI=-51° and is not appreciably skewed. The normal mean (+) of MD=30 MI=58 appears skewed. The unskewed reversed directions virtually rule out any significant tectonic rotation since deposition of the Harold Formation.

(b) Tilt-corrected EQPLOT of least-squares fit lines for both normal and reversed samples of the SPL sample series. The data describe a "girdle" that suggests that vector components are not being successfully separated during demagnetization. The scatter in these data preclude any judgement on the possibility of rotations. The normal vector mean (+) is MD=21° MI=57°. The reversed mean (X) is MD=184° MI=-21°.

(c) Geographic EQPLOT of least-squares fit lines for both normal and reversed samples of the MRF sample series. There is a suggestion of clockwise rotation of both normal and reversed directions 30-50°. More data should be gathered from the MRF site to improve the statistics and determine if this rotation is real. The normal vector mean (+) is MD=35° MI=51°. The reversed mean (X) is MD=199° MI=-56.

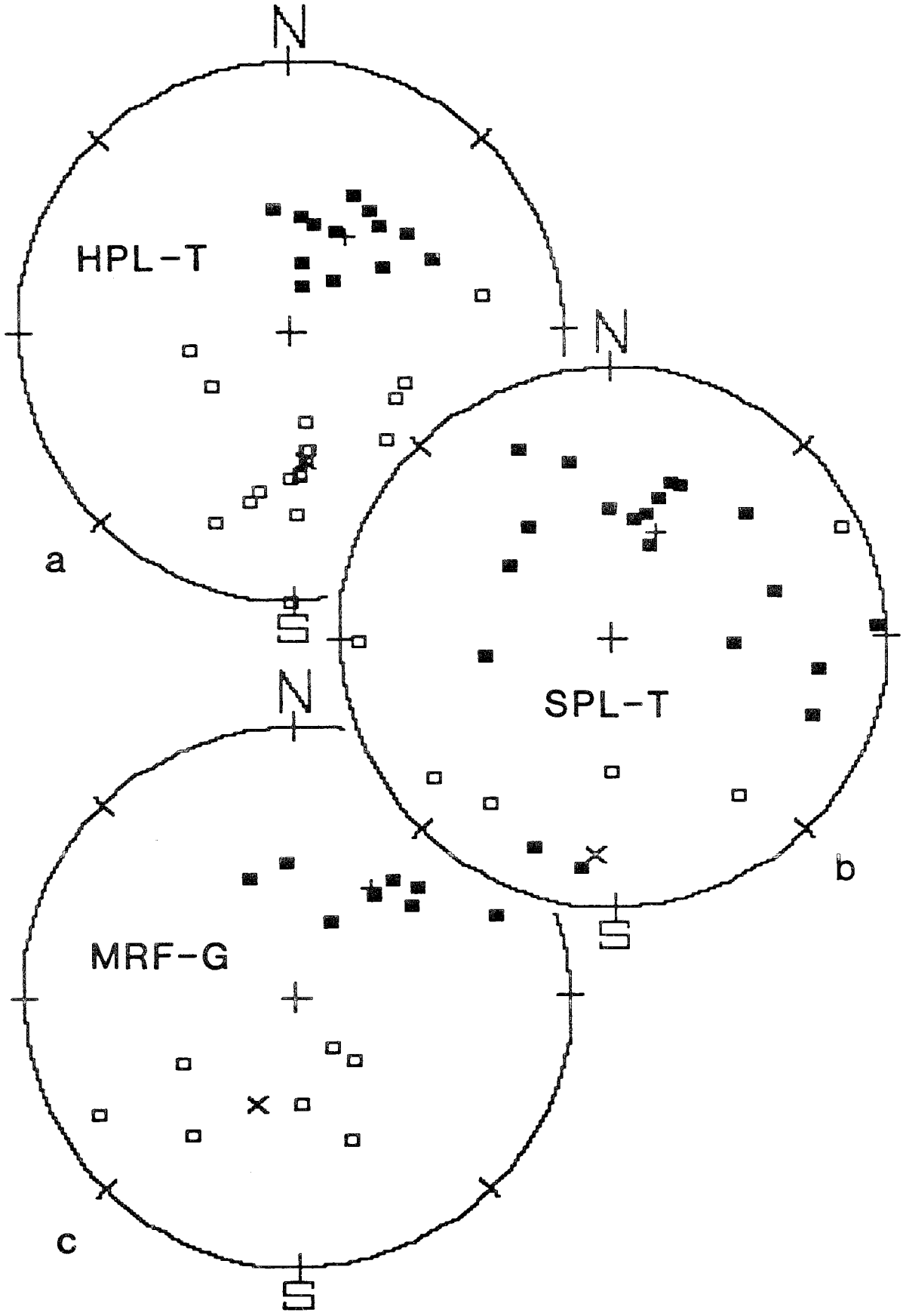
N
HPL-T
a
S
N
SPL-T
b
S
N
MRF-G
c
S

above the unconformity at the SPL site, however, is clearly reversed (SPL 14,16,17; Table 4-2), indicating that the age of the basal Older Alluvium may vary along strike.

A fold-test would establish whether normal directions in the upper Shoemaker and Older Alluvium are primary and pre-deformational, or secondary and post-deformational. Unfortunately, no suitable fold structures have been reported in these units.

4.4.2 The Age of the Victorville Fan

The Older Alluvium underlying the surface of the Victorville Fan is divided into older and younger units based on degree of dissection (Figure 4-1; Dibblee, 1965, 1967; Jennings, 1983). Dissected Older Alluvium underlies the topographic head of the Victorville Fan in a broad strip trending northwestward parallel to the inface bluffs in Cajon Pass, and along its southern shoulder between Summit Valley and Oro Grande Wash. Undissected Older Alluvium forms a large fan-shaped body north of Oro Grande Wash which underlies most of the town of Hesperia.

HRF 1 and 2, taken from beds exposed within the undissected Older Alluvium in Hesperia, are of normal polarity. They support the interpretation that part of the Older Alluvium is younger than the Brunhes/Matuyama polarity reversal, confirming the informal assignment of these beds to the late Irvingtonian land mammal age (Reynolds, pers. comm., 1982).

The map pattern of dissected alluvium coincides with the localities for which reversed sections have been measured. The MRF sample data reveal that this section, which underlies the dissected southern shoulder of the Victorville Fan, is unquestionably reversed and hence older than 730,000 years B.P. Part of the Older Alluvium in Cajon Pass is dissected and reversed.

4.4.3 The Age of Ord River Gravel and Arrastre Canyon Fan

The Ord River Gravel lies east of the Mojave River and is correlated with the Victorville Fan deposits on the basis of graded surfaces, lithology and degree of soil development. Clast lithologies within the Ord River Gravel require that a major north-flowing drainage once existed at the foot of the Ord Mountains, just east of the present-day Mojave River. This drainage was initially fed by Deep Creek and later by the western San Bernardino Mountains through Summit Valley.

ORD 2 and 4, collected from the early Ord River deposits derived from Deep Creek, are reversed and therefore older than the Brunhes/Matuyama polarity reversal. Coarse, angular alluvial fan gravel interfingers with and overlies the ancestral Ord River deposits, signaling a westward shift of the Ord River in response to development of integrated drainage in the western San Bernardino Mountains. ORD 3, which lies stratigraphically above ORD 2 and 4, was taken from the deep soil developed on these gravels. The normal polarity of ORD 3 suggests that the soil formed after the Brunhes/Matuyama polarity reversal. This deep soil may be the product of the same intense soil-forming episode that created the paleosol capping the Shoemaker Gravel at HPL. A deep soil is also found on the dissected surface along the southern shoulder of the Victorville Fan at MRF.

Ord River deposits underlie a well-graded geomorphic surface throughout the Apple Valley Highlands and Marianas Rancho areas in an obvious continuation of the undissected Older Alluvium west of the Mojave river in Hesperia. Clast lithologies in these exposures of the Ord River Gravel were derived from the western San Bernardino Mountains via an ancestral Summit Valley. Samples extracted from the upper few meters of this deposit include ORD 1 and ORM 1-4, all of unquestionably normal polarity. ORM 3 and 4, taken

from beds on the north side of Ocotillo Ridge which dip 55° to the north, display normal remanence that predates deformation; their remanence direction becomes fully normal only after tilt-correction. It is therefore likely that these samples possess a primary normal remanence, providing additional evidence to support the conclusion that the undissected Older Alluvium is younger than the Brunhes/Matuyama polarity boundary.

The Arrastre Canyon Fan represents an eastward continuation of the Ord River Gravel, as evidenced by continuous exposure from the Marianas Rancho area to Arrastre Canyon along the Ocotillo Ridge. The ACF sample series is normal in polarity, indicating that the bulk of the Arrastre Canyon Fan was deposited since the Brunhes/Matuyama polarity reversal, 730,000 years ago. The Arrastre Canyon Fan contains clasts derived exclusively from the Arrastre Canyon drainage basin to the south. The ancestral Arrastre Canyon drainage can be traced upstream in a discontinuous series of terrace deposits containing angular clasts composed of local crystalline basement lithologies. BRR 1 was taken from the southernmost terrace exposure, and is clearly of normal polarity. Thus, the terraces are younger than the Brunhes/Matuyama polarity reversal which suggests contemporaneity with the Arrastre Canyon Fan deposits.

A small patch of reversed sediment (RSR 1 and 2) is preserved beneath the Arrastre Canyon terraces along the Bowen Ranch Road at Rock Springs Road. It is composed of fine-grained silt and sand, possibly of lacustrine origin, and is of unknown age and affinity. These beds may be quite old, as they are tilted 30° to the east and seem to reflect more subdued relief than is now present in the area. They do suggest that the Arrastre Canyon area was a site of deposition before the Brunhes/Matuyama polarity reversal.

4.4.4 Rotations

Large clockwise block rotations have been reported in the Transverse

Ranges by Kamerling and Luyendyke (1979). It has been suggested that most of the western San Bernardino Mountains may be underlain by a major low-angle detachment surface (R. J. Weldon, pers. comm., 1983), possibly giving rise to complex rotations. Any large-scale mid- to late-Pleistocene tectonic rotation should be evident in the stable remanent vector directions measured in Cajon Pass.

In a systematic effort to explore for evidence of rotations, vector mean directions were calculated (Fisher, 1953) for least-squares lines fit to the data (Kirschvink, 1980) for samples in HPL, SPL and MRF displaying stable normal and reversed directions. The results are summarized in Figure 4-9.

When plotted in tilt-corrected coordinates, vector means for stable normal directions for HPL 1-39 appear to be rotated about 30 in a clockwise sense (Figure 4-9a). The mean for reversed directions, however, is not appreciably rotated. Since the reversed direction is the most stable and unquestionably ancient, it is the most reliable indicator of rotation. Hence there is no evidence for rotation. The skewed direction of the normal mean probably reflects variation in the present local field in the recent past. In any case, the scatter in the data includes the present local field direction and any apparent rotation cannot, therefore, be considered significant.

The data for SPL are too scattered to be useful in resolving rotations. The data describe a "girdle" on the equal-area plot, suggesting that the vector components were not sucessfully separated in many of the SPL samples (Figure 4-9b). The samples from MRF show a consistent clockwise rotation for both normal and reversed components (Figure 4-9c). The number of MRF samples, however, is small, and the data can only be considered suggestive. More data are required to improve the reliability of the mean result before

Figure 4-10. Correlation chart showing inferred relationship between sampled sections and the Brunhes/Matuyama polarity reversal.

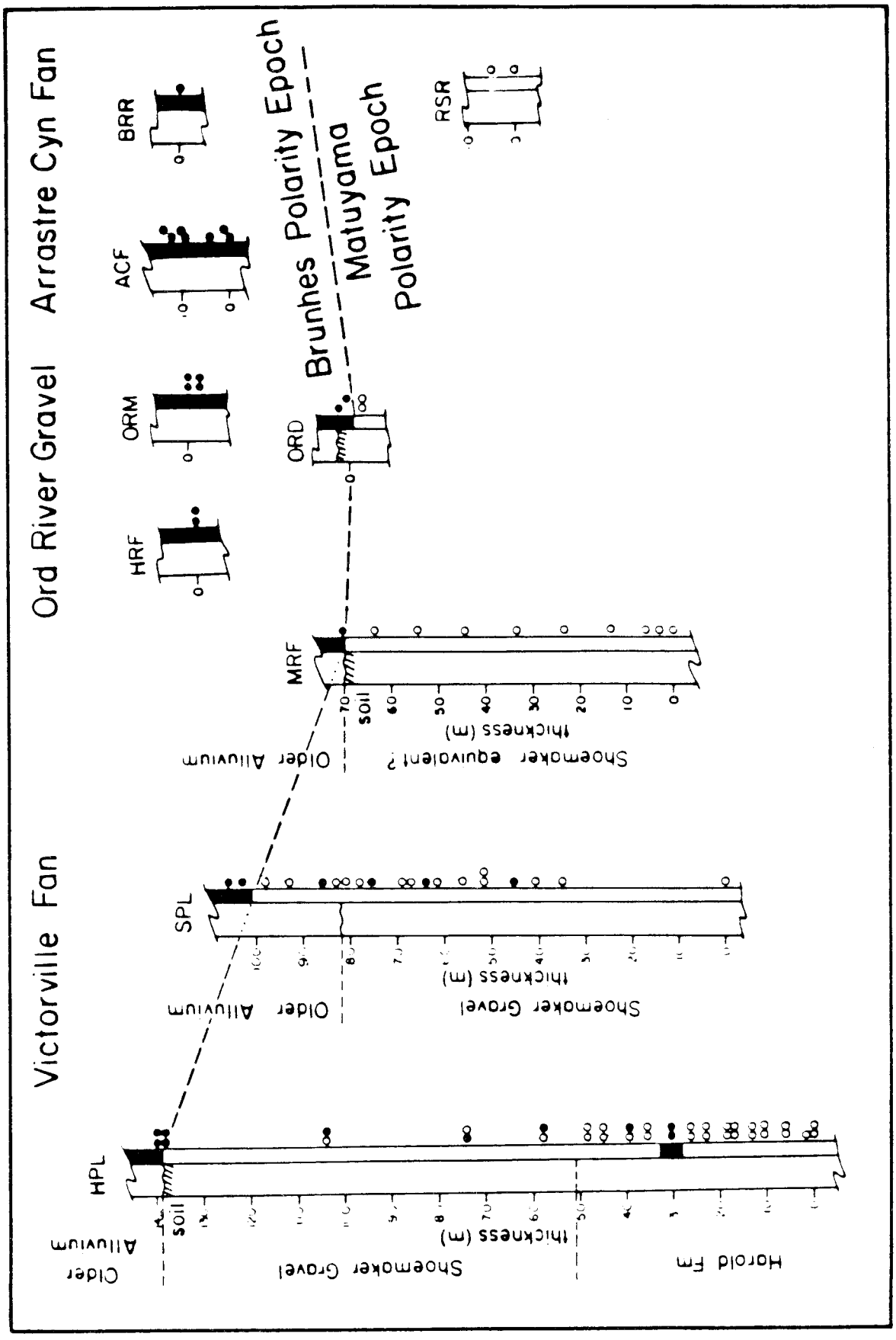
Victorville Fan
Ord River Gravel
Arrastre Cyn Fan
Brunhes Polarity Epoch
Matuyama Polarity Epoch
HPL
SPL
MRF
ORD
ORM
HRF
ACF
BRR
RSR
soil
thickness (m)
Older Alluvium
Shoemaker Gravel
Harold Fm
Older Alluvium
Shoemaker Gravel
thickness (m)
Older Alluvium
Shoemaker equivalent?
thickness (m)

any firm conclusion could drawn with regard to the existence of tectonic rotations.

Several possible mechanisms might create the appearance of rotation in the Cajon Pass sediments. Gentle folding on north-south axes, reported by Foster (1980), might couple with tilting to create a net rotation if bedding is not restored properly. Alternatively, northeast-flowing currents may have skewed grain orientation from true magnetic north during deposition. Antecedent drainages on the geomorphic surface underlain by the MRF section clearly reflect northeastward drainage directions, raising the possibility of current-induced skewing of depositional remanent directions. Incomplete separation of primary reversed and normal overprinted directions causes samples to lie in a planar "girdle" containing both vector component directions. The scatter of sample directions along the girdle demagnetization path may give the false appearance of rotations. Finally, sampling errors inherent in these poorly consolidated sediments introduce uncertainty as to the magnitude and sense of rotation.

4.4.5 Suggestions for Further Study

A great deal more can be learned about the paleomagnetism of Pleistocene sediments in the study area. The excellent exposures of Harold Formation, Shoemaker Gravel, and Older Alluvium along the inface bluffs in Cajon Pass might offer a rare opportunity to locate and study the Brunhes/Matuyama polarity transition in detail in fluvial/alluvial sediments. The time-transgressive nature of the Harold Formation and Shoemaker Gravel, suggested by Foster (1980) and Weldon (pers. comm., 1983), can easily be tested by following the polarity transition along the inface bluffs to the northwest. The success of the soft-sediment sampling techniques employed in this study shows that good results can be obtained for poorly-consolidated Pleistocene

fluvial and alluvial sediments.

4.5 CONCLUSIONS

The Brunhes/Matuyama polarity reversal (730,000 years B.P.) occurred during deposition of the Victorville Fan complex (Figure 4-10). Based on the results from progressive demagnetization of 50 paleomagnetic samples, the upper 50 meters of the Harold Formation and at least 88 meters of the overlying Shoemaker Gravel are of reversed polarity, and therefore older than 730,000 years old. The entire 70-meter-thick section of Victorville Fan sediments exposed in the bluffs along the Mojave River in Summit Valley is also reversed. The basal Older Alluvium capping the Victorville Fan complex in Cajon Pass is reversed, while higher levels within the Older Alluvium are normal.

Paleomagnetic samples from the Victorville Fan and related units permit preliminary age assignments, providing a much needed framework on which to base an interpretation of drainage development and depositional history. A border of dissected Older Alluvium that rims the Victorville Fan northeast of Cajon Pass and in Summit Valley is partly reversed. A central fan-shaped body of undissected Older Alluvium occupying the region underlying Hesperia is, in part, normal.

The Ord River Gravel east of the Mojave River on the west flank of the Ord Mountains is correlated with the Victorville Fan complex on the basis of similarity of geomorphic, lithologic and paleomagnetic characteristics. Reversed samples from exposures of the Ord River Gravel near Deep Creek are correlated with the dissected Older Alluvium that predates the development of Summit Valley. Well-graded deposits in the Apple Valley Highlands/Marianas area are normal and postdate the development of Summit Valley.

The sediments underlying the Arrastre Canyon Fan and terrace remnants

of its ancestral trunk stream are normal, hence younger than 730,000 y B.P. A small patch of reversed sediment which unconformably underlies the Arrastre Canyon Terrace deposits is of unknown age and affinity.

The techniques used in this study yield excellent results for unconsolidated alluvial deposits. Thus, paleomagnetic sampling can be a useful adjunct to detailed geological field mapping aimed at the resolution of depositional and drainage history. It is hoped that this work will lead to further application of these methods, thereby contributing to the understanding of complex Pleistocene sedimentary sequences elsewhere.

CHAPTER V

STRUCTURE

5.1 INTRODUCTION

5.1.1 Purpose

The primary objective of this study is to evaluate the seismic potential of faults along the northwestern range front of the San Bernardino Mountains. To this end, the faults of the range front were mapped in detail, with particular emphasis on their geometry, nature, and age. This chapter focuses on the features of each individual structural element, with the emphasis on description rather than interpretation. Implications for uplift history, origin, and tectonic context of faults are discussed in Chapter VI, "Tectonic Evolution". Consequences that pertain to earthquake hazard evaluation are considered in Chapter VII, "Seismic Risk".

5.1.2 Scope

The geometry, geomorphology, character, displacement, and age of each structure is discussed for each individual fault or group of related faults shown in Figure 5-1. Folding, warping, tilting, and cataclasis are also described. An effort is made to relate each structural element to adjacent structures, and establish a local geologic context.

Faults are discussed first, followed by folds. Structures are discussed from west to east. Exceptions to this order are made in the interest of continuity and clarity, and faults that have experienced more than one period of activity may be discussed more than once. The variety of styles of local deformation that have coexisted in the study area reflects the complex influence of pre-existing weaknesses on fault geometry, rather than a

Figure 5-1. Generalized map of the western San Bernardino Mountains with the names of individual faults and folds within the north frontal fault system of the San Bernardino Mountains (after Jennings, 1983). See Plates 1A and 1B for detailed fault patterns and text for detailed discussion of each structurte. AV = Apple Valley; LV = Lucerne Valley; V = Victorville.


Faults
5 mi
5 km
N
HELENDALE FLT.
LV
AV
V
SKY HI RANCH FAULT
WHITE MTN. THRUST
OCOTILLO RIDGE FOLD
LOVELACE CYN FLT.
BOWEN RANCH
RIDGE LINEAMENT
ORD MOUNTAINS FLT
SUMMIT VALLEY FLT ZONE
GRASSY FLT.
CLEGHORN FLT.
CEDAR SPRINGS SYSTEM
WATERMAN CYN FAULT ZONE
NOTCH
POWELL CYN
SAN ANDREAS FLT.
CLEGHORN FLT.
SQUAW PK.

complex regional stress regime.

The implications of these data for the timing and history of uplift of the San Bernardino Mountains and the nature and modes of deformation in the study area will be discussed in Chapter VI, "Tectonic Evolution". Quaternary activity, rates of deformation, cumulative offset for major structural elements are covered in Chapter VII.

The ideas presented in sections 5.2 and 5.3 were developed in close cooperation with Ray Weldon.

5.2 THE CEDAR SPRINGS REVERSE FAULT SYSTEM

A pervasive system of arcuate high-angle reverse faults displaying minor offset is expressed in the late Miocene erosion surface in the westernmost San Bernardino Mountains (Figure 5-1). This system has exerted a profound influence on the late Cenozoic structural development of the area around Silverwood Lake by providing a framework of pre-existing lines of weakness that were exploited by later faulting. Complex cross-cutting relationships suggest that the Cedar Springs fault system underwent a dynamic evolution that ultimately led to the development of the ancestral Cleghorn fault zone.

Major elements of the Cedar Springs system were recognized by Dibblee (1965, 1974) and appear on the map made by the California Department of Water Resources (1968a,b) of the Silverwood Lake area. Weldon et al. (1981) and Meisling and Weldon (1982a, 1982b) elucidated the complex relationships between the various members of the reverse fault system and the suggested the pivotal role of the Cedar Springs system in the structural evolution of the Silverwood Lake area.

The faults of the Cedar Springs system can be grouped into three categories on the basis of sense and magnitude of displacement: Faults

with (1) minor south-block-down separation, (2) minor north-block-down separation, and (3) major south-block-down separation (see Figure 5-2).

5.2.1 South-block-down Fault Set

An anastamosing set of high-angle reverse faults crosses the late Miocene erosion surface between Cajon Pass and the Pinnacles. Informally named the south-block-down set of the Cedar Springs fault system, the faults are best expressed on the Cleghorn and Pilot Rock ridges, and can be traced east at least as far as Tunnel Ridge and south as far as Crestline. The faults are very clearly expressed as lineaments on the late Miocene erosion surface. In fact, many faults could only be followed on aerial photographs due to the dense brush cover in the Silverwood Lake area. The south-block-down fault set strongly influences local drainage patterns.

Individual south-block-down faults are generally arcuate in plan, trending northwest at their western ends, east in their central regions, and northeast at their eastern extremities. Where arcuate faults intersect, a consistent geometric relationship is always observed: the trend of the younger trace is rotated clockwise through a small angle from the trend of the older trace (e.g. the northwest-trending member invariably cuts the east-trending member; the east-trending member invariably cuts the northeast-trending member etc.)[84]. Such consistent cross-cutting relationships suggest that the fault geometry of the Cedar Springs system evolved in a systematic way, perhaps in response to a migration of the locus of faulting, or a rotation of the compression axis.

The average trend of the south-block-down faults seems to change from west-northwest on Cleghorn ridge to east-northeast in the Pinnacles. This might suggest oroclinal bending of the western San Bernardino Mountains. The change in orientation is not evident in the Crowder Formation or the

Figure 5-2. Index Map of the Silverwood Lake area (Meisling and Weldon, 1982b). Diagram shows major faults and physiographic features, as well as the location of Figures 5-4 and 5-5. Minor faults are not shown; see Plates 1A and 1B for detailed fault pattern, and text for detailed discussion of each structure.

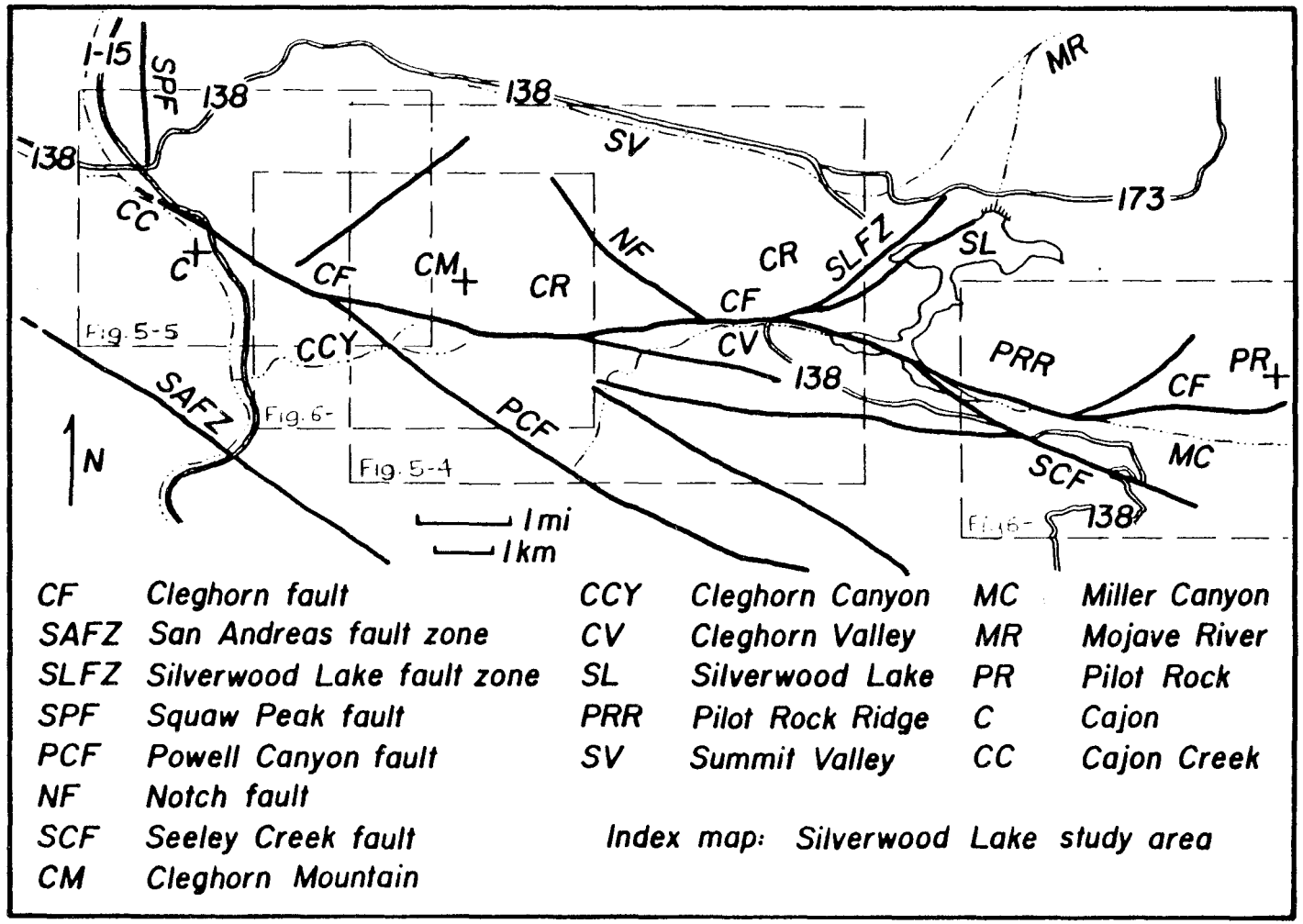
I-15
SPF
138
138
138
SV
MR
173
CC
C
CF
CM
CR
NF
CR
SLFZ
SL
CF
Fig. 5-5
CCY
CV
138
PRR
PR
CF
SAFZ
Fig. 6-
PCF
MC
N
Fig. 5-4
SCF
1 mi
1 km
Fig. 6-
138
CF Cleghorn fault
SAFZ San Andreas fault zone
SLFZ Silverwood Lake fault zone
SPF Squaw Peak fault
PCF Powell Canyon fault
NF Notch fault
SCF Seeley Creek fault
CM Cleghorn Mountain
CCY Cleghorn Canyon
CV Cleghorn Valley
SL Silverwood Lake
PRR Pilot Rock Ridge
SV Summit Valley
MC Miller Canyon
MR Mojave River
PR Pilot Rock
C Cajon
CC Cajon Creek
Index map: Silverwood Lake study area

Miocene erosion surface, however, and it appears to be a primary characteristic of the geometry of the south-block-down fault set.

About 30° of northward tilting must be subtracted from the present near-vertical dip of the south-block-down faults in order to reconstruct their original dip, which was approximately 50 to 70° to the north (Section 5.10.1). The faults seem to have inherited this orientation from the attitude of dikes and joints within the plutonic basement, which may have served to nucleate faulting.

Movement on the south-block-down set of the Cedar Springs fault system postdates the deposition of the Crowder Formation, as evidenced by numerous fault-bounded wedges of Crowder Formation throughout the western San Bernardino Mountains. Movement predates deposition of the Harold Formation, however, since the Harold Formation unconformably overlies related fold structures at Cajon Pass[85] (Section 5.10.3).

The south-block-down set is clearly truncated by lateral faults of the Cleghorn system[86]. Dibblee (1974) shows a member of the south-block-down set cutting the Tunnel Ridge lineament in Miller Canyon[87]. The set also cuts north-plunging monoclines developed in the Crowder Formation and the underlying late Miocene erosion surface[88].

Deformation associated with south-block-down faulting can be examined where the Crowder Formation is preserved adjacent to a fault, such as in the synclinal trough of one of the north-plunging monoclines. Gentle open drag folds are locally developed next to the larger faults[89]. Elsewhere, however, beds of the Crowder Formation are undisturbed adjacent to the fault trace[90]. The south-block-down faults appear to die out and become folds within the overlying Crowder Formation; these folds are best expressed within the Crowder Formation in Summit Valley[91] (Section 5.10.3).

Sense of displacement on the south-block-down set varies from simple dip-slip separation on east-trending segments to right-lateral strike slip on northwest-trending segments. The magnitude and sense of offset can be deduced for most faults from vertical displacement of the Miocene erosion surface and lateral offset of older members of the fault set. Pure dip-slip motion is demanded by the offset geometry of the plunging syncline southwest of Silverwood Lake[92].

The patterns of displacement and arcuate traces of the south-block-down reverse faults suggest a "shingling" of fault slices in response to north-south compression. It is noteworthy that south-block-down displacement is the wrong sense of motion for uplift of the western San Bernardino Mountains to the south. Mountain uplift was in fact accomplished by tilting (Section 5.10.1). Preservation of the Miocene erosion surface throughout the area and offset of the plunging monoclines rule out more that a few hundred meters of vertical and lateral offset on all but the ancestral Cleghorn fault zone.

Several northeast-trending splays from the Cleghorn fault appear to offset south-block-down faults in a left-lateral sense[93]. It is not known if this offset occurred in connection with motion on the Cedar Springs system or the Cleghorn lateral system. There is some evidence to suggest that the Silverwood Lake fault was once part of the ancestral Cleghorn reverse fault zone (Section 5.2.4).

5.2.2 North-block-down Set

Five faults within the Cedar Springs system display north-block-down, rather than south-block-down separation: The Squaw Peak fault, the Powell Canyon fault, the Notch fault, the Seeley Creek fault, and the Grass Valley fault (Figure 5-2). Restoration of strike-slip motion on the Cleghorn fault

(Section 5.3.1) aligns the Squaw Peak fault with the Powell Canyon fault and the Notch fault with the Seeley Creek fault, reducing the total number of north-block-down faults to three. The Grass Valley fault is discussed in Section 5.3.3.

The north-block-down faults are straighter and longer than the south-block-down faults, and continue out of the study area to the southeast where they are reported to display significant south-block-down separation (Weldon, 1982, pers. comm.). Strike-slip motion is therefore probably responsible for their north-block-down separation. They appear to represent larger versions of the arcuate south-block-down fault geometry.

The north-block-down faults truncate the south-block-down faults[94], and consequently must postdate them. Bends and cusps in the trace of the Cleghorn fault[95] suggest that movement on the north-block-down faults may have been partly contemporaneous with vertical motion on the ancestral Cleghorn fault zone. Their motion ceased, however, prior to the onset of strike-slip motion on the Cleghorn fault, and since then they have experienced the full amount of lateral offset on the Cleghorn fault. Thus, motion on the north-block-down faults represents a well defined phase in the dynamic evolution of the Cedar Springs fault system.

Lateral displacements on the north-block-down faults are difficult to estimate due to a lack of any suitable reference features. Inasmuch as the Squaw Peak/Powell Canyon fault zone defines the southwestern limit of the Crowder Formation, it is possible that it may have sustained major lateral displacement since the late Miocene.

5.2.2.1 The Squaw Peak Fault

Foster (1980) has suggested that vertical motion on the Squaw Peak fault (Figure 5-2) may have been contemporaneous with deposition of the

Crowder Formation. Foster concludes that dip-slip motion resulted in ponding of the Crowder Formation east of the fault. About 800 meters of dip-slip motion would be required to account for the ponded Crowder section. Shallow easterly dips and eastblock-down sense of motion on the Squaw Peak fault would require normal faulting, in sharp contrast with contemporaneous reverse faulting elsewhere in the western San Bernardino Mountains. Furthermore, ponding and dip-slip motion seem untenable in light of recent fossil evidence indicating that the Crowder Formation and Cajon beds of the Punchbowl Formation are of the same age (Reynolds, 1982, pers. comm.; Woodburne and Golz, 1972).

The juxtaposition of the Crowder Formation and the Cajon beds of Punchbowl Formation along the Squaw Peak fault is best explained by lateral faulting. Although the Crowder and Punchbowl Formations are of the same age, they differ markedly in provenance and depositional environment (Section 2.3.1). A large component of lateral translation would seem necessary to bring them together. Such translation could be accomplished on a shallow detachment surface (Weldon, 1983, pers. comm.), or on a lateral fault. Lateral faulting is the most effective means of bringing two widely separated basins into juxtaposition with a minimum of internal deformation. Deformation in the Crowder Formation is largely restricted to the immediate vicinity of the Squaw Peak fault, where deformation is intense. This is best explained by major lateral translation.

The Squaw Peak fault is overlain by the Harold Formation and appears to die out within Unit 5 of the Crowder Formation (Foster, 1980). Its motion is therefore early to middle Pleistocene or older. This is consistent with a notable lack of fault-related physiographic features along the Squaw Peak fault.

5.2.2.2 The Powell Canyon Fault

The Powell Canyon fault (Figure 5-2) is interpreted as the equivalent of the Squaw Peak fault south of the Cleghorn fault zone. In contrast to the Squaw Peak fault, vertical separation on the Powell Canyon fault cannot exceed a few tens of meters within the mapped area, based on the relative continuity of the late Miocene erosion surface and minimal offset of remnants of the Crowder Formation. Although there is no direct evidence for lateral motion on the Powell Canyon fault, its path is characterized by major linear drainages and other geomorphic features suggesting that it may have once been a significant tectonic element. The Powell Canyon fault is not well characterized outside the study area, but Weldon (1983, pers. comm.) reports evidence of significant south-block-down separation along its southern extension. The Powell Canyon fault appears to be part of a group of east- to southeast trending faults that also includes the Waterman Canyon fault (Weldon, 1983, pers. comm.).

5.2.2.3 The Notch and Seeley Creek Faults

The Notch/Seeley Creek fault zone shares many characteristics with the Squaw Peak/Powell Canyon fault zone. Its physiographic expression arises from its disruption of the Miocene erosion surface and has been accentuated by development of the drainage network. It is brought into alignment by restoration of the total lateral offset on the Cleghorn fault zone, and clearly truncates members of the south-block-down fault set[96]. Hence it was active during the same structural time period as the Squaw Peak/Powell Canyon fault zone. Its minimal north-block-down separation, linear trend, and northwest orientation are best explained by lateral faulting. It cuts the Crowder Formation[97] and is overlain by terrace deposits of middle Pleistocene age (Qt2)[98]. The evidence suggests that it has not sustained

major lateral offset, since both trend and attitude of members of the south-block-down fault set remain consistent across the fault zone.

5.2.3 The Ancestral Cleghorn fault

The Cleghorn fault (Figure 5-2) began as a major reverse fault which coalesced from a zone of concentrated faulting within the Cedar Springs fault system. The ancestral Cleghorn fault zone consisted of two arcuate faults, the west and east Cleghorn faults, which met at Silverwood Lake (Figure 5-3). The Silverwood Lake fault is believed to be the eastern extension of the west Cleghorn fault. The late Miocene erosion surface is displaced vertically across the Cleghorn fault zone in a south-block-down sense. Thus the ancestral Cleghorn fault was the largest south-side-down reverse fault in the Cedar Springs fault system.

Restoration of the lateral motion on the Cleghorn Fault yields some insights into the pre-existing reverse system that constituted the ancestral Cleghorn fault, and makes it possible to estimate its total displacement. The Cleghorn fault zone shows its greatest vertical separation between the Notch Fault and Little Horsethief Canyon. Vertical separation decreases to the west. In Cajon Pass all of the vertical separation can be satisfied by the postulated lateral motion. Near Silverwood Lake, vertical separation across the Cleghorn fault is also reduced. The separation increases to the east beneath Pilot Rock ridge, although some of this vertical relief can be explained by lateral faulting. The estimation of total vertical displacement on the ancestral Cleghorn fault zone is complicated by the fact that lateral faulting of folds within the Crowder Formation and underlying Miocene erosion surface has led to an apparent variation in separation along the fault trace. Despite these uncertainties, vertical displacement on the ancestral Cleghorn fault zone probably did not exceed 300 meters.

Figure 5-3. Schematic development of the Cleghorn fault system (Weldon et al., 1981). The Cleghorn fault system grew out of a pair of major south-block-down reverse faults of the Cedar Springs fault system. This diagram shows a possible sequence of events. (a) The west Cleghorn fault evolved from the integration of a zone of concentrated faulting in the south-block-down fault set of the Cedar Springs system. The west Silverwood Lake fault may have been the eastern extension of the west Cleghorn fault. (b) The east Cleghorn fault developed, cutting and offsetting the west Cleghorn fault in a right-lateral sense, consistent with the pattern displayed by lesser members of the Cedar Springs system. (c) The Squaw Peak/Powell Canyon and the Notch/Seeley Creek fault zones became active, offsetting the pre-existing faults right-laterally, again in a manner consistent with the Cedar Springs system pattern. (d) The lateral faulting began on the Cleghorn fault, integrating through the east-trending zone composed of segments of the pre-existing faults. (e) The east Silverwood Lake fault may have developed as a splay off the Cleghorn fault to transfer motion to the developing Summit Valley fault system.

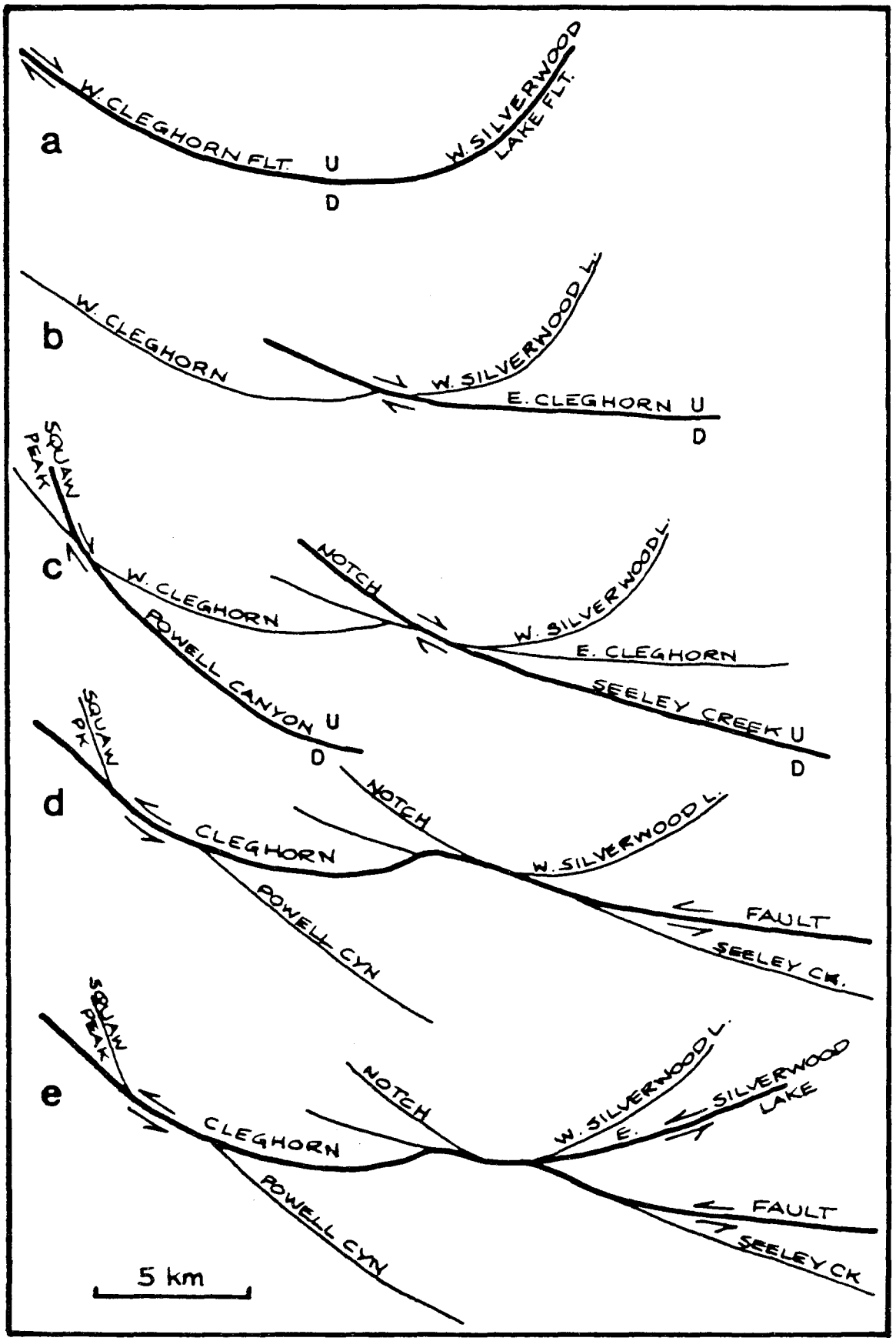
a
W. CLEGHORN FLT.
U
D
W. SILVERWOOD LAKE FLT.
b
W. CLEGHORN
W. SILVERWOOD L.
E. CLEGHORN
U
D
c
SQUAW PEAK
W. CLEGHORN
NOTCH
W. SILVERWOOD L.
E. CLEGHORN
POWELL CANYON
SEELEY CREEK
U
D
d
SQUAW PK
CLEGHORN
NOTCH
W. SILVERWOOD L.
FAULT
POWELL CYN
SEELEY CK.
e
SQUAW PEAK
CLEGHORN
NOTCH
W. SILVERWOOD L.
E.
SILVERWOOD LAKE
FAULT
POWELL CYN
SEELEY CK
5 km

5.2.4 Evolution of the Cedar Springs Fault System

The above observations, coupled with the nature of other faults in the Cedar Springs system, suggest the following model to explain all of the reverse faulting in the western San Bernardino Mountains. All of the dip-slip faults have the same arcuate pattern characterized by south-block-down dip-slip motion on east-west trending segments, and right-lateral motion on northwest-trending segments. The proposed motion is consistent with "shingling" of individual fault blocks under north-south regional compression. The locus of faulting migrated through the area from northwest to southeast, culminating in formation of the lateral north-block-down faults. A microcosm of this evolution is evident in the faulting on Cleghorn Ridge[99].

Weldon et al. (1981) envision the following scenario for the development of the Cleghorn fault (Figure 5-3). The earliest Cleghorn fault zone consisted of a major arcuate reverse fault that included the western part of the Cleghorn and the western branch of the Silverwood Lake fault zone. As faulting migrated south, fault trends became progressively more northwesterly. All faults have a similar spatial pattern of motion, but different parts of the pattern affect a given area as time progresses. Thus a single migrating pattern of deformation gave rise to changes in style of deformation with time. Lateral faulting began with integration of the weaknesses in a zone characterized by a higher concentration of reverse faults. It thereby incorporated the bends and cusps that existed at the intersection of the pre-existing reverse faults. Lateral motion on the eastern branch of the Silverwood Lake fault zone may have served to further emphasize the cusp formed near the Notch fault.

Besides unifying the dip-slip faulting into one deformational episode,

this model explains the somewhat curious course of the Cleghorn fault through the field area while all of the rest of the faults tend to have linear or smooth, arcuate trends.

5.3 THE CLEGHORN LATERAL FAULT SYSTEM

In the earliest Pleistocene, motion on the Cleghorn fault changed from south-block-down reverse to left-lateral strike-slip, following integration of the east and west branches of the Cleghorn fault to accomodate lateral displacement. Major discontinuities in the geology across the Cleghorn fault attest to substantial strike-slip motion, and suggest a cumulative left-lateral offset of 3.5 to 4.0 kilometers. The initiation of major strike-slip motion roughly coincided with the cessation of dip-slip motion on the ancestral Cleghorn fault. There are several related faults that are considered part of the Cleghorn lateral fault system. Three short northeast-trending faults diverge from the Cleghorn fault at Little Horsethief Canyon, Silverwood Lake and Pilot Rock ridge. The east end of the Cleghorn fault merges with the northeast-trending Tunnel Ridge lineament (Figure 5-1). There is some evidence to suggest that the Grass Valley and the Summit Valley fault zones may have sustained minor post-middle-Pleistocene lateral displacement. Many of the following ideas were developed jointly with Ray Weldon.

5.3.1 The Cleghorn Fault

Several unique structures demonstrate a cumulative left-lateral offset of 3 to 4 kilometers on the Cleghorn fault: (1) A north-plunging anticline-syncline pair in the Crowder Formation southwest of Silverwood Lake matches a similar flexure in the late Miocene erosion surface and Crowder Formation 3 to 4 kilometers to the west on the north side of the Cleghorn fault.

(2) The steeply dipping basement contact that forms the eastern limit of the Cajon beds of the Punchbowl Formation in Cajon Pass is offset along the Cleghorn fault approximately 4 kilometers. (3) Restoration of 3-4 km of cumulative left-lateral offset results in the alignment of unique members of the Cedar Springs fault system, permitting a refined offset estimate of 3.5 to 4.0 kilometers of total left-lateral displacement.

A set of north-plunging, east-block-down monoclinal warps form anticline/syncline pairs in the basal Crowder Formation and underlying late Miocene erosion surface (Section 5.10.1), which are offset 3 to 4 kilometers in a left-lateral sense on the Cleghorn fault zone (Figure 5-4). The major plunging anticline/syncline pair just southwest of Silverwood Lake is correlated with a similar feature responsible for an embayment and salient in the Miocene erosion surface in lower Little Horsethief Canyon and Cleghorn Mountain respectively. The northern end of the Silverwood Lake reservoir is largely underlain by Crowder Formation (California DWR, 1968b), which occupies a structural trough which appears to be part of another north-plunging monocline, somewhat modified by later faulting. This feature is believed to correspond to a series of smaller folds on the south side of the Cleghorn fault in Miller Canyon[100]. An estimate of offset for these folds is obtained after following their axes to the Cleghorn fault. This can be done with considerable accuracy since the folds are clearly expressed in the late Miocene erosion surface even in the absence of Crowder Formation[101]. The plunging monoclines indicate a cumulative left-lateral offset of 3 to 4 kilometers on the Cleghorn fault.

Another basis for measurement of cumulative offset is the steep eastern limit of the Cajon beds of the Punchbowl Formation, which is offset 3 to 4 kilometers left-laterally (Figure 5-5). Restoration of this motion aligns

Figure 5-4. Offset of north-plunging monoclines east of Cleghorn Mountain (Meisling and Weldon, 1982). A north-plunging monocline, or anticline/syncline pair, is offset 3 to 4 kilometers in a left-lateral sense along the Cleghorn fault. Fold axes can be projected with confidence due to their expression in the late Miocene erosion surface that is present throughout the area. Folds were also cut and displaced is a south-block-down, dip-slip sense prior to offset on the Cleghorn fault zone.

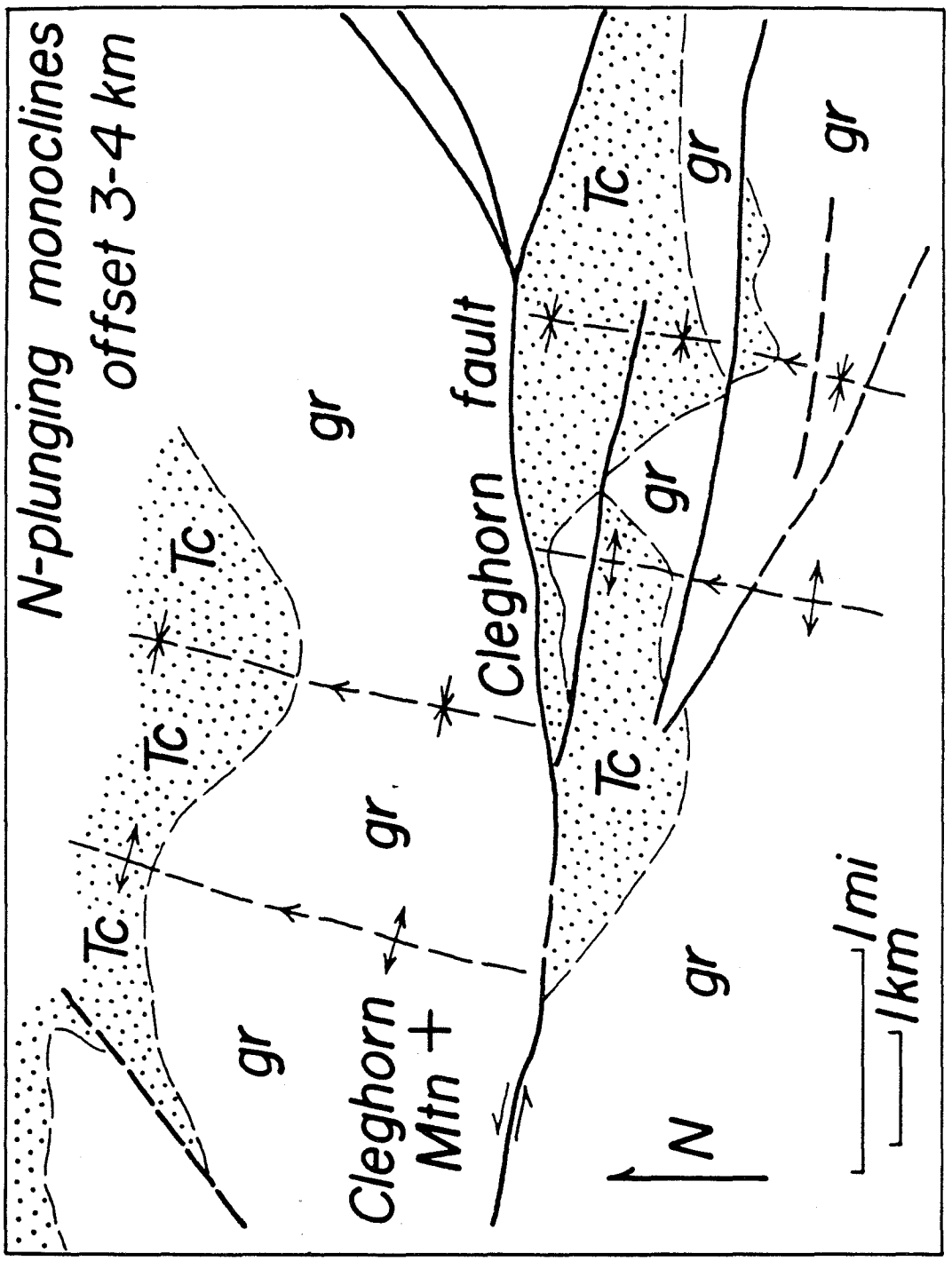
N-plunging monoclines
offset 3-4 km
Tc
Tc
Tc
gr
Cleghorn fault
Tc
gr
gr
gr
Cleghorn Mtn
Tc
gr
gr
N
1 mi
1 km

Figure 5-5. Offset high-angle eastern limit of the Punchbowl Formation (Meisling and Weldon, 1982). A unique spatial arrangement of structural and stratigraphic elements is offset 3 to 4 kilometers left-laterally along the Cleghorn fault near Cajon Pass. The high-angle contact between the Punchbowl Formation and the granodiorite of Squaw Peak was interpreted as a buttress unconformity by Woodburne and Golz (1972). The high-angle contact bounds the west side of the granodiorite of Squaw Peak, while the Squaw Peak fault bounds the east side, down-dropping the Crowder Formation. The same unique arrangement of features is found on the south side of the Cleghorn fault. The features are offset approximately 3 to 4 kilometers.

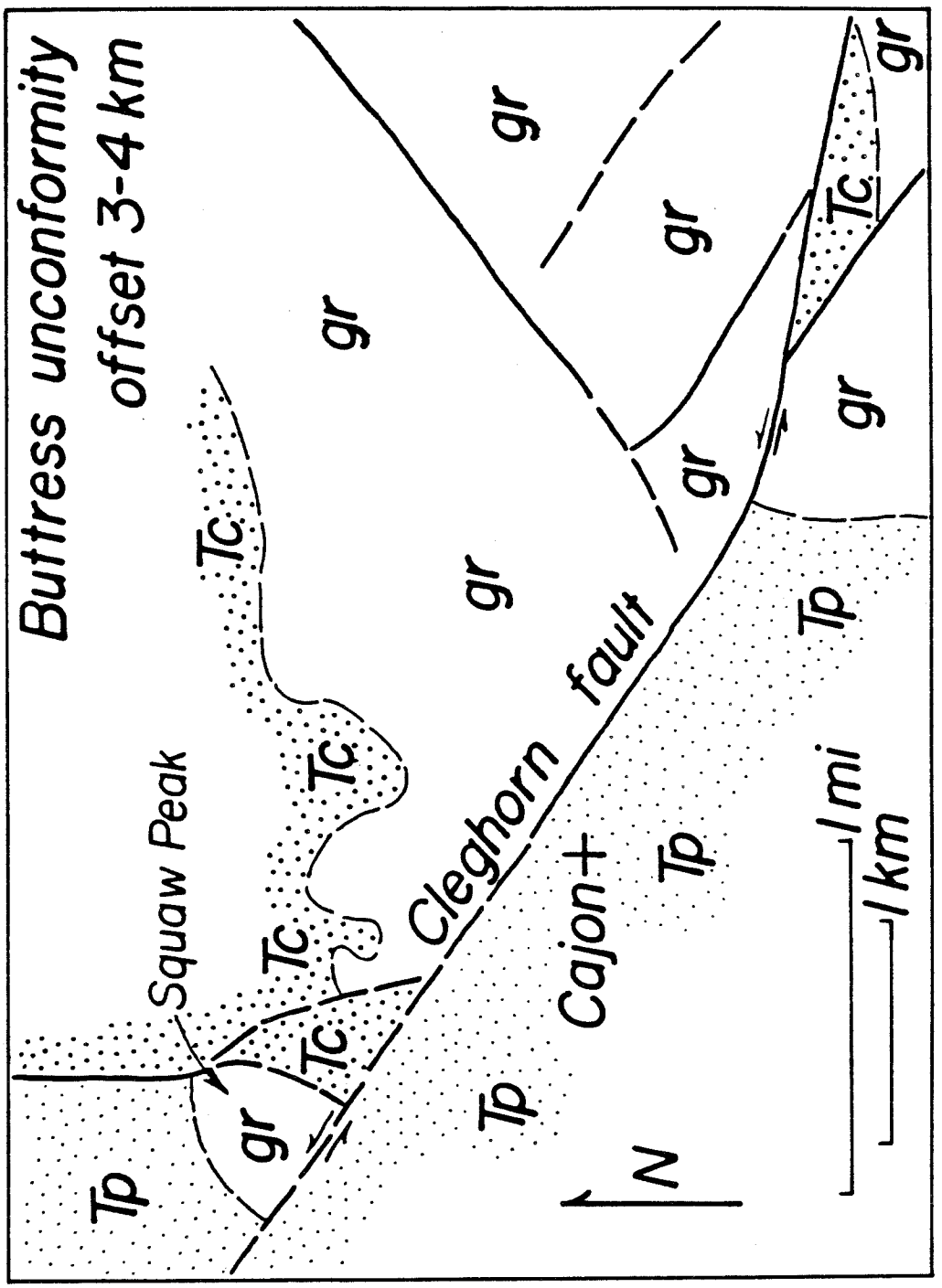
Buttress unconformity
offset 3-4 km
Squaw Peak
Cleghorn fault
Cajon
Tp
Tc
gr
N
1 mi
1 km

the Squaw Peak and Powell Canyon faults, both of which place Crowder Formation on the east against granodiorite on the west. The Punchbowl Formation, granodiorite, major north-block-down faulting and Crowder Formation form a unique spatial arrangement not found anywhere else in the area. A very complex sequence of structural events would be required to juxtapose these elements by some means other than simple left-lateral offset of 3 to 4 kilometers on the Cleghorn fault.

Restoration of 3 to 4 kilometers of left-lateral offset on the Cleghorn fault aligns the Squaw Peak/Powell Canyon fault zone and the Notch/Seeley Creek fault zone (Figure 5-3). These fault zones are unique members of the Cedar Springs fault system since they display north-block-down separation (Section 5.2.2). The fault zones intersect the Cleghorn fault at a significant angle[11], and can therefore be used as piercing points. This technique results in a refined estimate of 3.5 to 4.0 kilometers of cumulative left-lateral offset on the Cleghorn fault. This estimate is consistent with the less accurate, but possibly more compelling, offset estimates outlined above. In summary, all of the pre-Quaternary geologic features point to a total left-lateral offset of 3.5 to 4.0 kilometers on the Cleghorn fault.

East of the study area the Cleghorn fault itself appears to turn northeast and join the Tunnel Ridge lineament, which crosses the western San Bernardino Mountains from Tunnel Ridge to Fifteen-Mile Valley (Dibblee, 1974). West of the study area, the Cleghorn fault turns northwest and goes beneath the alluvium of a northwest-trending linear valley, from which it never emerges. It is not known if the motion on the Cleghorn fault dies out to the west, or is replaced by deformation of another kind. There is no evidence to support a direct connection with the San Andreas fault.

5.3.2 Northeast-Trending Splays

The Silverwood Lake fault zone splays off of the Cleghorn fault just west of Silverwood Lake and crosses to the range front in Summit Valley. Similar northeast-trending splays are found in Little Horsethief Canyon and on Pilot Rock ridge east of the reservoir. The manner in which these splays offset the Cedar Springs fault system and late Miocene erosion surface is suggestive of left-lateral and southeast-block-down motion. The Tunnel Ridge lineament, much farther to the east and outside the study area, also bears a remarkable geometric similarity to the these splays. All of these structures may be responsible for linking the Cleghorn fault with the north frontal fault system of the San Bernardino Mountains, possibly via the Summit Valley fault zone.

The northeast-trending splays show evidence of late Pleistocene motion (California DWR, 1968b), indicating that they should be considered part of the lateral Cleghorn fault system. The splays may well have played an earlier role in the Pliocene and Pleistocene Cedar Springs fault system.

5.3.3 The Grass Valley Fault

The Grass Valley fault (Figure 5-1) shows clear evidence of lateral displacement. Grass Valley itself follows this fault for about a kilometer. Several smaller drainages to the west of Grass Valley show signs of disruption and diversion. All the drainages west of Grass valley terminate abruptly at the fault zone[102]. One drainage, about a kilometer east of Grass Valley, traverses a wide valley[103] and large dissected fan-shaped pediment surface[104], but draws on a very small upstream drainage basin area. This drainage may once have carried greater runoff, perhaps from Grass Valley. If so, the Grass Valley fault may have a kilometer of left-lateral slip on it. These geomorphic features seem too fresh to be due only

to lateral motion in the middle Pleistocene. By analogy with the Cleghorn fault zone, the Grass Valley fault may have experienced more than one type of motion during its history.

Vertical offset on the Grass Valley fault is not more than several tens of meters, based on the separation on the basal Crowder Formation and the late Miocene erosion surface. The Grass Valley fault bounds the north side of a prominent ridge that confines Silverwood Lake on its north side[105]. The south side of this ridge is defined by one of the larger members of the south-block-down fault set. Thus, this ridge appears to be compressional in origin. There is no comparable structure in the Cedar Springs fault system. A similar ridge is associated with the Arrastre Canyon Narrows fault, which is believed to be a middle to late Pleistocene structure. Evidence points to post-middle-Pleistocene movement in the Grass Valley fault, although it was probably originally part of the Cedar Springs system, and has been reactivated as a lateral fault.

5.3.4 The Summit Valley Fault Zone

Geomorphic features in Summit Valley (Figure 5-1) raise the possibility of an east-trending fault zone buried beneath the alluvium of the valley floor. West Summit Valley is remarkably linear. Dibblee (1965) shows a buried fault beneath the valley fill. Abundant lineaments in central and east Summit Valley trend east-northeast to east. A system of east-trending faults cuts the Miocene erosion surface, the volcanogenic eastern facies of the Crowder Formation and north-northeast-trending lineaments in the Pinnacles area. No youthful fault-related geomorphic features are evident.

Although the Summit Valley fault system shows separation indicative of minor north-block-down or right-lateral displacement at the east end of Summit Valley, marker beds in the volcanogenic eastern facies of the Crowder

Formation is not significantly offset by it. Furthermore, lineaments in the verdant valley floor to the west are discontinuous, and some may be due to simple damming of groundwater by impermeable strata, rather than faulting.

Vertical bedding, suggestive of lateral faulting, is exposed adjacent to a thick clay-rich zone in a roadcut exposure along the Goat Trail Road in central Summit Valley[106]. This exposure coincides with an east-trending lineament that is expressed in the Qt2 terrace surface to the west. The lineament cannot be followed farther to the west, but vertical bedding is again found in the northeastern exposures of the volcanogenic eastern facies of the Crowder Formation near Deep Creek[107]. It seems possible that evidence for a through-going structure once existed in Summit Valley but has been obliterated by livestock and human activity. Whatever the merits of evidence for an integrated fault zone in Summit Valley might be, it must be considered a potentially significant, if minor, tectonic element. It may have sustained some vertical motion during the activity of the Cedar Springs system, and then been incipiently reactivated as a lateral fault zone during the development of the Cleghorn system. It is difficult to put much cumulative offset on the system since the late Pliocene deposition of the volcanogenic eastern facies of the Crowder Formation.

5.4 THE TUNNEL RIDGE LINEAMENT

The Tunnel Ridge lineament (Figure 5-1) is a major northeast-trending physiographic feature that extends from Miller Canyon in the western San Bernardino Mountains to the northern range front at Arrastre Canyon. Although it lies outside the study area and was not mapped, it appears to be a significant tectonic element linking the Cleghorn fault zone and the Sky Hi Ranch fault zone via the Arrastre Canyon graben.

The Tunnel Ridge lineament is made up of a series of broad linear

valleys developed on the late Miocene erosion surface. It bounds the west side of Tunnel Ridge in east Miller Canyon, continues northeast along Kinley Creek, where it merges with the Cleghorn fault zone and several other east-northeast-trending lineaments from the Pinnacles area. It crosses Deep Creek and splays out into several diverging fault traces, known as the Arrastre Canyon graben.

Dibblee (1974) maps the Tunnel Ridge lineament as a continuous fault between Miller Canyon and Deep Creek. MacColl (1964) shows the diverging splays of the Tunnel Ridge lineament cutting the margin of the Rattlesnake Mountain Pluton north of Deep Creek. Both Dibblee and MacColl stop short of actually connecting the diverging northern splays of the Arrastre Canyon graben to the Tunnel Ridge lineament. Dibblee (1974), however, does connect the Lovelace Canyon fault with the Tunnel Ridge lineament near Deep Creek. For the purposes of this study, the Tunnel Ridge lineament is considered essentially continuous, and of potential neotectonic significance. The term "lineament" is chosen to reflect the possibility that the feature may actually be a collection of related tectonic elements, rather than a single continuous fault zone. The physical continuity of Tunnel Ridge lineament and its splays north of Deep Creek has yet to be shown.

Parts of the Tunnel Ridge lineament must have had motion since the middle Pleistocene. Just east of the study area, the Cleghorn fault zone enters a broad valley which turns northeast and merges with the Tunnel Ridge lineament. This suggests that the lineament has probably experienced Pleistocene motion north of the junction. The Bowen Ranch fault and the Arrastre Canyon Narrows fault, both part of the Arrastre Canyon graben Section 5.7), cut middle Pleistocene terrace gravels, supporting this conclusion. The lineament must also have sustained motion prior to the

development of the Cleghorn fault zone, since it is offset by a south-block-down member of the late Pliocene Cedar Springs fault system south of the Cleghorn fault zone in east Miller Canyon (Dibble, 1974). Dibblee shows the Tunnel Ridge lineament truncating west-northwest-trending lineaments near Deep Creek. Faults of this trend are thought to predate uplift of the San Bernardino Mountains in the late Pliocene (Section 5.6). The Tunnel Ridge lineament possibly originated in the middle to late Pliocene during incipient uplift of the San Bernardino Mountains. Its motion continued through, or was reactivated during, the middle Pleistocene.

There is conflicting evidence for the magnitude and sense of displacement on the Tunnel Ridge lineament. At the junction with the Cleghorn fault, sizeable left-lateral motion might be transferred to the Tunnel Ridge system. Relative continuity of the late Miocene erosion surface south of Deep Creek rules out any large component of vertical displacement. There is evidence for right-lateral, reverse, and normal faulting in the Arrastre Canyon graben. The apparent ambiguity in the sense of these displacements points to the need for further work on the Tunnel Ridge lineament. Much could be learned by examining the drainage patterns, relict erosion surface, and young deposits along the Tunnel Ridge lineament.

5.5 THE ORD MOUNTAINS FAULT ZONE

The north frontal fault system of the San Bernardino Mountains trends north along the west flank of the Ord Mountains between Grass Valley and the Marianas Rancho of Apple Valley (Figure 5-1). The system can be divided into high-angle and low-angle faults, active at different times. The low-angle faults are expressed in a long scarp in the older (Qf2) fanglomerates of the range front. The high-angle faults, apparently responsible for creating most of the range-front relief, are older. There is some evidence

to suggest an earlier episode of low-angle faulting.

5.5.1 Low-angle Faults

5.5.1.1 The Deep Creek Fault Zone

The Deep Creek fault zone (Figure 5-1) is the westernmost member of the highly varied group of range-bounding reverse faults that are collectively referred to as the "north frontal fault system". The Deep Creek fault zone begins just east of Grass Valley, replacing the Grass Valley warp as the range-bounding structure. It extends north-northeast as far as the SCE Powerline Road, where it abruptly turns east-northeast to join the Apple Valley Highlands fault zone. The east-northeast-trending structure appears to be a tear fault, although a warp or reverse fault cannot be ruled out.

The Deep Creek fault zone cuts the late Miocene erosion surface just east of Grass Valley, exposing fresh bedrock in the steep west-facing slopes along the range front[108]. The deeply weathered erosion surface is relatively continuous from the Pinnacles to the range front, where it is clearly broken. The erosion surface reappears beneath the volcanogenic eastern facies of the Crowder Formation on the downthrown side of the fault zone. The Miocene erosion surface is also offset by several east-trending faults that are part of the Summit Valley fault zone. Numerous natural springs occur along the trace of the Deep Creek fault zone south of the Mojave River, especially at intersections with east-west trending faults.

In the vicinity of the Mojave River Dam, the ground surface has been extensively modified by dam construction activity and later offroad vehicle use. Fortunately, the location of the Deep Creek fault zone in the immediate area of the dam is well documented in the Mojave River Dam construction reports (U. S. Army Corps of Engineers, 1982).

Range-front alluvial fan deposits (Qf2) are abruptly truncated along a

north-trending scarp just south of the SCE Powerline Road[109]. This feature resembles the scarp on the Apple Valley Highlands fault zone, and is interpreted as the continuation of the Deep Creek fault zone north of the dam.

The Deep Creek fault zone is best exposed in the east abutment of the wing dike of the Mojave River Dam. It dips 45° east and into the abutment, putting sheared basement rock over siltstones correlated with the volcanogenic eastern facies of the Crowder Formation[110]. U. S. Army Corps of Engineers (1982) shows the fault cutting and deforming sediments referred to the Harold Formation, almost certainly part of the Victorville Fan section. Relationships south of the Mojave River also place basement rocks topographically over the volcanogenic eastern facies of the Crowder Formation[111], without any occurence of basement clasts in the Crowder sediment. Although the fault surface is not exposed, outcrop patterns suggest that is a low- to medium-angle reverse fault. Parallel shears exposed in the Mojave River Dam foundation excavations and roadcuts on the SCE Powerline Road dip as shallowly as 20° to the east.

In an effort to reconstruct displacements on the faults east of Grass Valley, the base of the late Miocene weathering profile was mapped as a marker bed[112]. Vertical separation of the relict erosion surface increases to the northeast along the Deep Creek fault zone. East-trending members of the Summit Valley fault zone also offset the Miocene erosion surface vertically with a north-block-down or right-lateral sense of motion[113] (Section 5.3.3). Members of the Cedar Springs fault system further complicate the picture, displacing the relict surface in a southeast-block-down sense. Warping on the Grass Valley warp is also involved. The range front between Grass Valley and Deep Creek is one of the most complex

structural knots in the study area. The total vertical displacement of the Miocene erosion surface across all of these structural elements is about 250 meters, northwest-block-down.

The clast lithologies in the alluvial fan gravels along the Deep Creek fault zone north of the Mojave River Dam show no evidence of being displaced laterally from their source drainages by the fault. The surfaces of the fans are truncated, however, and down-dropped at least 30 meters to the west. Although the Deep Creek fault zone clearly cuts the Victorville Fan sediments at the Mojave River Dam, the magnitude of the west-block-down displacement is unknown.

The east-northeast-trending structure that connects the north end of the Deep Creek fault zone with the south end of the Apple Valley Highlands fault zone appears to be intimately related to these faults[114]. The connecting structure does not affect the crystalline rocks east of the Apple Valley Highlands fault zone; the Apple Valley Highlands fault zone does not appear to continue into the crystalline basement south of the connecting fault. These observations suggest that the east-northeast-trending structure is not following a pre-existing weakness, but rather is related to the development of the reverse structures. Either a reverse fault or a lateral tear fault could account for the observed range-front relief.

5.5.1.2 The Apple Valley Highlands Fault Zone

A prominent scarp cuts the older alluvial fans along the western flank of the Ord Mountains from Powerline Canyon to the Marianas Rancho. The fault surface is not exposed, but the topographic expression of the fault trace suggests a medium- to low-angle, east-dipping reverse fault. This structure, herein named the Apple Valley Highlands fault zone, is linked to the Deep Creek fault zone at its southern end by an east-northeast-trending connecting

structure interpreted as a probable tear fault. At its northern end, the Apple Valley Highlands fault zone becomes a fold in the Ord River Gravel, probably in response to faulting in the underlying basement. The faulting may represent a reactivation or continuation of motion on the reverse fault originally responsible for uplift of the Ord Mountains.

The Apple Valley Highlands fault zone cuts the Qf2 fanglomerates that mantle the base of the slope of the Ord Mountains[115]. The fanglomerates topographically overlie the Ord River Gravel in the Marianas Rancho area [116]. No other units are cut, the faulting being restricted almost exclusively to the lower slope of the Qf2 fans.

The maximum vertical offset of the surface of the Qf2 fans is 70 meters, in a west-block-down sense. Vertical separation on the scarp decreases southward to 30 meters or less at the Juniper Ranch. These offset measurements were made where the Qf2 surface is locally preserved west of the fault zone. The Apple Valley Highlands fault zone dies out into folding northward, consistent with relatively small displacements since the deposition of the Ord River Gravel in the middle Pleistocene.

The clasts in all of the alluvial fans are consistent with derivation from the local drainage presently upstream. Thus, there is no evidence of appreciable lateral offset of the Qf2 fanglomerate.

No evidence of disruption was found in the small fans that exit the steep-walled gullies along the scarp face. The lack of weathering products developed on the boulders in these small fans results in a grey appearance on color airphotos, and is interpreted as indicating possible Holocene age. No geomorphic features suggestive of Holocene motion were found along the scarp face. These observations might be misleading, however, since the age of the young fans is unknown, and delicate evidence of surface rupture could

disappear very rapidly.

Both the surficial weathering profile and internal stratification of the older fanglomerate (Qf2) are warped adjacent to the fault. Dips as steep as 50° to the northwest can be measured on layers within the fans[117]. Laminated caliche deposits and a reddish surficial oxidized layer associated with soil developed on the fan surface are warped down at the fault scarp. Such warping adjacent to the fault trace could lead to low estimates of vertical separation.

The scarp itself is inclined about 30° at its steepest point and notably lacks evidence of landslides, slumping or hummocky ground to indicate fresh scarp formation or mass wasting. The scarp surface lacks resistant outcrops of cemented fanglomerate being covered with a mantle of loose clasts. These characteristics of the scarp surface contrast sharply with the near-vertical walls of the incised gullies. They suggest that the scarp is either much older than the gully walls, or originated as a composite feature produced by complex motion on several related fault planes. Unfortunately, the Apple Valley Highlands fault zone is unsuitable for trenching due to the coarse, strongly-cemented nature of the older fanglomerate. Shearing would be hard to recognize in the coarse fan gravels, especially for small displacements; carbonate cementation virtually rules out backhoe excavation.

The largest of the younger fans disgorges from precipitous Juniper Canyon, south of the Juniper Ranch. The fan surface is undisturbed across the fault trace as projected, based on nearby scarps[118]. Juniper Ranch itself is sited on the fault projection, making it impossible to rule out any small-scale topographic disruption. No shearing is evident in cutbank exposures of the Qf1 fanglomerate where the Juniper Canyon drainage crosses the fault zone just south of the Juniper Ranch.

Despite the impressive geomorphic expression of the Apple Valley Highlands fault zone, there is no conclusive evidence to suggest Holocene activity. The Qf2 fanglomerate, which is clearly cut by the fault, is correlated with the Summit Valley facies of the Ord River Gravel, and both are thought to be middle to late Pleistocene in age. The total displacement of the fan surface is not great, which suggests that most of the uplift of the Ord Mountains was accomplished during an early to middle Pleistocene episode of faulting. This raises the possibility that there exists a buried fault system that was responsible for the uplift of the Ord Mountains.

Just south of the point where the Apple Valley Highlands fault zone steps away from the range front in the Marianas Rancho area, a splay diverges eastward along the northern base of the Ord Mountains[119]. This splay can be traced in the Qf2 deposits but is buried by the younger Qf1 fan gravels. It does suggest that a buried reverse fault zone lies beneath the fans on north side of the Ord Mountains. The topographic relief decreases eastward along the north flank, and total vertical displacement of the Miocene erosion surface decreases and dies out. By inference, vertical displacement on the postulated eastern extension of the Apple Valley Highlands fault zone probably dies out. These observations lend credence to the hypothesis that the reverse faulting that breaks the fans on the west flank of the Ord Mountains is a reactivated strand of an older system that was active during uplift of the Ord Mountains.

The Apple Valley Highlands fault zone cannot be traced south of Powerline Canyon. It appears to turn southwest and join the Deep Creek fault zone. There is some brecciation of the bedrock adjacent to the fan/basement contact on the north side of Powerline Canyon, which indicates that faulting does not die out there [120].

5.5.2 High-angle Faults

5.5.2.1 The Powerline Road Fault Zone

The Powerline Road fault zone is made up of three parallel north-northeast-trending high-angle faults that are exposed on the west side of the Deep Creek pendant north of the Mojave River Dam and south of Powerline Canyon. These faults show west-block-down motion, and cut the Deep Creek facies of the Ord River Gravel. Folding of the Ord River Gravel is evident adjacent to the fault zone in several exposures[121]. They may be correlative with the Juniper Ranch fault zone.

Aside from the obvious physiographic relief of the range front, the Powerline Road fault zone is not well expressed geomorphically. The faults do not appear to disturb the upper surface of Qf2, although they do break the basal deposits of the Qf2 fanglomerate[122]. Lineaments associated with the faults appear to reflect the juxtaposition of different lithologies rather than the displacement of landforms.

Maximum vertical displacement across the Powerline Road fault zone is ultimately limited by the lack of Ord River Gravel on the erosion surface that caps the Deep Creek pendant. The Ord River deposits occur on the west side of the fault zone, and the late Miocene erosion surface must have been at or above their level during the middle to late Pleistocene to escape deposition. Thus vertical separation can not have exceeded the 300-350 meters that now separate the Ord River Gravel and the Miocene surface. There is no evidence to constrain vertical offset since the deposition of Qf2, since what little alluvium is preserved east of the fault zone is of questionable age.

The possibility that the Powerline Road fault zone was once a lateral fault system cannot be ruled out. The alluvial fans west of the Powerline

Road fault zone contain clasts that are derived from the drainage basin presently upstream, however, ruling out any significant lateral offset since Qf2 fan deposition.

Movement on the Powerline Road fault zone is interpreted as predating the latest movement on the Deep Creek fault zone, and largely postdating deposition of the Deep Creek Facies of the Ord River Gravel, >730,000 y ago (Section 4.4.3).

5.5.2.2 The Juniper Ranch Fault Zone

The Juniper Ranch fault zone trends north-northeast from the vicinity of Juniper Canyon along the west flank of the Ord Mountains to the Marianas Rancho area, where it joins the Apple Valley Highlands fault zone. It may be the northward continuation of the Powerline Road fault zone. The fault zone is near-vertical in dip.

The Juniper Ranch fault zone is geomorphically evident in a series of saddles, benches, and drainage irregularities which combine to form a lineament. Geomorphic expression is not fresh, however, and the fault is difficult to trace on the ground. The geomorphic expression seems to be due to vertical offset of the late Miocene erosion surface, which is still locally preserved in the form of knobs and benches on the down thrown side of the fault zone[123].

A cemented breccia (Qb) composed of angular fragments of dolomitic limestone and quartz-monzonite is spatially associated with the trace of the Juniper Ranch fault[124]. There is no evidence of shearing in the matrix to suggest that the cemented breccia was produced by fault movement <u>per se</u>, yet fault movement was almost certainly responsible for the steep slopes that must have existed for such a breccia to form. Old fanglomerates (Qf2) are deposited on crystalline bedrock in a steep buttress unconformity[125]

which also suggests deposition along a youthful, fault-related mountain front. The cemented breccia is therefore interpreted as a talus deposit developed on oversteepened slopes along a receding mountain front.

The Juniper Ranch fault traverses primarily crystalline basement rocks but does appear to define the eastern limit of the lower parts of the older fans (Qf2)[126]. It cannot be shown to cut the Qf2 surface, however, and it is unclear whether the Juniper Ranch fault cuts the Ord River Gravel at its northern end. These observations are consistent with the Juniper Ranch fault being the northern extension of the Powerline Road fault zone.

There is no basis for estimating cumulative offset for the Juniper Ranch fault zone, as no suitable datum exists. A total vertical offset of the Miocene erosion surface of <400 meters since the deposition of the Ord River Gravels would seem to be an unavoidable consequence of the lack of Ord River Gravel preserved on the erosion surface east of the zone. The character of sediments in the Juniper Flats area is further evidence that the Ord Mountains were an effective barrier to the sediments of the Victorville fan during the middle to late Pleistocene. Hence, the Juniper Ranch/Powerline Road fault zone may have been responsible for substantial uplift in the Ord Mountains.

There are several lineaments along the west flank of the Ord Mountains that parallel the Juniper Ranch fault. The contact between the Summit Valley facies of the Ord River Gravel and the Qf2 fanglomerate is very linear south of the Marianas area[127]. Lack of exposure makes it difficult to determine whether this feature is a fault, fold or cutbank. It is shown as a lineament and must be considered a potential member of the Juniper Ranch fault zone until proven otherwise. Dibblee (1974) shows a north-northeast-trending fault disrupting the surface of the Qf2 fan surface just east of the Apple

Valley Highlands fault zone[128]. The lineament associated with this feature may simply be an artifact of fan segmentation patterns.

The Juniper Ranch fault zone must be also be considered in the context of other north-northeast-trending fault zones in the study area. The trend of the fault zone suggests a relationship with the Bowen Ranch fault, Lovelace Canyon fault system, Silverwood Lake fault zone, Tunnel Ridge lineament, and northeast-trending lineaments in the Pinnacles area. The Pinnacles lineaments are interpreted as a disarticulated southern extension of the Juniper Ranch/Powerline Road fault zone. A strong pattern of pre-existing weaknesses appears to have dictated the trend of all of the north-northeast-trending faults. The Arrastre Canyon graben suggests that these structures may have developed in a localized environment of extension. The west flank of the Ord Mountains could have been formed by normal faulting on the high-angle faults.

The Juniper Ranch fault may have, in turn, provided a pre-existing weakness for the Apple Valley Highlands fault zone to follow. The Juniper Ranch fault zone descends across a broad bench and joins the Apple Valley Highlands fault zone at the point where it steps away from the range front [129]. The Apple Valley Highlands fault zone may have explioted this weakness in jumping out from the range front. The geometry could also be explained by offset of an older thrust system along the Juniper Ranch fault zone, followed by reactivation of the thrust.

Brown (1979) shows the Juniper Ranch fault cut by one of the northwest trending faults in the Ord Mountains pendant. This would make the Juniper Ranch fault early Tertiary or latest Mesozoic in age. No evidence was found in the field to support this conclusion.

5.6 THE POWERLINE CANYON FAULT ZONE AND RELATED STRUCTURES

A half-kilometer-wide zone of deformed phylonite is exposed in Powerline Canyon at the contact between the Ord Mountains pendant and the Deep Creek pendant. The zone is considered a fault on the basis of its straight course and the highly disconformable nature of the contact.

The Powerline Canyon fault is near-vertical in dip, linear, and at least 2 km long. Phylonite, developed on the metasediments of the Ord Mountains pendant adjacent to the fault zone, displays tight folding and boudinage indicative of intense deformation[130].

The fault can be traced to the east, where it appears to cut the biotite quartz monzonite of the Mesozoic batholith[131]. In a regional sketch map, MacColl (1964) shows the fault dying out in the batholithic rocks, but its precise eastern limit is not known. There is no evidence to suggest that the Powerline Canyon fault displaces the fan gravels at the mouth of Powerline Canyon. It is possible that the Powerline Canyon fault provided a pre-existing weakness that led to the development of the tear fault that connects the Deep Creek and Apple Valley Highlands fault zones (Section 5.5.1.2).

The Powerline Canyon fault zone is overlain by terraces deposits preserved high on the south wall of Powerline Canyon[131]. These terraces are of unknown age. They appear to be graded to the same level as a long linear bedrock ridge on the north side of Powerline Canyon. The topographic height of this undisturbed terrace deposit offers further proof that motion of the Powerline Canyon fault predates most of the uplift in the Ord Mountains.

Powell (1982, pers. comm.) observed that the metamorphic grade of the metasediments in the Deep Creek pendant is higher than that in the Ord Moun-

tains pendant, north of the Powerline Canyon fault. Foliation within the Ord Mountains pendant is parallel to the fault zone in the immediate vicinity of the structure. These observation, plus the phylonite zone, suggest that the Powerline Canyon fault may have sustained a large component of motion.

Parallel faults, mapped by Brown (1979) and Coffman (1980), cut both metasedimentary and batholithic rocks in the Ord Mountains[132]. The faults in the Ord Mountains to the north are high-angle structures that trend west-northwest and are frequently associated with fault breccias (Ely, 1982; Coffman, 1980). They are believed to be members of a set of northwest-trending faults in the Mojave block which predate uplift of the San Bernardino Mountains.

The northwest-trending faults in the Ord Mountains cannot be traced in the alluvial gravel of the Juniper Flats area, indicating that they are middle Pleistocene or older. They do not appear to interrupt the Juniper Ranch fault, suggesting that they predate range-front uplift. Northwest-trending faults in the Ord Mountains do not appear to be expressed as lineaments on the Miocene erosion surface, indicating that they may be pre-late-Miocene in age.

Coffman (1980) indicates that lamprophyric dikes of unknown age are contemporaneous with northwest-trending faults in the Ord Mountains, suggesting that the faults may have developed on early Tertiary zones of weakness. The northwest trend of these structures is obliquely transverse to the north-south, low-angle axial planes of the isoclinal folding in the Ord Mountains (Brown, 1979), indicating that development of the Powerline Canyon fault may be unrelated to pre-batholithic deformation.

Northwest-trending faults are mapped by Dibble (1974) to the southeast of the Ord Mountains. These faults lie east of the Tunnel Ridge lineament,

and are truncated by it. Sadler (1981) interprets many of the northwest-trending structures in the central and eastern San Bernardino Mountains as older Mojave-block structures. He indicates that some of these structures may have been locally reactivated in the Quaternary, especially along the projection of the Helendale and Sky Hi Ranch faults.

5.7 THE ARRASTRE CANYON GRABEN

The Arrastre Canyon graben is a group of northeast-trending faults that diverge from the north end of the Tunnel Ridge lineament and may connect with the north frontal fault system in Fifteenmile Valley. The graben includes the Bowen Ranch fault, Arrastre Canyon Narrows fault zone, and Lovelace Canyon fault system (Figure 5-1). These faults show evidence of early right-lateral motion, followed by dip-slip motion leading to formation of the Arrastre Canyon graben, and finally reverse motion in response to compression.

Collectively, members of the Lovelace Canyon fault system form the eastern limit of the Arrastre Canyon graben. The western limit of the graben is defined by the Bowen Ranch fault. Although the amount of down-faulting is minimal, the graben structure is significant in that it indicates that an extensional environment existed locally within a prevailing compressional regime. The fact that Arrastre Canyon has been a site of sedimentation throughout the Pleistocene, and possibly part the Pliocene, is indicative of graben formation. Tilting and warping accompanied faulting during graben formation as evidenced by the attitude of the Miocene erosion surface in Arrastre Canyon. Down-bowing of the erosion surface in Arrastre Canyon is probably due in part to the nature of deformation within the coarse crystalline Rattlesnake Mountain pluton. Faulting may have been secondary to warping in graben formation.

Many faults in the western San Bernardino Mountains share the north-northeast trend of the Arrastre Canyon graben faults. Although most of these faults show evidence of activity since middle Pleistocene, their common trend suggests that they may have all exploited a pre-existing system of weaknesses. The Lovelace Canyon fault system may represent the least-modified part of this older fault set. Other faults that trend north-northeast include the Tunnel Ridge lineament, Silverwood Lake fault zone, Powerline Road fault, Bowen Ranch fault, and Juniper Ranch fault.

5.7.1 The Bowen Ranch Fault

The Bowen Ranch fault trends north-northwest from where it enters the map area in the vicinity of the Bowen Ranch to head of the Arrastre Canyon fan at the range front. Although the fault cannot be followed north of the Bowen Ranch Road at the head of the Arrastre Canyon fan, it may continue north under the alluvium along the fan-head trench to Roundup Way. The fault extends out of the area to the south, where Dibblee (1974) shows meta-sedimentary exposures that apparently preclude direct connection with the colinear Tunnel Ridge lineament. The Bowen Ranch fault is high-angle, linear, and anastamosing.

The trace of the Bowen Ranch fault is largely confined to the late Miocene erosion surface developed on the Rattlesnake Mountain pluton. It is expressed as a lineament in the weathered erosion surface, which roughly follows a linear body of diorite interpreted by MacColl (1964) as a septum between two intrusive tongues of the pluton. The fault trace is characterized by numerous fault-related geomorphic features such as disturbed drainage patterns, linear stream courses, saddles, and notches. A zone of greenish-white clay gouge is locally up to a half a meter in width along the fault[133], acting as an effective groundwater barrier. Springs occur

where stream channels cross the fault trace.

The Bowen Ranch fault clearly cuts middle Pleistocene(?) terrace gravel in roadcut exposures along the Bowen Ranch Road[134], although the fault cannot be traced into sediments of the Arrastre Canyon fan at its northern end. Youthful, possibly Holocene(?), terrace deposits appear undisturbed at the fault trace[135]. MacColl (1964) shows the Bowen Ranch fault cutting the margin of the Rattlesnake Mountain Pluton. The fault clearly disrupts the late Miocene erosion surface. Cross-cutting relationships with other faults are unknown, since there are no intersections with other faults within the map area. Based on its trend, the Bowen Ranch fault is considered part of the north-northeast-trending regional fault pattern.

The sense of separation on the Bowen Ranch fault is east-block-down and right lateral. A maximum vertical offset is constrained by the Miocene erosion surface and middle Pleistocene(?) terrace gravel to be less than 30 meters. Middle Pleistocene terrace gravel is offset in an east-block down sense at both ends of the fault trace[136]. Right-lateral separation of the margin of the Rattlesnake Mountain pluton is half a kilometer or less[137] (MacColl, 1964). Stream channel offsets are suggestive of left-lateral displacement[138], although this may be due to drainage diversion or capture. The somewhat conflicting evidence points to a small amount of late-Pleistocene vertical offset, with possible previous right-lateral offset.

5.7.2 The Arrastre Canyon Narrows Fault Zone

The Arrastre Canyon Narrows fault zone enters the map area near Round Mountain trending northeast, turns east-northeast and finally joins the Sky Hi Ranch fault east of Grapevine Canyon. Dibblee (1974) extends the fault zone southwest to within a kilometer of the Tunnel Ridge lineament, but does

not show a direct connection. The junction with the Sky Hi Ranch fault is complex, and may involve local reactivation of part of the White Mountain thrust system. The central segment of the fault is a zone of high-angle faults one half kilometer in width, which contains a major compression ridge. The geomorphic expression of the fault trace is highly variable, and ambiguities exist with regard to the youthfulness of the features.

The late Miocene erosion surface forms a northwest-dipping ramp on both sides of the fault trace. This surface is also present on top of the ridge within the fault zone, as evidenced by the presence of residual boulders and a rounded lag gravel[139]. Despite the pressure ridge, the overall effect of the fault zone is to drop the erosion surface down to the northwest.

The northeast-trending fault-bounded ridge acts as a barrier to northwest-trending drainages, which coalesce and pass through the ridge in bedrock narrows[140]. Downcutting of these drainages has accentuated relief on the ridge, since the fault trace is commonly found well up on the flank of the ridge[141]. Small drainages on the slopes of the ridge cross the fault without apparent offset.

To the northeast, the fault zone is characterized by a physiographic trough which follows an easily eroded gouge zone[142]. The gouge zone on this segment of the fault seems to be a characteristic response of the granulite and biotite quartz monzonite to deformation. Where the fault traverses the coarse quartz monzonite of the Rattlesnake Mountain pluton, the fault zone is characterized by a broad band of crushed and granulated rocks[143], rather than the interlacing network of gouge zones common to the east. It is hard to determine if geomorphic features along the fault trace such as troughs, saddles, and benches reflect Quaternary displacement of the ground surface, or merely differential erosion due to juxtaposition

of rocks in various degrees of decomposition and/or granulation.

The fault zone is made up of several segments which follow pre-existing weaknesses. The southern segment follows the trend of the north-northeast-trending Tunnel Ridge lineament. At the Arrastre Canyon narrows, the fault zone abruptly swings east-northeast and follows the trend of the east-northeast set of the Lovelace Canyon fault system. Finally, at Lovelace Canyon, the Arrastre Canyon Narrows fault zone turns east and appears to follow the White Mountain thrust fault zone until it joins the Sky Hi Ranch fault east of Grapevine Canyon. The fault zone seems to have evolved out of the integration of pre-existing fault zones, in a style reminiscent of the Cleghorn fault zone (Section 5.3.1).

East of Lovelace Canyon, the Arrastre Canyon Narrows fault zone is hard to trace. It may follow the pre-existing weakness of the White Mountain thrust fault system east[144], although the thrust shows little geomorphic evidence of reactivation. Alternatively, the fault zone may continue east-northeast and leave the range front[145]. There is no evidence of disruption in the fans on this trend. Although neither of these possible paths is entirely satisfactory, the White Mountain fault system seems to provide the most likely connection with the range front in light of its involvement with the Sky Hi Ranch fault zone.

A major ridge within the fault zone at Arrastre Canyon Narrows appears to be compressional in origin. The eastern trace seems better expressed to the north, whereas the western trace is better delineated to the south, suggesting that the ridge zone may be an en echelon step in the fault system. Splays appear to originate at the points where the fault turns abruptly, and may simply represent sections of pre-existing faults not used during the integration.

Cumulative displacement on the Arrastre Canyon Narrows fault zone is less that 60 meters vertical and 250 meters horizontal. Middle Pleistocene terrace gravel are displaced by the fault zone at the LeVan Ranch[146], in a northwest-block-down sense. A doubly plunging arch in the basement rocks at Lovelace Canyon is displaced laterally less than a quarter kilometer (Figure 5-6). This lateral offset is consistent with the small amount of right-lateral offset of the edge of the Rattlesnake Mountain pluton shown by MacColl (1964).

Since the Arrastre Canyon Narrows fault zone truncates members of north-northeast set of the Lovelace Cayon fault system[147], it must be younger. The right-lateral motion on the Arrastre Canyon Narrows fault zone is interpreted as having originated on incorporated elements of the Lovelace Canyon system prior to fault integration. West-block-down motion followed right-lateral motion during the formation of the Arrastre Canyon graben. The pressure ridge is the youngest feature and indicates a third phase of transpressive deformation. This complex evolutionary sequence is in agreement with the timing constraints on other faults in the study area. It is illustrative of the way in which faults in the study area serve different functions at different times.

5.7.3 The Lovelace Canyon Fault System

5.7.3.1 North-northeast-trending Faults

The Lovelace Canyon fault trends north-northeast across the ramp defined by the late Miocene erosion surface west of White Mountain and east of the Arrastre Canyon Narrows fault zone. It extends out of the study area to the south, where Dibblee (1974) shows it connecting directly to the Tunnel Ridge fault near Deep Creek. It extends two miles northward to the range front, where it is apparently truncated by the Arrastre Canyon Narrows fault zone

Figure 5-6. Offset axis of basement doubly-plunging antiform west of Lovelace Canyon. Exposures of a dome-shaped antiform in the basal contact of the Rattlesnake Mountain pluton are offset in a right-lateral sense by the Lovelace Canyon fault and the Arrastre Canyon Narrows fault zone. Offset on the Arrastre Canyon Narrows fault zone is minimal, probably less than half a kilometer in a right-lateral sense. Offset on the Lovelace Canyon fault is about a kilometer, right-lateral. Other parallel faults of the Lovelace Canyon system also show a small component of right-lateral separation.
Kr= Rattlesnake Mountain pluton; a = alaskite of MacColl (1964); gr = granulite of MacColl; Kb = Cretaceous biotite-quartz monzonite; Trhm = Triassic hornblende monzonite (Fawnskin Monzonite).

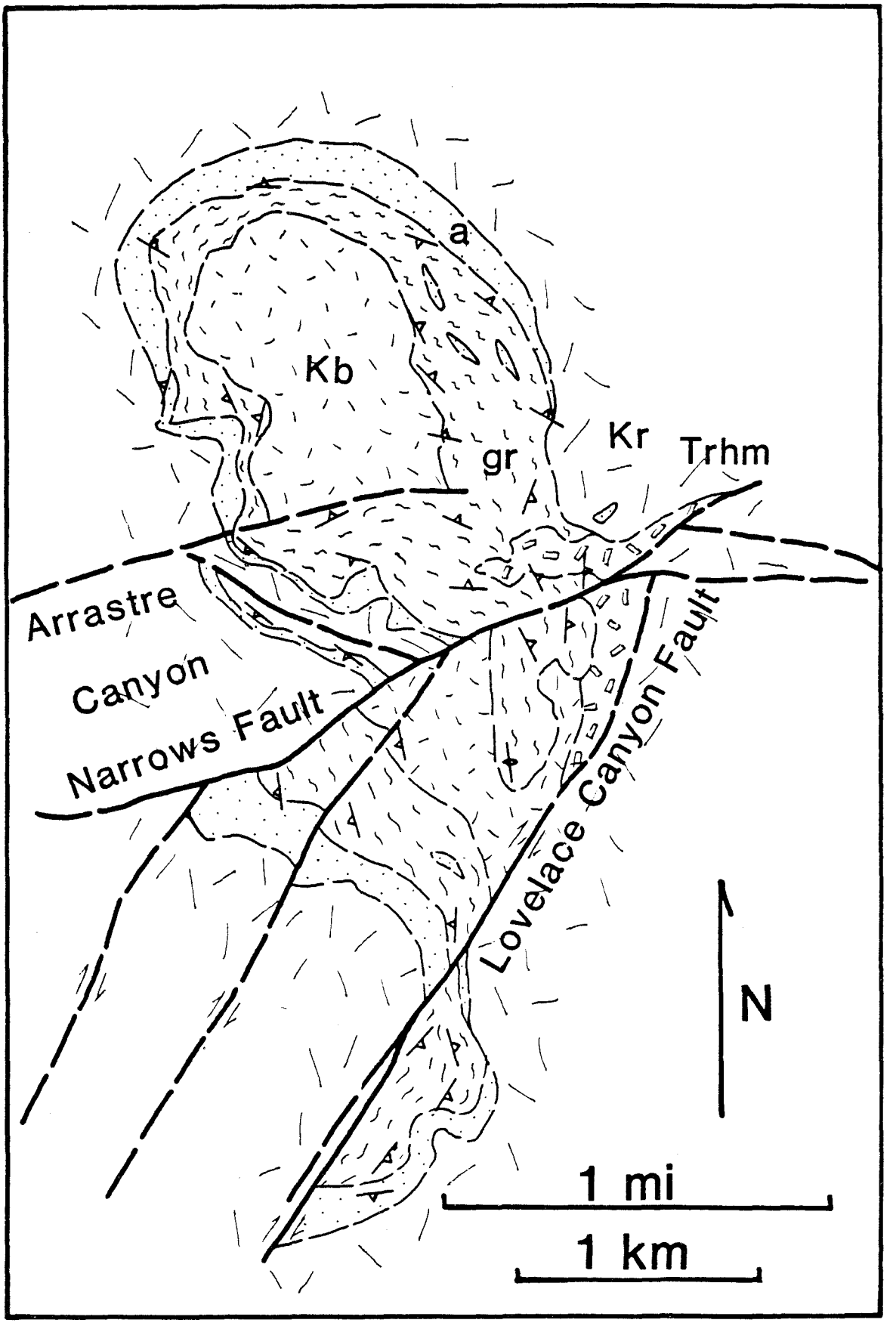
a
Kb
gr
Kr
Trhm
Arrastre
Canyon
Narrows Fault
Lovelace Canyon Fault
N
1 mi
1 km

at the mouth of Lovelace Canyon. It is exposed in the walls of upper Lovelace Canyon but is buried by alluvium in the lower part.

The Lovelace Canyon fault is recognizeable as a lineament on airphotos. A gouge zone, locally a meter or more in width, is present along the fault trace in Lovelace Canyon[148], giving rise to springs near the junction with the Arrastre Canyon Narrows fault zone.

The fault truncates the structural dome defined by the granulite and alaskite of MacColl (1964) and displaces its axis about 1.0 kilometer in a right-lateral sense (Figure 5-6). The late Miocene erosion surface is stepped down to the west across the fault, indicating a minimal component of vertical separation. There are no latest Tertiary or Quaternary deposits along the fault trace to constrain recency of motion. Geomorphic expression of the fault is largely due to the linearity of Lovelace Canyon and the contrast in rock types in juxtaposition across the fault.

The Lovelace Canyon fault clearly cuts east-northeast-trending faults[149], which are therefore inferred to be older. The Lovelace Canyon fault is, in turn, truncated by the Arrastre Canyon Narrows fault zone at the range front[150]. No geomorphic features could be found to indicate youthful motion. The Lovelace Canyon fault is therefore thought to be pre-middle-Pleistocene in age.

There are several faults that parallel the Lovelace Canyon fault and appear to be part of a larger system of north-northeast-trending faults. Faults to the west of the Lovelace Canyon fault offset the granulite and alaskite contacts several tens of meters in a right-lateral sense. These faults also show minor dip-slip motion that drops the Miocene erosion surface down to the west.

5.7.3.2 East-northeast-trending Faults

A set of east-northeast-trending faults is expressed as lineaments in the late Miocene erosion surface southeast of Lovelace Canyon. Other structures in the area that trend east-northeast include a fault in the Milpas Road area, folding along Ocotillo Ridge, and the tear structure that joins the Deep Creek and Apple Valley Highlands fault zones.

The east-northeast-trending structures postdate formation of the late Miocene erosion surface, since they form clear topographic lineaments on it. These faults are cut by members of the Lovelace Canyon fault system, which makes them some of the oldest faults in the area. Their relationship to the southwest-trending faults in the Ord Mountains is unknown, but Sadler (1982) and Dibblee (1974) show northeast trending-lineaments cut by northwest-trending lineaments west of Big Bear Lake.

Little is known about their displacement or history. The late Miocene erosion surface is displaced no more than 20 meters down to the northwest, constraining post-Miocene dip-slip motion. There is no basis for estimating lateral offset, however. Separation of a mafic body on one of the east-northeast trending faults just southeast of Lovelace Canyon is suggestive of left-lateral motion[151].

An east-northeast-trending fault bounds the north side of a mafic body in the Milpas Road area. It appears to cut the Arrastre Canyon fan deposits, although a buttress unconformity cannot be ruled out[152]. An unconformity would suggest that the fault line was topographically expressed at the time of deposition of the Arrastre Canyon fan gravel. This member of the east-northeast set must be considered to have moved, possibly as a result of reactivation, during the middle Pleistocene.

The Ocotillo Ridge fold follows an east-northeast trend, parallel to

faint lineaments on the north flank of the Ord Mountains. It is possible that pre-existing weaknesses attributable to the east-northeast fault set may be responsible for this trend.

The east-northeast-trending connecting structure between the Deep Creek and the Apple Valley Highlands fault zone may also follow a pre-existing fault trend. If this feature was offset by the Juniper Ranch fault, it might explain why the east-northeast-trending connecting structure is not expressed in the bedrock east of the Juniper Ranch fault.

5.8 THE SKY HI RANCH FAULT ZONE

The Sky Hi Ranch fault zone trends northwest between Sky Hi Ranch and Silver Creek. The fault zone is composed of a primary high-angle lateral fault, and secondary low-angle reverse faults. Geomorphic evidence of strike-slip displacement includes offset drainages, ponded alluvium, scarps, and shutter ridges. Secondary low-angle faulting appears to have occurred on segments of the White Mountain thrust system that were isolated by lateral faulting, and reactivated to accomodate transpressional strain. Both types of faulting displace older Qf2 and Qf3 fanglomerates.

5.8.1 High-angle Faults

High-angle faulting occurs along a single linear break, the Sky Hi Ranch fault, between Sky Hi Ranch and the foot of White Mountain. To the northwest of the Sky Hi Ranch, the fault splays into several strands[153] which appear to connect east to the Arrastre Canyon Narrows fault zone via a segment of the White Mountain thrust system (Section 5.7.2). The fault zone also appears to continue northwest as a fold[154] which joins the Ocotillo Ridge fold (Section 5.10.4). To the southeast, the Sky Hi Ranch fault turns east and joins the White Mountain thrust system[155]. A complex zone of north-

west-trending faults, shown by Sadler (1981) offsetting the White Mountain thrust system, may be an extension of the Sky Hi Ranch fault zone[156].

The Sky Hi Ranch fault posesses many geomorphic features indicative of lateral slip. Remnants of the Qf3 fans form shutter ridges on the north side of the fault[157]. Alluvial deposits indicate localized ponding upstream of the fault trace in response to damming by these shutter ridges[158]. Movement on the fault since Qf2 fan deposition has been just enough to permit capture of most drainages by the adjacent drainage[159]. Those drainages that have not been captured show signs of being disturbed at the fault trace[160].

The range front grows higher, steeper and more sharply dissected east from Grapevine Canyon. This may suggest greater cumulative displacement on range-bounding faults, lateral offset of the range front following uplift, or simply a difference in rapidity and character of erosion due to a change in lithology.

The Sky Hi Ranch fault, where exposed[161], is vertical. It is 11.2 kilometers in length, and splits into three traces at Sky Hi Ranch. Northwest of the Sky Hi Ranch, the fault trace leaves the range front and crosses a bajada composed of Qf1 fans. Although there is some evidence to suggest folding of the fan surface[162], it is not possible to demonstrate that the fault actually breaks the Qf2 fans. The fault trace is characterized by vegetation indicating local damming of groundwater. The resulting springs are used as a water supply for several properties in the vicinity of Sky Hi Ranch. There is a northwest-trending groundwater divide beneath Fifteenmile Valley which suggests a continuation of the Sky Hi Ranch to the northwest.

The above geomorphic evidence suggests right-lateral displacement on the Sky Hi Ranch fault of up to 0.5 kilometers since deposition of the Qf2

fans. This amount of offset is consistent with the observed displacement of drainages by one drainage basin interval. The lithology of clasts within the Qf2 and Qf3 fans does not permit more than one drainage basin interval of offset.

The possibility exists that greater right-lateral displacement occurred prior to fan deposition. This idea is purely speculative, since there is a total lack of late Tertiary and early Quaternary sediments along the range front between Arrastre Canyon and Furnace Creek. It is possible that this absence of older sediments reflectes a right-lateral displacement of the range front in the early Pleistocene. This notion is supported by the fact that the range front is much fresher than elsewhere where relief was accomplished by thrust faulting range front. An earlier episode of high-angle dip-slip faulting on the Sky Hi Ranch fault zone could account for this fresh relief.

The Sky Hi Ranch fault cuts the Qf2 fanglomerate but is overlain by the Qf1 fans. The fault zone cuts the White Mountain thrust system, and the displacement of its elements is consistent with about 0.5 kilometers of right-lateral offset. This would tend to argue against any post-uplift dip-slip motion on the fault. The White Mountain thrust is extensively broken by complex faulting in the White Mountain area, and it is hard to be sure how many traces there are and whether of not they are repeated. Although the age of the fans along the range front is not known, they are estimated to be late Pleistocene in age. Therefore, the Sky Hi Ranch fault is inferred to have been active in the latest Pleistocene, and possibly much earlier.

The trend of the Sky Hi Ranch fault suggests comparison with the northwest trending Helendale fault. There is a barrier to groundwater flow

that trends northwest in Fifteenmile Valley. It is possible that the Sky Hi Ranch fault is a member of the northwest-trending set of Mojave-block faults, and that its history spans the time before, during and after uplift of the San Bernardino Mountains. The Sky Hi Ranch fault resembles other members of the range front fault system in that is exploits pre-existing weaknesses.

5.8.2 Low-angle Faults

Low-angle faults that cut Qf2 fan surfaces are spatially associated with the high-angle Sky Hi Ranch fault. These low-angle faults are believed to be reactivated segments of the older White Mountain thrust system, probably relieving a compressional component of strain across the range-front system.

The low-angle faults dip gently south to gently north, based on their reaction to topography[163]. In this respect, their geometry is reminiscent of the White Mountain thrust. Low-angle faults seem to cut younger fan materials exclusively on the northern, downslope side of the fault trace, indicating that gravitational sliding may be a contributing factor in reactivation. The thrust faults on the south side of the Sky Hi Ranch fault do not cut Qf2 fanglomerates[164]. The occurrence of the younger low-angle structures coincides with the predicted occurrence of the White Mountain thrust based on bedrock exposures and lateral offset on the Sky Hi Ranch fault.

Vertical displacements of the Qf2 surface by these low-angle faults probably did not exceed 40 meters at most. In many places subsequent alluviation has filled in against the base of the scarp, reducing its height [165]. The Qf1 fans are clearly undisturbed and deposited against the scarp in at least one locality[166]. Thus, the younger low-angle

structures appear to be part of the Sky High Ranch fault zone, and were probably active in concert with it to relieve transpressional strain across the range front. The low-angle structures are probably developed on reactivated segments of the White Mountain thrust system.

5.9 THE WHITE MOUNTAIN THRUST SYSTEM

The White Mountain thrust is the eastern equivalent of the range-bounding thrust system that includes the Santa Fe thrust of Sadler (1982) and Shreve (1968) and the Crystal Creek thrust of Richmond (1960). These thrust systems become disrupted by later faulting and landslides, and it becomes very difficult to be sure how many distinct thrust surfaces in fact exist.

There appear to be at least two distinct thrust surfaces along the range front between Dry Canyon and Lovelace Canyon. One thrust surface, the Crystal Creek thrust of Richmond (1960), can be followed west to Grapevine Canyon and tentatively extrapolated as far as Lovelace Canyon[168]. This thrust may join the Arrastre Canyon Narrows fault zone. Another thrust fault is evident in the lower fan surface at Dry Creek[169]. This structure follows the trace of the Sky Hi Ranch fault zone west and may be the structure responsible for the Ocotillo Ridge fold. The connection is buried, however, and therefore hard to demonstrate. There is no suggestion in the range-front geomorphology that the thrust system connects to buried reverse structures on the north side of the Ord Mountains. Thrusting may not have been the preferred form of deformation within the Rattlesnake Mountain pluton.

The White Mountain system has a thrust/slide geometry, as described by Sadler (1982) for thrusts to the east. The fault surface dips to the south as steeply as 45° within the canyons[170], but dips shallowly north on ridges

and within the range-front alluvium[171].

The rock below the Crystal Creek thrust is a highly fractured and chloritized cataclasite[172] suggestive of brittle deformation at shallow depth. The cataclastic rock may be restricted to the zone between the thrust planes, possibly representing a crushed plate within the thrust fault zone. Unfortunately, bedrock below the lowest thrust plane is buried, and this hypothesis cannot be readily tested.

The cumulative displacement on the White Mountain and related thrust zones is not known. The White Mountain thrust in the area of White Mountain is overlain by both Qf2 and Qf3 fanglomerates, suggesting that it has not moved since at least the middle Pleistocene. Sadler (1982) indicates that range-front uplift began to the east along thrust faults as early as 3.0 my ago, and that high angle faulting has prevailed more recently. The White Mountain thrust appears to be part of an older range-front thrusting event, and may well have been inactive since the beginning of the Pleistocene. Reactivation of older thrust surfaces in connection with later high-angle faulting is common, however, and many of these reactivated surfaces are connected with scarps in the alluvial fans. It is believed that cumulative motion on these structures is small, and that range-front relief was accomplished prior to most of the fan-building on thrusts such as the White Mountain system. Sadler (1981) shows a system of high-angle, northwest-trending faults that displace the thrust faults on the projection of the Sky Hi Ranch fault zone.

5.10 FOLDING

5.10.1 Tilting

Both the bedrock erosion surface and overlying Crowder Formation consistently dip 30° north over a broad area of the range front between Cajon

Pass and Grass Valley, suggesting that tilting was the dominant mechanism for uplift in the western San Bernardino Mountains. The regional consistency of dip suggests that tilting was not related to local faulting, although it may have been due to major reverse faulting south of the study area. In Cajon Pass, an east-trending, high-angle reverse fault is buried by the Pleistocene Harold Formation, which dips about 25° northeast. Thus tilting may largely postdate motion on the Cedar Springs fault system, and south-block-down members of this system probably dipped 50° to 70° north prior to being rotated to their present vertical orientation.

Weldon (1982, pers. comm.) believes that tilting occurred on the north flank of a northwest-trending arch in the basement rocks of the western San Bernardino Mountains.

Foster (1980) invokes episodes of tilting to explain angular unconformities as far back as the Punchbowl/Crowder boundary. The present study indicates that tilting began after the deposition of the Harold Formation, in the middle to late Pleistocene. Detailed study of the Lost Lake terrace series (Qta) in Cajon Pass (Weldon and Sieh, 1980) and releveling of railroad tracks over the last 50 years (Shelton, 1966) suggest that northward tilting is still going on.

5.10.2 North-plunging, East-block-down Monoclines

The earliest deformational event recorded in the Crowder Formation is a set of north-trending, east-block-down monoclines. The monoclines have been tilted about 30° northward during later arching of the western San Bernardino Mountains and now appear as asymmetric anticline/syncline pairs. These features probably represent draping of sediment over basement steps.

The largest plunging monocline is exposed in the Crowder Formation and

underlying erosion surface about 2 kilometers southwest of Silverwood Lake[173]. This anticline/syncline pair indicates east-block-down motion and is truncated at its north end by the Cleghorn fault. The syncline is represented by a broad fold in the Crowder Formation. The anticline is represented by a broad antiformal bedrock ridge that trends slightly east of north from Sugarpine Mountain to the Cleghorn Fault.

North of Cleghorn Ridge are several broad embayments in Crowder Formation separated by broad bedrock ridges. The bedrock surface north of Cleghorn Ridge is the exhumed late Miocene erosion surface; hence its topography reflects later folding. Despite faulting on the Cedar Springs fault system, the monoclinal warps can still be clearly seen in the erosion surface. The most prominent antiformal ridge trends north-northeast from Cleghorn Mountain to Little Horsethief Canyon[174]. This plunging monocline is considered the offset equivalent of the structure southwest of Silverwood Lake (Section 5.3.1).

Numerous minor plunging monoclines are exposed south of the Cleghorn fault in Miller Canyon[175]. The north end of Silverwood Lake is underlain by Crowder Formation (California DWR, 1968b) and is considered another of these monoclinal down warps.

The north-plunging monoclines are clearly cut by members of the south-block-down set of the Cedar Springs fault system[176]. The folding must therefore be older than the Cedar Springs system. The folding must postdate deposition of the basal Crowder Formation in the western San Bernardino Mountains. The folding is consequently post-late-Miocene, and perhaps younger, depending on the correlation used for the Crowder Formation.

5.10.3 East-trending, South-block-down Monoclines

A set of west- to west-northwest-trending monoclines, or anticline/syncline pairs, is expressed within the Crowder Formation in Summit Valley and Cajon Pass. These folds were first mapped by Foster (1980), who showed that the Harold Formation overlies them in Cajon Pass[177]. The folds are interpreted as the effect of draping of Crowder Formation over steps in the underlying basement.

Displacement on each fold is not more than a few tens of meters, yet Foster notes a dramatic thickening of the Crowder Formation from Cajon Pass to Summit Valley that could be due to multiple folds of this type. It is possible that many more such folds are buried by the Victorville Fan.

The small magnitude of offset on individual structures and the south-block-down sense of motion suggests that the west-trending monoclines should be considered part of the south-block-down set of the Cedar Springs fault system. The folds postdate the deposition of the Crowder Formation, and predate the deposition of the Harold Formation. Thus they developed during roughly the same period of time as the Cedar Springs fault system.

There is little evidence of west-trending faulting in the Crowder Formation in Cajon Pass and west Summit Valley. West-trending lineaments can be followed for short distances in central Summit Valley, but through-going structures are hard to demonstrate. West-trending faulting becomes clearly evident at the east end of Summit Valley at the base of the Crowder Formation near the contact with bedrock. These observations are consistent with faulting of the basement which extends a short distance into the overlying Crowder Formation and then dies out into folding.

5.10.4 The Ocotillo Ridge Fold

The Ocotillo Ridge fold is the single surficial structural element constituting the north frontal fault system of the San Bernardino Mountains between the Marianas Rancho area and the Sky Hi Ranch. At its west end the fold turns sharply southward and becomes the Apple Valley Highlands fault zone[178]. At the east end, it becomes the Sky High Ranch fault zone[180]. In between, the Ocotillo Ridge fold changes trend from east-northeast in the Marianas Rancho area to due east at Arrastre Canyon to west-northwest at Grapevine Canyon. The fold is developed in the Ord River Gravel and Arrastre Canyon Fan Gravel, and appears also to affect possibly younger (Qf2) fan gravels at the mouth of Grapevine Canyon[181]. The Ord River Gravel underlying Ocotillo Ridge is of normal paleomagnetic polarity, making the folding younger than 730,000 y B.P.

The fold is interpreted as a monoclinal warp; developed over a fault in the basement. This buried fault is an apparent continuation of either the Apple Valley Highlands fault zone or the Juniper Ranch fault zone. The fold is an asymmetric anticline/syncline pair, and has a north-block-down sense of motion. Although the trend of this fold is the same as that of the east-trending folds in Summit Valley, the sense of motion is different.

The folding of the Ord River Gravel over a fault in the basement probably reflects a reactivation of an earlier low-angle structure. This tends to support the hypothesis that there was a low-angle fault system that existed prior to the deposition of the Ord River Gravel. A pre-existing structure may have been partly responsible for uplift of the Ord Mountains.

The Ocotillo Ridge fold is discussed in some detail in Section 7.3.1, Chapter VII, in connection with the Ocotillo Ridge trench. No fault was found on the north side of the ridge, confirming the original interpretation

of Dibblee (1974) that the ridge was underlain by a fold.

5.10.5 Range-front Warping

In several areas along the northern range front warping seems to have been a locally important mechanism for range-front deformation. Warping is evident in the vicinity of Arrastre Canyon, Grass Valley, and along the range front east of Lovelace Canyon.

The Arrastre Canyon warp is a bowl-shaped depression in the late Miocene erosion surface east of the Ord Mountains and west of White Mountain. It is roughly coincident with, and probably related to, the Arrastre Canyon graben. The warp is confined to the exposure of the Rattlesnake Mountain pluton, which suggests that warping may be lithologically controlled.

The Grass Valley warp is expressed just east of Grass Valley[182] and has been extensively modified by faulting. The warp is clearly not a fault, as the Miocene erosion surface can be clearly seen to flex at the range front. The Grass Valley warp dies out to the west and merges with the north-dipping ramp defined by the erosion surface in the vicinity of Silverwood Lake. At its northeast end, the warp becomes increasingly tight until the erosion surface is broken and it becomes the Deep Creek fault zone. The warping seems to be confined to the range front and has a north-block-down sense of motion.

East of Lovelace Canyon, the thrust plane of the White Mountain thrust commonly dips northward at the extreme northern end of its lobes. It is possible that the White Mountain thrust faults originally dipped shallowly southward and have since been warped into their present north-dipping configuration. This interpretation offers a possible alternative to the thrust/slide model of Sadler (1982). It may be that slow rates of deformation that are occurring along the range front have favored warping over

faulting at certain times in the past.

5.11 CATACLASTIC DEFORMATION

A detailed discussion of cataclastic deformation is beyond the scope of this study. The most obvious occurrences of cataclasis in the study area are mentioned here for sake of completeness.

The oldest structural event recognized in the area is manifested by the subhorizontal cataclastic fabric in the crystalline rocks southwest of Silverwood Lake. This fabric is probably related to low-angle thrusting at depth (R. Powell, 1982, pers. comm.). The subhorizontal fabric has since been warped into a broad antiform that trends north-northwest across the southeast edge of the map. Foliation attitudes and a string of marble pendants help delineate the fold. Extensive recrystallization is associated with the cataclastic fabric in these rocks, suggesting that deformation occurred at some depth.

The rocks that lie beneath the Crystal Creek thrust of the White Mountain thrust system are highly fractured and chloritized. They appear to have suffered deformation under near-surface conditions. These chloritized cataclastic rocks may be confined to the plate that lies between the multiple fault planes of the White Mountain thrust system. This would explain the cataclasis observed in these rocks and the brittle nature of the deformation. If this is the case, the cataclasis woulkd be late Pliocene in age.

Phyllonites developed along the trace of the Powerline Canyon fault zone are discussed in Section 5.6.

5.12 SUMMARY AND CONCLUSIONS

The oldest structure to deform the Crowder Formation is a series of north-trending, east-cascading monoclines, now tilted into plunging

asymmetric anticline-syncline pairs. These structures may represent folding above faults at depth. Although most obvious within the Crowder Formation, these folds are also evident as broad undulations in the stripped late Miocene(?) erosion surface.

The plunging monoclines are cut by a pervasive set of arcuate, northwest- to east-trending high-angle reverse faults called the Cedar Springs fault system. The sense of motion on these reverse faults is south-block-down; a small component of right-lateral motion seems to accompany dip-slip in the northwest-trending segments of these faults. This motion is consistent with "shingling" of individual fault blocks under north-south regional compression. Preservation of the late Miocene(?) erosion surface throughout the area and minimal vertical offset of plunging monoclines rules out a total cumulative displacement on these faults of more than a few hundred meters. Northwest-trending fault segments systematically cut east-trending ones, suggesting that the conditions that gave rise to this structural episode migrated to the south and east.

Five major northwest-trending dip-slip faults show anomalous southwest-side-up separation: the Squaw Peak, Powell Canyon, Notch and Seeley Creek, and Grass Valley faults. At least one of these faults can be shown to post-date several high-angle reverse faults of the typical south-block-down variety. To the southeast, motion on the north-block-down faults becomes north-side-up, consistent with the hypothesized "shingling" of fault blocks. No exposures of Crowder Formation are found southwest of the Squaw Peak and Powell Canyon faults, suggesting that the faults may have accumulated significant cumulative lateral motion. Lateral motion seems to be required by the juxtaposition of the contemporaneous, yet contrasting Punchbowl and Crowder basins.

A major vertical offset of the late Miocene(?) erosion surface in the Silverwood Lake area occurs along the Cleghorn Fault. This offset cannot be accounted for by lateral motion. It is therefore postulated that the Cleghorn fault began as a major arcuate reverse fault west of Silverwood Lake. As the locus of reverse faulting migrated southeast across the area, first the eastern branch of the Cleghorn and then the north-block-down faults experienced reverse motion. Bends and cusps on the Cleghorn fault provide evidence of this pre-existing reverse fault geometry.

Both the bedrock erosion surface and overlying Crowder Formation consistently dip about 30° north over a broad area of the range front, suggesting that tilting was the dominant mechanism for mountain uplift. The regional consistency of dip suggests that tilting was not related to local faulting, although it may have been due to major reverse faulting south of the study area. In Cajon Pass an east-trending high-angle reverse fault is buried by the Pleistocene Harold Formation, which dips about 25° northeast. Thus tilting may largely postdate the reverse faulting, and the steep high-angle reverse faults probably dipped 50° to 70° north prior to being rotated to their present vertical orientation.

In the earliest Pleistocene, motion on the Cleghorn fault changed from reverse to left-slip, following integration of the east and west branches of the Cleghorn fault to accomodate lateral displacement.

Several unique structures demonstrate a cumulative left-lateral offset of 3 to 4 kilometers on the Cleghorn system. A north-plunging anticline/syncline pair in the Crowder Formation southwest of Silverwood Lake matches a similar flexure in the erosion surface and Crowder Formation 3 to 4 kilometers to the west on the north side of the Cleghorn fault. The steeply dipping basement contact that forms the eastern limit of the Punchbowl

Formation in Cajon Pass is offset along the Cleghorn fault approximately 3 to 4 kilometers.

Restoration of 3-4 km of cumulative left-lateral offset results in the alignment of unique members of the Cedar Springs reverse fault system, suggesting that vertical faulting ended before the onset of lateral faulting. Using the Squaw Peak, Powell Canyon, Notch and Seeley Creek faults as piercing points, a refined offset estimate of 3.5 to 4.0 kilometers can be made.

East of the study area the Cleghorn fault itself appears to turn northeast and join the prominant Tunnel Ridge lineament that crosses the western San Bernardino Mountains from Tunnel Ridge to Fifteenmile Valley. Lesser northeast-trending splays, most notably the Silverwood Lake fault zone, show minor left-lateral and southeast-block-down displacement. These structures may serve to link the Cleghorn fault with the north frontal fault system of the San Bernardino Mountains via the discontinuous Summit Valley fault zone.

Uplift of the Ord Mountains and Pinnacles occurred along a complex north-northeast-trending fault system that can be followed from Grass Valley to Arrastre Canyon. Southwest of Grass Valley, the system spreads out into a multitude of minor north-block-down fault traces accompanied by range-front warping. The Ord Mountains fault zone consists of a middle to late Pleistocene high-angle fault set and a late Pleistocene low-angle fault set. The high-angle faults are nearly vertical, west-block-down, and displace the middle to late Pleistocene(?) Ord River Gravel. The low-angle faults cut the high angle faults. The entire system is cut by east-trending high-angle lateral faults of the Summit Valley fault zone in east Summit Valley. The low-angle system turns east and becomes a fold in the alluvium on the north flank of the Ord Mountains, traverses the Arrastre Canyon Fan, and

rejoins the range front south of Fifteenmile Valley.

The northern extension of the Tunnel Ridge fault, called the Arrastre Canyon graben, also joins the range front near Fifteenmile Valley. The north-northeast-trending faults that make up the Arrastre Canyon graben show evidence of both right-lateral and dip-slip motion. The right-lateral motion is believed to reflect the earliest displacement on these faults. Dip-slip motion followed lateral motion with west-block-down on the east side of the graben and east-block-down on the west side. At least one of the faults, the Arrastre Canyon Narrows fault zone, has been reactivated for a third time under compression. The Arrastre Canyon Narrows fault zone turns east at the range front and joins range-front folding to form the Sky Hi Ranch fault zone.

The Sky Hi Ranch fault is a high-angle northwest trending zone which displaces late Pleistocene Fan gravels along the range front in a right-lateral sense between Sky Hi Ranch and White Mountain. It may have sustained significant dip-slip and/or strike-slip motion prior to deposition of the fans. Minor low-angle faulting accompanies strike-slip motion on the Sky Hi Ranch fault zone and probably represents reactivation of pre-existing faults of the White Mountain thrust system.

The White Mountain thrust system is primarily responsible for range-front relief east of Grapevine Canyon. Members of the White Mountain thrust system are cut by the Sky Hi Ranch fault zone and overlain by middle Pleistocene(?) fanglomerate. The White Mountain thrust zone is believed to have been active since at least middle Pleistocene.

Thus, range-front deformation reflects a two-phase history of development in which late Pliocene to early Pleistocene thrusting led to a pulse of uplift that immediately gave way to middle to late Pleistocene high-angle

faulting. This history has led a wide variety of structures within the system, each responding to range-front deformation in a manner appropriate for its location and geometry. These conclusions are developed fully in the following chapter, "Tectonic Evolution".

CHAPTER VI

TECTONIC EVOLUTION

6.1 INTRODUCTION

6.1.1 Purpose

Two of the primary goals of this study were to (1) establish a better constrained uplift history for the northwestern San Bernardino Mountains, and (2) elucidate the nature and modes of deformation acting on the northern range front. The following chapter is an effort to bring together and the detailed results of field work presented in the preceding chapters and integrate them into a working chronology for the late Tertiary structural development of the northwestern San Bernardino Mountains. A history of range-front uplift is proposed and the nature, origin and tectonic implications of deformation are addressed.

6.1.2 Scope

Uplift history of the northwestern San Bernardino Mountains is herein examined by considering the structural and stratigraphic constraints on the timing of tectonic events in the study area. Related structures are grouped and the tectonic events responsible for uplift are identified. Particular emphasis is placed on constraining the timing of uplift along range-front structures.

A discussion of the nature and modes of deformation in the study area is aimed at determining the origin of structural geometries and their relationship to the regional tectonic context of the northwestern San Bernardino Mountains. Possible models for the origin of important structural elements within the study area are reviewed.

Stratigraphic and structural histories of the study area are presented

in Figures 6-1 and 6-2, which summarize the neotectonic evolution of the northwestern San Bernardino Mountains. Offsets, slip-rates, and earthquake potential of faults studied are discussed in Chapter VII, "Seismic Risk".

6.2 UPLIFT HISTORY OF THE WESTERN SAN BERNARDINO MOUNTAINS

Uplift of the northwestern San Bernardino Mountains took place during the late Pliocene and early Pleistocene. Late Pliocene inception of thrusting along the north frontal fault system is recorded by a change in the nature of sediment deposited in the Old Woman Sandstone. Uplift on the north-central range front by thrust faulting was apparently completed by middle Pleistocene. Uplift in the westernmost San Bernardino Mountains was the result of tilting which postdated the deposition of the early Pleistocene(?) Harold Formation and is still ongoing in Cajon Pass. Thus, uplift was roughly synchronous throughout the northwestern San Bernardino Mountains.

Since the middle to late Pleistocene, lateral faulting has been the dominant style of deformation along the northern range front, apparently due to a re-assertion of the northwest-trending faults of the Mojave block following early Pleistocene cessation of vertical deformation. Since the early Pleistocene, compression in the western San Bernardino Mountains has been accommodated by lateral translation of fault-bounded wedges, rather than by uplift on dip-slip faults. Local extension seems to have accompanied lateral faulting. The Ord Mountains appear not to have been uplifted during range-front thrusting, and some of their relief may have originated under extensional conditions.

6.2.1 Constraints on the Timing of the Cedar Springs Fault System

The inception of motion on the Cedar Springs fault system postdates deposition of the basal Crowder Formation in the western San Bernardino

Figure 6-1. Summary of constraints on ages of principal late Cenozoic stratigraphic units. A generallized stratigraphic column is shown for each of seven principal range-front areas. Together, the columns portrays a stratigraphic history of the range-front study area and provide a basis for the discussion of neotectonic evolution in the text. Non-horizontal lines bounding a unit signifies the range of uncertainty in the age of the top or bottom of that unit and do not imply a change in age across the site of an individual column. Age divisions of the north American land mammal and paleomagnetic timescales are included for reference. "Bone" symbol in unit shows age of fossil locality; "atom" indicates radiometric date; "magnet" indicates paleomagnetic age constraint. Dotted lines are inferred correlations, solid lines are unconformable unit boundaries, and dashed lines are conformable unit boundaries. SV = Summit Valley facies of the Ord River Gravel; DC = Deep Creek facies of the Ord River Gravel; ACF = Arrastre Canyon Fan; RSR = Rock Springs Road deposits. "Weathering" indicates timing of weathering on the late Miocene bedrock erosion surface.

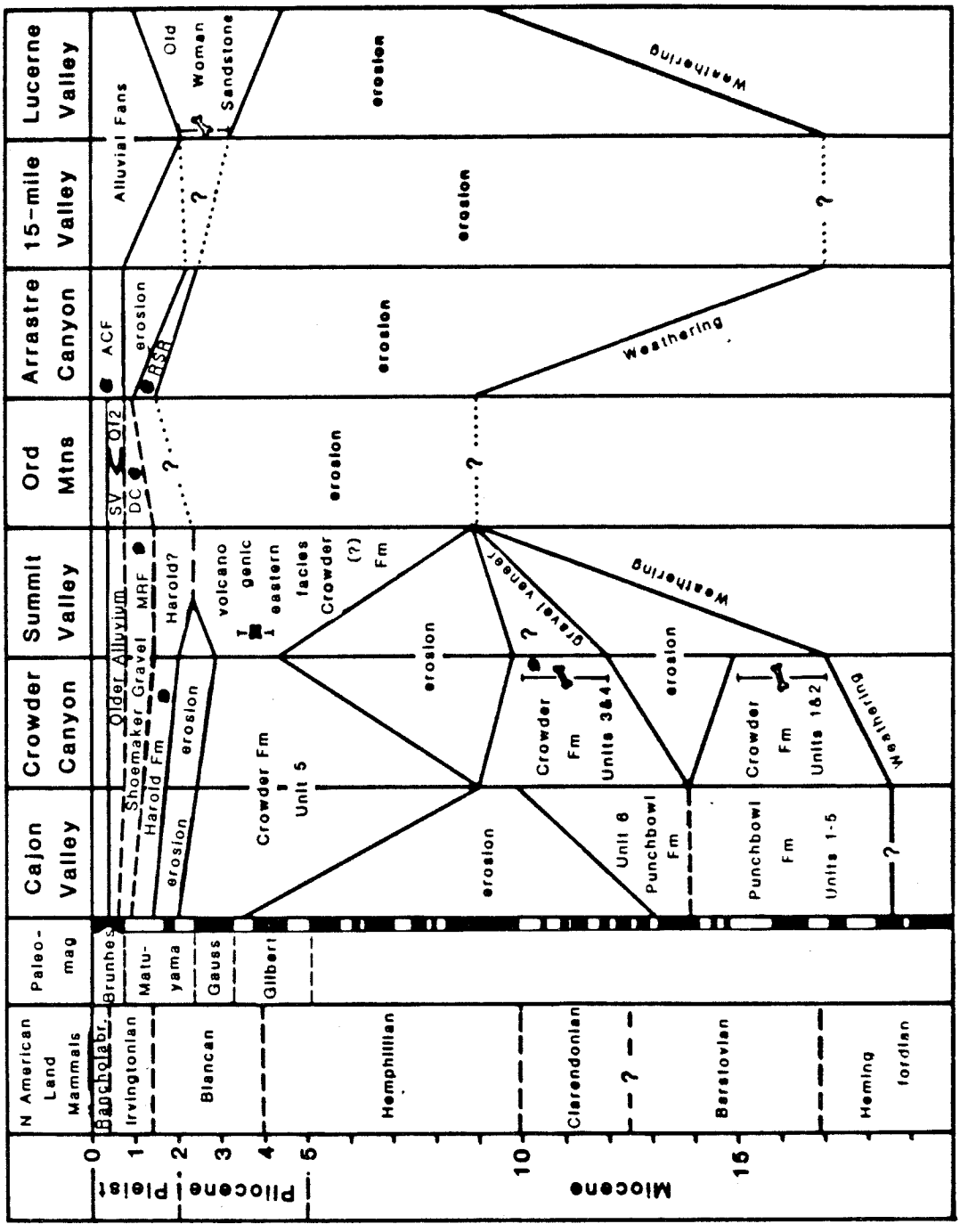
Lucerne Valley
15-mile Valley
Arrastre Canyon
Ord Mtns
Summit Valley
Crowder Canyon
Cajon Valley
Paleo-mag
N American Land Mammals
Pliocene
Pleist
Miocene
Alluvial Fans
Old Woman Sandstone
Older Alluvium
Shoemaker Gravel
Harold Fm
Harold?
MRF
ACF
RSR
SV
DC
Q12
volcano genic
eastern facies
Crowder (?) Fm
Crowder Fm
Unit 5
Crowder Fm
Units 3&4
Crowder Fm
Units 1&2
Punchbowl Fm
Unit 6
Punchbowl Fm
Units 1-5
gravel veneer
erosion
weathering
Brunhes
Matu-yama
Gauss
Gilbert
Irvingtonian
Blancan
Hemphillian
Clarendonian
Barstovian
Hemingfordian

Figure 6-2. Summary of constraints on ages of principal Pliocene and Pleistocene structural events. A generalized chronologic sequence of development of structures is shown for each of seven principal range-front areas. Together, the columns map out a history of deformation for the range-front study area, and provide a reference for the discussion of neotectonic evolution in the text. Non-horizontal lines bounding an event signify the range in uncertainty in the age of the inception or cessation of that event, deduced from the involvement and ages of units from Figure 6-1, and do not imply a change in age across the site of a structural event. Age divisions of the North American land mammal and paleomagnetic timescales are included for reference. Dotted lines are inferred correlation of structural events.

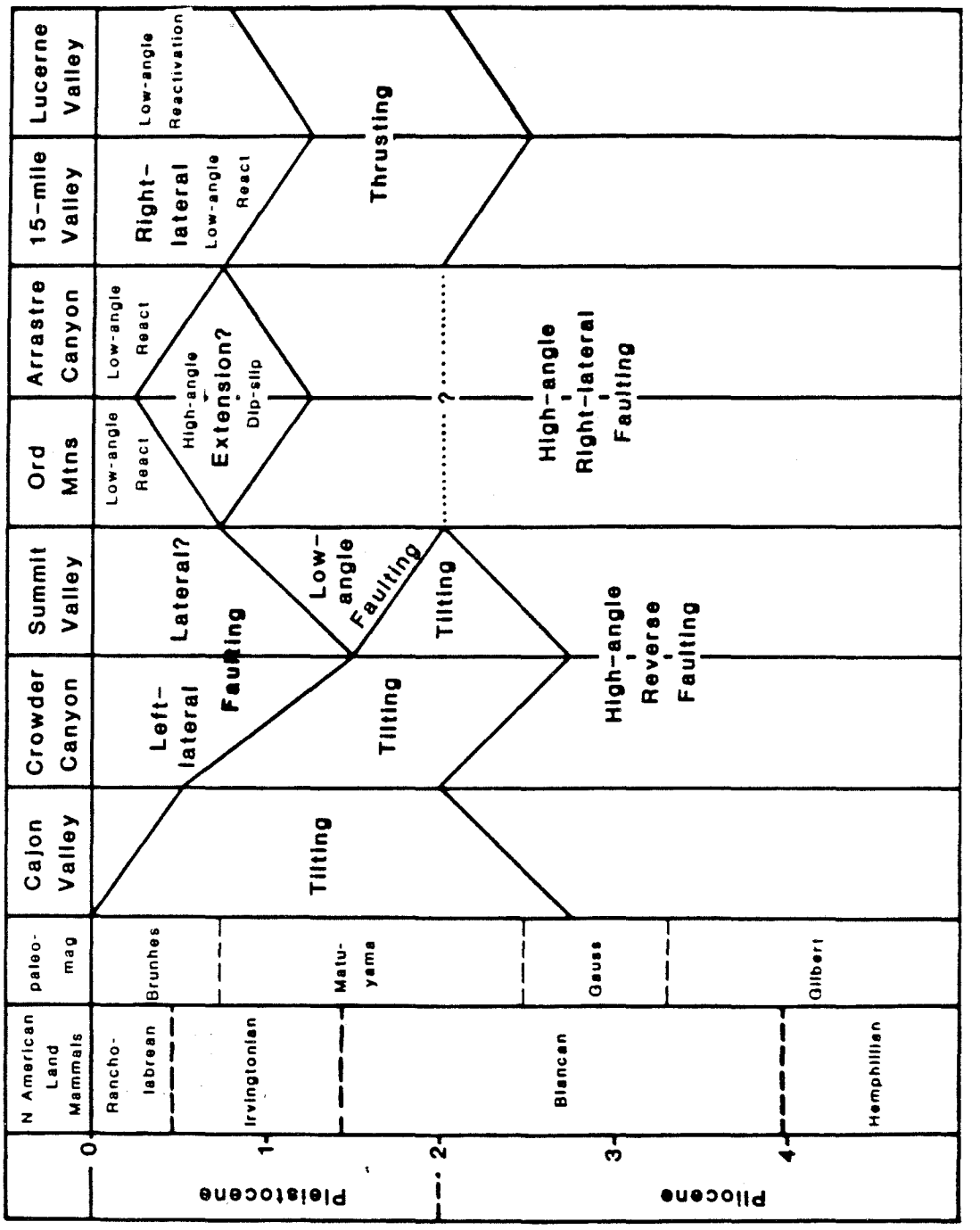
Lucerne Valley
15-mile Valley
Arrastre Canyon
Ord Mtns
Summit Valley
Crowder Canyon
Cajon Valley
paleo-mag
N American Land Mammals
Pleistocene
Pliocene
0
1
2
3
4
Rancho-labrean
Irvingtonian
Blancan
Hemphillian
Brunhes
Matu-yama
Gauss
Gilbert
Low-angle Reactivation
Right-lateral
Low-angle React
Thrusting
Low-angle React
High-angle Extension?
Dip-slip
Low-angle React
High-angle Right-lateral Faulting
Left-lateral Faulting
Lateral?
Low-angle Faulting
Tilting
Tilting
Tilting
High-angle Reverse Faulting

Mountains. Although the Crowder Formation in the western San Bernardino Mountains could be as old as middle Miocene (Hemingfordian/Barstovian; ~16 my), an abundance of quartzite clasts suggests a correlation with late Miocene (Barstovian/Clarendonian; ~11 my) Units 3 or Pliocene(?) Unit 5 of the Cajon Pass section (Sadler, 1983, pers. comm.; Foster, 1980). No compelling evidence was found in the Crowder Formation to support the assertion made by Foster (1980) that faulting was syndepositional. Motion on the Cedar Springs fault system cannot have begun prior to middle Miocene, and it probably began in the late Miocene or Pliocene.

The Cedar Springs fault system is expressed in the volcanogenic eastern facies of the Crowder(?) Formation. The geometric pattern, sense of displacement, and pervasive nature of faulting in east Summit Valley are all characteristic of the Cedar Springs fault system. Although some of the observed faulting is certainly due to the Deep Creek and Summit Valley fault zones, south-block-down folding on east-trending axes within the volcanogenic eastern facies of the Crowder(?) Formation closely resembles similar deformation affecting Crowder Unit 5 in west Summit Valley. Later faulting may have exploited pre-existing fault geometry, however, and the conclusion that motion on the Cedar Springs system postdates deposition of the 3.8 ± 0.4 volcanogenic facies of the Crowder(?) Formation must be considered tentative.

Motion on the Cedar Springs system had ceased by early to middle Pleistocene. East-trending, south-cascading folds in Unit 5 of the Crowder Formation in west Summit Valley are overlain with angular unconformity by the basal Harold Formation in Cajon Pass (Foster, 1980). The age of the basal Harold Formation is unknown but must be appreciably greater than 730,000 y B.P. (middle Pleistocene) and cannot be greater than ~2.75 my (late Pliocene) in age (Section 6.2.3). Faults of the Cedar Springs system

are overlain by ~400,000 y B.P. terrace deposits (Qt2) in Cleghorn Valley, indicating that no movement has occurred in the western San Bernardino Mountains since middle to late Pleistocene.

The Cedar Springs system continues eastward into the Pinnacles area, where lineament patterns suggest that it may have merged with the Tunnel Ridge lineament. Dibblee (1974) shows the southern extension of the Tunnel Ridge lineament as truncated by a member of the south-block-down fault set of the Cedar Springs system in east Miller Canyon. The arcuate lineaments of the Cedar Springs fault system curve northeast and merge with the Tunnel Ridge lineament, suggesting that the Cedar Springs system once fed into it. These observations can be explained if motion on the Cedar Springs system and Tunnel Ridge lineament overlapped in time.

6.2.2 Constraints on the Timing of Tilting

Uplift in the western San Bernardino Mountains took place primarily by tilting in response to arching and reverse faulting on the south flank of the range. The late Miocene(?) erosion surface, basal Crowder Formation and the volcanogenic eastern facies of the Crowder(?) Formation are all tilted northward about 30°. Thus, tilting clearly postdates deposition of the eastern facies of the Crowder(?) Formation, 3.8 ± 0.4 my ago.

Tilting was, for the most part, complete by late Pleistocene. Qt2 terrace surfaces, estimated to be ~400,000 years in age, and Qt1 terrace surfaces, about 60,000 years old, are not obviously tilted northward in Cleghorn Valley and Miller Canyon. Nevertheless, tilting appears to be going on today in Cajon Pass (Shelton, 1966).

6.2.3 Stratigraphic Constraints on Timing of Uplift

Uplift began in the western San Bernardino Mountains between the middle

Pliocene and early Pleistocene. Stratigraphic evidence for stripping of the Crowder Formation from the western San Bernardino Mountains during uplift is found in the sediments of the Victorville Fan (Figure 6-1). Victorville Fan sediments in Summit Valley were clearly derived from the western San Bernardino Mountains since they contain abundant well-rounded clasts of quartzite and volcanic lithologies recycled as a result of stripping of the Crowder Formation from the range in response to uplift. The Deep Creek facies of the Ord River Gravel contains well-rounded clasts that originated in the drainage area of Deep Creek. Both the Victorville Fan sediments of Summit Valley (MRF; Section 4.3.3) and the Deep Creek facies of the Ord River Gravel (ORD; Section 4.3.5.1) are reversed and therefore older than 730,000 years B.P. Thus uplift was well under way, and sediment was being shed off the rising western San Bernardino Mountains, by the middle Pleistocene. This is in agreement with the constraints on tilting and the structures responsible for uplift outlined above.

The Harold Formation in Cajon Pass contains the earliest appearance of clasts from the San Gabriel Mountains crystalline terrane on the Mojave block, and it records the arrival of the San Gabriel Mountains as a source area. The San Gabriel Mountains source was introduced to the area by both lateral movement on the San Andreas fault zone and vertical uplift of the San Gabriel Mountains. At a slip-rate of ~2.5 cm/yr on the San Andreas (Weldon and Sieh, 1983) the San Gabriel Mountains would not have been in a position to deliver Pelona Schist clasts to the Cajon basin prior to about 3.5 my ago, regardless of their rate of uplift. The paleomagnetic data provide a further constraint on the age of the basal Harold Formation. The worst-case assumption that the 175 meters of predominantly reversed section measured in Cajon Pass spans the entire 1.75 my length of the Matuyama

polarity epoch leads to a deposition rate of ~1 meter/10,000 years (175 meters/1.75 my). The ~25 meters of Harold Formation that lie below the lowest measured sample might span 25,000 years of deposition (25 meters x 10,000 y/m), making the base of the Harold Formation ~2.75 my old. Consequently, the Harold Formation in Cajon Pass is probably less than 2.75 my old and records the appearance of the San Gabriel Mountains as a source of sediment and topographic relief.

The Harold Formation and the volcanogenic eastern facies of the Crowder(?) Formation can both be interpreted as syntectonic deposits that reflect deformation associated with uplift of the western San Bernardino Mountains and the arrival of the San Gabriel Mountains in Cajon Pass. The topographic effect of these deformational events was to completely reverse the prevailing drainage direction from southerly transport in the lower Crowder Formation to northerly transport in the Victorville Fan. The fine-grained nature of both the Harold and eastern facies of the Crowder(?) Formation is indicative of local ponding which must have accompanied the intial stages of this drainage reversal. The Harold Formation and the volcanogenic Crowder(?) Formation contain the earliest occurrence of clasts derived from the San Gabriel and western San Bernardino Mountains, and both are overlain by deposits that contain evidence of a massive influx of sediment from the adjacent mountain source areas.

The nature and age of the Harold and eastern Crowder(?) Formations suggest that the uplift of the western San Bernardino Mountains was contemporaneous with the arrival of the San Gabriel Mountains in the Cajon Pass area. This may indicate that uplift of the western San Bernardino Mountains occurred in response to compressional forces generated by the San Gabriel crystalline mass impinging on the western San Bernardino Mountains

block. Although tilting was largely accomplished prior to late Pleistocene time, tilting appears still to be going on in Cajon Pass (Shelton, 1966).

Northerly paleocurrent directions from Unit 5 of the Crowder Formation record localized reversal in drainage direction (Foster, 1980). This may reflect the inception of deformation that eventually led to ponding and reversal of the prevailing drainage direction. This would imply that Unit 5 of the Crowder Formation is Pliocene in age. This hypothesis is speculation at this time and needs to be tested. The Unit 5 paleocurrent data could be the result of an earlier deformation, perhaps associated with the passage of the Sierra Pelona past the site along the San Andreas fault.

6.2.4 Timing of Lateral Faulting

The Cleghorn lateral fault zone evolved through the integration of a concentrated zone of Cedar Springs reverse faults during the late Pliocene or early Pleistocene. The Cleghorn fault clearly cuts, and therefore postdates, the late Miocene(?) basal Crowder Formation in the western San Bernardino Mountains as well as south- and north-block-down members of the Cedar Springs fault system. The arcuate geometry of the Cleghorn fault suggests that it began as a reverse fault. Qt2 terrace gravels are offset over a kilometer laterally with a negligible vertical component (Section 7.2.2), however, indicating that motion on the Cleghorn fault zone had become largely strike-slip by the middle Pleistocene.

Lateral motion on the Cleghorn fault appears to have been facilitated by tilting which rotated the reverse faults of the Cedar Springs system to their present near-vertical orientation. Tilting affects the Harold Formation, which buries Cedar Springs folds (Section 5.2.1). If lateral faulting began prior to tilting, it would have to have occurred on fault planes dipping 50 to 70° northward, because no fault planes exist that would have

been near vertical prior to tilting. Since the middle Pleistocene, lateral faulting has exclusively exploited near-vertical surfaces in the western San Bernardino Mountains. Thus lateral faulting probably began during the final stages of tilting in the late Pliocene or early Pleistocene, after the Cedar Springs fault planes were rotated to a vertical orientation.

Slip-rate estimates for the Cleghorn fault of ~2 mm/yr and a total cumulative offset of 3.5 to 4.0 kilometers (Section 7.4.1) suggest that lateral motion began about 2 my ago. This is generally consistent with lateral faulting following tilting in Cajon Pass, since tilting postdates deposition of the Harold Formation less than 2.75 my ago. The continuity of the Harold Formation with the Shoemaker Gravel and Older Alluvium suggests that the Harold Formation may be significantly younger 2.75 my old, which would imply a higher slip-rate for the Cleghorn fault.

The timing of motion on the Summit Valley fault zone is very poorly constrained. It clearly affects the volcanogenic eastern facies of the Crowder(?) Formation. Bedding is locally vertical, which is uniquely characteristic of nearby lateral faulting within the Silverwood Lake area. East-trending faults of the Summit Valley fault zone offset both the Deep Creek and Powerline Road fault zones, which demonstrably cut the Ord River Gravel of middle Pleistocene age. There is some indication that the Qt2 terrace surface is disturbed, which suggests late Pleistocene motion. Thus motion on the Summit Valley fault zone was contemporaneous with the development of lateral faulting on the Cleghorn fault zone. The Summit Valley fault zone has sustained minimal cumulative offset since the middle Pliocene, however, since the stratigraphy of the eastern volcanogenic facies of the Crowder(?) Formation remains basically intact.

Several lines of evidence suggest that the Tunnel Ridge lineament was

once a lateral fault. There is minimal displacement of the late Miocene(?) erosion surface across the lineament, yet geomorphic expression of the feature is strong and continuous. Virtually every northeast-trending fault along the northern extension of the Tunnel Ridge lineament displaces the southern margin of the Rattlesnake Mountain pluton in a right-lateral sense, despite differences in senses and magnitudes of vertical offsets and later reactivation histories. This strongly suggests that the original north-northeast-trending fault system was a right-lateral system. Total cumulative displacement on this system is small, however, as evidenced by minimal offset of the southern margin of the Rattlesnake Mountain pluton.

6.3 DEFORMATION AND UPLIFT ON THE NORTH FRONTAL FAULT SYSTEM

Range-front thrusting is discontinuous, occurring along the west flank of the Ord Mountains/Pinnacles and along the northern range front east of Lovelace Canyon. There is some suggestion that thrusting propagated westward with time but was never established in the westernmost San Bernardino Mountains prior to the onset of lateral faulting.

A replacement of thrusting with high-angle faulting along the range front seems roughly to coincide with the development of lateral faulting in the Silverwood Lake area. Thrusting appears to have occurred in a distinct pulse associated with uplift in the Pliocene and early Pleistocene, followed by readjustment on high-angle faults to accommodate motion on pre-existing structures.

6.3.1 Timing of Range-front Thrusting

The inception of thrusting along the range front in Lucerne Valley is recorded by a dramatic change in character and provenance of the central facies of the Old Woman Sandstone (Sadler, 1982). A sudden influx of

monolithologic marble breccias contrasts with underlying fine-grained, well-sorted fluvial sediments, marking the first appearance of lithologies from the nearby range-front source area in the Old Woman Sandstone basin. The central facies of the Old Woman Sandstone has been paleontologically dated at 2.0 to 3.2 my (May and Repenning, 1982). The fine-grained sediment of the western facies of the Old Woman Sandstone apparently predates uplift and contains vertebrate fossils that are 2.5 to 3.0 my in age (May and Repenning, 1982). Sadler (1983, pers. comm.) suggests that the Old Woman Sandstone basin may owe its existence to down-warping associated with incipient range-front thrusting. Hence, stratigraphic evidence suggests that range-front thrusting began in the Lucerne Valley area during the latest Pliocene.

There is little evidence to constrain the time when thrusting ceased along the range front in Lucerne and Fifteenmile Valley. The White Mountain thrust system is cut by the Sky Hi Ranch fault along the range front, suggesting that the system has been inactive since at least late Pleistocene. The White Mountain thrust is overlain by Qf3 fanglomerate. The age of Qf3 is unknown, but it is almost certainly late Pleistocene or older based on the degree of dissection, soil development, and full offset on the Sky Hi Ranch fault. Where thrusting is well expressed geomorphically, an argument can usually be made for late Pleistocene reactivation of low-angle surfaces as secondary faults or landslide surfaces.

Thrusts are reported to override Pleistocene(?) fanglomerates near Cushenbury Canyon (Richmond, 1960), suggesting Quaternary activity. Sadler (1983, pers. comm.) argues that it is difficult to distinguish late Pliocene fanglomerates from late Pleistocene ones, making it dangerous to infer recency of faulting on the basis of such a relationship. Furthermore, Shreve (1959, 1968) has amply demonstrated the importance large-scale landsliding

along the range front, which could easily be mistaken for youthful thrusting. Landsliding must be carefully ruled out before low-angle structures are interpreted as thrusts. Sadler (1982) concludes that range-front thrusts were responsible for uplift, but have not been active since the early to middle Pleistocene.

Range-front thrusts becomes less distinct westward, and there is a steady reduction in relief of the range front. Thrusting cannot be traced west of Lovelace Canyon and, hence, late Pliocene thrusting is interpreted as having died out westward, possibly terminating in a tear structure. The Tunnel Ridge lineament would seem to be an obvious candidate for such a structure, but its sense of displacement is right-lateral, rather than the left-lateral motion that would be expected at the west end of a north-directed thrust fault.

6.3.2 Timing of Cataclasis

Cataclasis appears to have been associated with range-front thrusting. The uppermost thrust plane of the White Mountain system is commonly underlain by highly fractured and chloritized rocks, for which the protolith is unknown. Some of the fractured rock appears to have developed from a cataclastic protolith. The pervasive fracturing and shearing in these rocks require that deformation occurred under near-surface conditions, and that the rocks have not been subjected to significant burial since. The fracturing and shearing of the rock are therefore tentatively interpreted as having been developed in the sheets that lie between the fault surfaces of the White Mountain thrust zone.

Silver (1983, pers. comm.) has raised the possibility that some of the low-angle zones of cataclasis exposed along the range front may be early Tertiary structures related to a major episode of westward displacement of

the upper crust on shallow sub-horizontal surfaces. The "granulite" and "alaskite" of MacColl (1964) may represent deformation associated with an early Tertiary surface. Sadler (1983, pers. comm.) and Smith (1982) have defined older zones of cataclasis that they believe are developed along the margins of the Triassic Fawnskin monzonite. Further study is needed in order to develop a history of cataclasis on the range front.

6.3.3 Constraints on the Timing of the Ord Mountains Fault Zone

There is no evidence to suggest that range-front thrusting ever connected through from Lovelace Canyon to the north flank of the Ord Mountains. The Ocotillo Ridge fold is the only structure in the north frontal fault system to affect the range front across the mouth of Arrastre Canyon since at least middle Pleistocene. There is a complete lack of the dramatic range-front relief characteristic of the thrust-bounded range front to the east. A gentle warping or ramping seems to accomplish deformation across the front instead. Had thrusting occurred here during the latest Pliocene or early Pleistocene some residual evidence of range-front relief would be expected.

The low-angle fault zone on the west flank of the Ord Mountains has been active as recently as late Pleistocene. The fault is strongly expressed in a series of scarps that break the surface of the Qf2 fanglomerate, interpreted to be late Pleistocene in age. The zone also displaces middle Pleistocene sediments (MRF) of the Victorville Fan at the Deep Creek Dam. The Ord Mountain low-angle faults postdate the middle Pleistocene high-angle faults, but are displaced by the east-trending Summit Valley fault system. The complexity of this sequence of structural events, and short period of time during which they occurred, recall the dynamic nature of deformation in the westernmost San Bernardino Mountains.

Offset on the low-angle structures appears inadequate to account for uplift of the Ord Mountains block. Middle Pleistocene high-angle faults could have been largely responsible for uplift of the Ord Mountains, but the presence of low-angle structures suggests the possible existence of a Pliocene or early Pleistocene thrust system analogous to the White Mountain system. This system might have been reactivated following uplift on the high-angle faults. The Ord Mountains are enigmatic in that high-angle faulting was followed by low-angle faulting, rather that vice-versa.

Cumulative offset on the low-angle structures of the Ord Mountains range front is thought to be small, since the eastern contact of the Ord River Gravel with the Ord Mountains fanglomerates is still exposed adjacent to the range. Small displacements are also indicated by the fact that the low-angle fault zone dies out to the south near Grass Valley and to the northeast near Arrastre Canyon.

Numerous north-block-down faults north of the Grass Valley fault are suggestive of an incipient range-front reverse fault zone. It seems that frontal faulting began, but never got under way on the north side of the westernmost San Bernardino Mountains.

6.3.4 Timing of High-angle Faulting

The Sky Hi Ranch fault appears to be a reactivated member of the northwest-trending, right-lateral fault set developed in the Mojave block. An abundance of northwest-trending faults cut within the basement rocks of the range front on the projection of the Sky Hi Ranch fault. The lack of geomorphic expression along most of these faults indicates that they have long been inactive. The lateral faults probably existed within the Mojave block prior to range-front deformation. The Sky Hi Ranch fault zone is interpreted to represent the first stage of re-establishment of the Mojave-

block fault system across the range front. The pre-existing weakness of the Sky Hi Ranch fault zone also appears to have been incorporated by the north frontal fault system as an efficient means of accomodating lateral motion.

The Helendale fault is another member of this fault set. It gives way southeastward to a complex zone of faulting within the crystalline rocks of the San Bernardino Mountains, which suggests an overall sense of right-lateral displacement according to Sadler (1983, pers. comm.). Sadler suggests that small sedimentary basins on top of the range may actually be pull-apart structures related to a right-lateral shear.

The high-angle faults along the west flank of the Ord Mountains may have originally been lateral faults. The high-angle faults cut the Deep Creek facies of the Ord River Gravel and therefore have sustained motion during the middle Pleistocene or later. Although there is no evidence to support significant lateral offset in the basement rocks, their trend and timing match those of the faults of the Tunnel Ridge/Arrastre Canyon system.

6.3.5 Timing of Local Extension

The configuration of the Arrastre Canyon graben suggests that the north-northeast-trending faults may have once experienced dip-slip motion under conditions of local extension (Section 6.3.4).

The Arrastre Canyon graben has been a site of deposition since at least middle Pleistocene time, as evidenced by the fine-grained sediment (RSR; Section 4.3.5.4) that lies with angular unconformity beneath the terrace gravels along the Bowen Ranch Road. These sediments are magnetically reversed, and therefore older than 730,000 y B.P. Late Tertiary sediments are rare within the range, and the Arrastre Canyon deposit is distributed over several kilometers along the Bowen Ranch Road. Sadler (1982, pers.

comm.) has suggested that other depositional sites interior to the range are preserved in small pull-apart basins that indicate local extension in a right-lateral shear zone. The Arrastre Canyon graben is a topographic depression and has been a site of deposition since middle Pleistocene time.

6.4 NATURE AND MODES OF DEFORMATION

As can be seen by the preceding discussion, there is no through-going thrust fault system along the entire northwestern range front of the San Bernardino Mountains. The north frontal fault system is a collection of unique elements, each of which accommodates regional stress in a different way. Pre-existing weaknesses have strongly influenced subsequent fault patterns, and many faults have experienced more than one type of motion during their histories.

The central San Bernardino Mountains are bounded by low-angle structures on both sides, whereas the westernmost part of the range is asymmetric, with significant frontal reverse faulting restricted to the south side. This seems to be due to the early development of lateral faulting in the western San Bernardino Mountains. Lateral faulting may have obviated the need for major reverse structures, accomplishing shortening by squeezing material out laterally, rather than vertically. Tilting, range-front warping, and arching have served to elevate parts of the range front without range-front faulting.

6.4.1 Origin of Low-angle Range-front Structures

Low-angle structures clearly played an important role in uplift and early deformation along the range front. Several different hypotheses are proposed for the nature and origin of these low-angle structures:

6.4.1.1 Transpressional Welt

Sadler (1982) proposes a "flower structure" geometry for deformation of

the basement rocks in the San Bernardino Mountains (Figure 6-3). In this model, thrust faulting developed to accommodate a vertical "squeezing out" of the San Bernardino Mountains block in response to compressional forces across the San Andreas fault. Fuis and Lamanuzzi (1978, pers. comm.) made a cross-section of seismicity in the central San Bernardino Mountains that shows a V-shaped lower limit to the depth of seismic events, in general agreement with Sadler's model. If transpressional uplift straddled the San Andreas fault, the frontal faults on the south side of the San Gabriel Mountains may represent the other side of the uplift structure and would be analogs of the north frontal fault system. This would imply that the San Bernardino Mountains and the San Gabriel Mountains, representing the two halves of the flower structure, both developed at a time when the mountain ranges were juxtaposed along the San Andreas fault. Such an origin for the uplift of the San Bernardino Mountains is generally consistent with the timing of uplift observed on the north side of the San Bernardino Mountains, assuming a uniform Quaternary slip-rate for the San Andreas fault. Following uplift, the northwestward movement of the San Gabriel Mountains along the San Andreas fault relieved the stresses on the San Bernardino Mountains block, allowing it to be modified by the northwest-trending faults of the Mojave block.

6.4.1.2 Early Tertiary Low-angle Structures

Silver (1983, pers. comm.) has proposed major translation of crustal sheets westward on low-angle surfaces during the early Tertiary. In his model, the San Bernardino Mountains are an allochthonous slab which overlies the autochthonous basement on a major subhorizontal discontinuity at unknown depth. He speculates that vertical uplift in the San Bernardino Mountains may have exposed and exploited parts of this older discontinuity, leading to

Figure 6-3. "Transpressional" model of uplift for the San Bernardino Mountains (Sadler, 1982). In this model basement rocks of the San Bernardino Mountains are "squeezed up" vertically as the result of compression developed in association with lateral faulting on the San Andreas fault. (A) The fracture pattern produced as a result of convergent lateral faulting in a limestone slab (Bartlett et al., 1981). A cross-section view is presented, cut transverse to direction of lateral displacement. (B) An interpretive isometric cutaway diagram looking west-southwest across the San Bernardino Mountains (Sadler, 1982). Note thrusting on north and south side of the range, and northwest trending, right-lateral faults of the Mojave block that cross the range-front on the north side. The inferred geometry of internal deformation for the San Bernardino Mountains bears a strong similarity to the clay-cake deformation of Bartlett et al. (1981).

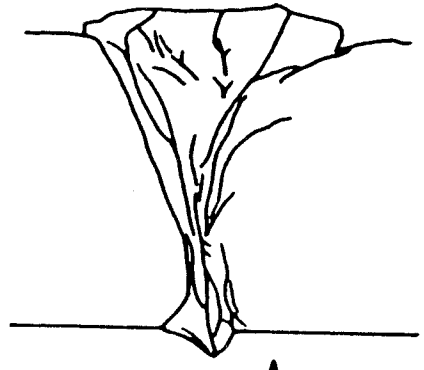

A

BARTLETT et al.
1981

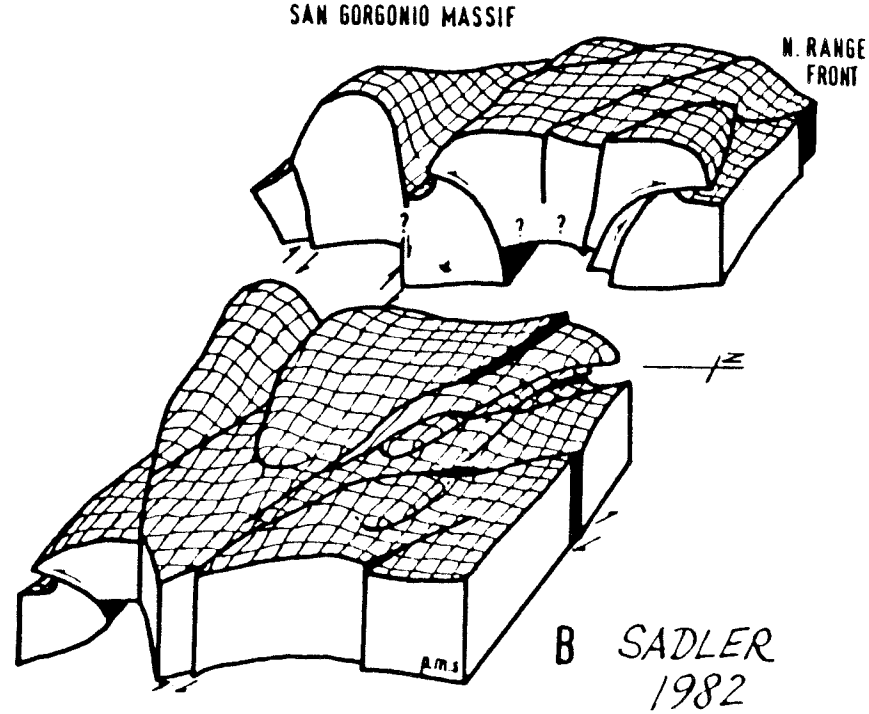

B SADLER
1982

the observed stack of thrusts.

Several lines of evidence support Silver's model. The arcuate pattern and pervasive nature of the Cedar Springs fault system suggest that these structures may be rooted in a shallow discontinuity beneath the western San Bernardino Mountains. Weldon (1982, pers. comm.) reports that a stack of low-angle structures is exposed on the south side of the western San Bernardino Mountains. These structures parallel foliation in the cataclastic gneiss in the westernmost San Bernardino Mountains. Such a shallow, low-angle discontinuity might explain the manner in which the Cleghorn fault follows the traces of the pre-existing Cedar Springs faults. Furthermore, the pervasive nature of deformation and proposed "shingling" of fault blocks in the westernmost San Bernardino Mountains would seem most consistent with deformation internal to a thin slab.

6.4.1.3 Shallow Crustal Discontinuity

Corbett and Hearn (1981) report that the maximum depth of seismicity is 10 kilometers beneath most of the northern San Bernardino Mountains and southern Mojave Desert (Figure 6-4). By contrast, the deepest seismicity in southern California occurs beneath San Gorgonio Pass on the southwest side of the San Andreas fault. A shallow floor to the seismicity under the San Bernardino Mountains raises the possibility of a discontinuity in rock properties and/or deformational behavior in the upper crust. The San Bernardino Mountains appear to be undergoing brittle deformation to a depth of about 10 kilometers and behaving plastically beneath that level. This seismicity pattern might be explained by a contrast in rock type across a low-angle structural discontinuity. Such behavior could also occur as a consequence of changing rock properties with depth.

Figure 6-4. Cross-sections of seismicity in the San Bernardino Mountains (Corbett and Hearn, 1981). The top cross-section shows a shallow floor to seismic events in the western San Bernardino Mountains. The section trends due north through east Summit Valley and includes events within 15 km of the section line. The San Andreas fault defines the southern margin of the San Bernardino Mountains at +20 km, and Summit Valley defines the northern limit of the range at +40 km. The bottom section shows a similar lower limit to the occurrence of seismic events under the central San Bernardino Mountains. It trends due north through White Mountain, with events being projected to the section from up to 15 km on either side. In the lower section, the San Andreas fault is at +12 km, and the northern range-front fault system is at +50 km.

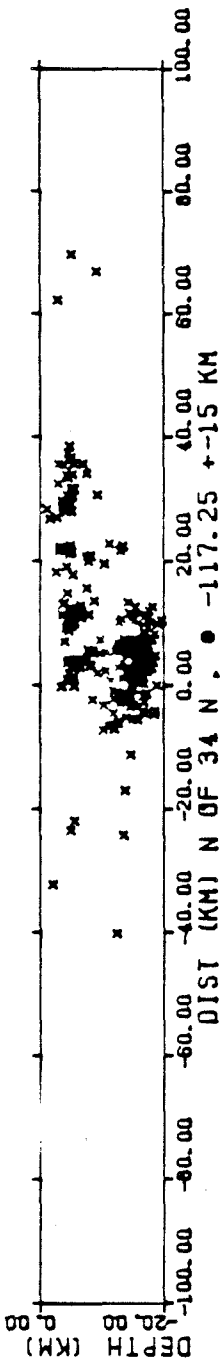
DEPTH (KM)
0.00
-20.00
-100.00
-80.00
-60.00
-40.00
-20.00
0.00
20.00
40.00
60.00
80.00
100.00
DIST (KM) N OF 34 N. • -117.25 +-15 KM

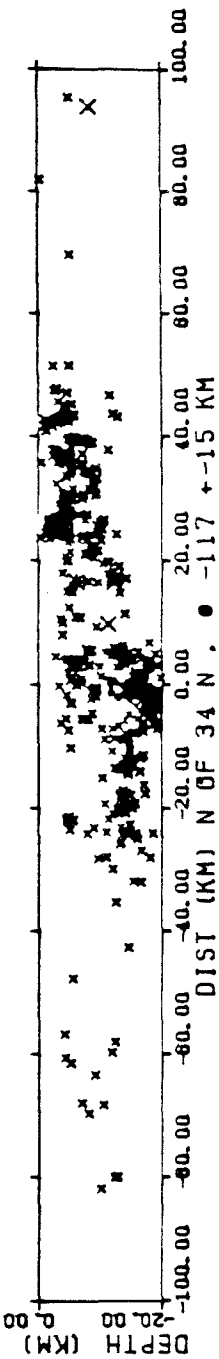
DEPTH (KM)
0.00
-20.00
-100.00
-80.00
-60.00
-40.00
-20.00
0.00
20.00
40.00
60.00
80.00
100.00
DIST (KM) N OF 34 N. • -117 +-15 KM

6.4.1.4 Upper Mantle Discontinuity

Hadley and Kanamori (1977) propose that the upper mantle boundary between the North American and Pacific plates diverges from the crustal boundary located at the San Andreas fault (Figure 6-5). Traction, exerted locally across a low-angle decoupling zone between the divergent traces, might result in a dynamic crustal buckling response, giving rise to low-angle structures in the San Bernardino Mountains. This model implies that the northern Transverse Ranges boundary east of the San Andreas fault is migrating northward and propagating eastward.

6.4.1.5 Regional Rotation

Antipodal symmetry displayed by the frontal fault systems of the San Bernardino and San Gabriel Mountains has caused some authors to propose rotation of the entire Transverse Ranges province about a vertical axis near its center (Baird et al., 1974). Baird et al. point out that the required 55° counterclockwise rotation, with overthrusting northeastward east of center and overthrusting southwestward west of center, leads to an enormous great-circle overlap of 190 kilometers at the extreme ends of the range. In this model the San Bernardino Mountains would be allochthonous. Paleomagnetic data in the western Transverse Ranges tend to support rotations, but of smaller blocks in a regional right-lateral shear couple (Kamerling and Luyendyk, 1979).

6.4.1.6 Differential Offset on the San Andreas Fault

Many workers believe that the Transverse Ranges divide the San Andreas fault into two parts with different movement histories (e.g. Baird et al., 1974), and they invoke large components of upward relief and thrusting in the Transverse Ranges to alleviate strain accumulation resulting from

Figure 6-5. Block diagram of the proposed divergence of the crust and mantle plate boundaries. "The crust and mantle boundaries are assumed to be coincident within the Salton Trough. The mantle boundary extends northwest along the strike of the structural elements of the Salton Trough and passes . . . in the vicinity of the Helendale-Lenwood-Camprock faults. The resulting differential motions between the crust and upper mantle, which must occur under southern California if the crust and mantle plate boundaries diverge, would have a profound effect on the crust in this region of greater drag. . . . The morphological Transverse Ranges (extending across the San Andreas fault) should appear as a constant phenomenon associated with the [observed] high velocity upper mantle structure and thin decoupling layer. As the Pacific plate moves northwest the Transverse Ranges should likewise migrate. . . . The Transverse Ranges are viewed as a ripple in the crust that reflects a major upper mantle structure" (Hadley and Kanamori, 1977).

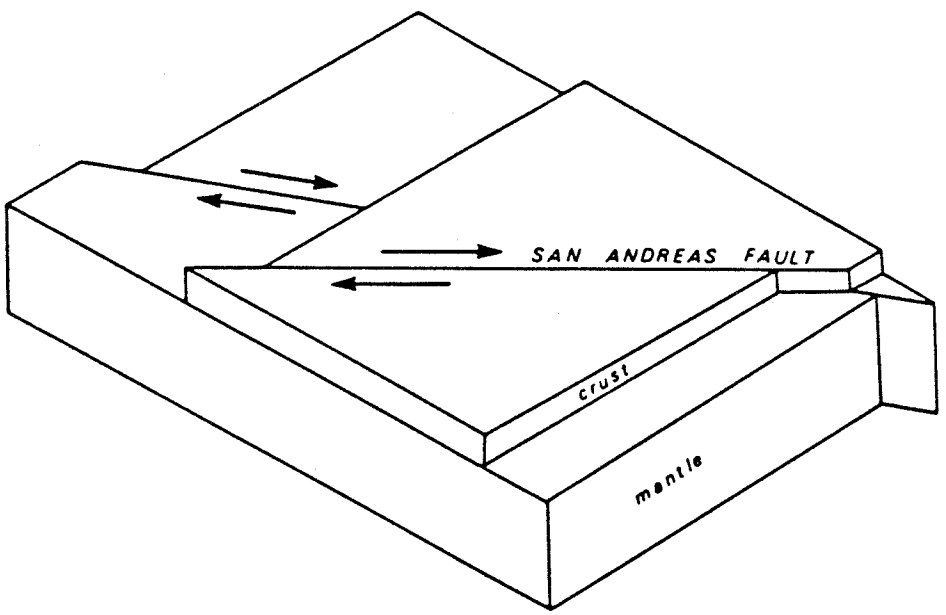
SAN ANDREAS FAULT
crust
mantle

different slip rates on the San Andreas north and south of the province.

6.4.1.7 Discussion

Although the results of this study do not permit any of the above hypotheses to be ruled out, some relevant observations can be made. There is no evidence to support late Tertiary horizontal displacements of more than a few kilometers on the range-front thrust faults, which argues against the major displacements required by large-scale rotation. Paleomagnetic data from both the Harold Formation and Unit 4 of the Crowder Formation (Kirschvink, 1983, pers. comm.) indicate that no appreciable rotation has occurred in Cajon Pass since the late Miocene. Neither does the evidence support northward or eastward propagation of range-front faulting with time, which argues against the notion that uplift in the central Transverse Ranges is the product of coupling across a deep-seated lithospheric discontinuity experiencing motion at the plate-rate. Differential movement history on the San Andreas fault should produce structures analogous to those predicted for the end of a strike-slip fault (Chinnery, 1966a,b; see Section 6.3.2; Figure 6-6). Although such structures are observed locally adjacent to the San Andreas fault in Cajon Pass, fault geometries in the San Bernardino and San Gabriel Mountains as a whole would not seem to be consistent with this hypothesis.

The most plausible hypothesis for the nature and origin of low-angle structures in the San Bernardino Mountains would seem to be a combination of hypotheses (1), (2), and (3). The cross-section of Fuis and Lamanuzzi (1978, pers. comm.) would support a model in which a transpressional welt is rooted beneath the central San Bernardino Mountains. The profile of Corbett and Hearn (1981), on the other hand, suggests a subhorizontal limit to seismicity in the San Bernardino Mountains and a maximum depth along the

Figure 6-6. Modes of secondary faulting, deduced from the results of theoretical modeling of maximum shear stress trajectories at the end of a strike-slip fault (Chinnery, 1966b). In this model, secondary faulting is considered as an end effect of movement on a "master" fault. For each mode of secondary faulting, A through F, the left-hand pattern corresponds to formation of the master fault under conditions of pure shear, and the right-hand pattern results from a uniaxial compression. All of the shear stress trajectories shown coexist within the context of the stress distribution at the end of fault. The differences shown from A to F reflect conditions at the end of the fault (A,B), tensional quadrant (C,D) and compressional quadrant (E,F). Each pair of stress trajectories (A,B; C,D; E,F) represent a conjugate set. If the "master" fault is considered to be the southern segment of the San Andreas, or the San Jacinto fault, the "type D" pattern bears a remarkable resemblance to the pattern of faulting in the western San Bernardino Mountains, particularly the Cleghorn fault.

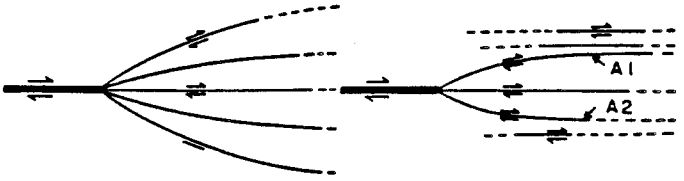

TYPE A

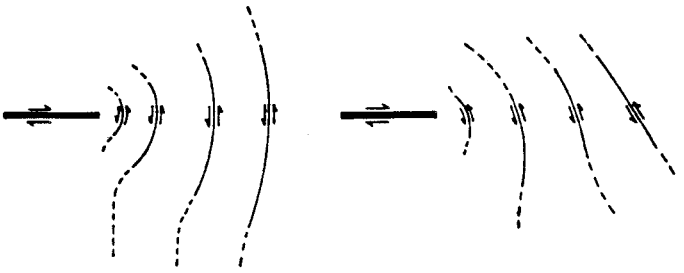

TYPE B

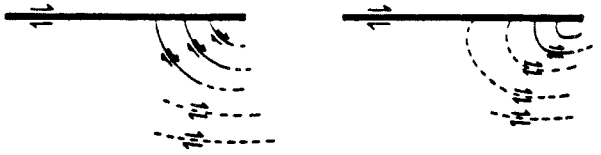

TYPE C

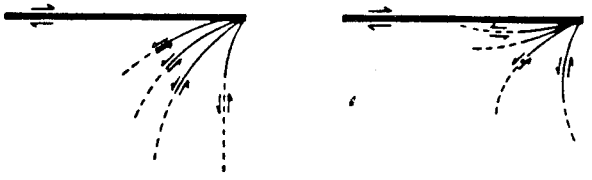

TYPE D

TYPE E

TYPE F

San Andreas fault, which would tend to support a larger welt including the San Gabriel Mountains. Their profile indicates the possible existence of a low-angle floor to seismicity beneath the San Gabriel Mountains as well. Hypotheses (1), (2) and (3) can be combined into one model in which a transpressional welt, developed across the San Andreas fault in response to compression, was locallized and facilitated by pre-existing early Tertiary low-angle structures.

6.4.2 Origin of Deformation in the Western San Bernardino Mountains

Fault patterns in the westernmost San Bernardino Mountains are very similar to predictions by mathematical modeling of the pattern of slip-planes that occur near the end of a strike-slip fault (Chinnery, 1966a,b; Figure 6-6). The arcuate pattern, spatial distribution and sense of motion on the Cedar Springs fault system, Cleghorn lateral fault system, and the Tunnel Ridge lineament can be explained as the product of a change in slip-rate on the San Andreas fault in Cajon Pass. Such a change would lead to a build-up of stresses and result in structures similar to those predicted for the end of a strike-slip fault. Chinnery (1966b), in fact, identifies the Cajon Pass area as an ancient "end point" of the San Andreas fault. Late Pliocene and early Pleistocene structures in the western San Bernardino Mountains can be explained as "secondary" faults that developed under the direct influence of the San Andreas "master" fault.

Weldon (1982, pers. comm.) has suggested that right-lateral motion on the San Jacinto fault may have begun about 2 my ago, when it would have impinged on the San Andreas fault opposite the southern projection of the Tunnel Ridge lineament. Weldon's hypothesis suggests that the San Jacinto fault may have temporarily hindered motion on the San Andreas fault. The southern segment of the San Andreas fault could have been the "master" fault

which dictated the original fault geometries in the western San Bernardino Mountains. The San Jacinto fault effectively ended against the San Andreas, and would have had the right orientation to produce the arcuate pattern of faulting in the Cedar Springs fault system. While the geometry of the Cedar Springs system suggests secondary faulting, the sense of displacement on the arcuate faults clearly relates to north-south compression and shortening. Thus the Cedar Springs faults may have originated as "type D" faults, which were modified to accomodate shortening (Figure 6-6). The migrating nature of Cedar Springs fault patterns might be understood in terms of the evolution of the San Jacinto/San Andreas junction.

Weldon's hypothesis also offers an explanation for the enigmatic right-lateral offset and geometry of the Tunnel Ridge lineament. As the west side of the San Jacinto fault moved northward, it would have impinged on the San Andreas fault and forced material west of the fault junction northward. This might result in small right-lateral displacement on the north-northeast-trending fault set of the Tunnel Ridge lineament. In terms of Chinnery's model (1966b), the Tunnel Ridge lineament can be thought of as a "type F" fault produced by southern end point of the northern branch of the San Andreas fault at Cajon Pass (Figure 6-6).

The interaction with the San Jacinto fault, and temporarily locking of the San Andreas fault, could also have resulted in the rapid uplift by arching of the western San Bernardino Mountains. The location, magnitude and shape of arching in the west San Bernardino Mountains is, in general, consistent with mathematical predictions for vertical deformation near the end of a strike-slip fault (Chinnery, 1965).

Any detailed comparison of deformation and uplift with Chinnery's model predictions would have to take account both the San Jacinto and the San

Andreas fault. Any pre-existing, early Tertiary fault zones may also have influenced the course of structural evolution. While the above ideas are highly speculative, they do offer a possible unifying explanation for the complex fault geometries in the western San Bernardino Mountains.

6.4.3 Origin of Late Pleistocene High-angle Faulting

6.4.3.1 Development of the Cleghorn Fault

The east-west orientation of the Cleghorn fault would seem to be incorrect for left-lateral motion, since north-south compression should produce northeast-trending left-lateral faulting. The case has already been made (Section 5.2.4) that the Cleghorn fault began as a Cedar Springs reverse fault, correctly oriented to accommodate north-south compression, and that motion has subsequently become left-lateral. Possible models to explain the misorientation of the Cleghorn fault are discussed below.

One obvious explanation for the origin of this misorientation is that the Cleghorn fault began as a northeast-trending left-lateral fault and has since been rotated into its present orientation by oroclinal bending or block rotation in response to a right-lateral shear couple. The consistent azimuth of the northward dip in the late Miocene erosion surface and basal Crowder Formation in Summit Valley argues against oroclinal bending in the western San Bernardino Mountains since tilting in the early Pleistocene. Furthermore, preliminary paleomagnetic work in the Crowder Formation in Cajon Pass rules out rotation since the middle Miocene. Thus, it appears that the development of left-lateral motion occurred with the Cleghorn fault in its present orientation.

Hill (1982) has calculated that "active" fault zones are 20 to 50% weaker than block interiors, favoring motion on pre-existing fault surfaces even if they are rotated as much as 60° from their optimal orientation.

Deformation in southern California is generally consistent with a simple hexagonal-block model under north-south compression with (1) reverse faults trending east, (2) normal faults trending north, and (3) right- and left-lateral faults trending northwest and northeast respectively. Hill argues, however, that the abundance of pre-existing fault zones may imply that the region is behaving more like an aggregate of fault-bounded crustal blocks separated by relatively weak fault zones in a structurally heterogeneous crust (Hill, 1982). This line of reasoning leads to the hypothesis that the Cleghorn and San Andreas faults are acting as weak zones permitting the westernmost San Bernardino Mountains to be "squeezed out" eastward by converging blocks under north-south compression. Such block-motion might be contributing to the rapid uplift of the San Gorgonio block (Morton and Herd, 1980). Evidence for the role and importance of pre-existing weaknesses in later fault patterns is presented in Section 6.3.5.

The Cleghorn fault is perhaps best interpreted as a secondary fault originating as an "end effect" of a strike-slip fault. The "type D" faults of Chinnery (1966b) are a perfect match for the Cleghorn fault in terms of geometry, spatial arrangement and sense of displacement (Figure 6-6). The "master" fault would be either the southern segment of the San Andreas fault or the San Jacinto fault. The modeling of Chinnery (1966b) suggests that the stress axes in the western San Bernardino Mountains may well be strongly influenced by the nearby San Andreas fault. The evolution from arcuate reverse faults to left-lateral strike-slip faults may be a natural consequence of progressive deformation. In Chinnery's model, the Cleghorn fault is not misoriented at all!

Thus, the most satisfactory explanation for the complex structural evolution of the western San Bernardino Mountains is that fault patterns,

initially developed as an "end effect" of the San Andreas, have themselves become weak zones which have profoundly influenced subsequent deformation.

6.4.3.2 Origin of Northwest-trending Faults of the Mojave Block

A set of northwest-trending, right-lateral faults existed in the Mojave block prior to the development of range-front structure in the San Bernardino Mountains. In the middle Pleistocene the northwest-trending faults began to re-establish themselves across the north frontal fault system (Section 6.3.2). Motion on these right-lateral faults has offset range-front structures (e.g. Sky Hi Ranch fault) and may have led to the development of complex zones of right-lateral shear in the interior of the range (Sadler, 1983, pers. comm.).

6.4.4 Evidence for Local Extension

The combined effect of the northwest-trending Mojave faults and the east-trending Cleghorn fault zone is to create a local extensional regime in the Ord Mountains/Arrastre Canyon area.

Local extension in the vicinity of the Arrastre Canyon graben can be explained in terms of the consequence of lateral faulting along the range front. Faults bounding the Arrastre Canyon graben are near-vertical and linear, reflecting their origin as lateral faults. Left-lateral motion on the Cleghorn fault implies that the main mass of the San Bernardino Mountains is moving eastward relative to the Mojave block at a rate of ~2 mm/yr. The Cleghorn fault does not appear to continue east, but rather turns north-northeast and follow the Tunnel Ridge lineament into the Arrastre Canyon graben. Neglecting internal deformation within the range, the main mass of the San Bernardino Mountains is separating from the Victorville Fan at a rate of 2 mm/yr. Extension in the Arrastre Canyon graben is therefore a

logical consequence of motion of the Cleghorn fault zone.

Carrying this reasoning one step further leads to an examination of the high-angle, north-northeast-trending frontal faults of the Ord Mountains. Many characteristics of the west flank of the Ord Mountains suggest normal faulting. The cemented talus breccia associated with the high-angle faults can be interpreted as the product of a receding mountain front uplifted along normal faults. The range-front fanglomerates are in buttress contact with basement rocks. Basement rocks show none of the signs of cataclasis that are observed along the northern range front. The Ord Mountains block tilts northeastward into the Arrastre Canyon graben; this eastward tilt is reflected in the attitude of the older RSR sediments along the Bowen Ranch Road. Thus the Ord Mountains can be interpreted as a tilted fault block bounded by the Arrastre Canyon graben on the east and normal range-front faults on the west. This hypothesis explains both the Arrastre Canyon depression and range-front relief on the west flank of the Ord Mountains. Extensional deformation must have occurred in the middle Pleistocene or later, as all of the structures involved cut middle to late Pleistocene deposits.

Motion on the Sky Hi Ranch fault also has the effect of producing extension in the Arrastre Canyon graben. Right-lateral movement on the northwest-trending faults of the Mojave block has the effect of moving the main mass of the San Bernardino Mountains southeast with respect to the Ord Mountains. This produces a net extensional component of strain across the range-front on the southwest side of the fault, and a net compressional component on the northeast side. This situation is especially acute since the right-lateral Mojave block faults die out at the range front and their motion must somehow be absorbed by deformation on the range front and

internal to the range.

6.4.5 The Role of Pre-existing Weaknesses

There is abundant evidence that pre-existing weaknesses in the San Bernardino Mountains have exerted a profound influence on the pattern of subsequent faulting and deformation.

The evolution of the Cleghorn fault zone is a particularly instructive example of how the geometry of pre-existing weaknesses can dictate the course of later deformation. A concentrated zone of faults within the Cedar Springs fault zone coalesced to form the Cleghorn fault after being rotated to a vertical orientation by regional tilting. The path that the Cleghorn fault adopted has many cusps and bends at intersections with members of the Cedar Springs reverse fault system. Northeast-trending segments of the old reverse fault system may have been exploited as splays to accommodate minor adjustments related to motion on the Cleghorn fault zone.

The history of the Grass Valley fault is similar. It resembles a member of the Cedar Springs fault in its arcuate geometry, yet it displays evidence of lateral motion. It also may have sustained north-block-down motion as a result of incipient reverse faulting on an aborted extension of the north frontal fault zone. Evidence for more than one sense motion on the same fault plane indicates that it is more efficient for faulting to proceed on an existing fault plane than to establish a new one.

North-northeast-trending faults have been involved in many different types of deformation. The abundance of north-northeast-trending structures with a variety of motion histories points to a natural tendency for faulting to follow a set of pre-existing weaknesses. The original weaknesses for the north-northeast-trending fault set may have been joints or fractures, dikes, or linear septa of weak rock. The north-northeast-trending weaknesses have

been exploited as right-lateral faults (Lovelace Canyon fault), dip-slip faults in an extensional regime (Arrastre Canyon graben), as well as reverse faults under compression (Arrastre Canyon Narrows fault zone).

Reactivation of the east-northeast-trending faults commonly involves the north-northeast-trending faults. Structures following the east-northeast trend include the tear fault between the Deep Creek and Apple Valley Highlands fault zones, the Ocotillo Ridge fold in the Mariannas Rancho area, and the Arrastre Canyon Narrows fault zone.

The northwesterly trend of faults in the Mojave block predates uplift along the range front. Many northwest-trending faults mapped by Sadler (1981) within the San Bernardino Mountains block are apparently inactive based on their lack of geomorphic expression. These northwest-trending weak zones have clearly been utilized by the north frontal fault system where they were favorably oriented to accommodate range-front deformation. This suggests that many of these older weaknesses could potentially be exploited to accommodate readjustments along the range front following major uplift.

The White Mountain thrust system has been reactivated. Although the thrust has clearly been inactive since the middle Pleistocene, segments of the thrust plane have been locally activated to accomodate a compressional component of motion across the Sky Hi Ranch fault zone. The White Mountain thrust itself may have followed an early Tertiary weakness. The low-angle structures along the west flank of the Ord Mountains may indicate a pre-existing thrust zone. The Arrastre Canyon Narrows fault zone appears to utilize the White Mountain thrust zone as a path for linking with the north frontal fault system east of Lovelace Canyon.

The following example sums up the importance of pre-existing weaknesses

in the study area. The Arrastre Canyon Narrows fault zone follows a north-northeast-trending weakness north from the Deep Creek area, changes trend to east-northeast along another old fault zone, turns east and follows the White Mountain thrust zone until it swings southwest and joins the right-lateral Sky Hi Ranch fault. It thereby exploits four different fault trends while negotiating a right-angle bend!

6.5 Summary

This study clearly shows that the concept of a single, unified range-bounding thrust is incorrect. The north frontal fault system is, in fact, a disparate collection of structures, many of which follow pre-existing weaknesses, and each of which accommodates range-front deformation in whatever way it can, given its orientation and attitude.

Thrusting and tilting led to uplift along the northern range front in Lucerne Valley during a pulse of compression in the latest Pliocene and early Pleistocene. Thrusting along the range front in Lucerne and Fifteenmile Valley seems to have been roughly contemporaneous with tilting in the westernmost San Bernardino Mountains. Both thrusting and tilting were accomplished during the latest Pliocene to early Pleistocene. The Cedar Springs system was inactive by early Pleistocene, and may have been begun to form as early as late Miocene.

Since the middle to late Pleistocene, high-angle faulting has dominated over low-angle faulting in the range-front study area. Lateral faults in the western San Bernardino Mountains are believed to reflect an eastward "squeezing out" of the San Bernardino Mountains in response to transpressional forces along the San Andreas fault. Northwest-trending faults along the northern range front represent a reassertion of the prevailing fault trend in the Mojave block prior to uplift. There is some evidence to

suggest that localized extension accompanied the development of the lateral faulting.

Both low-angle and high-angle faults can ultimately be related to the influence of the San Andreas fault zone. Low-angle structures, while possibly developed on early Tertiary structures, appear to be part of a transpressional welt developed across the San Andreas fault. High-angle faulting in the western San Bernardino Mountains can be understood in terms of secondary fault patterns predicted for stress buildup associated with the end of a strike-slip fault. All systems appear to accommodate north-south compression in may also be responding to local transpressional forces generated by convergence across the San Andreas fault zone.

CHAPTER VII

SEISMIC HAZARD EVALUATION

7.1 INTRODUCTION

7.1.1 Purpose

Two of the primary objectives of this study were: (1) to estimate Holocene rates of deformation along the northern range front, and (2) to estimate recurrence intervals and vertical/lateral offsets, both cumulative and for single earthquakes, for the frontal fault system. The following is a summary of the evidence for offset, slip-rate, and earthquake potential for the major faults in the area covered by this investigation.

Trenching was carried out at two sites along the north frontal fault system in order to (a) determine whether or not the north frontal fault system is a continuous structure, inasmuch as its continuity bears on its earthquake potential, (b) study the nature and geometry of faulting and deformation along the range-front fault system in order to understand better its geomorphic expression and role in a regional tectonic context, and (c) document deformation in young, hopefully datable, deposits that would constrain the recency of activity along the north frontal fault system.

7.1.2 Scope

Activity is assessed for each major fault in the study area (Table 7-1), under a scheme which classifies faults according to their degree of activity, and includes a category for faults of uncertain activity. The scheme used conforms to the guidelines established for the State of California under the Alquist-Priolo Special Studies Zones Act (California Division of Mines and Geology, 1980). Critical evidence used in evaluating activity is briefly summarized and keyed to specific localities on Plates 1A and 1B. Principal

fault parameters, including length, cumulative offset, slip-rate, maximum credible earthquake magnitude, and recurrence interval are estimated where data permit. This geologic study naturally focuses on earthquakes which result in surface rupture; seismic events which do not involve surface faulting must be studied by means other than surficial geologic mapping. The most damaging seismic events usually produce surface rupture.

In order to study the recency, nature, and continuity of faulting on the range-front system, trenches were excavated on the Arrastre Canyon Narrows fault zone in Lovelace Canyon and on the Ocotillo Ridge fold in the Marianas Rancho. No fault was encountered at either site, and it was not possible directly to constrain earthquake recurrence intervals, as had originally been hoped. Some important insights were gained, however, into the style and rates of deformation along the north frontal fault system.

A measure of offset can be obtained for many of the faults and fault systems within the study area, and an attempt is made to present maximum, minimum, and preferred values for both offset and ages of offset features. Estimates of the limiting values of offset and age for poorly constrained faults and units are necessarily based on the geologic and geomorphic arguments considered most consistent with the neotectonic evolution developed in Chapter VI.

Maximum, minimum, and preferred slip-rates are calculated based on the range in amount of offset and age of each offset feature. A lack of age control on alluvial units makes the range of possible slip-rates for certain faults considerable. In these cases, it is felt that an appreciation for the geology, geomorphology, and history of the study area leads to a qualitative limitation on what constitutes a geologically "reasonable" slip-rate. Slip-rate data are accompanied by a qualitative measure of the uncer-

tainty in offset data and quality of reasoning that went into each slip-rate estimate.

Finally, a comparison is made between the faults of the study area and other active faults in the region to provide a context for the the relative degrees of seismic hazard they pose.

7.2 CRITERIA FOR ACTIVITY

In the following sections, evidence bearing on the late Quaternary activity of each major fault or fault system in the study area is presented. Since data do not exist to constrain the activity of many faults in the study area, faults are first grouped according to the scheme for classification of fault activity based on available data developed by Cluff et al. (1972), as modified by Slemmons (1977), The geologic criteria for activity are presented in Table 7-1, which has been further modified from Slemmons.

For the purposes of the present study, "the planned project" referred to in this classification scheme is assumed to be a residential development. The scheme has therefore been interpreted in conformance with the guidelines set forth by the Alquist-Priolo Special Studies Zones Act of 1972 (California Division of Mines and Geology, 1980), wherein an "active fault" is defined as one which has "had surface displacement within Holocene time (about the last 11,000 years)", and a potentially active fault is one which shows "evidence of surface displacement during Quaternary time (last 2 to 3 million years)". Interpreted in this way, the system of Cluff et al. (1972) stresses the dependence of "activity" on the lifespan of the particular project planned. For residential development, the project lifespan is herein assumed to be 50 years, and Alquist-Priolo criteria for activity are therefore considered appropriate.

Faults for which slip-rate data can be calculated are further classified

Table 7-1. Classification of fault activity based on available data¶.

Activity Classification	Geologic Criteria
Active - a tectonic fault with a history of strong earthquakes or surface faulting, or a fault with a short recurrence interval relative to the life of the planned project.	(1) Geologically young* deposits cut by fault (2) Youthful geomorphological features that are characteristic of geologically young* displacements along the fault trace. (3) Groundwater barriers in geologically young* or unconsolidated deposits.
Potentially Active - a tectonic fault without historic surface offset, but with a recurrence interval that could be sufficiently short to be significant to the particular project.	(1) Geomorphic features that are characteristic of active faults, but with subdued, eroded and discontinuous form. (2) Faults not known to cut or displace youngest alluvial deposits, but offset older Quaternary† deposits. (3) Water barriers in older deposits†. (4) Geological setting in which the geometry in relation to active or potentially active faults suggest similar degree of activity.
Activity Uncertain - a fault with insufficient evidence to define past activity or recurrence interval. The following classifications can be used until the results of additional studies provide definitive evidence.	Available information is insufficient to provide criteria that are sufficiently definitive to establish fault activity. This lack of information may be due to the inactivity of the fault or to lack of investigations needed to provide definitive criteria.
(Tentatively Active) - predominant evidence suggests that the fault may be active even though its recurrence interval is very long or poorly defined.	Available information suggests evidence of fault activity, but evidence is not definitive.
(Tentatively Inactive) - predominant evidence suggests that the fault is not active.	Available information suggests evidence of fault inactivity, but evidence is not definitive.
Inactive - A fault along which it can be demonstrated that surface faulting has not occurred in the recent past, and that the requirement interval is long enough to be of significance to the particular project.	Geomorphic features characteristic of active fault zones are not present and geological evidence is available to indicate that the fault has not moved in the recent past and recurrence is not likely within a time period considered significant to the site. Should indicate age of last movement: Holocene, Pleistocene, Quaternary,

* geologically young <11,000 y † 11,000 y > older Quaternary < 2 my
¶ modified from Cluff et al. (1972), after Slemmons (1977)

Table 7-2. Fault classification criteria for degrees of fault activity*.

FAULT CLASSIFICATION CRITERIA

Class 1
Slip-rate ≥ 10 mm/yr
Slip per event ≥ 1 m
Rupture length ≥ 100 km
Seismic moment ≥ 10^{26} dyne-cm
Magnitude ≥ M_S 7.5
Recurrence interval ≥ 500 yrs

Class 1A
Same as Class 1, except
Slip-rate ≥ 5 mm/yr
Recurrence interval ≤ 1000 yrs

Class 1B
Same as Class 1, except
Slip per event < 1 m
Magnitude < M_S 7.0
Recurrence interval generally ≤ 100 yrs

Class 2
Slip-rate 1-10 mm/yr
Slip per event ≥ 1 m
Rupture length 50-100 km
Seismic moment ≥ 10^{25} dyne-cm
Magnitude ≥ M_S 7.0
Recurrence interval 100-1000 yrs

Class 2A
Same as Class 2, except
Slip per event < 1 m
Magnitude < M_S 7.0
Short (<100 yrs) recurrence interval

Class 2B
Same as Class 2, except
Slip per event ≥ 5 m
Rupture length ≥ 100 km
Recurrence interval ≥ 1000 yrs

Class 3
Slip-rate 0.5-5 mm/yr
Slip per event 0.1-3 m
Rupture length 10-100 km
Seismic moment ≥ 10^{25} dyne-cm
Magnitude ≥ M_S 6.5
Recurrence interval 500-5000 yrs

Class 4
Slip-rate 0.1-1 mm/yr
Slip per event 0.01-1 m
Rupture length 1-50 km
Seismic moment ≥ 10^{24} dyne-cm
Magnitude ≥ M_S 5.5
Recurrence Interval 1000-10,000 yrs

Class 4A
Same as Class 4, except
Slip per event ≥ 0.5 m
Rupture length ≥ 10 km
Seismic moment ≥ 10^{25} dyne-cm
Magnitude ≥ M_S 6.5

Class 5
Slip-rate < 1 mm/yr
Recurrence interval ≥ 10,000 yrs

Class 6
Slip-rate < 0.1 mm/yr
Recurrence interval ≥ 100,000 yrs

*from Cluff *et al.*, 1983

by "degree of activity" according to the scheme suggested by Cluff et al. (1983) (Table 7-2). The classification scheme reflects the natural grouping of more than 50 faults and fault segments with respect to six principal fault activity characteristics: slip-rate, slip per event, rupture length, seismic moment, magnitude, and recurrence interval. Faults are grouped into six classes based on these parameters (Table 7-2); five sub-classes are also recognized. Faults in the study area for which these principal parameters can be estimated are assigned to a class according to this system.

No effort has been made herein to interpret fault activity under the more stringent requirements of the U. S. Nuclear Regulatory Commission (NRC), as these requirements are not considered applicable to any forseeable development in the nearby high desert communities.

Table 7-3 summarizes the activity classification for each major fault or fault system in the study area, along with the principal fault characteristics which form the basis for determining the maximum credible earthquake. Critical geological and geomorphological evidence bearing on the recency of faulting is briefly summarized in Table 7-3 and keyed to the map by the numbers in parentheses in the text and the circled numbers on Plates 1A and 1B.

In the discussion that follows, faults are treated in order of decreasing earthquake hazard.

7.3 THE CLEGHORN LATERAL FAULT SYSTEM

The Cleghorn fault is classified as active. Although there have been no significant historic events attributed to the Cleghorn fault (VanderHoof, 1955), the fault trace shows many signs of Holocene movement, including scarps and offset drainages. These features permit the calculation of a late Pleistocene slip rate of about 3 mm/yr. The maximum credible earthquake

Table 7-3. Activity classifications and key characteristics for faults in study area.

Fault	Location	Length	Strike	¶Style	§Cum. Offset	*Activity	Evidence
Cedar Springs system	WSBM	24 km (15 mi)	arcuate avg 090 070-180	R	†1830 m vertical	inactive	overlain by Qt2 offset by Cleghorn lateral fault
Cleghorn lateral fault	WSBM	24 km (15 mi)	arcuate avg 090 070-135	S	3.5-4.0 km left-lateral	active Class 3	scarplet offset gulleys offset terraces
Grass Valley fault	East Summit Valley	9.7+ km (6+ mi)	arcuate avg 090 080-110	S?	1 km? left-lateral	activity uncertain (tentatively active)	springs beheaded drainage possible offset of Grass Valley?
Summit Valley fault zone	Summit Valley	22 km (14 mi)	arcuate avg 090 080-100	S?	<<1 km? lateral?	activity uncertain (tentatively active)	deformed Qt2 offset Crowder Fm dammed groundwater in alluvium
Tunnel Ridge linea-ment	Pinnacles & Miller Canyon	11.2 km (7 mi)	linear 040	S?	1-2 km? right-lateral	activity uncertain (tentatively active)	Cleghorn merger linear valley truncates all lineaments
Ord Mtns low-angle faults	Deep Ck/ Marianas Rancho	12.9 km (8 mi)	sinuous 010	R	<70 m? vertical	potentially active Class 5	scarp in late Pleistocene alluvial fans
Ord Mtns hi-angle faults	Deep Ck/ Marians Rancho	6.5 km (4 mi)	linear 025	N?	<410 m? vertical	inactive	no geomorphic expr. overlain by Qf2 offset Ord Riv Gr.

* See Section 7.2 for explanation of terms/§ See Table 7-2 for full offset/slip-rate data
† From Weldon et al., 1981. ¶ R = reverse, S = strike-slip, N = normal, ? = uncertainty

Table 7-3(cont.). Activity classifications and key characteristics for faults in study area

Fault	Location	Length	Strike	¶Style	§Cum Offset	*Activity	Evidence
Powerline Canyon fault	Power-line Canyon	2.7 km (1.7 mi)	linear 135	S?	large unknown	inactive	overlying terraces no geomorphic expr. overlain by Qf1,Qf2
Oco-tillo Ridge fold	Marianas Ranch	9.7 km (6 mi)	arcuate avg 090 070-110	R?	<100 m vertical	activity uncertain (tentatively active)	connects active faults fracture, liquefac. in trench
Arrastre Canyon graben	Arrastre Canyon	9.7 km (6 mi)	linear 045	N? S?	<200 m vertical	activity uncertain (tentatively active)	disrupted drainage offset late Pleist terrace gravel joins Tunnel R.lin.
Arrastre Canyon Narrows fault	Arrastre Canyon	12.9 km (8 mi)	segment 050-130	S	<0.5 km horizontal <100 m vertical	potentially active	joins active flts. offset late Pleist terrace gravel groundwater dammed
Sky Hi Ranch fault zone	Fifteen-mile Valley	11.2+ km (7+ mi)	linear 135	S	<0.5 km horizontal	potentially active Class 5	dammed groundwater scarp shutter ridges offset drainage
White Mountain thrust system	15-mile, Lucerne Valley	16+ km (10+ mi)	sinuous avg 090	R	<2 km? horizontal <1000 m vertical	inactive (local reactivation)	overlain by Qf2,Qf3 no geomorphic expr. discontinuous

* See Section 7.2 for explanation of terms/§ See Table 7-2 for full offset/slip-rate data
† From Weldon et al., 1981. ¶ R = reverse, S = strike-slip, N = normal, ? = uncertainty

is estimated to be M_S 6.8 with a recurrence interval of about 7000 years.

7.3.1 Activity

A scarp (1) along the trace of the Cleghorn fault in Cleghorn Valley suggests Holocene surface rupture (Weldon et al., 1981). The scarp is apparent on aerial photographs where it crosses several steep granodiorite ridges on the south flank of Cleghorn Ridge (Figure 7-1). The scarp appears to extend intermittently for roughly a kilometer on the 1939 aerial photographs (U.S. Army Corps of Engineers). The topographic expression of the scarp is consistent with pure left-lateral displacement. The scarp is about a meter high and faces uphill, yet the space behind the scarp is not yet filled with colluvial material. Although the scarp might endure in a relatively undegraded state for several thousands of years in bedrock, it seems unlikely that the depression behind the scarp would escape rapid infilling. Hence, the scarp is considered Holocene. The scarp may reflect sympathetic motion on the Cleghorn fault in response to a major pre-historic earthquake elsewhere in southern California.

Offset streams (2) and disrupted terraces provide abundant evidence in support of Holocene activity on the Cleghorn fault (Meisling and Weldon, 1982b). Stream offsets can be viewed in Cleghorn Valley, where the Cleghorn fault splits into three traces (Figure 7-1). Offset terrace remnants and stream channels suggest consistent rates of motion on the Cleghorn fault throughout the late Pleistocene (Figures 7-2 and 3-6). This supports the designation of the Cleghorn fault as active.

7.3.2 Offset and Slip-rate

Several lines of evidence support significant Quaternary left-lateral motion on the Cleghorn fault (Meisling and Weldon, 1982a,b). The topography

Figure 7-1. Scarps and offset drainages along the Cleghorn fault on south side of Cleghorn Ridge (from Weldon, et al., 1981). The scarp (a) is about one meter high and one kilometer long. Crests of small ridges are offset in a left-lateral sense across the fault, creating a one-meter-high back-facing scarp on the east side of each ridge. The Cleghorn fault splits into three traces, each of which displace two incised stream channels in a left-lateral sense (b). Cumulative displacement across the three traces of the fault is about 200 meters. The stream channels are incised into a terrace surface that is believed to correlate with the ~60,000-year fill event in Cajon Pass (Weldon and Sieh, 1983). Both features strongly suggest Holocene activity on the Cleghorn fault.


b´
a´

Figure 7-2. Proposed correlation of Qt2 terraces across the Cleghorn fault in Cleghorn Canyon, yielding an estimated offset of about 1 kilometer (from Meisling and Weldon, 1982b). A patch of terrace gravel (A) on the north side of the Cleghorn fault just west of Cleghorn Mountain contains angular clasts of metasedimentary quartzite derived from a small quartzite body on Cleghorn ridge. Angular quartzite clasts are found in another patch of terrace gravel south of the Cleghorn fault, with no source in the drainage basin upstream. Quartzite bodies are extremely rare in the western San Bernardino Mountains, suggesting that the two terraces, which are at the same elevation, were once part of the same drainage system. The terraces are estimated to be about 500,000 years old, and drainage reconstructions indicate that they were deposited prior to the abandonment of the surface of the Victorville Fan. The estimate for their offset has been refined to 1.1 kilometers since this figure was published. These offset terrace remnants are considered strong evidence for significant left-lateral motion on the Cleghorn fault in late Pleistocene time.

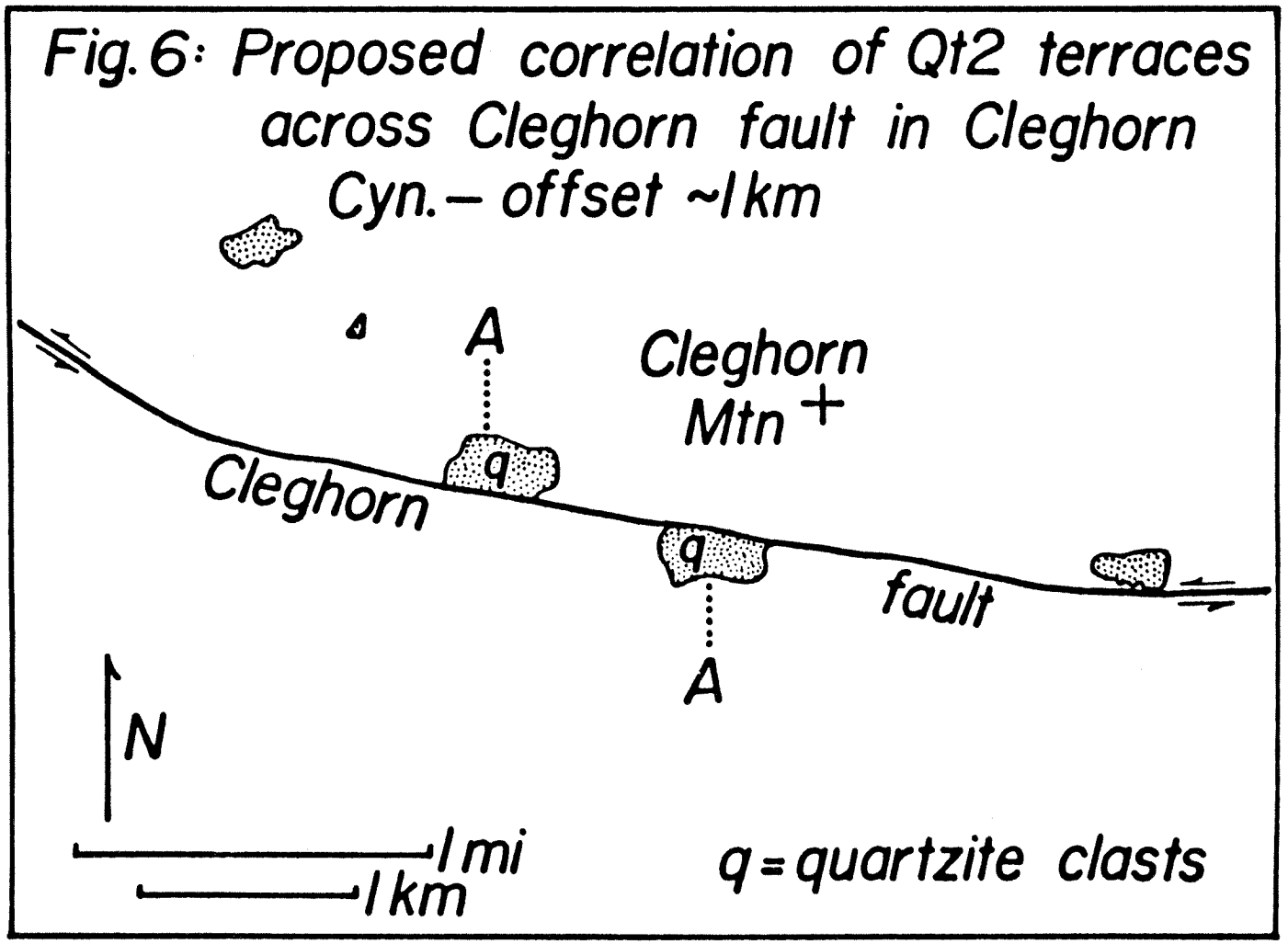
Fig. 6: Proposed correlation of Qt2 terraces across Cleghorn fault in Cleghorn Cyn. – offset ~1 km
A
Cleghorn Mtn
q
Cleghorn
q
fault
A
N
1 mi
1 km
q = quartzite clasts

of the scarps strongly suggests offset in a left-lateral sense. Older alluvial fan deposits in Miller Canyon (Figure 3-6) and terrace remnants above Cleghorn Canyon (Figure 7-2) appear to be offset left-laterally about 1.1 kilometer. These Qt2 terraces are estimated to be 400,000 years in age (Section 3.3.2). Their intense soil development and height above dated terraces in Cajon Pass preclude an age of less than about 60,000 years for Qt2. They are correlated with terraces that are incised into the Older Alluvium of the Victorville Fan, which rules out an age of greater than 730,000 years.

Streams cut into the Qt1 terrace level in Cleghorn Valley appear to be offset up to 200 meters left-laterally (Meisling and Weldon, 1982b). These terraces represent a major fill event in Cleghorn Valley. Soil development is much greater than on the Qta terraces of the last major fill event in Cajon Pass, and therefore cannot be younger than 12,400 y B.P. (Weldon and Sieh, 1983). An upper age limit of 100,000 years is indicated by soils and correlation with the Cajon Pass terrace sequence of Weldon and Sieh. An age of 60,000 years is preferred since it corresponds to a major fill event in the Cajon Pass terrace sequence (Weldon and Sieh, 1983).

It could be concluded that the offset of these incised streams channels is due to deflection of their course by topographic irregularities at the fault trace rather than by actual fault offset. The configuration of the streams argues against this hypothesis. There are two parallel stream courses close to each other with each course displaced left-laterally by approximately the same amount across each of three traces of the Cleghorn fault (Figure 7-1). If deflection were responsible for the observed configuration, it would be extremely fortuitous for the both streams to be displaced by the same amount. Furthermore, if the two streams were prone to

diversion they would have been likely to flow together. The two streams maintain separate paths across the terrace surface, although they are presently separated by only a few meters at several points. Although it cannot be proven, the configuration of the two streams suggests that they have been tectonically offset, rather than deflected, along the trace of the Cleghorn fault zone.

The streams channels are probably Holocene in age if the terrace is correlative with the 12,400 y B.P. fill event in Cajon Pass. If the terraces are 12,400 years old, the offset of 200 meters implies a slip rate of 16 mm/yr (Table 7-4). Although possible, this rate is considered geologically unreasonable, since it closely approaches the slip rate for the San Andreas fault, a Class 1 fault (Cluff et al., 1983) with much stronger and more continuous evidence for Holocene movement than the Cleghorn fault. Therefore it is believed that the Qtl terrace is correlative with the 60,000 y fill event and that the streams may be pre-Holocene.

Offset of older terraces in Cleghorn and Miller Canyons (1.1 km since 0.4 my) suggest an average left-lateral slip-rate of about 2.75 mm/yr on the Cleghorn fault (Figures 7-2 and 3-6). Offset of 60,000-year-old terraces up to 200 meters yields a similar average slip-rate of 3.3 mm/yr. At 3.0 mm/yr, the 4.0 kilometers of offset on the Cleghorn fault since the deposition of the Crowder Formation could have been accumulated in 1.3 my. This is roughly consistent with the onset of lateral faulting following deposition of the Harold Formation and subsequent early Pleistocene tilting. The slip-rate values presented here are greater than the 2.0 mm/yr reported by Meisling and Weldon (1982b) and reflect the revised age estimates for the Cajon Pass terrace sequence of Weldon and Sieh (1983).

Table 7-4. Slip-rate estimates for principal active and potentially active faults in study area.

Fault/Location	Style/ Component	Slip (m) mn	mx	pf	Age of offset feature (x1000y) mn	mx	pf	Slip-rate (mm/yr) mn	mx	pf	Feature Offset/ Dating Method†	*Uncertainty Us	Ua
Cleghorn fault § (Cleghorn Valley, Miller Canyon)	lateral left-slip	—	—	200	12.4	100	60	2.0	16	3.3	streams cut in terrace deposits (1) (2) (3) (4)	B	C
Cleghorn fault § (Cleghorn Valley)	lateral left-slip	—	—	1100	60	730	400	1.5	18	2.75	dissected terrace remnants (1) (4) (5)	C	D
Ord Mountains low-angle faults (Apple Valley Highlands)	reverse vertical	0	480	70	400	730	500	0	1.2	0.14	Summit Valley facies, Ord River Gravel (4) (5) (6)	D	D
Ord Mountains low-angle faults (Apple Valley Highlands)	reverse vertical	30	70	70	100	730	400	0.04	0.7	0.10	Surface of Qf2 fanglomerate (4) (5) (6)	B	D
Sky Hi Ranch fault (Fifteenmile Valley)	lateral right-slip	250	750	500	50	730	400?	0.34	15	1.25	Qf2 fanglomerate (1) (5) (6)	C	D

† Dating Methods: (1) correlation; (2) vertebrate fossils; (3) radiometric; (4) paleomagnetism; (5) soils; (6) geomorphology

* from Clark et al., (1983): Us - qualitative uncertainty associated with slip estimate
Ua - qualitative uncertainty both in analyitical method used to reckon ages and in the assumptions made linking them to the age of the offset feature.
A - small uncertainty; B - significant uncertainty; C - distinct uncertainty
D - major uncertainty

§ modified from Meisling and Weldon (1982b)

7.3.3 Degree of Activity, Magnitude, and Recurrence Interval

The Cleghorn fault is classified as a Class 3 fault according to the criteria of Cluff et al. (1983) (Table 7-2), based on its Pleistocene average slip rate of 3 mm/yr and total length of 24 kilometers. The total length of the Cleghorn fault zone is much less than the 50-to 100-km rupture length of Class 2 or 2B faulting, and there is no historic evidence to suggest a recurrence interval of less than 100 years for Class 2A faulting. Earthquake magnitudes for other Class 3 faults are M_S 6.5, with recurrence intervals ranging in the range of 500 to 5000 years, and slip per event between 10 cm and 3 meters (Table 7-2).

Assuming, for the sake of argument, that the one-meter-high scarp on Cleghorn Ridge was product of a single earthquake of three meters lateral offset, it might represent a characteristic earthquake for the Cleghorn fault. Although this would be a large surface displacement for a scarp of less that a kilometer in length, evidence for more extensive surface rupture may have been removed by geomorphic processes. At a slip-rate of 3.0 mm/yr, such a three-meter event would be expected to occur every 1000 years (Table 7-5). At the minimum slip-rate for the Cleghorn fault of 1.5 mm/yr, the recurrence interval would be 2000 years. Even if ten meters of lateral slip is postulated for each event, the minimum slip-rate of 1.5 mm/yr (Table 7-5) yields a recurrence interval of 6667 years. A lesser offset magnitude would correspond to a shorter recurrence interval. If the scarp on the Cleghorn fault is the product of more than one event, the recurrence interval would also be shorter. Clearly the slip-rate estimates demand that for any geologically reasonable offset magnitude, the Cleghorn fault must have experienced an event during Holocene time.

The maximum earthquake that might be expected to occur on the Cleghorn

Table 7-5. Recurrence intervals for various slip-rates and displacement magnitudes.

Slip-rate (mm/yr)	Recurrence interval (years)				
	0.1 m event	0.5 m event	1.0 m event	3.0 m event	10 m event
0.5	200	1000	2000	6000	20,000
1.0	100	500	1000	3000	10,000
2.0	50	250	500	1500	5000
3.0	33	167	333	999	3333
10.0	10	50	100	300	1000
20.0	5	25	50	150	500
40.0	2.5	12.5	25	75	250

Figure 7-3. Regression relationships between earthquake magnitude (M_S) and length of surface rupture for surface rupture length (L, in km) for world-wide (WW) and North America (NA) data (from Slemmons, 1983)

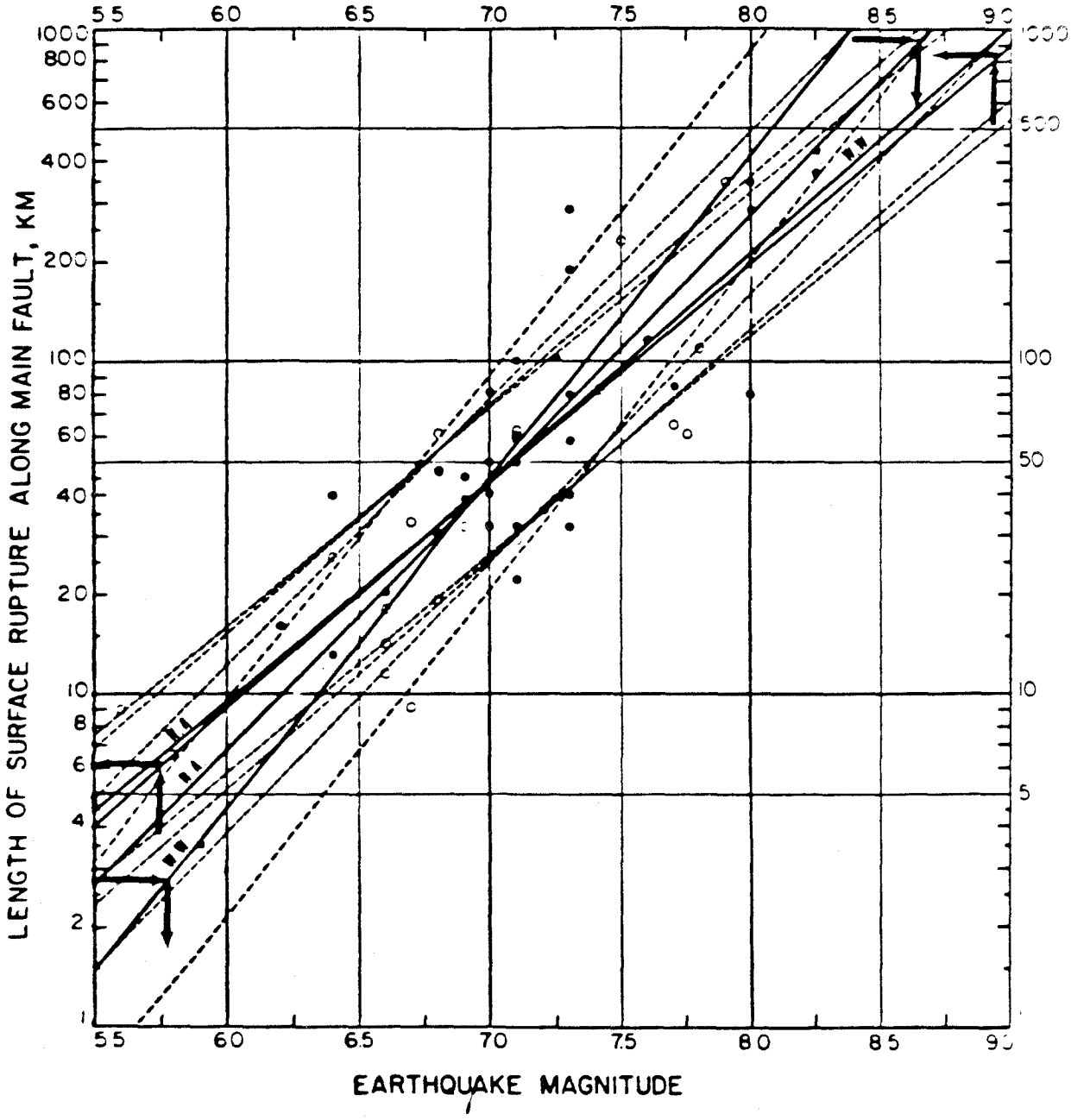
LENGTH OF SURFACE RUPTURE ALONG MAIN FAULT, KM
EARTHQUAKE MAGNITUDE
5.5
6.0
6.5
7.0
7.5
8.0
8.5
9.0
1000
800
600
400
200
100
80
60
40
20
10
8
6
4
2
1
500
50
5

fault can be estimated on the basis of empirical relationships between earthquake magnitude and either surface rupture length or maximum surface displacement (Slemmons, 1983). If surface rupture is assumed to occur along the entire 24-kilometer length of the Cleghorn fault zone, regression relationships predict an earthquake of magnitude (M_S) 6.7 (Figure 7-3). If only 10 kilometers of surface rupture were to occur, between Cajon Pass and Silverwood Lake, for instance, an M_S of 6.2 would be expected. Lesser rupture lengths would result in smaller earthquakes. Assuming that the one-meter-high scarp is the product of one earthquake, empirical data for maximum surface displacement (Figure 7-4) would suggest an event of magnitude M_S 6.8. Thus, the maximum credible earthquake for the Cleghorn fault lies in the range of M_S 6.2 to M_S 6.8, which is consistent with $M_S \geq 6.5$ observed for Class 3 faults (Table 7-2).

When percent of total fault length ruptured during a maximum earthquake is regressed on total fault length (Figure 7-5), the resulting curve predicts that only 10 to 20 percent of a fault less than 100 kilometers long should rupture during its maximum earthquake. If this is the case, 2.5 to 5 kilometers of rupture might be expected on the Cleghorn fault, corresponding to maximum magnitude of M_S 5.5 to M_S 5.8.

It is possible that motion occurs on the Cleghorn fault in response to major events on the San Andreas fault. Perhaps the scarp on Cleghorn Ridge was formed during the 1857 Fort Tejon earthquake. Such a causative relationship between events on the San Andreas and events on the Cleghorn fault would seem logical in the context of the observed "end effect" geometry of the the latter fault trace (Section 6.4.2). If this hypothesis is correct, frequency of events on the Cleghorn fault might be much greater than otherwise predicted, and maximum earthquake magnitude correspondingly smaller.

Figure 7-4. Regression relationships between earthquake magnitude (M_S) and maximum surface displacement (D, in m) for worldwide (WW) and North America (NA) data (from Slemmons, 1983).

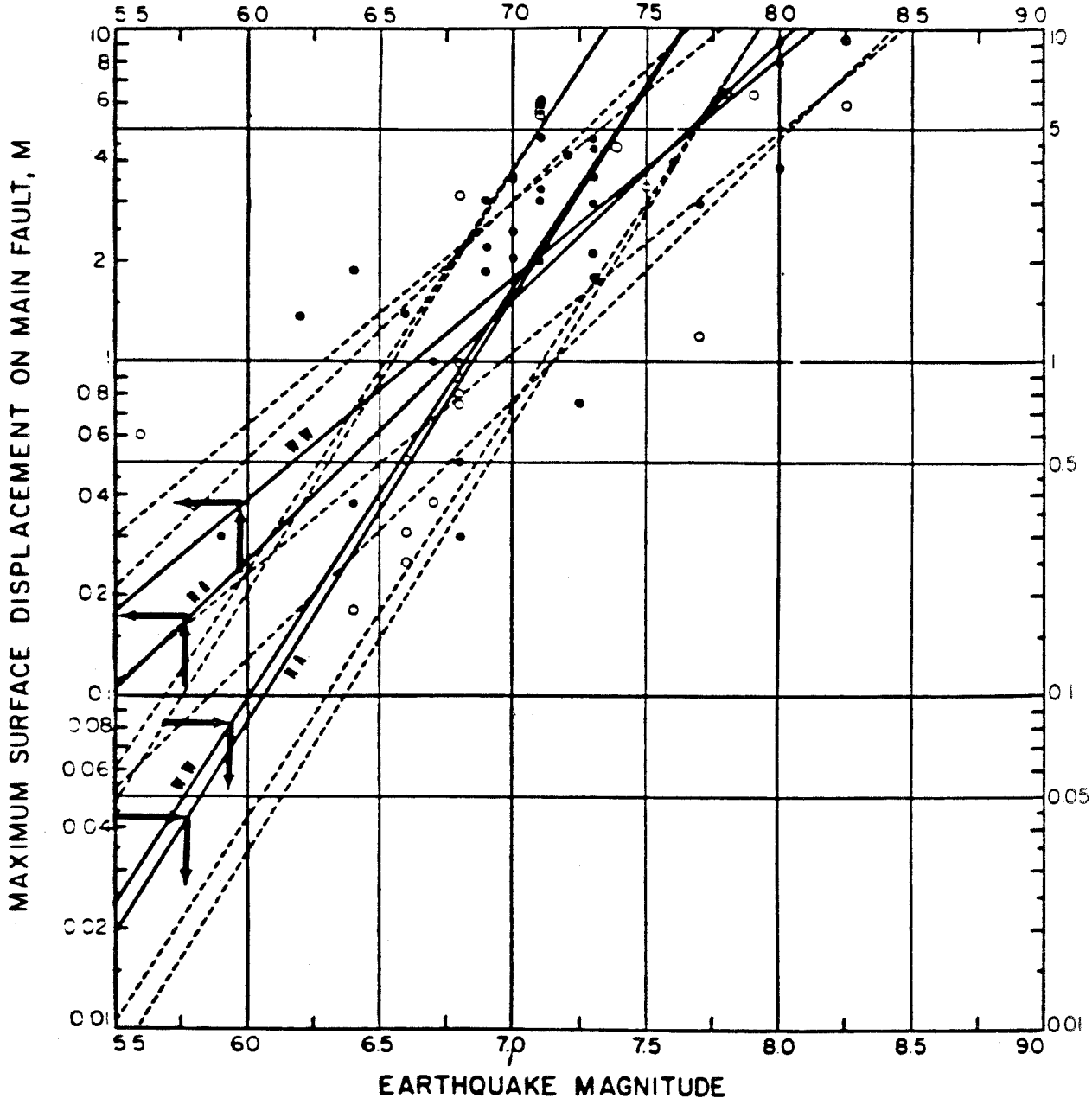
MAXIMUM SURFACE DISPLACEMENT ON MAIN FAULT, M
EARTHQUAKE MAGNITUDE
5.5
6.0
6.5
7.0
7.5
8.0
8.5
9.0
10
8
6
4
2
1
0.8
0.6
0.4
0.2
0.1
0.08
0.06
0.04
0.02
0.01
5
1
0.5
0.1
0.05
0.01

Figure 7-5. Percent of total fault length (Pr) ruptured during a maximum earthquake regressed on total fault length (L, in km) for strike-slip faults (from Slemmons, 1983).

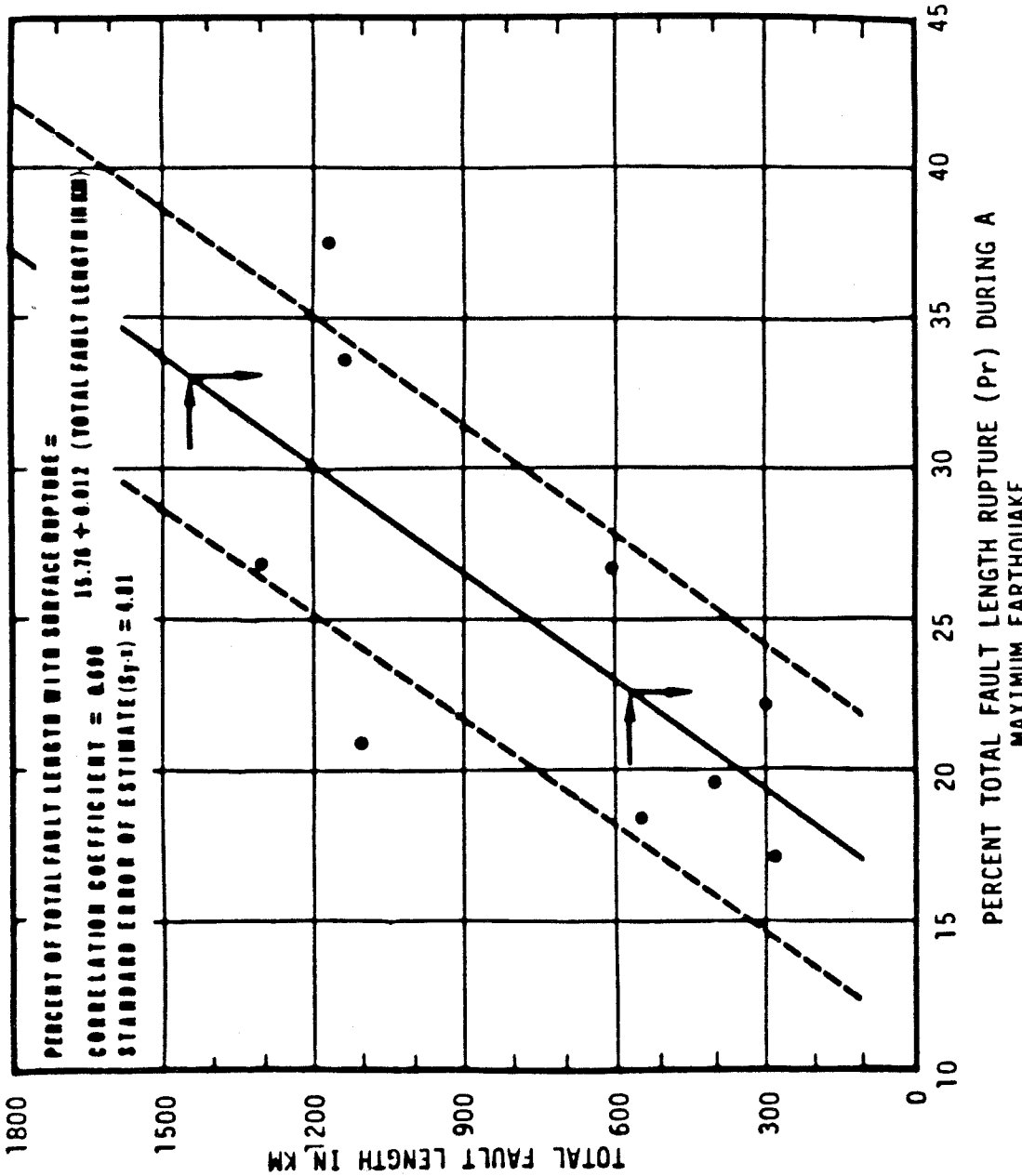
PERCENT OF TOTAL FAULT LENGTH WITH SURFACE RUPTURE =
CORRELATION COEFFICIENT = 0.000
STANDARD ERROR OF ESTIMATE (Sy·x) = 4.81
TOTAL FAULT LENGTH IN KM
1800
1500
1200
900
600
300
0
10
15
20
25
30
35
40
45
PERCENT TOTAL FAULT LENGTH RUPTURE (Pr) DURING A MAXIMUM EARTHQUAKE

If rupture of the Cleghorn fault were to occur in association with an earthquake on the San Andreas fault, however, the latter event would be so damaging as to render the event on the Cleghorn fault insignificant by comparison.

The most conservative estimate of the maximum credible earthquake for the Cleghorn fault is M_S 6.8. This number should be used until evidence to constrain earthquake magnitude further becomes available. Certainly the evidence indicates that the Cleghorn fault zone is both sufficiently "active" and "well located," according to the definition of the Alquist-Priolo Act (California Division of Mines and Geology, 1980) to be considered in zoning.

7.3.4 Related faults

Northeast-trending splays, such as the Silverwood Lake fault zone, are directly connected to the Cleghorn fault zone and must be considered active by association. The splays merge with the Cleghorn fault and truncate late Pleistocene (Qt2) pediment surfaces (3) and Holocene(?) terrace gravels beneath Silverwood Lake (California Department of Water Resources, 1968). Aerial photographs and detailed topographic maps predating the construction of the Cedar Springs Dam suggest that the surface of low terraces excavated during dam construction may have been disrupted by faulting (California Department of Water Resources, 1968). Faults beneath the dam were recognized and were considered "active" in the design and placement of the dam itself (Sherard et al., 1974).

The Grass Valley and Summit Valley fault zones are classified in the category of uncertain activity, but should be considered tentatively active (Table 7-1). This assignment is based on their geometric and evolutionary similarity to the Cleghorn fault, and evidence already presented (Section 6.2.4) for middle to late Pleistocene lateral motion. Both faults truncate

all other intersecting faults. Unfortunately it is not possible to determine slip rates or rupture lengths for either of these faults based on the present study. Hence they cannot be classified as to degree of activity or maximum credible earthquake. The Summit Valley fault is not "well defined", in the terminology of the Alquist-Priolo criteria, and therefore may not be amenable to site-specific investigation.

7.4 THE SKY HI RANCH FAULT ZONE

The Sky Hi Ranch fault zone is classified as potentially active (Table 7-1). There is abundant evidence of Quaternary movement, including scarps and offset drainages. It is a Class 5 fault, has a preferred slip-rate of 1.25 mm/yr, and is considered capable of producing a M_S 6.6 earthquake.

7.4.1 Activity

The Sky Hi Ranch fault zone is classified as potentially active. A half-meter-high scarp cuts the surface of the Qf2 fanglomerate (4) (Figure 7-6). The scarp is expressed for only a few tens of meters, and faces upslope. The Qf3 fans are deformed and offset along the fault trace to form shutter ridges (5). Although the ages of these alluvial fans are not known, the degree of preservation of their geomorphic form indicates late Quaternary age. The degree of preservation of such a small scarp in alluvial materials certainly indicates late Pleistocene displacement.

The fault trace displays an abundance of other geomorphic features indicative of Quaternary faulting, such as vegetation anomalies and springs in alluvial materials, ponded alluvium, offset drainages, as well as scarps. The youngest alluvial fans crossing the fault trace show no signs of disruption, however, and no compelling evidence could be found to support Holocene displacements. Hence, the Sky Hi Ranch fault is classified as

Figure 7-6. Geomorphic features indicative of strike-slip faulting along the Sky Hi Ranch fault in Fifteenmile Valley. This aerial photograph shows a scarp (a) cutting the Qf1 fan surface. Other features suggestive of late Pleistocene activity include shutter ridges (b), captured (c) and diverted (d) drainages, and ponded alluvium (e). The airphoto also shows arcuate scarps (f) believed to represent low-angle surfaces of the early Pleistocene White Mountain thrust fault system that have been reactivated as secondary faults to accommodate compression across the Sky Hi Ranch fault zone.

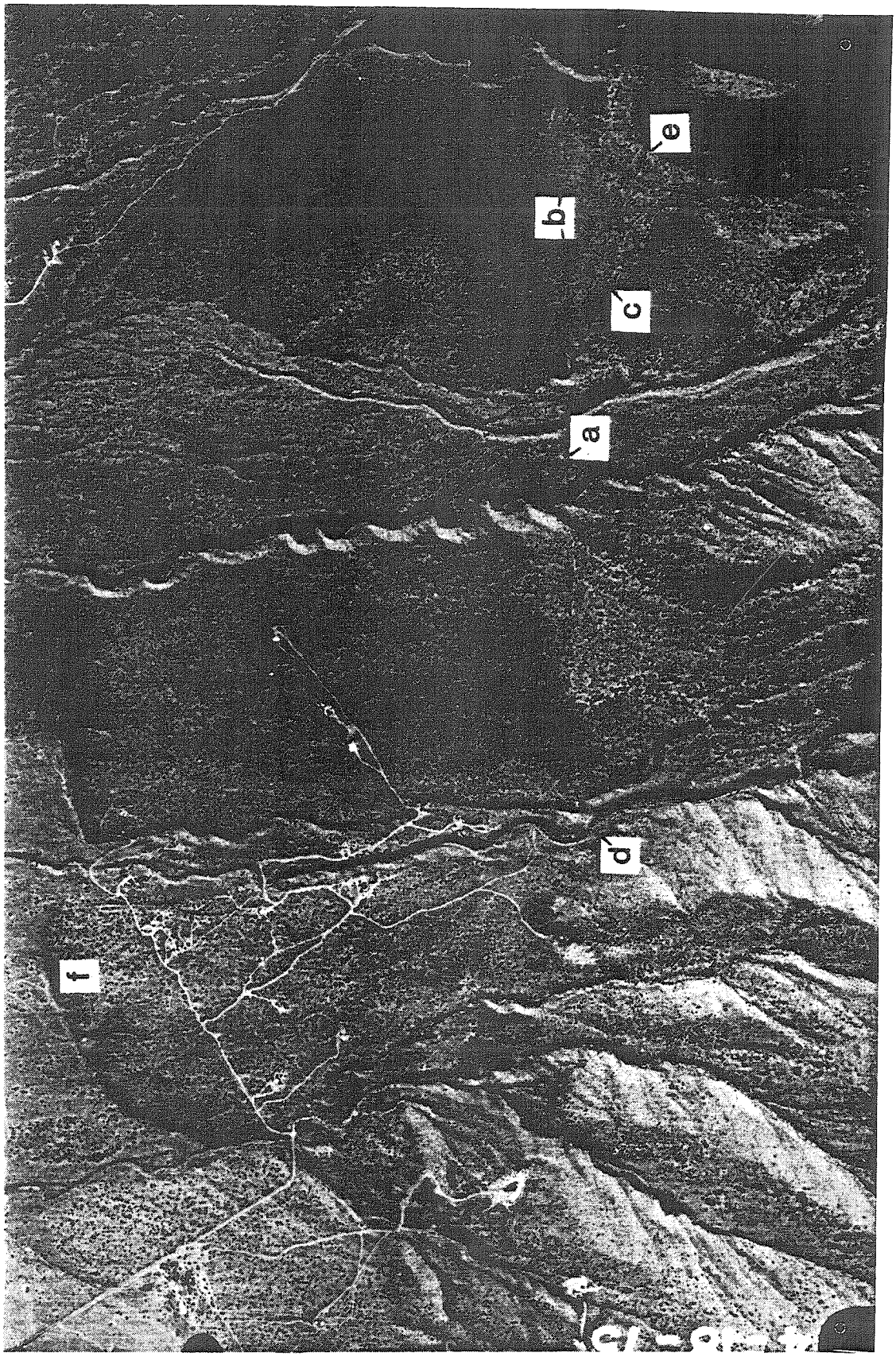
a
b
c
d
e
f

potentially active.

7.4.2 Offset and Slip Rate

Late Pleistocene alluvial fans shed off the north flank of the San Bernardino Mountains have been displaced laterally from their source drainages by movement on the Sky Hi Ranch fault. Distinctive clasts in the alluvial fans can be uniquely matched with their small range-front drainage basin sources. The Qf2 fan deposit just west of Sky Hi Ranch is dominantly made up of grus and residual boulders derived from the Rattlesnake Mountain pluton. The range-front drainage basin immediately upstream of it is underlain by subequal exposures of Rattlesnake Mountain Pluton and Fawnskin Monzonite. The next range-front drainage basin to the west, Grapevine Canyon, is exclusive underlain by the Rattlesnake Mountain pluton. Thus the grus-bearing fans west of the Sky Hi Ranch are interpreted as having been derived from Grapevine Canyon, rather than the canyon they are presently opposite. A right-lateral horizontal displacement of about 0.5 kilometers would be required to create this juxtaposition. The first appearance of metasedimentary lithologies in the Qf2 fans is similarly displaced about 0.5 kilometer right-laterally from its drainage basin source area. Lateral displacement of as much as 0.75 kilometers or as little as 0.25 kilometers cannot be ruled out, however, since there is much latitude with regard to the precise location of the fan deposits with respect to the drainage basins at time of deposition.

The age of the displaced Qf2 alluvial fans is not known, but deep weathering and stratigraphic constraints suggest an age of 0.05 to 0.7 my. Qf2 fans to the west in the Milpas Ridge area overlie the Arrastre Canyon Fan deposits, which are paleomagnetically constrained to be younger than 730,000 y B.P. The fans could be much younger, but depth and intensity of

weathering argues strongly for an age in excess of 50,000 y B.P. The Qf2 fans are tentatively considered to be 400,000 years in age based on general stratigraphic and geomorphic similarity with the Qf2 fans in the Ord Mountains, and the 500,000 year age estimate for the Arrastre Canyon fan deposits.

Based on the above limits for the ages of the alluvial fans along the Sky·Hi Ranch fault, and the estimated range of allowable lateral offsets, the average late Pleistocene slip-rate for the Sky Hi Ranch fault lies between limits of 0.34 and 15 mm/yr, with the preferred value being 1.25 mm/yr (Table 7-4).

7.4.3 Degree of Activity, Magnitude, and Recurrence Interval

The Sky Hi Ranch fault is classified as a Class 5 fault according to the criteria of Cluff *et al.* (1983) (Table 7-2), based on its estimated average Pleistocene slip rate of 1.25 mm/yr, total length of 11 km, and lack of evidence of Holocene displacement. If the fault extends northwestward across Fifteenmile Valley under the alluvium, its rupture length might be much greater, which might suggest a Class 4 designation. If Holocene displacement could be shown on the Sky Hi Ranch fault, a Class 3 designation might even be indicated. Class 6 can be ruled out on the basis of limits on slip rate alone. Lacking definitive evidence of Holocene movement, the Sky Hi Ranch fault is considered Class 5.

Although there is no compelling evidence for Holocene movement on the Sky Hi Ranch fault, the preservation of a small scarp feature could be interpreted as indicative of Holocene movement. Assume that the scarp developed in Qf2 on the Sky Hi Ranch fault was originally one meter high. If a ten meter lateral event is postulated, the preferred slip-rate would suggest a recurrence interval of 8000 years. At the minimum slip-rate of

0.34 mm/yr, a ten-meter event would occur every 29,411 years. A more realistic two-meter event would occur every 5882 years at the minimum slip-rate. Thus, if the Sky Hi Ranch fault has not moved in the Holocene, it must experience > 2 meters of offset per event. Although definitive of Holocene activity is lacking, the Sky Hi Ranch fault is herein deemed potentially active in conformance with the Alquist-Priolo criteria.

The maximum credible earthquake magnitude for the Sky Hi Ranch fault can be estimated on the basis of maximum surface displacement and rupture length using Figures 7-4 and 7-5. For 11 kilometers of surface rupture, M_S 6.3 is predicted. For a half meter of maximum surface displacement, M_S 6.6 is indicated. Too little is known about the possible continuation of the fault to the northwest and southeast to speculate as to the likelihood of greater surface rupture length; lesser surface rupture length would produce a smaller magnitude event. If the scarp on Qf2 were produced in more than one event, a lesser magnitude would also follow.

Thus M_S 6.6 is considered a conservative maximum credible earthquake for the Sky Hi Ranch fault. This would seem to be at odds with its designation as a Class 5 fault, probably reflecting the poor constraints on the fault parameters. The fault is "well located" in the terminology of the Alquist-Priolo Act, and should be probably be considered "sufficiently active" to warrant consideration for zoning based on the possibility of unrecognized evidence for Holocene movement.

7.4.4 Related Faults

The northwest-trending fault set of the Mojave block appears to have become reactivated following cessation of motion on the range-front thrusts. Some of the fault planes of the range-front thrust system have become involved as secondary faults (6), taking up compression across the Sky Hi

Ranch fault, and they must therefore be considered potentially active as well. The Sky Hi Ranch fault is geomorphically the freshest member of the north frontal fault system.

7.5 THE ORD MOUNTAINS FAULT ZONE

7.5.1 Activity

The low-angle faults of the Ord Mountains fault zone are considered potentially active (Table 7-1), by the criteria of the Alquist-Priolo Act, because they cut and deform middle to late Pleistocene Qf2 fanglomerates, but do not cut Holocene alluvial fans. Displacement of the Pleistocene fanglomerates has produced a continuous scarp 6 kilometers long and up to 70 meters in height (7) (see Figure 3-7). The crest of this scarp is rounded and is incised by steep-walled gullies. The Qf2 fanglomerate is very well indurated and and may approach bedrock in its resistance to erosion. These observations suggest that the scarp may not be as young as it appears.

There is no evidence to indicate offset of any of the Qf1 fans that disgorge from gullies cut in the scarp face (8). The walls of these gullies are nearly vertical, and the material eroded from the older fans to create them is believed to be deposited in the small Holocene(?) fans along the scarp face. The scarp face is much less steep than the gullies, and is therefore probably older. The intermediate Qf1 fans deposits also do not appear to be cut. The Qf1 fans overlie the Pelona-Schist-bearing Qt2 terrace fill along the Mojave River, and are correlated with the Qt1 terrace deposits. This may suggest that the low-angle faults have not moved since latest Pleistocene.

In the absence of evidence for Holocene movement, the low-angle faults of the Ord Mountains fault zone are classified as potentially active.

The high-angle faults of the Ord Mountains frontal zone are considered

inactive, based on their lack of fresh geomorphic expression and the fact that they appear to be overlain by undisturbed Qf2 fanglomerate (9). They are largely confined to bedrock, where there is no evidence of a scarplet. They may cut the base of the Qf2 fan, suggesting that they have been active during middle to late Pleistocene time. They disappear at intersections with low-angle faults. Although they may well be responsible for uplift of the Ord Mountains, the high-angle faults are thought to have ceased movement in late Pleistocene time, according to the tectonic evolution of the area (Section 6.3.3).

7.5.2 Offset and Slip Rate

The Summit Valley facies of the Ord River Gravel provides a rough measure of the vertical offset on the Apple Valley Highlands and Deep Creek fault zones since middle Pleistocene time (Table 7-2). The Summit Valley facies was deposited by drainage flowing north from the western San Bernardino Mountains, confined between the toe of the Victorville Fan and the Ord Mountains (Section 2.4.4). The Ord Mountains were a positive topographic feature at the time of deposition of the Ord River Gravel, because the gravel contains angular blocks of coarse, white quartzite from the Deep Creek metasedimentary roof pendant. Thus the upper depositional surface of the Summit Valley facies of the Ord River Gravel must have been topographically lower than the crest of the Ord Mountains. This inference is supported by the lack of any vestige of rounded river gravel on the late Miocene erosion surface on top of the Ord Mountains, and by the lack of any such sediment in the correlative Juniper Flats and Bowen Ranch Road deposits on the other side of the Ord Mountains.

The crest of the Ord Mountains is about 480 meters above the upper surface of the Ord River Gravel in the Apple Valley Highlands, providing a

maximum vertical offset value. The Ord River Gravel is cut by the low-angle faulting in the Marianas area, and underlies a scarp which has a displacement of 70 meters nearby. Thus, vertical displacement would seem to be a minimum of about 70 meters. The Apple Valley Highlands fault zone is interpreted as reactivated, and the vertical uplift in the Ord Mountains is thought to have occurred on high-angle faults. For this reason, the lesser offset of 70 meters is believed to be the entire cumulative displacement since reactivation of the low-angle surfaces.

The Summit Valley facies of the Ord River Gravel is of normal polarity and therefore less than 730,000 years in age. The Ord River Gravel is capped by a deep soil profile including a $CaCO_3$ horizon which suggests an age of at least 100,000 years. The Summit Valley facies predates the Pelona-Schist-bearing fill terraces along the Mojave River, and is thought to be about 500,000 years in age. The preferred estimates for offset and age of the Ord River Gravel yield an average vertical slip-rate of about 0.14 mm/yr. Under no circumstances can the average slip-rate have been greater than 1.2 mm/yr.

Another line of reasoning in support of a low average slip-rate for the late Pleistocene can be developed using the offset of the Qf2 fan surfaces along the scarp in the Apple Valley Highlands. The fan surface is locally preserved at the foot of the scarp, allowing a maximum and minimum vertical displacement of 70 and 30 meters, respectively, to be measured at the scarp face. Degradation of the scarp with time will tend to reduce its height, and hence the maximum figure of 70 meters is preferred. The Qf2 fans are thought to be roughly correlative with the Qt2 terrace fill event of about 400,000 y B.P. Laminated carbonates (K-horizon) are developed in the soil profile on the Qf2 fans, indicating an age of at least

100,000 years (Birkland, 1974). This soil is correlated with the soil developed on the Qf2 fans that overlie the Deep Creek facies of the Ord River Gravel; it is paleomagnetically normal, and therefore less the 730,000 years old. These constraints yield a maximum vertical slip-rate of 0.7 mm/yr, and a preferred vertical slip-rate of 0.10 mm/yr for the low-angle fault zone of the Ord Mountains. This is in general agreement with the result for the displacement of the Ord River Gravel. Although there is a high degree of uncertainty in the slip and age data used for these calculations, the limiting slip-rates are believed to represent realistic bounding values.

7.5.3 Degree of Activity, Magnitude and Recurrence Interval

The Ord Mountains fault zone is classified as a Class 5 fault, in the scheme of Cluff et al. (1983), on the basis of slip rate and lack of evidence of Holocene movement. The low preferred slip rate estimates argue against both Class 4 and Class 6 designations.

The Ord Mountains low-angle fault zone has a preferred slip-rate of about 0.1 mm/yr, which would correspond to a one-meter event every 10,000 years. The minimum slip-rate of 0.04 would allow one-meter events to be as rare as one per 25,000 years.

The Ord Mountains fault zone dies out into the Ocotillo Ridge fold at its north end, and range-front warping at its south end. If its 13-km-length broke at one time, it could produce a M_S 6.5 earthquake, based on the surface-rupture-length/magnitude relationship (Figure 7-4). The irregular and discontinuous trace of the fault makes this seem unlikely. If the fault ruptured over half its length, from Ocotillo Ridge to Powerline Canyon, for instance, a M_S 6.2 event might be expected. This is considered a much more likely scenario, and M_S 6.2 is favored as a conservative estimate

of the magnitude of the maximum credible earthquake magnitude for the Ord Mountains fault zone. Unfortunately, there are no data to constrain the maximum displacement per event.

7.6 THE TUNNEL RIDGE LINEAMENT

The Tunnel Ridge lineament lies outside the study area and was not mapped or examined in detail for evidence of activity. Although there is some question as to the continuity of the lineament (Section 5.4), the Cleghorn fault zone appears to merge with it, and there is evidence for late Pleistocene offset on the Cleghorn fault in Miller Canyon (Figure 3-6). This implies that motion may have been transferred onto the Tunnel Ridge lineament as recently as latest Pleistocene, possibly even during the Holocene. The mechanical relationship between the Cleghorn fault and the Tunnel Ridge lineament is not fully understood. It would seem prudent to regard the Tunnel Ridge lineament as tentatively active until it can be examined in detail.

7.7 THE OCOTILLO RIDGE FOLD

7.7.1 Activity

The Ocotillo Ridge fold is considered a potentially active structure by association with the low-angle faults of the Ord Mountains zone. Based on the results of the Ocotillo Ridge trench (Section 7.7.2) there is no through-going fault along the north side of Ocotillo Ridge. The feature is interpreted as a fold over most of its length, and it merges with the Sky Hi Ranch fault at its east end and the Apple Valley Highlands fault zone at its west end. The fold is presumed to be the result of faulting in the basement at some depth. The depth to basement is not known but cannot be great given the tightness of the fold. Since the fold joins two potentially

active fault zones, it must be considered potentially active itself, at least insofar as a fold can be so classified.

7.7.2 The Ocotillo Ridge Trench

A trench was excavated on the north flank of Ocotillo Ridge (10) (Figure 7-7). This site was chosen in order to determine whether or not the Ord Mountains fault zone is connected to the north frontal fault system, and to study the nature of deformation that produced the ridge itself. The

Ocotillo Ridge trench was excavated on County of San Bernardino right-of-way at the corner of Ocotillo Way and Pioneer Road (sec 15, R3W T4N) in the Marianas Rancho area of Apple Valley (Figure 7-7). The site lies on the steepest part of the northwest slope of Ocotillo Ridge, just west of a scarp-like lineament on the 1939 airphotos (Figure 7-8). The trench was 65 feet (19.8 m) long, and a maximum of 13 feet (3.3 m) deep. The trench site was chosen on the projection of a lineament on the 1939 airphotos that was thought to be a fault scarp.

The Ocotillo Ridge trench (Figure 7-9) exposed a 55° north-dipping section of coarse fluvial sand and gravel (Figure 7-9, #1) underlain by several massive debris-flow units (Figure 7-9,#2). These sediments, part of the "Ord River Gravel" deposits, are correlated with the "Old Alluvium" of Dibblee (1974) underlying the Victorville Fan to the west and estimated to be about 500,000 years in age (Section 4.4.3). A soil (Figure 7-9, #3) developed on the debris-flow unit and the presence of rotten diorite clasts support this age; no C^{14}-datable material was found in this unit.

At the south end of the trench, alluvial material in a younger channel-fill (Figure 7-9, #4) contained traces of charcoal in insufficient quantity to allow dating by C^{14} methods. Bedding in this younger deposit, was nearly horizontal. It was deposited by one of many small alluvial fans

Figure 7-7. Sketch diagram of Ocotillo Ridge trench site, located at the corner of Pioneer Road and Ocotillo Way in the Marianas Rancho area of the unincorporated city of Apple Valley. The trench is on the north side of the topographic feature herein named "Ocotillo Ridge". See Plate 1B for location of trench site.

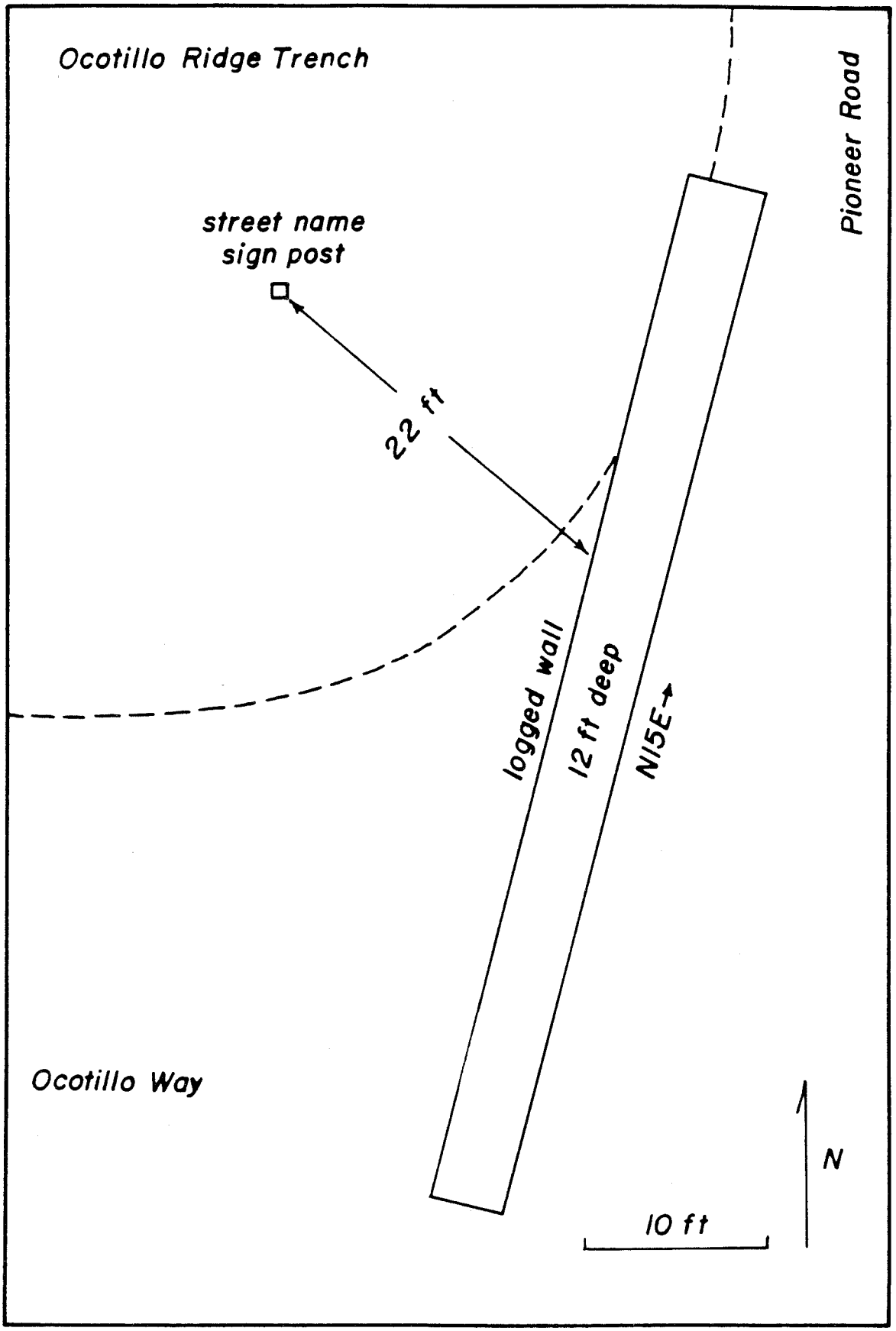
Ocotillo Ridge Trench
Pioneer Road
street name
sign post
22 ft
logged wall
12 ft deep
N15E
Ocotillo Way
N
10 ft

Figure 7-8. Aerial photograph of "Ocotillo Ridge" taken in 1939 (Army Corps of Engineers). This airphoto shows the Marianas Rancho area prior to any development. The scarp-like feature (a) that can be seen on the north side of the anticlinal ridge is now largely obscured by cultural features. The "scarp" turned out to be a resistant layer in the steeply north-dipping strata on the north flank of the anticline (b), rather than a fault scarp as first thought. The Ocotillo Ridge is believed to be a fold developing over a tentatively active(?) reverse fault in the basement beneath the alluvium. (c) indicates the north end of the Apple Valley Highlands fault zone, part of the Ord Mountains fault zone.

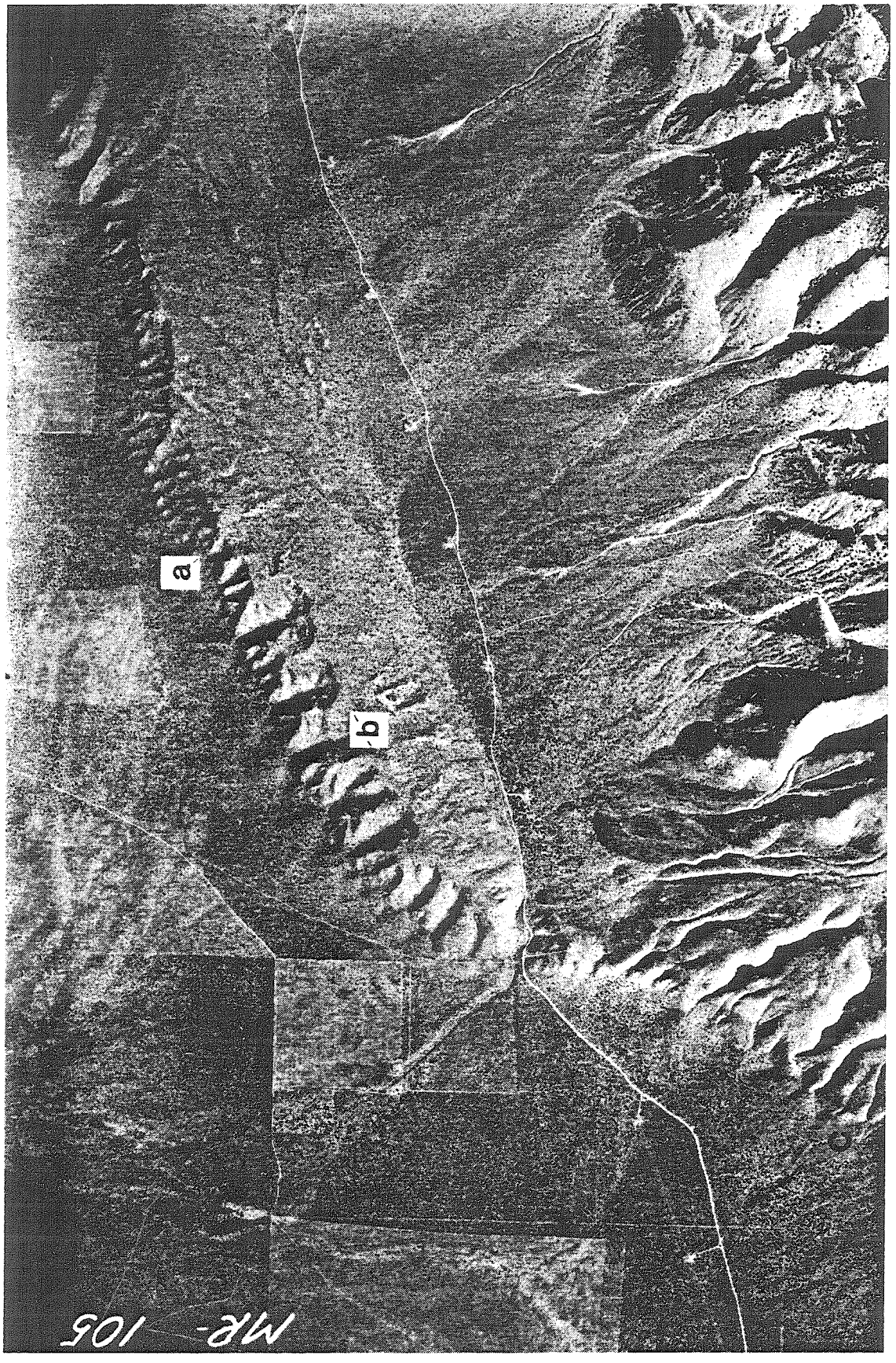
a
b
ME- 105

Figure 7-9. Trench log of the Ocotillo Ridge trench. Numbered features are discussed in text. The excavation exposed a north-dipping homoclinal sequence of fluvial sand, gravel and debris-flows. No faulting was found. Carbonate-filled tension fractures are believed related to folding, and liquefaction features suggest seismic shaking occurred after formation of the tension fractures. These observations are interpreted as evidence of co-seismic folding on the the Ocotillo Ridge fold which is developing over a buried reverse fault.

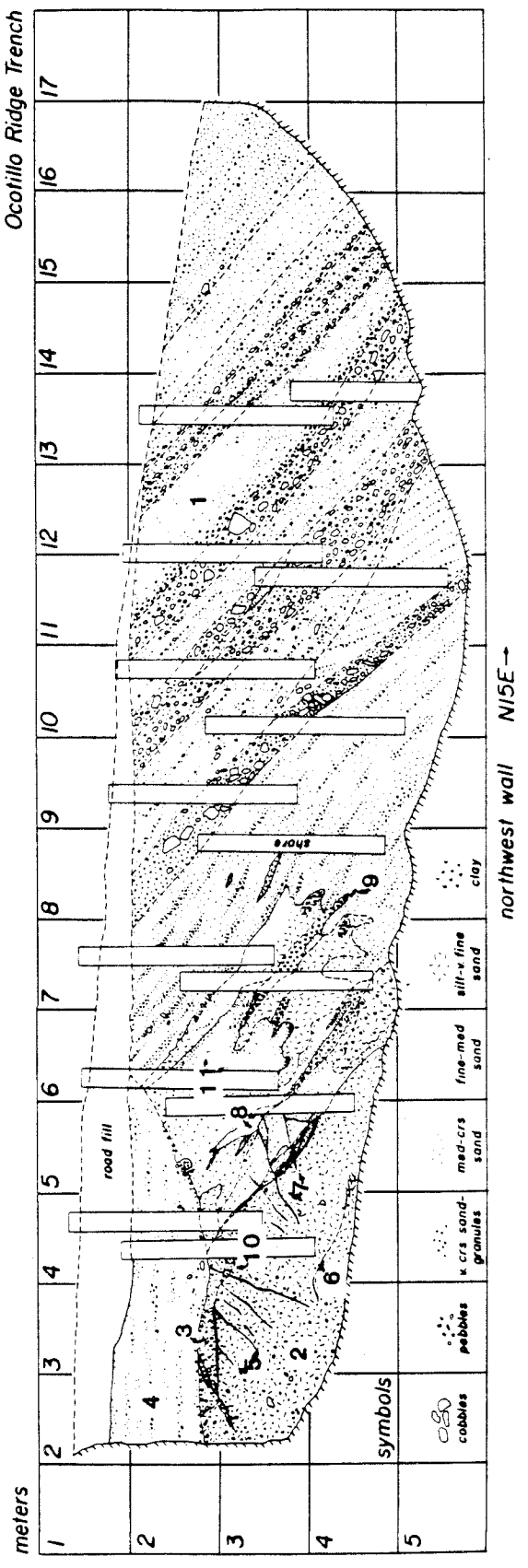
Ocotillo Ridge Trench
meters
1
2
3
4
5
6
7
8
9
10
11
12
13
14
15
16
17
symbols
cobbles
pebbles
v crs sand-granules
med-crs sand
fine-med sand
silt-v fine sand
clay
road fill
shore
northwest wall N15E→

derived by erosion from embayments in Ocotillo Ridge. Together, they define a little bajada, the outer limit of which can be readily traced on the 1939 airphotos (Figure 7-8). It is clear that these small fans were derived from Ocotillo Ridge, following or coincident with its uplift.

The structure underlying Ocotillo Ridge appears to be continuous with the structure responsible for the impressive scarps on the west flank of the Ord Mountains. Dips measured on the Ocotillo Ridge deposits in many natural and man-made exposures clearly define an asymmetric anticline, with steep northern and shallow southern limb. Ocotillo Ridge was mapped as a simple anticline by Dibblee (1974), and as a fault-bounded anticline by Fred Miller (pers. comm., 1981). Although no evidence of faulting was found in the Ocotillo Ridge excavation, calcium-carbonate-filled fractures and liquefaction structures indicative of post- or syn-depositional deformation were present.

Multiple $CaCO_3$-filled fractures were evident in the debris-flow deposit at the south end of the trench. These fractures were confined to the better-indurated, $CaCO_3$-cemented soil-zone in the debris-flow unit, dying out in the softer underlying material. The majority of the fractures dipped steeply to the south (Figure 7-9, #5); a lesser set dipped shallowly north (Figure 7-9,#6). There was no evidence of offset across any of the fractures (Figure 7-9,#7). Several of the fractures could be traced into the fluvial sand unit that overlies the debris-flow, where they were abruptly truncated by liquefaction structures (Figure 7-9,#8).

The steep, south-dipping fractures are interpreted as tension cracks developed in the brittle $CaCO_3$-cemented soil zone of the debris-flow deposit in response to the bending moment applied to the beds during folding. Shallow north-dipping fractures possibly represent similar features, now

rotated out of alignment by folding. Alternately, these shallow fractures may be basal shears for small slumps developed on the oversteepened hillslope.

Liquefaction structures were abundant throughout the coarse sand body immediately overlying the debris-flow unit. A large, amorphous sand, silt and clay intrusion appears to have invaded the fluvial unit along bedding planes (Figure 7-9,#9). Evidence of in-situ liquefaction was also noted, included pods of well-sorted, structureless, medium-grained sand (Figure 7-9,#10), and coherent blocks of laminated sand surrounded by chaotic laminations (Figure 7-9,#11).

Liquefaction can occur in response to depositional loading or seismic shaking of saturated sand. In this case, sediment loading can be ruled out, since liquefaction structures cut tension cracks in the soil developed on the Ocotillo Ridge deposits (Figure 7-9,#8).

Collectively, these findings seem best explained by co-seismic folding of the Ocotillo Ridge deposits in response to movement on a buried reverse fault. Thus, the structure seems to be a straightforward extension of the low-angle faulting on the west flank of the Ord Mountains. The scarps on the 1939 airphotos appear, upon careful re-examination, to be the expression of a resistant gravel bed within the Ocotillo Ridge deposits. There is no compelling evidence of faulting on the north side of Ocotillo Ridge.

7.8 THE ARRASTRE CANYON GRABEN

7.8.1 Activity

The faults of the Arrastre Canyon graben are considered tentatively active, except for the Arrastre Canyon Narrows fault zone which is considered potentially active, due to its association with both the Sky Hi Ranch fault and the Tunnel Ridge lineament. A pressure ridge developed within the

Arrastre Canyon Narrows fault zone contrasts with the strike-slip faulting and graben-style deformation that is characteristic of all other faults within the Arrastre Canyon graben. The pressure ridge, which is capped by middle to late Pleistocene gravel, indicates that the most recent conditions on the fault have been compressional or transpressional. The Arrastre Canyon Narrows fault zone feeds into the Sky Hi Ranch fault zone, and it seems likely that it has moved in latest Pleistocene time. Geomorphic expression of the Arrastre Canyon Narrows fault zone is consistent with low-rates of activity, its continuity is difficult to show in detail, and the Lovelace Canyon trench did not uncover a fault in the top 3 meters of stream deposits (Section 7.3.1).

Although the Bowen Ranch fault cuts middle to late Pleistocene terrace gravels, it does not express itself in Holocene(?) alluvial terraces that it crosses (13), and it cannot be traced north of the head of the Arrastre Canyon Fan. It does appear to affect the pattern of small drainages that cross its trace, but this may be explained by variation in strength or weakness of material along the fault line.

There are no constraints on the activity of the Lovelace Canyon fault system, except that the system seems to terminate against the Arrastre Canyon Narrows fault zone. Dibblee (1974) shows a connection between the Lovelace Canyon fault and the Tunnel Ridge lineament; therefore it is considered tentatively active by association.

Insufficient data exist for even a preliminary slip-rate estimate to be made for the Arrastre Canyon Narrows fault zone. Cumulative displacement does not exceed 0.5 kilometers based on offset of the domal structure expressed in units "a" and "gr" of MacColl (1964). There are no distinctive alluvial units on which to base an offset or age estimate.

Figure 7-10. Sketch diagram of the Lovelace Canyon trench site, located on the property of L. E. and Marsha Alter in Lovelace Canyon, south of Fifteen-mile Valley. The trench site is on the projection of the Arraste Canyon Narrows fault zone in the alluvium of the stream channel. See Plate 1B for location of trench site.

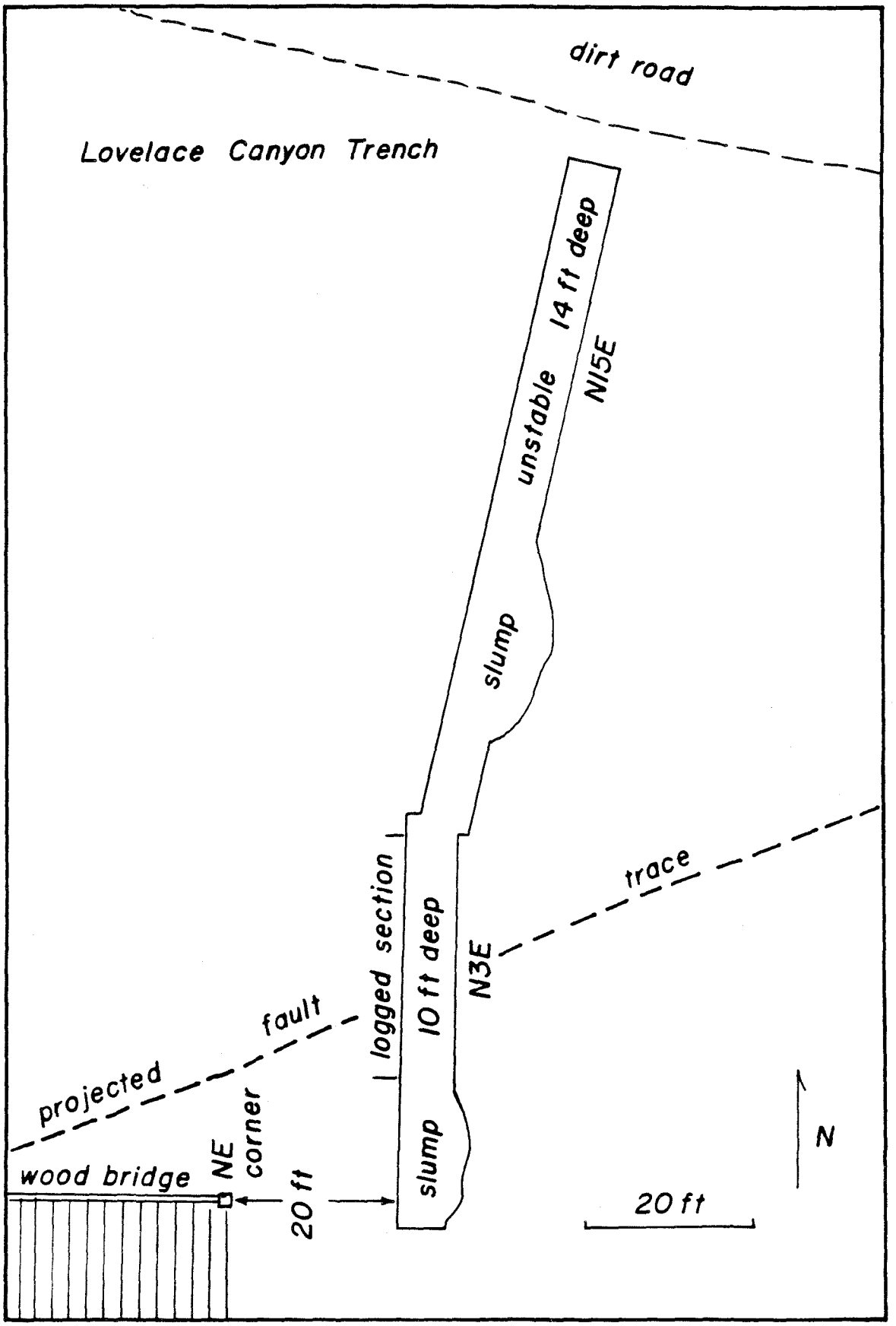
dirt road
Lovelace Canyon Trench
unstable 14 ft deep
N15E
slump
logged section
10 ft deep
N3E
trace
fault
projected
NE corner
wood bridge
20 ft
slump
N
20 ft

7.8.2 The Lovelace Canyon Trench

The Lovelace Canyon trench was excavated on the property of L. E. and Marcia Alter (sec 27, R2W T4N; Figure 7-10). The site lies in the modern stream bed on the projection of a wide gouge zone cutting bedrock in the canyon walls. Although the trench was 120 feet long, and reached a depth of 14 feet, it was only possible to safely shore 50 feet of the excavation to a depth of 10 feet due to extremely unstable soil conditions.

The ground surface at the trench site had clearly been disturbed by the property owners prior to trenching (Figure 7-10). A sprinkler system had to be disassembled before, and reconstructed after, operations. A dirt road crossing the channel immediately downstream of the site is constructed entirely of fill with no culvert; it is, in effect, a dam across the stream channel.

Nevertheless, several geomorphic features at the trench site suggest the presence of a fault in the natural alluvium. A vegetation anomaly that defines a linear zone of moisture in the alluvium on line with gouge exposed in the west canyon wall leads to a shallow linear depression across the canyon. High on the east wall of the canyon, Pleistocene(?) alluvial fan deposits terminate abruptly against bedrock along the projection of the gouge zone; although the contact is not exposed, they appear to be faulted. The object of the trench was to find C^{14}-datable deposits buried beneath the modern channel fill and see if they were deformed or faulted.

The excavation at Lovelace Canyon revealed several massive debris-flow deposits overlain by more than a meter of moderate- to well-bedded, moderately sorted coarse sand interpreted as historic channel fill (Figure 7-11). The modern channel sands grade laterally to massive silts which abut and overlie old road-fill at north end of the trench. Thus the upper meter

Figure 7-11. Trench log of the Lovelace Canyon trench. Numbered features are discussed in the text. The excavation did not expose any faulting in the upper 3 meters of stream deposits. The upper 1.5 meters of stream deposits turned out to be a modern channel fill associated with the effect of a road across the stream course. The Lovelace Canyon trench by no means rules out a through-going fault at a depth of greater than 3 meters.

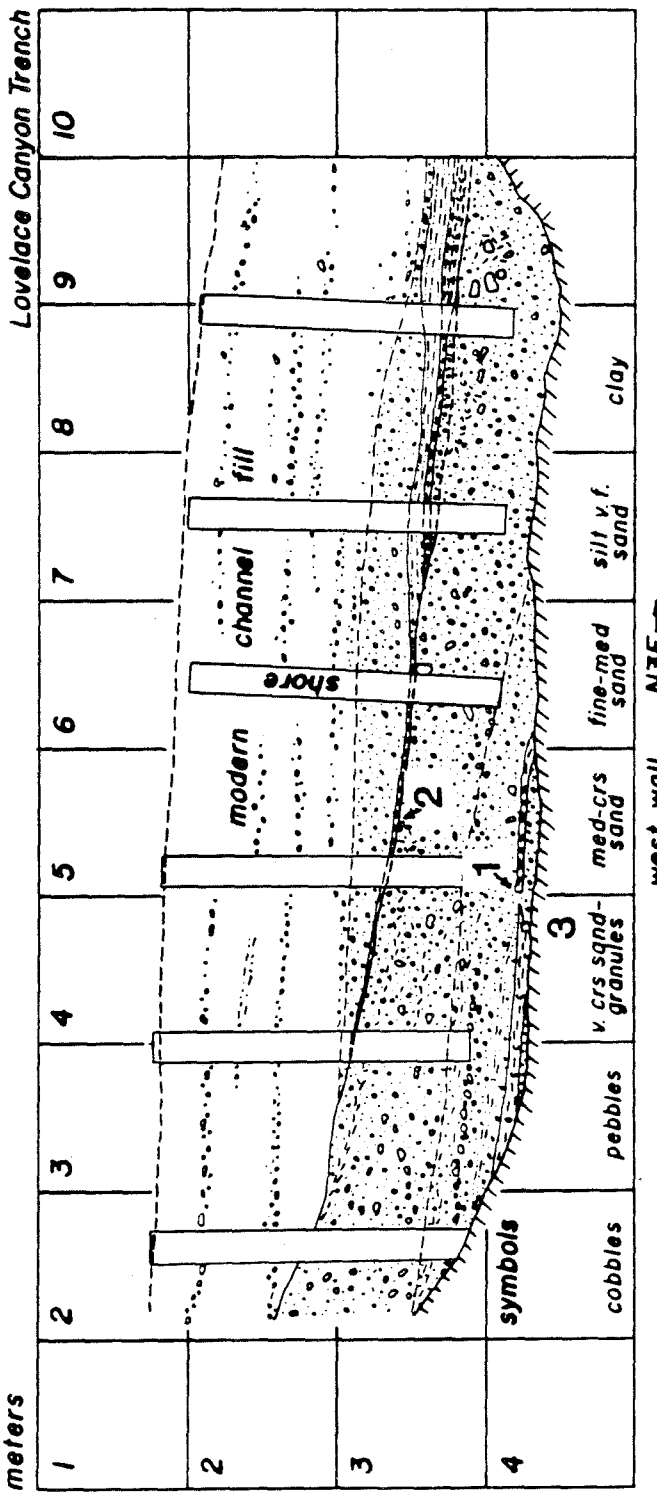
Lovelace Canyon Trench
meters
1
2
3
4
5
6
7
8
9
10
modern
channel
fill
shore
1
2
3
symbols
cobbles
pebbles
v. crs sand-granules
med-crs sand
fine-med sand
silt v.f. sand
clay
west wall
N3E→

of channel fill in the trench is historic.

The debris-flow deposits appear to have been derived from a small alluvial fan emerging from the canyon wall east of the trench. Their upper surface is in line with the projection of its present day geomorphic surface. The age of the debris-flow deposit appears to be no greater than 300 years, or three major flood/depositional events.

About a meter of massive fluvial(?) sand underlies the debris-flow unit in the north end of the trench. This deposit was moist and highly unstable, undermining the overlying units and making it impossible to shore this segment of the trench. Hence, it was not possible to map the sand in detail or search for datable material.

No conclusive evidence of faulting or deformation was found in the Lovelace Canyon trench. A disarticulated clay layer within the debris-flow unit (Figure 7-11,#1) and a gentle rise in its upper surface (Figure 7-11,#2) coincided with a moist zone (Figure 7-11,#3) at the base of the excavation. Detailed mapping did not reveal any evidence of internal shearing or deformation. Based on inspection from outside the excavation, the contact between the massive fluvial sand and overlying debris-flow deposit did not appear to be offset. We conclude that faulting has not occurred since deposition of the debris-flow unit and that, quite possibly, all of the above features are the result of a groundwater barrier created by the bedrock gouge zone depth. It is felt, however, that the materials in the Lovelace Canyon trench were far too young to warrant any conclusion regarding the activity of the Arrastre Canyon Narrows fault zone.

7.9 THE CEDAR SPRINGS FAULT SYSTEM

The Cedar Springs fault system is, as a whole, considered inactive because undisturbed Pleistocene deposits overlie several structures within

the system. Most faults that are not constrained by an overlying unit are truncated by other faults of the Cedar Springs system that are demonstrably dead. The entire system is thus considered inactive (Table 7-3). Certain faults that originated as members of the Cedar Springs system have subsequently become lateral faults, and are treated in separately.

A crude measure of the cumulative vertical offset on the Cedar Springs reverse fault system as a whole can be obtained from the south-block-down displacement of the late Miocene erosion surface across the western San Bernardino Mountains (Table 7-3).

7.9.1 The South-block-down Set

The south-block down set of the Cedar Springs fault system is inactive. Most of the arcuate faults belonging to this set are demonstrably truncated by the Notch, Seeley Creek, Cleghorn, or Silverwood Lake fault zone, which are in turn truncated by the Cleghorn fault zone. Several members of the south-block-down set are overlain by undisturbed Qt2 terraces (11,12), indicating that they have not been active since the middle to late Pleistocene (Weldon et al., 1981). Folds of the south-block down geometry occur in west Summit Valley where they are overlain by the relatively undisturbed Harold Formation (13), implying inactivity since at least the middle Pleistocene, and possibly since the late Pliocene (Section 6.2.1). The Cedar Springs faults share their orientation and geometry with the Cleghorn, Grass Valley and Summit Valley faults, which implies that they could become reactivated should favorable conditions arise.

7.9.2 The North-block-down Set

The Squaw Peak, Powell Canyon, Notch and Seeley Creek fault zones, which constitute the north-block-down set of the Cedar Springs fault system,

are considered inactive. The Squaw Peak fault lacks geomorphic expression, is truncated by the Cleghorn fault zone, and is overlain by undisturbed late Pleistocene Qya terraces deposits (14) (Foster, 1980). The Notch fault is demonstrably overlain by undisturbed Qt2 terrace deposits and truncated by the Cleghorn fault zone. Both the Squaw Peak and Notch faults have been inactive since at least the late Pleistocene. The Powell Canyon fault is also truncated by the Cleghorn fault zone, but lacking definitive evidence of inactivity, it is considered tentatively inactive. The Seeley Creek fault does not show any geomorphic signs of activity, and it is overlain by undisturbed Qt1 terrace deposits (15), suggesting that it is inactive.

The history of the development of the north-block-set (Section 5.2.2) suggests that all of the above faults were active at the same time during the early Pleistocene prior to uplift of the western San Bernardino Mountains by tilting (Section 6.2.1). The Squaw Peak, Powell Canyon, Notch, and Seeley Creek fault zones are therefore all classified as inactive by association with an inactive system.

7.10 THE POWERLINE CANYON FAULT ZONE AND RELATED STRUCTURES

The Powerline Canyon fault is inactive. It is overlain by high-elevation terrace deposits of unknown age in Powerline Canyon (16) and has no geomorphic expression suggestive of Quaternary movement. It does not disrupt the Qf1 or Qf2 fans on its projection at the mouth of Powerline Canyon. It is believed to be a northwest-trending fault of the Mojave block that was active before uplift of the San Bernardino Mountains.

7.11 THE WHITE MOUNTAIN THRUST SYSTEM

The White Mountain thrust system in Fifteenmile Valley appears to have been inactive since the oldest fans recognized (Qf3) were deposited in the

middle-Pleistocene(?). A major, continuous thrust within the White Mountain system, the Crystal Creek thrust of Richmond (1960), is overlain by the deposits of Qf3 (17). The age of Qf3 is not known, but it is highly indurated and has a deep soil developed on it, suggesting an age of late if not middle Pleistocene. Some thrusting is evident in the Qf2 fan surface; however this faulting is believed to represent secondary reactivation of older thrust planes (18) (Section 5.8.2). Total displacement on these reactivated surfaces is believed to be small.

7.12 UPLIFT RATES

Uplift of the northern range front began about 2.5 my ago, and was over by 0.5 my ago. The northern escarpment, which is about 1000 meters high, was therefore uplifted in about 2 my. These rough figures lead to an estimate of uplift rate for the late Pliocene and early Pleistocene of 0.5 mm/yr. Thus, uplift need not have proceeded at a very high rate to establish the requisite relief on the range front in the time allowed.

Early Holocene uplift rates for the San Bernardino Mountains of between 18 and 36 mm/yr have been proposed by Morton and Herd (1980), based on studies of glacial sediments in the San Gorgonio Peak area. There is no evidence on the northern range front to support uplift at rates this high. The uplift of the San Gorgonio block may be a response to the stresses produced as a result of lateral motion on the Cleghorn and other faults rather than pure north-south compression.

7.13 SEISMIC HAZARD RELATIVE TO OTHER ACTIVE FAULTS

Slip rates derived for the faults in the study area can be put in perspective by comparing them to known slip-rates for faults of the Los Angeles region, recently compiled by Ziony et al.(1983). Vertical slip-

rates for various segments of the Newport-Inglewood fault zone range from 0.07 to 0.63 mm/yr. Estimates for the San Jacinto fault zone range from 3 to 6 mm/yr vertical, and from 8 to 12 mm/yr lateral. For comparison, 20 to 30 mm/yr slip rates have been derived for the San Andreas fault in southern California. Slip-rates for strike-slip faulting seem generally higher than for reverse faulting. The Sierra Madre/Raymond/Cucamonga fault system has vertical slip-rates in the range from 0.13 to 2.8 mm/yr, and that of the Malibu/Santa Monica system is estimated at 0.04 to 0.46 mm/yr.

It should be stressed that in terms of the impact of ground shaking on structures in the southwestern Mojave desert, the hazard posed by the nearby San Andreas fault greatly overshadows the hazard due to all of the faults evaluated in this study. Seismic events on the San Andreas fault, due to their great magnitude and short recurrence interval, will undoubtedly dictate the design parameters used for structures within the study area. Faults in the study area might be expected to experience sympathetic ground breakage during an event on the San Andreas fault.

Although none of the faults in the study area poses as great a seismic hazard as does the San Andreas fault, the 3 mm/yr lateral slip-rate on the Cleghorn fault is a significant fraction of the 8-12 mm/yr estimated for the San Jacinto fault, which has several historic earthquakes attributed to it. The vertical slip-rate on the Ord Mountains fault zone is comparable to rates for the eastern Sierra Madre fault zone, a part of the system that produced the damaging San Fernando earthquake of February 9, 1971. Clearly the faults in the study area identified as active and potentially active represent a seismic hazard and should be considered for Alquist-Priolo zoning.

7.14 CONCLUSIONS

The Cleghorn fault is classified as "Class 3," according to the terminology of Cluff et al. (1983), and "active," under the criteria of the Alquist-Priolo Act. As such, it clearly poses the greatest seismic hazard to the nearby desert communities of all faults in the study area except the San Andreas fault. The Sky Hi Ranch and Ord Mountains low-angle fault zones are classified as "Class 5" and "potentially active," and must also be considered to represent a seismic hazard. Slip-rates appear to be much lower on the Ord Mountains low-angle faults (0.10 to 0.14 mm/yr vertical) than on the Sky Hi Ranch fault zone (1.25 mm/yr lateral).

The Cleghorn fault is by far the most significant seismic element with a slip rate of 2.75 to 3.3 mm/yr. The slip-rates of the Arrastre Canyon Narrows fault and Tunnel Ridge lineament are not known, but their physical connection with both the Cleghorn and Sky Hi Ranch faults makes significant slip-rates a distinct possibility. It is recommended that all of the above faults be considered for zoning under the Alquist-Priolo Special Studies Zones Act.

Slip-rate estimates for the Cleghorn, Sky Hi Ranch, and Ord Mountains fault zones suggest that they should be taken into account in planning for development in the high-desert communities. They are capable of producing significant earthquakes within time intervals on the order of a few hundred to a thousand years. The maximum credible earthquake for the Cleghorn fault is estimated to be M_S 6.8. For the Sky Hi Ranch fault, M_S 6.6 is considered the maximum credible magnitude, and M_S 6.2 is the limit derived for the Ord Mountains fault zone. The San Andreas fault, however, poses by far the greatest seismic hazard to the communities in the study area.

CHAPTER VIII

SUMMARY AND CONCLUSIONS

8.1 STUDY GOALS

The primary goals of this study, as stated at the outset, were (1) to establish a better constrained Quaternary uplift history for the San Bernardino Mountains, (2) to elucidate the nature and modes of deformation along the northern range front, (3) to estimate Holocene rates of deformation along the range front, and (4) to estimate, if possible, recurrence intervals of earthquakes and vertical/lateral offsets for the north frontal fault system.

8.2 RESULTS

The most important conclusion of this study is that the north frontal fault system is not a continuous structure, but rather a collection of unique elements that accommodate range-front deformation in a variety of ways. The disparate nature of the north frontal fault zone reflects a two-phase history of development in which late Pliocene to early Pleistocene uplift of the northwestern San Bernardino Mountains was followed by middle to late Pleistocene modification of the range front by high-angle faulting.

Constraints on the timing of deformation and uplift in the westernmost San Bernardino Mountains are provided by late Cenozoic stratigraphy. The late Miocene to Pliocene(?) Crowder Formation was deposited by south-flowing streams which originated in the Victorville area and crossed the San Andreas fault in the vicinity of the western San Bernardino Mountains. Vertebrate fossils pf 16- and 11-my age have been extracted from Units 1-4 of the Crowder Formation. The late Miocene Cajon beds of the Punchbowl Formation are in fault contact with the lower Crowder Formation, yet are overlain by

the upper Crowder Formation. The relationship between the Punchbowl and lower Crowder Formations is an unsolved stratigraphic problem in that they share the same age and paleocurrent direction, yet differ substantially in both provenance and sediment character. Any solution would seem to require substantial lateral translation of at least one of these units. The lower Crowder Formation clearly predates uplift and deformation.

The upper Crowder Formation records the emergence of local source areas, which may signal the onset of uplift and deformation in the western San Bernardino Mountains. The upper Crowder Formation may be as young as Pliocene, since it unconformably overlies the late Miocene "Cajon beds" of the Punchbowl Formation, displays northerly paleocurrent directions, and resembles the overlying Harold Formation in areal distribution. Patches of Crowder Formation throughout the westernmost San Bernardino Mountains are of unknown age, but clast lithologies suggest correlation with the upper Crowder Formation. Volcanogenic sediments in east Summit Valley, dated at 3.8 ± 0.4 my, are interpreted as an eastern facies of the upper Crowder Formation.

The middle to late Pliocene onset of deformation and incipient uplift is recorded in the stratigraphic sequence by the appearance of fine-grained sediments, new clast lithologies, and northerly paleocurrent directions. The volcanogenic eastern facies of the Crowder(?) Formation is believed to be a syntectonic deposit indicative of ponding that accompanied the reversal in drainage direction brought on by incipient uplift of the western San Bernardino Mountains. The fine grained, lacustrine character of the Harold Formation can be interpreted in the same way; the base of the Harold Formation is <2.75 my old on the basis of paleomagnetic constraints. The Old Woman Sandstone in Lucerne Valley records an abrupt change from fine-grained

sediments indicative of incipient uplift to coarse, angular debris signalling the emergence of the range front as a topographic element. The influx of range-front debris is estimated to have occurred <2.5 my ago. Several small, deformed patches of fine-grained sediment in Arrastre Canyon appear to be of similar origin.

Deposition of the Victorville Fan sequence (Harold Formation, Shoemaker Gravel, and Older Alluvium) was the direct result of uplift of the western San Bernardino Mountains and emergence of the San Gabriel Mountains southwest of the San Andreas fault. These units are characterized by northerly transport directions and a distinctive clast suite indicating derivation from the rising mountain ranges to the south and west. The Ord River Gravel along the west flank of the Ord Mountains is correlative with the Older Alluvium of the Victorville Fan sequence; paleomagnetic results constrain the 730,000 y B.P. (Brunhes/Matuyama) polarity reversal to have occurred during deposition of the Older Alluvium and Ord River Gravel. The Juniper Flats gravel, Bowen Ranch Road terraces and the Arrastre Canyon Fan gravel were also deposited during late Pleistocene time, as these units are of normal paleomagnetic polarity.

A deeply weathered bedrock erosion surface of late Miocene(?) age is widely preserved throughout the study area and serves as a useful index to deformation within the crystalline rocks in the absence of sedimentary rocks. Late Cenozoic faults express themselves as lineaments on the weathered surface, permitting the observation of critical cross-cutting and geometric relationships that constrain the relative ages of faults. The erosion surface also provides a crude datum for measuring cumulative vertical offsets on these faults. Warping and folding are evident in the erosion surface, which provides a critical insight into the nature of deformation on

the range front.

The Cedar Springs fault system is a complex sequence of cross-cutting fault sets expressed in the Crowder Formation and underlying late Miocene(?) erosion surface in the western San Bernardino Mountains. The oldest structures in the system are north-plunging anticline/syncline pairs that are interpreted as a draping of sediment over basement "steps". The folds are truncated by a set of south-block-down reverse faults, including the late Pliocene reverse fault zone that is ancestral to the Cleghorn lateral fault zone. A still younger set of faults with north-block-down separation is thought to be right-lateral. Members of the Cedar Springs system all have arcuate traces, with vertical motion on their east-trending segments and right-lateral motion on their northwest-trending segments. This geometry suggests a shingling of fault blocks rooted in a shallow sub-horizontal discontinuity. Their pattern also suggests that they originated as secondary faults in response to a differential in slip-rate on the San Andreas fault north and south of Cajon Pass. The Cedar Springs system was dead by late Pliocene to early Pleistocene time, since folds interpreted as contemporaneous with Cedar Springs faults are truncated and overlain by the <2.75 my old basal beds of the Harold Formation in Cajon Pass.

Uplift was accomplished by tilting in the westernmost San Bernardino Mountains. About 30° of northward tilting rotated the fault zones of the Cedar Springs system to a near-vertical orientation, which then favored lateral faulting over reverse motion. The tilting affects the Harold Formation and is therefore latest Pliocene to early Pleistocene in age. Tilting is thought to have been roughly synchronous with thrusting on the White Mountain thrust fault system in Lucerne Valley. The Cleghorn lateral fault grew out of the integration of major elements in the Cedar Springs

reverse fault system, following their rotation to a vertical attitude.

Several lines of evidence suggest 3.5 to 4.0 kilometers of cumulative left-lateral displacement on the Cleghorn fault since deposition of the Crowder Formation in the western San Bernardino Mountains. North-plunging anticline/syncline pairs can be matched across the fault, yielding about 4 kilometers of left-slip. The coincident eastern limit of the Punchbowl Formation and the western limit of the lower Crowder Formation are displaced approximately 4 kilometers on the Cleghorn fault. Finally, unique members of the Cedar Springs fault system can be matched across the Cleghorn fault, giving a refined estimate of 3.5 to 4.0 kilometers of total left-slip.

The Cleghorn fault turns northeast and joins the Tunnel Ridge lineament, the longest in a set of northeast-trending fault zones which includes the Arrastre Canyon graben, Arrastre Canyon Narrows fault zone, Lovelace Canyon fault system, and the high-angle frontal faults of the Ord Mountains. The persistence of the northeast structural trend is believed to be due to a "pirating" of older zones of weakness by younger fault systems. The Tunnel Ridge fault may have been the master element in the older northwest-trending system. It lies outside the study area and has yet to be examined in detail. The cumulative slip on the Tunnel Ridge lineament is thought to be small and right-lateral, based on the offset of the southern contact of the Rattlesnake Mountain pluton. Several splays on the Cleghorn fault, most notably the Silverwood Lake fault, share this northeasterly trend.

The Grass Valley fault and Summit Valley fault system in Summit Valley are considered possible analogs of the Cleghorn fault zone, with cumulative displacement of ≤ 1 kilometer. These faults also continue east and join the Tunnel Ridge lineament, cutting all other lineaments they encounter.

The frontal fault system of the Ord Mountains can be divided into high-

and low-angle fault sets. Both sets cut the middle to late Pleistocene Ord River Gravel, but uplift appears to have been accomplished primarily on the high-angle Powerline Road and Juniper Ranch faults. Displacement on these faults is not considered to have been great, and the evidence suggests that the Ord Mountains were a topographic element prior to uplift on the western San Bernardino Mountains. Although the low-angle faults postdate the high-angle faults, they appear to have minimal displacement on them, and may reactivated older weaknesses. Range-front relief dies out to the south in a warp near Grass Valley, and to the northeast in a ramp at Arrastre Canyon. The Ord Mountains were apparently uplifted later than the range front in Lucerne Valley, and the Ord high-angle faults may have developed under local extensional conditions related to lateral motion on the Cleghorn and Sky Hi Ranch faults.

Local extensional conditions are postulated to have existed at the time of formation of the Arrastre Canyon graben, which is the northern extension of the Tunnel Ridge lineament. The graben is developed within a set of northeast-trending faults on which dip-slip offset was superimposed on earlier right-lateral displacement. The graben has been a site of deposition since middle Pleistocene time. The Arrastre Canyon Narrows fault zone, occupying the center of the graben, includes a prominent pressure ridge, suggesting that the extensional regime has since given way to a lateral or compressional regime. The Arrastre Canyon Narrows fault zone curves east and joins the Sky Hi Ranch fault zone via a reactivated segment of the White Mountain thrust system.

The north end of the low-angle fault zone in the Ord Mountains becomes the Ocotillo Ridge fold, which is interpreted as a draping of sediment over a reverse fault in the basement. The Ocotillo Ridge fold turns east

and joins the Sky Hi Ranch fault zone. There is no evidence of substantial Pleistocene uplift on the range front in the vicinity of Arrastre Canyon. It appears that the late Miocene(?) erosion surface ramps down to the floor of Fifteenmile Valley in the vicinity of Arrastre Canyon. Late Pleistocene displacement on the Ocotillo Ridge fold is considered to be small and compatible with the small displacement postulated for the Ord Mountains low-angle fault zone.

The Arrastre Canyon Narrows fault zone and the Ocotillo Ridge fold join to form the Sky Hi Ranch fault, which continues southeast as the primary late Pleistocene range-front structure. The Sky Hi Ranch fault is right-lateral with cumulative displacement of about 0.5 kilometers. It is interpreted as a member of the northwest-trending fault set of the Mojave block which has reasserted itself following cessation of activity on the White Mountain thrust system. Low-angle faults cutting Pleistocene alluvial fans along the trace of the Sky Hi Ranch fault zone are considered reactivated segments of the White Mountain thrust system.

The White Mountain thrust system is the system on which the prominant northern escarpment of the San Bernardino Mountains was developed. The trace of the White Mountain thrust is now overlain by late Pleistocene(?) alluvial fans, and is cut by the Sky Hi Ranch fault zone, indicating current inactivity. The White Mountain thrust system and associated relief along the northern range front die out to the west near Lovelace Canyon. Although many segments of the White Mountain thrust appear to cut alluvial fans, this is believed to be due to reactivation. High-angle faulting has dominated rangefront deformation since the middle to late Pleistocene.

Deformation in the study area is thought to be related to motion on the San Andreas fault through two principal mechanisms. Uplift of the San

Bernardino Mountains accompanied the development of a transpressional welt across the San Andreas fault, possibly locallized by pre-existing zones of weakness. The San Gabriel Mountains may represent the other side of the welt, subsequently laterally offset. Fault geometries in the westernmost San Bernardino Mountains are interpreted to be the consequence of a slip-rate differential on the San Andreas fault at Cajon Pass, which led the formation of an arcuate pattern of secondary faults. Such fault geometries are predicted and observed for secondary faults produced as an "end effect" near the termination of a lateral master fault. The "transpressional welt" and "end effect" models for deformation are fully compatible, insofar as Pleistocene lateral motion on the arcuate faults has accomodated north-south compression by permitting an eastward "squeezing out" of the San Bernardino Mountains between convergent blocks.

8.3 SUMMARY OF RESULTS

The following conclusions can be drawn from the above summary, and constitute the essential contributions of this study:

(1) The north frontal fault system is not a single thrust fault zone, but rather a collection of disparate structural elements, each of which accommodates range-front deformation in its own way, as dictated by its individual geometry.

(2) The northern range front and the westernmost San Bernardino Mountains were uplifted during a pulse of deformation in the late Pliocene to early Pleistocene. Uplift was largely complete by middle Pleistocene time.

(3) The northern range front was uplifted by thrusting, and the westernmost San Bernardino Mountains were uplifted by tilting related to arching. These events were roughly contemporaneous.

(4) Thrusting and tilting are consistent with the formation of a transpressional welt across the San Andreas fault, the southern half of which may have been the San Gabriel Mountains, and which was initiated in Pliocene time.

(5) High-angle faulting has been the dominant style of deformation in the northwestern San Bernardino Mountains since middle to late Pleistocene.

(6) Pleistocene lateral faulting in the westernmost San Bernardino Mountains has had the effect of squeezing the San Bernardino Mountains block out to the east, thereby accomplishing relative shortening of the central Transverse Ranges.

(7) Northwest-trending faults of the Mojave block were active prior to uplift along the north frontal fault system and reasserted themselves following cessation of its activity.

(8) Localized extension, with concomitant graben formation, appears to have been associated with lateral motion on the Sky Hi Ranch fault zone and the Cleghorn fault zone.

(9) Arcuate patterns of faulting in the western San Bernardino Mountains can be understood in terms of the pattern of faulting predicted for secondary faults near the end of a strike-slip fault. In this case the "end effect" is produced by a change in slip-rate on the San Andreas fault in Cajon Pass, possibly related to motion on the San Jacinto fault.

(10) All faulting in the study area can be thought of as the product of compressional forces across the San Andreas fault.

(11) The slip rate on the Cleghorn fault zone is estimated to be about 3.0 mm/yr. Cumulative offset on the Cleghorn fault is 3.5 to 4.0 kilometers

(12) The slip rate on the Sky Hi Ranch fault is estimated to be about 1 mm/yr, with a late Pleistocene offset of about 0.5 kilometers.

(13) The slip rate on the Ord Mountains frontal fault zone is thought to be about 0.1 to 0.2 mm/yr.

(14) The Cleghorn fault is classified as Class 3, in the terminology of Cluff et al., (1983), and "active", according to the criteria set forth under the Alquist-Priolo Special Studies Zones Act.

(15) The Sky Hi Ranch and Apple Valley Highlands/Deep Creek fault zones are classified as "potentially active", by Alquist-Priolo criteria, and both faults are Class 5, in the terminology of Cluff et al. (1983).

(16) The Tunnel Ridge lineament and Arrastre Canyon Narrows fault zones are of unknown activity, but are considered tentatively active. They should be examined in detail prior to development of adjoining areas.

(17) Although the San Andreas fault is by far the most potentially damaging structure in the study area, the Cleghorn, Sky Hi Ranch and Ord Mountains fault zones should be taken into account in planning for development of the high desert communities. It is recommended that these faults be considered for Alquist-Priolo zoning.

REFERENCES CITED

Armstrong, R., and Suppe, J., 1973, Potassium-argon geochronometry of Mesizoic igneous rocks in Nevada, Utah, and southern California: Geol. Soc. Am. Bull., v. 84, p. 1375-1392.

Baird, A. K., Morton, D. M., Woodford, A. O., and Baird, K. W., 1974, Transverse Ranges province: A unique structural-petrochemical belt across the San Andreas fault system: Geol. Soc. Am. Bull., v. 85, p. 163-174.

Bartlett, W. L., Friedman, M., and Logan, T. M., 1981, Experimental folding and faulting of rocks under confining pressure: Part IX. Wrench faults in limestone layers: Tectonophysics, v. 79, p. 255-277.

Bingham, C., 1974, An antipodally symmetric distribution on the sphere: Ann. Stat., v. 2, p. 1201-1225.

Bird, P., 1980, Fault slip rates, microplate velocities, and mantle flow in southern California: EOS, v. 61, no. 46, p. 1125.

Birkeland, P. W., 1974, Pedology, Weathering, and Geomorphological Research: Oxford University Press, New York, 285 pp.

Blackwelder, E., 1925, Exfoliation as a phase of rock weathering: Jour. Geol., v. 33, p. 789-806.

Brown, Howard, 1979, Unpublished map of the Ord Mountains, 1:24,000.

_____, 1982, Unpublished map of the White Mountain area, ~1:6000.

California Department of Water Resources, 1968a, Geology and construction materials data, Cedar Springs Dam: Cal. Dept. Water Res., Southern District Design and Construction Branch, Project Geology Report D-102.

California Department of Water Resources, 1968b, Areal Geology of the Cedar Springs Dam: Cal. Dept. Water Res., Southern District Design and Construction Branch, Project Geology Map, Scale 1:12,000, A. B. Arnold, Project Chief.

California Division of Mines and Geology, 1980, Fault-rupture hazard zones in California: Cal. Div. of Mines and Geology, Special Publication 42 by Earl W. Hart.

Cameron, C. S., 1981, Geology of the Sugarloaf and Delamar Mountain areas, San Bernardino Mountains, California: Ph.D. thesis, Massachusetts Institute of Technology, 399 pp.

Chinnery, M. A., 1965, The vertical displacements associated with transcurrent faulting: Jour. Geophys. Res., v. 70, no. 18, p. 4627-4632.

_____, 1966a, Secondary faulting: I. Theoretical aspects: Can. Jour. Earth Sci., v. 3, p. 163-174.

_____, 1966b, Secondary faulting: II. Geological aspects: Can. Jour. Earth Sci., v. 3, p. 175-190.

Cluff, L. S. et al., 1972, Site evaluation in seismically active regions--an interdisciplinary team approach: International Conference on Microzonation.

_____, Coppersmith, K. J., and Knuepfer, P. L., 1983, Assessing degrees of fault activity for seismic microzonation: Proceedings of the Third International Microzonation Conf., v. 1.

Coffman, R. L., 1980, A study of igneous-matamorphic contact zone in the Juniper Flats region of the San Bernardino Mountains, San Bernardino County, California: Senior Thesis, Univ. Cal. Riverside.

Corbett, E. J., and Hearn, T. M., 1981, The depth of the seismic zone in the Transverse Ranges of southern California: Informal paper presented at the John Muir Geophysical Society meeting, Lake Arrowhead, California.

Davis, W. M., 1938, Sheetfloods and streamfloods: Geol. Soc. Am. Bull., v. 49, p. 1337-1416.

Dibblee, T. W., Jr., 1964, Geologic map of the Lucerne Valley quadrangle, San Bernardino County, California: U.S. Geol. Survey Misc. Geol. Inv. Map I-426.

_____, 1965, Geologic Map of the Hesperia 15' quadrangle San Bernardino County, California: U.S.G.S., Open File Map 65-43.

_____, 1967, Areal geology of the western Mojave Desert: U.S. Geological Survey Prof. Paper 522, 153 pp.

_____, 1974, Geologic Map of the Lake Arrowhead 15' quadrangle, San Bernardino County, California: U.S.G.S., Open File Map 73-56.

_____, 1975, Late Quaternary Uplift of the San Bernardino Mts on the San Andreas and Related Faults, in San Andreas Fault in Southern California: Cal. Div. Mines and Geology, special report 118, p. 127-135.

Ehlig, Perry L., 1975, Basement rocks of the San Gabriel Mountains, south of the San Andreas fault, southern California: in San Andreas Fault in Southern California, J.C. Crowell ed.: Cal. Div. Mines Geol., Spec. Rep. 118, p. 177-186

Ely, Marion II, 1982, Stratigraphy of Tortoise Canyon, Ord Mountains, San Bernardino County, California: unpublished manuscript to be submitted to the South Coast Geologic Society for Transverse Ranges volume.

Foster, J. H., 1980, Late Cenozoic tectonic evolution of Cajon Valley, southern California: Ph.D. thesis, Univ. of Cal., Riverside, 235 pp.

Gillou, R. B., 1953, Geology of the Johnston Grade area, San Bernardino County, California: Cal. Div. Mines Geol. Spec. Rept. 31, 18 pp.

Goree, W. S., and Fuller, M., 1976, Magnetometers using R-F-driven squids and their applications in rock magnetism and paleomagnetism: Rev. Geophys. Space Phys., v. 14, no. 4, p. 591-608.

Hadley, D., and Kanamori, H., 1977, Seismic structure of the Transverse Ranges, California: Geol. Soc. Am. Bull., v. 88, p. 1469-1478.

Hill, D. P., 1982, Contemporary block tectonics: California and Nevada: Jour. Geophys. Res., v. 87, no. B7, p. 5433-5450.

Hollenbaugh, K. M., 1970, Geology of a portion of the north flank of the San Bernardino Mountains, California: Geol. Soc. Am. Abstr. with Prog., v. 2, no. 2, p. 103.

Jahns, R. H., 1973, Tectonic evolution of the Transverse Ranges province as related to the San Andreas fault system: Stanford Univ. Pub. Geol. Sci., v. 13, p. 149-170.

Jennings, C. W., 1983, in preparation, Geologic Map of California, San Bernardino Sheet: Cal. Div. Mines Geol., 1:250,000.

Jenkins, O. P., 1969, Geologic Map of California, San Bernardino Sheet: Cal. Div. Mines and Geology, State Map Sheet, scale 1:250,000.

Kamerling, M. J., and Luyendyk, B. P., 1979, Tectonic rotations of the Santa Monica Mountains region, western Transverse Ranges, California,suggested by paleomagnetic vectors: Geol. Soc. Am. Bull., v. 90, p. 331-337.

Kirschvink, Joseph L., 1980, The least-squares line and plane and the analysis of palaeomagnetic data: Geophys. J. R. astr. Soc., v. 62, p. 699-718.

_____, 1981, A quick, non-acidic chemical demagnetization technique for dissolving ferric minerals: EOS, v. 62, no. 45 (abstr.)

MacColl, Robert S., 1964, Geochemical and structural studies in batholithic rocks of southern California: Part 1, Structural geology of the Rattlesnake Mountain pluton: Geol. Soc. Am Bull., v. 75, no. 9, p. 805-822.

Mankinen, E. A., and Dalrymple, G. B., 1979, Revised geomagnetic polarity time scale for the interval 0-5 my B.P.: J. Geophys. Res., v. 84, p. 615-626.

May, S. R., and Repenning, C.A., 1982, New evidence for the age of the Old Woman Sandstone, Mojave Desert, California: in Sadler, P.M., and Kooser, M.A., eds., Late Cenozoic stratigraphy and structure of the San Bernardino Mountains: Geol. Soc. Am., Cordilleran Section Field Trip Guide, 6, p. 93-96.

_____, and Sadler, P. M., 1981, Emerging evidence for the stratigraphic and tectonic position of the Old Woman Sandstone, southern Mojave Desert, California: Informal abstract circulated at the 1981 U.S. Geol. Survey Conference on the Tectonics of the Mojave Desert region, 2 pp.

Mehra, O. P., and Jackson, M. L., 1958, Iron oxide removal from soils and clays by a dithionite-citrate system buffered with sodium bicarbonate: Clays and Clay Minerals, v. 7, p. 317-327.

Meisling, K. E., and Weldon, R. J., 1982a, Slip-rate, offset, and history of the Cleghorn fault, western San Bernardino Mountains, southern California: Geol. Soc. Am. Abstr. with Prog., Cordilleran Section Mtg., p. 215.

Meisling, K. E., and Weldon, R. J., 1982b, The late-Cenozoic structure and stratigraphy of the western San Bernardino Mountains: in Geologic Excursions in the Transverse Ranges, J. D. Cooper ed., p. 55-106, Cal. State Univ. Fullerton.

Morton, D. M., and Herd, D. G., 1980, Earthquake hazards studies, Upper Santa Ana Valley and adjacent areas, southern California: Summaries of Technical Reports, v. IX, N.E.H.R.P., U.S,G.S. Open File Rept. 80-6, p. 15.

Mendenhall, W. C., 1905, The hydrology of the San Bernardino Valley, California: U. S. Geol. Survey, Water Supply Paper 142.

Miller, C. F., 1977, Alkali-rich monzonites, California: Origin of near silica saturated alkaline rocks and their significance in a calc-alkaline batholithic belt: Ph.D. thesis, Univ. of Cal., Los Angeles, 283 pp.

Miller, F. K., and Morton, D.M., 1975, K-Ar geochronology for the eastern Transverse Ranges: Geol. Soc. Am. Abstr. with Prog., v. 7, no. 3, p. 348.

_____, 1980, Potassium-argon geochronology of the eastern Transverse ranges and southern Mojave Desert, southern California: U.S.G.S. Professional Paper 1152, 30 pp.

Noble, L. F., 1932, The San Andreas rift in the desert region of southeastern California: Carnegie Inst. Washington Yearbook 31, p. 355-363.

_____, 1953, Geology of the Pearland Quadrangle, California: U.S. Geol. Survey Geol. Quad. Map GQ-24.

_____, 1954a, Geology of the Valyermo Quadrangle and vicinity, California: U.S. Geol. Survey Geol. Quad. Map GQ-50.

_____, 1954b, The San Andreas fault zone from Soledad Pass to Cajon Pass, California: Cal. Div. Mines Geol. Bull. 170, Ch. IV, p. 32-48.

Oberlander, T. M., 1972, Morphogenesis of granitic boulder slopes in the Mojave Desert, California: Jour. Geol., v. 80, p. 1-20.

Powell, Robert E., 1981, Geology of the crystalline basement complex, eastern Transverse Ranges, southern California: Constraints on regional tectonic interpretation: Ph.D. thesis, California Institute of Tech., 441 pp.

Repenning, C. A., 1982, Preliminary report on the U.C. Riverside Barrel Springs faunal locality: U. S. Geological Survey Preliminary Report on Referred Fossils, 2 pp.

Richmond, J. F., 1960, Geology of the San Bernardino Mountains north of Big Bear Lake, California: Cal. Div. Mines Geol. Special Report 65, 68 pp.

Robinson, P. T., and Woodburne, M. O., 1971, Source of volcanic clasts in the Punchbowl Formation, Valyermo and Cajon Valley, California: Program, 67th ann. meeting, Cordilleran Section, Geol. Soc. Am., p. 185-186.

Roy, J. L., and Park, J. K., 1974, The magnetization process of certain red beds: Vector analysis of chemical and thermal results: Can. Jour. Earth Sci., v. 11, p. 437-471.

Sadler, P. M., 1981, Structure of the northeast San Bernardino Mountains: Report and Open File Maps submitted to Cal. Div. Mines and Geology in response to RFP-SMPI.

_____, 1982, Late Cenozoic stratigraphy and structure of the San Bernardino Mountains, in Geologic Excursions in the Transverse Ranges, J. D. Cooper ed., p. 55-106, Cal State Univ. Fullerton.

Sadler, P. M., and Reeder, W. A., 1983, Upper Cenozoic, quartzite-bearing gravels of the San Bernardino Mountains, southern California: Recycling and mixing as a result of transpressional uplift: manuscript submitted to the A.A.P.G. for inclusion in field trip guidebook.

Shelton, J. S., 1966, Geology Illustrated, Freeman Press, San Francisco, 434 pp.

Sherard, J. L., Cluff, L. S., and Allen, C. R., 1974, Potentially active faults in dam foundations: Geotechnique, vol. 24, no. 3, 367-428.

Shreve, R. L., 1959, Geology and mechanics of the Blackhawk landslide; Ph.D. thesis, California Institute of Tech.

_____, 1968, The Blackhawk landslide: Geol. Soc. Am. Spec. Paper 108, 47 pp.

Slemmons, D. B., 1977, State-of-the-art for assessing earthquake hazards in the United States; Report 6, Faults and Earthquake Magnitude: Miscellaneous Paper S-73-1, 129 pp.

_____, 1983, Determination of Design Earthquake Magnitudes for Microzonation: Proceedings of the Third International Microzonation Conference, vol. 1.

Smith, David K., 1982, Petrology of Mesozoic alkaline and calc-alkaline igneous rocks northwest of Holcomb Valley, San Bernardino County, California: Masters thesis, Univ. of Cal., Riverside, 87 pp.

U. S. Army Corps of Engineers, 1982, Mojave River Dam Foundation Report: U. S. Army Engineer District, Los Angeles, Corps of Engineers, C. W. Orvis, Project Geologist, 66 pp., 13 Figs., 11 Tables, 53 Dwgs.

Vaughan, F. E., 1922, Geology of the San Bernardino Mountains north of San Gorgonio Pass: Univ. Cal., Dept. Geol. Sci. Bull, v. 13, p. 319-411.

VanderHoof, V. L., The major earthquakes of California: A historical summary: Colorado Division of Mines Bulletin 171, p. 137-141.

Weldon, R. J., and Meisling, K. E., 1982, Late Cenozoic tectonics in the western San Bernardino Mountains; Implications for the uplift and offset of the central Transverse Ranges: Geol. Soc. Am. Abstr. with Prog., Cordilleran Section Meeting, Apr. 1982.

Weldon, R. J., Meisling, K. E., Sieh, K. E., and Allen, C. R., 1981, Neotectonics of the Silverwood Lake area, San Bernardino County: Report to the California Department of Water Resources, 22 pp., 11 figures, 1 map.

Weldon, R.J., and Sieh, K.E., in preparation, Holocene rate of slip along the San Andreas fault near Cajon Pass, southern California: manuscript to be submitted to Geol. Soc. Am. Bull., 25 pp., 9 figures.

Weldon, R. J., and Sieh, K. E., 1980, Holocene rate of slip along the San Andreas fault and related tilting near Cajon Pass, southern California: in Abstracts with Programs, Cordilleran Section, Geol. Soc. Am., v. 12, no. 3, p. 159.

Woodburne, M. O. and Golz, D. J., 1972, Stratigraphy of the Punchbowl Formation Cajon Valley, Southern California: Univ. Cal. Pubs. Geol. Sci., v.92, 57 pp.

Woodford, A. O., and Harriss, T. F., 1928, Geology of Blackhawk Canyon, San Bernardino Mountains, California: Cal. Univ. Pub. Geol. Sci., V. 17, p. 265-304.

Woodring, W. P., 1942, Marine Miocene mollusks from Cajon Pass, California: Jour. Paleont., v. 16, no. 1, p. 78-83.

Zijderveld, J. D. A., 1967, A. C. demagnetization of rocks: Analysis of results: in Methods in Paleomagnetism, D. W. Colinson, K. M. Creer, and S. K. Runcorn eds., Elsevier.

Ziony, J. I., et al., 1983, Seismic zonation of the Los Angeles Region--A progress report: Proceedings of the Third International Microzonation Conf., v. 1.

APPENDIX A

PALEOMAGNETIC DATA

The progressive demagnetization data for paleomagnetic samples from the Harold Formation, Shoemaker Gravel, Older Alluvium and other key Pleistocene deposits are presented in the pages that follow. These data are summarized in Tables 4-1 to 4-5 of Chapter IV.

An EQPLOT and ZPLOT is included for each sample. Section 4.2.4, "Data Analysis" and Figure 4-2 of Chapter IV give an explanation of the vector projections used in these plots. The relevant parts of Section 4.2.4, along with Figure 4-2 (Figure A-2), are repeated here for convenience.

The data for progressive demagnetization of each sample are summarized by plotting the remnant vectors on an equal-area stereographic projection (EQPLOT). Open points plot in the upper hemisphere and solid points plot in the lower hemisphere (Figure A-2a). The EQPLOT can be presented in either geographic coordinates or tilt-corrected coordinates which restore bedding and sample to their original depositional orientation.

Progressive demagnetization data are also plotted on a modified Zijderveld, or Roy-Park, diagram (ZPLOT) in which two useful projections of the paleomagnetic vector are combined (Zijderveld, 1967; Roy and Park, 1974; Figure A-2b). For open points, the x-axis is the radial component of the vector in the horizontal plane (horizontal intensity) and the y-axis is the vertical component of the vector (vertical intensity: positive above the x-axis, and negative below). This projection plane can be thought of as a vertical slice through both upper and lower hemispheres of the EQPLOT that passes through each point when plotted. Solid points are the projection of the paleomagnetic vector on the horizontal plane, with the positive x-axis pointing east and the positive y-axis pointing north; this projection plane

is simply a horizontal slice through the equator of the EQPLOT. In both of these projections, the length of the vector is proportional to its intensity.

Data for samples requiring bedding restoration have been plotted in both geographic and tilt-corrected coordinates. In tilt-corrected coordinates, paleomagnetic vector directions are plotted relative to the local bedding plane, measured at the sample site and restored to horizontality by a single rotation about the the strike-line of the bedding. Samples for which dip of bedding measured less than 10° were not tilt-corrected, since bedding attitudes were found to be quite variable in the studied units and primary dips of 5-10° are not uncommon.

Table A-1 lists the pages on which plots for each sample series can be found. ZPLOT axis divisions are 1 x 10^{-5}emu/g unless otherwise labeled.

Table A-1. Key to data of Appendix A

Site Code	#Samples	Coords*	Page
HPL†	39	G	A-5
HPL†	39	T	A-15
SPL	19	G	A-25
SPL	19	T	A-30
MRF	10	G	A-35
ACF	8	G	A-38
RSR	2	G	A-41
RSR	2	T	A-41
BRR	1	G	A-42
ORD	4	G	A-43
HRF	2	G	A-44
ORM	4	G	A-45
ORM	4	T	A-46

*(-G) suffix = geographic coords.; (-T) suffix = tilt-corrected coords.
†samples HPL-30 & 31 are omitted since they were too strong to measure.

Figure A-2. (a) Left: Equal area stereographic projection (EQPLOT) showing the direction of the paleomagnetic vector during progressive thermal demagnetization of sample MRF-1. Open points plot in the upper hemisphere; solid points plot in the lower hemisphere. "NRM" is the natural remanent magnetic vector prior to demagnetization, which is the sum of a stable reversed paleomagnetic vector and a less stable normal vector overprint due to the present local magnetic field (PLF). As the normal overprint is removed by progressive thermal demagnetization, the vector sum tracks across the plot to a reversed direction. The vector remains at this ancient declination and inclination during further heating, decreasing only in intensity. When the blocking temperature of the minerals carrying the ancient field direction is exceeded, the vector drifts randomly across the plot. (b) Right: Zijderveld diagram (ZPLOT) as modified by Roy and Park (1974) for MRF-1 in which two useful projections of the paleomagnetic vector are combined. For open points, the x-axis is the radial component of the vector in the horizontal plane (horizontal intensity) and the y-axis is the vertical component of the vector (vertical intensity: positive above the x-axis, and negative below); this projection plane is a vertical slice through both upper and lower hemispheres of the EQPLOT that passes through each point when plotted. Solid points are the projection of the paleomagnetic vector on the horizontal plane, with the positive x-axis pointing east and the positive y-axis pointing north; this projection plane is simply a horizontal slice through the equator of the EQPLOT. Except where otherwise noted, divisions on axes are 10^{-6} emu/g. The ZPLOT for MRF-1 clearly shows that a strong normal component is completely removed after heating to the 200° demag step, leaving a remanent paleomagnetic vector of reversed polarity which decreases in intensity and remains constant in direction with stepwise heating.

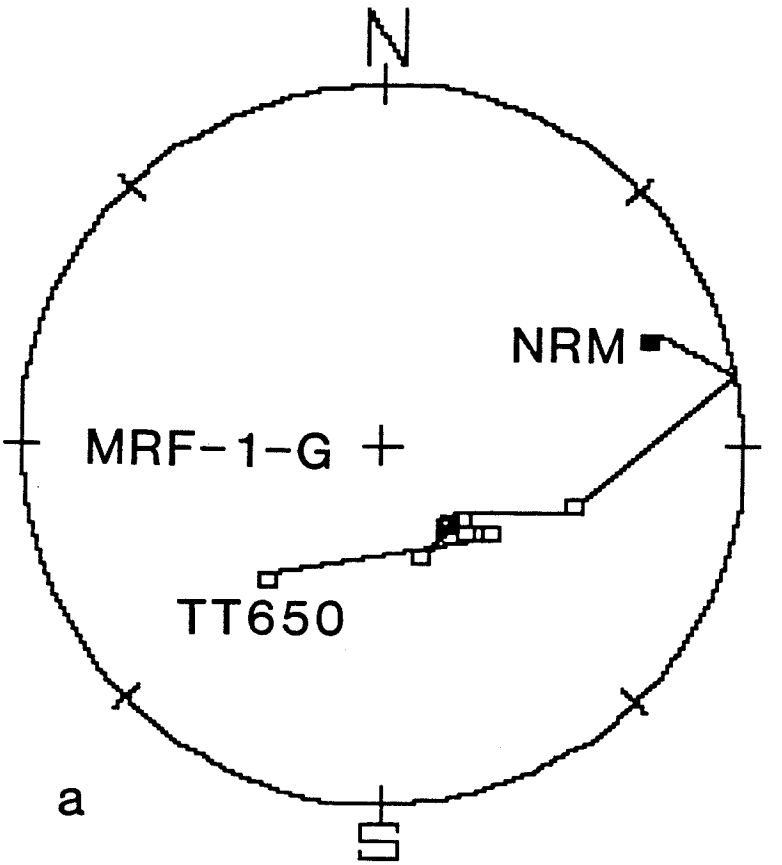
N
NRM
MRF-1-G
TT650
a
S

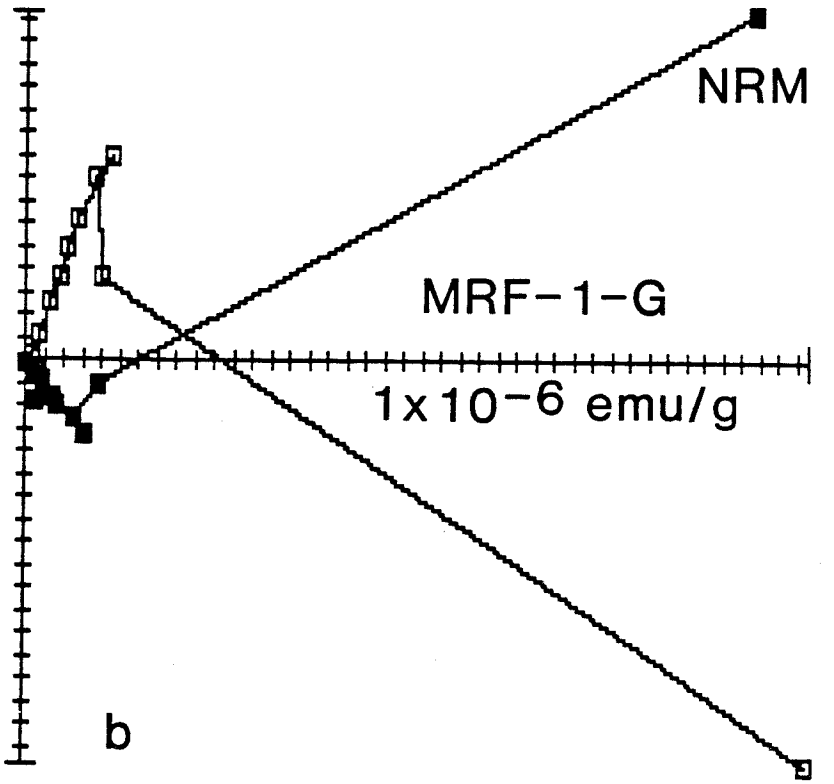
NRM
MRF-1-G
1x10⁻⁶ emu/g
b

HPL-1-G
NRM
N
S
HPL-1-G
10⁻⁵emu/g
HPL-2-G
NRM
N
S
HPL-2-G
10⁻⁵emu/g
HPL-3-G
NRM
N
S
HPL-3-G
10⁻⁵emu/g
HPL-4-G
NRM
N
S
HPL-4-G
10⁻⁵emu/g

HPL-5-G
NRM
N
S
HPL-5-G
10⁻⁵emu/g
HPL-6-G
NRM
N
S
HPL-6-G
10⁻⁵emu/g
HPL-7-G
NRM
N
S
HPL-7-G
10⁻⁵emu/g
HPL-8-G
NRM
N
S
HPL-8-G
10⁻⁵emu/g

HPL-9-G
NRM
N
S
HPL-9-G
10^{-5}emu/g
HPL-10-G
NRM
N
S
HPL-10-G
10^{-5}emu/g
HPL-11-G
NRM
N
S
HPL-11-G
10^{-5}emu/g
HPL-12-G
NRM
N
S
HPL-12-G
10^{-5}emu/g

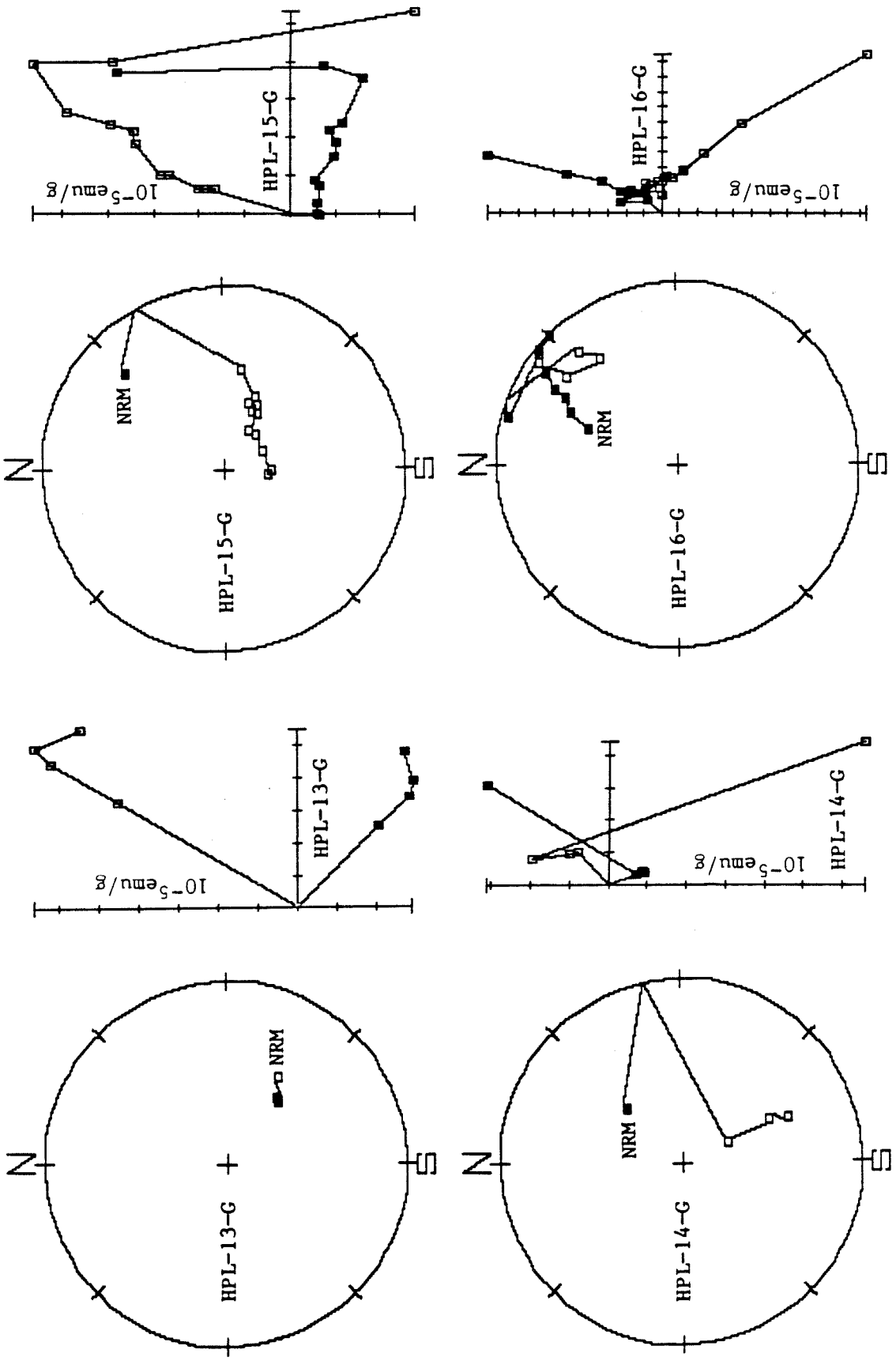
HPL-15-G
10⁻⁵emu/g
HPL-16-G
10⁻⁵emu/g
NRM
N
S
HPL-15-G
NRM
N
S
HPL-16-G
HPL-13-G
10⁻⁵emu/g
HPL-14-G
10⁻⁵emu/g
NRM
N
S
HPL-13-G
NRM
N
S
HPL-14-G

HPL-17-G
NRM
N
S
HPL-17-G
10^{-5}emu/g
HPL-18-G
NRM
N
S
HPL-18-G
10^{-5}emu/g
HPL-19-G
NRM
N
S
HPL-19-G
10^{-5}emu/g
HPL-20-G
NRM
N
S
HPL-20-G
10^{-5}emu/g

HPL-23-G
10⁻⁵emu/g
N
S
NRM
HPL-23-G
HPL-24-G
10⁻⁵emu/g
N
S
NRM
HPL-24-G
HPL-21-G
10⁻⁵emu/g
N
S
NRM
HPL-21-G
HPL-22-G
10⁻⁵emu/g
N
S
NRM
HPL-22-G

HPL-25-G
NRM
N
S
HPL-25-G
10^{-5}emu/g
HPL-27-G
NRM
N
S
HPL-27-G
10^{-5}emu/g
HPL-26-G
NRM
N
S
HPL-26-G
10^{-5}emu/g
HPL-28-G
NRM
N
S
HPL-28-G
10^{-5}emu/g

HPL-29-G
NRM
N
S
HPL-29-G
10^{-5}emu/g
HPL-32-G
NRM
N
S
HPL-32-G
10^{-5}emu/g
HPL-33-G
NRM
N
S
HPL-33-G
10^{-5}emu/g
HPL-34-G
NRM
N
S
HPL-34-G
10^{-5}emu/g

HPL-37-G
10⁻⁵emu/g
HPL-38-G
10⁻⁵emu/g
N
S
NRM
HPL-37-G
NRM
HPL-38-G
HPL-35-G
10⁻⁵emu/g
HPL-36-G
10⁻⁵emu/g
N
S
NRM
HPL-35-G
NRM
HPL-36-G

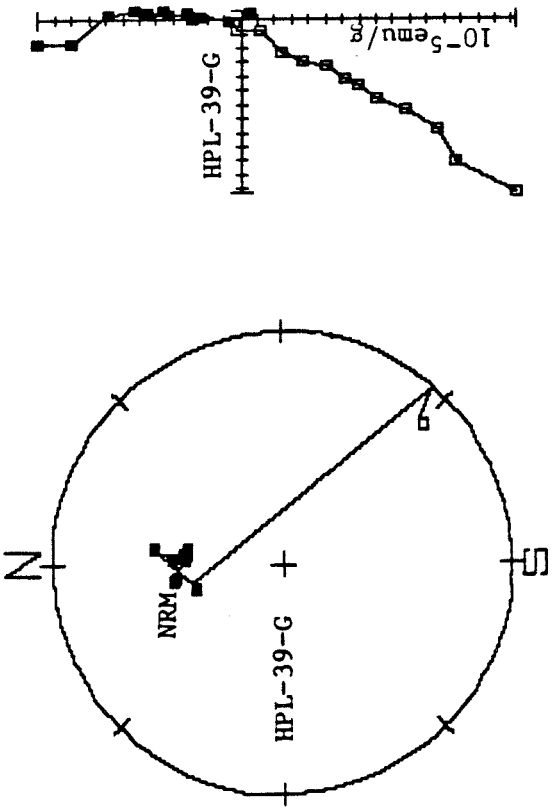
10^-5emu/g
HPL-39-G
N
S
NRM
HPL-39-G

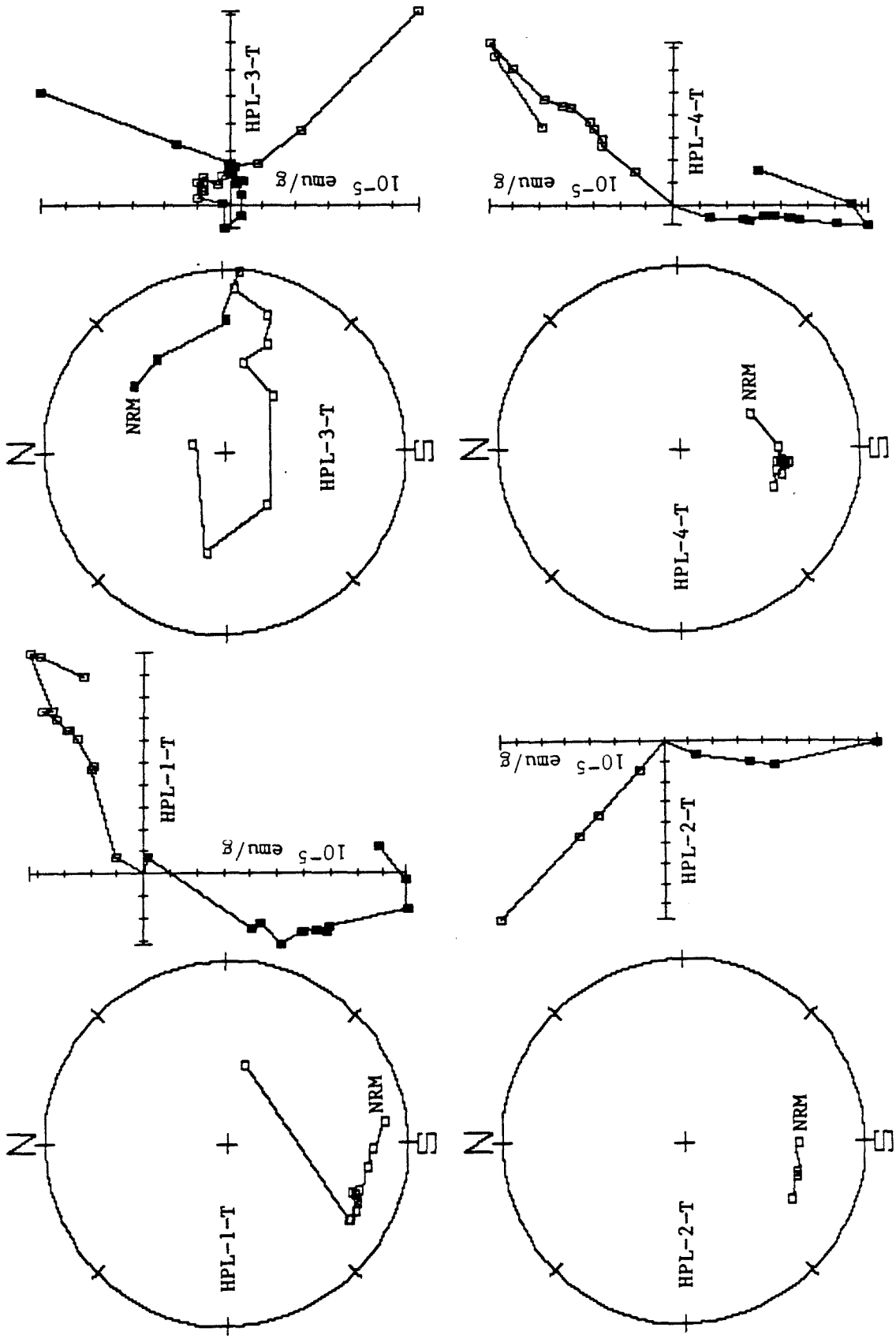
HPL-3-T
10⁻⁵ emu/g
N
S
NRM
HPL-3-T
HPL-4-T
10⁻⁵ emu/g
N
S
NRM
HPL-4-T
HPL-1-T
10⁻⁵ emu/g
N
S
NRM
HPL-1-T
HPL-2-T
10⁻⁵ emu/g
N
S
NRM
HPL-2-T

HPL-5-T
NRM
N
S
HPL-5-T
10⁻⁵ emu/g
HPL-6-T
NRM
N
S
HPL-6-T
10⁻⁵ emu/g
HPL-7-T
NRM
N
S
HPL-7-T
10⁻⁵ emu/g
HPL-8-T
NRM
N
S
HPL-8-T
10⁻⁵ emu/g

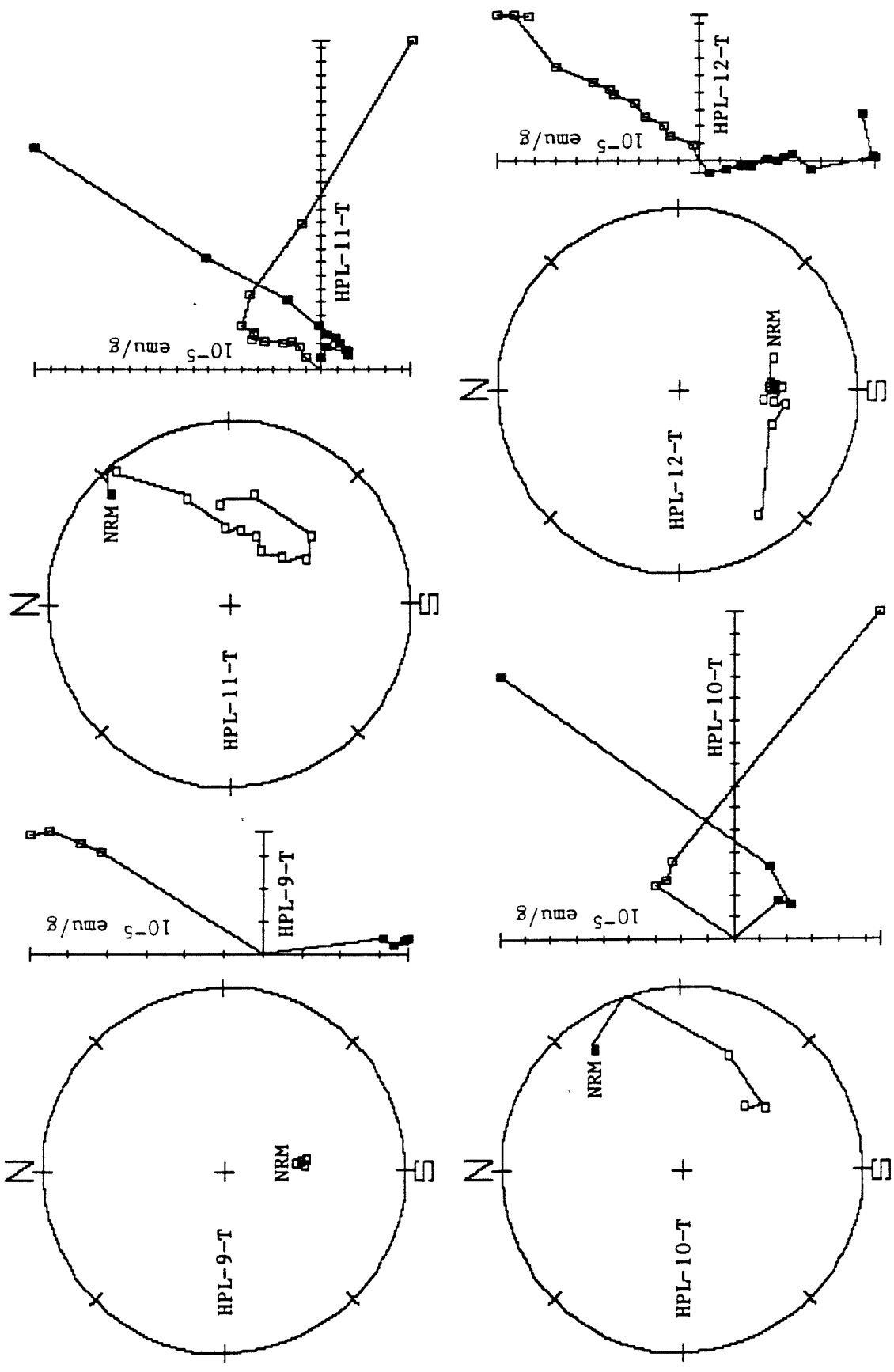
HPL-9-T
NRM
N
S
HPL-9-T
10⁻⁵ emu/g
HPL-11-T
NRM
N
S
HPL-11-T
10⁻⁵ emu/g
HPL-10-T
NRM
N
S
HPL-10-T
10⁻⁵ emu/g
HPL-12-T
NRM
N
S
HPL-12-T
10⁻⁵ emu/g

HPL-13-T
NRM
N
S
HPL-13-T
10^{-5} emu/g
HPL-15-T
NRM
N
S
HPL-15-T
10^{-5} emu/g
HPL-14-T
NRM
N
S
HPL-14-T
10^{-5} emu/g
HPL-16-T
NRM
N
S
HPL-16-T
10^{-5} emu/g

HPL-19-T
10⁻⁵ emu/g
NRM
N
S
HPL-19-T
HPL-20-T
10⁻⁵ emu/g
NRM
N
S
HPL-20-T
HPL-17-T
10⁻⁵ emu/g
NRM
N
S
HPL-17-T
HPL-18-T
10⁻⁵ emu/g
NRM
N
S
HPL-18-T

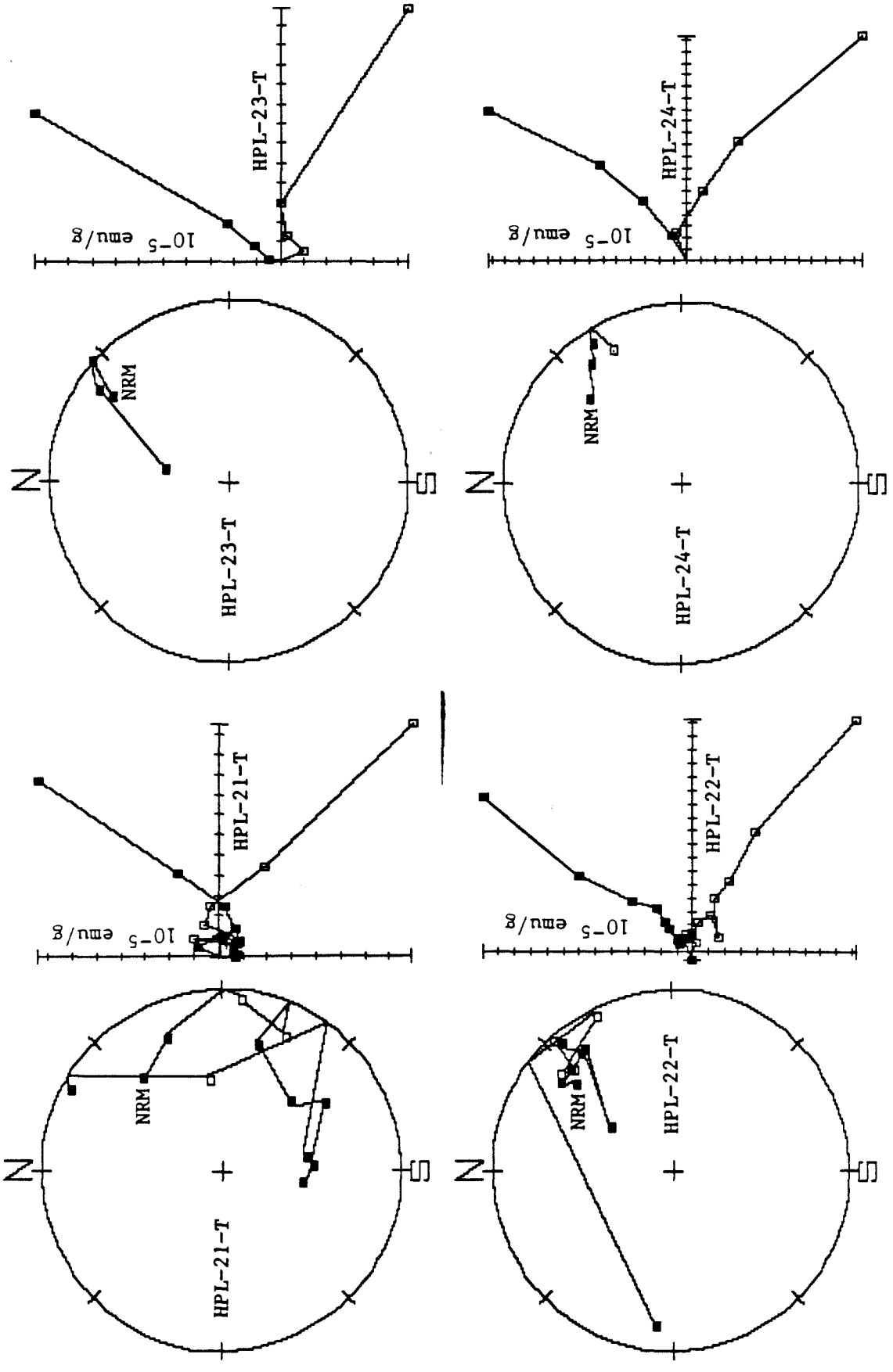
HPL-23-T
10⁻⁵ emu/g
NRM
N
S
HPL-23-T
HPL-24-T
10⁻⁵ emu/g
NRM
N
S
HPL-24-T
HPL-21-T
10⁻⁵ emu/g
NRM
N
S
HPL-21-T
HPL-22-T
10⁻⁵ emu/g
NRM
N
S
HPL-22-T

HPL-25-T
NRM
N
S
10⁻⁵ emu/g
HPL-25-T
HPL-27-T
NRM
N
S
10⁻⁵ emu/g
HPL-27-T
HPL-26-T
NRM
N
S
10⁻⁵ emu/g
HPL-26-T
HPL-28-T
NRM
N
S
10⁻⁵ emu/g
HPL-28-T

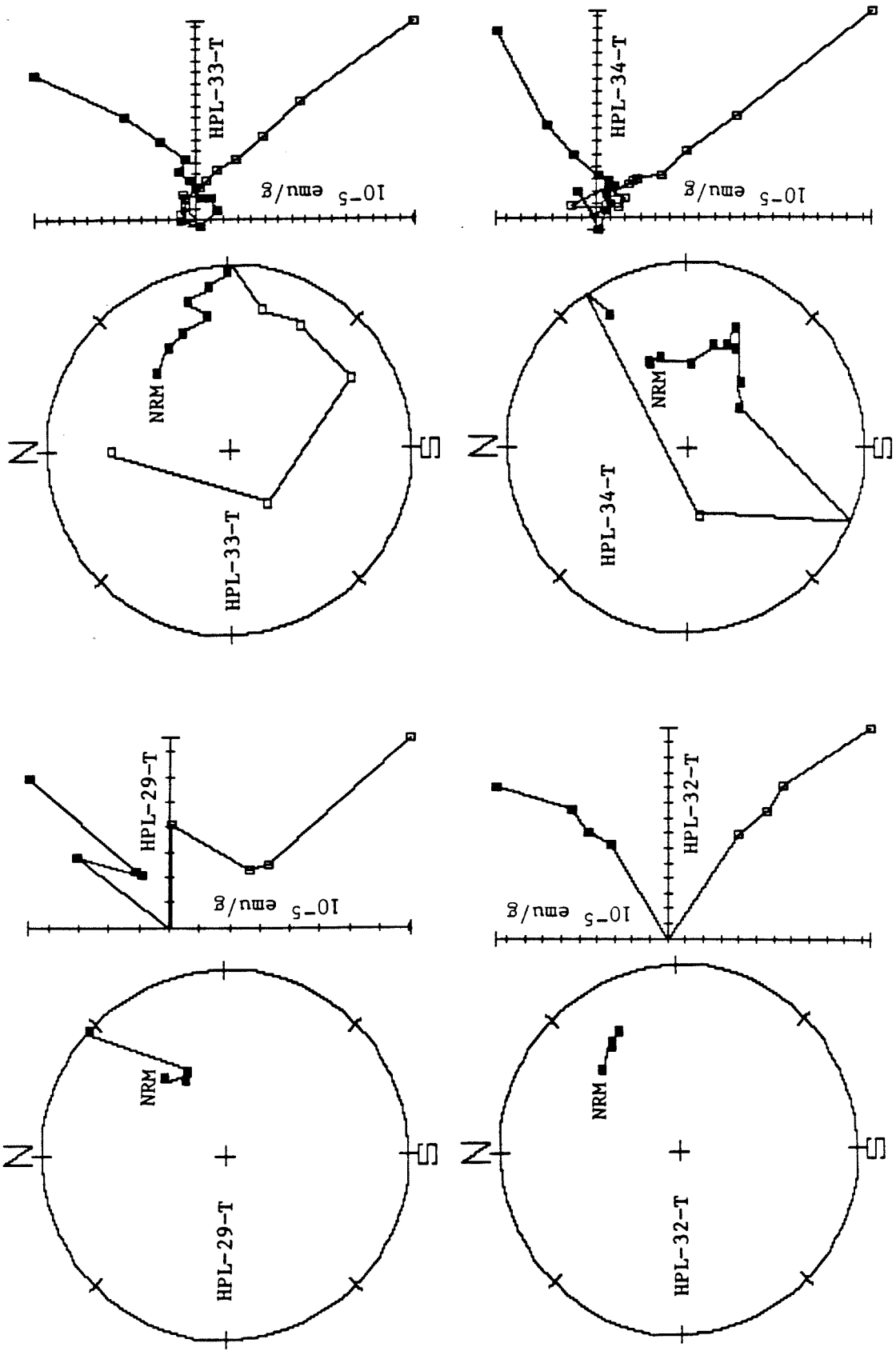
HPL-33-T
10⁻⁵ emu/g
NRM
N
S
HPL-33-T
HPL-34-T
10⁻⁵ emu/g
NRM
N
S
HPL-34-T
HPL-29-T
10⁻⁵ emu/g
NRM
N
S
HPL-29-T
HPL-32-T
10⁻⁵ emu/g
NRM
N
S
HPL-32-T

HPL-37-T
10⁻⁵ emu/g
NRM
HPL-37-T
N
S
HPL-38-T
10⁻⁵ emu/g
NRM
HPL-38-T
N
S
HPL-35-T
10⁻⁵ emu/g
NRM
HPL-35-T
N
S
HPL-36-T
10⁻⁵ emu/g
NRM
HPL-36-T
N
S

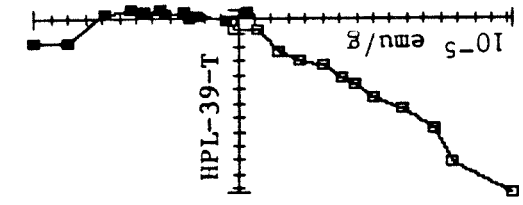
10⁻⁵ emu/g
HPL-39-T

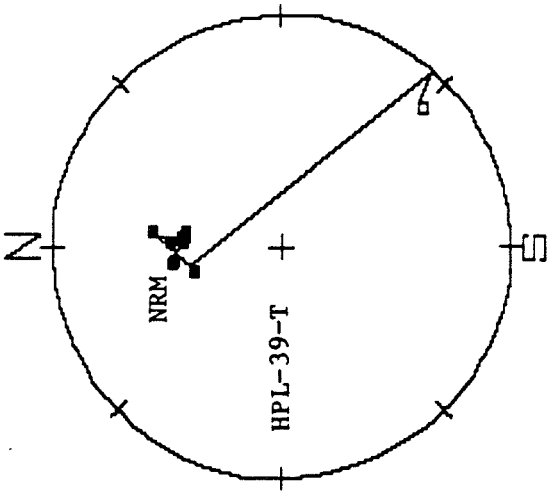
N
S
NRM
HPL-39-T

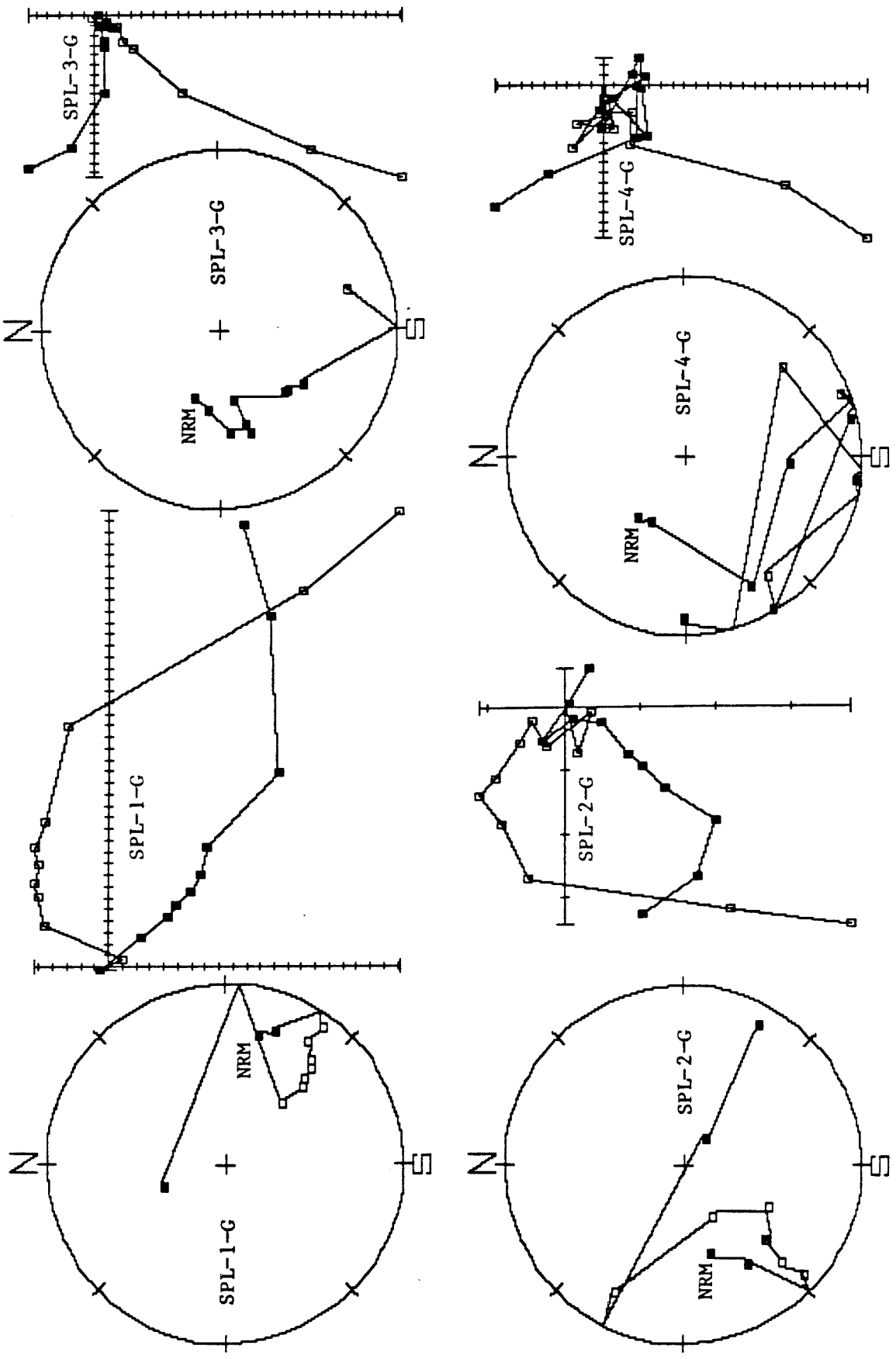
SPL-3-G
N
S
NRM
SPL-1-G
SPL-4-G
SPL-2-G

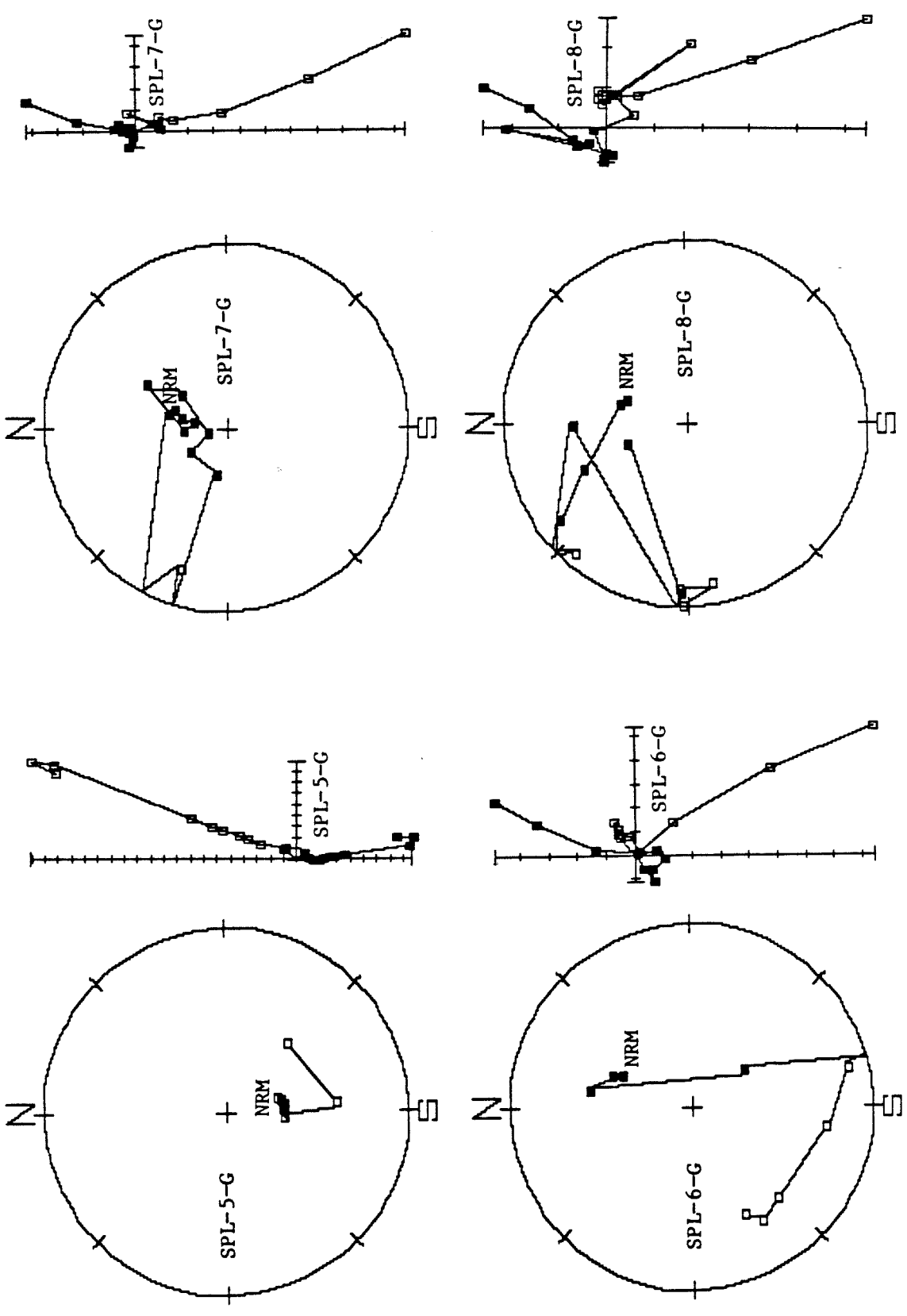
SPL-5-G
NRM
N
S
SPL-5-G
SPL-6-G
NRM
N
S
SPL-6-G
SPL-7-G
NRM
N
S
SPL-7-G
SPL-8-G
NRM
N
S
SPL-8-G

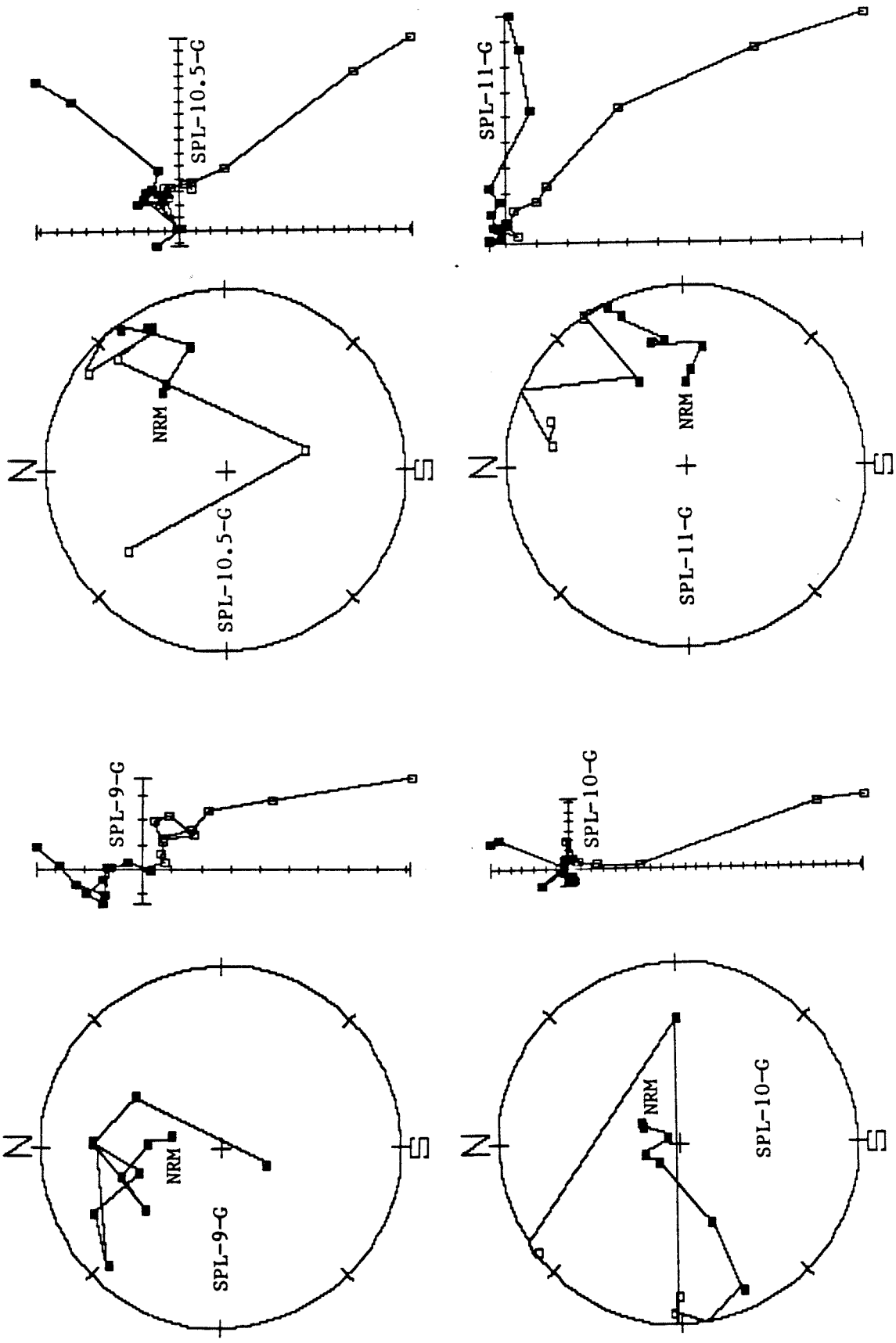
SPL-10.5-G
SPL-11-G
SPL-9-G
SPL-10-G
NRM
N
S

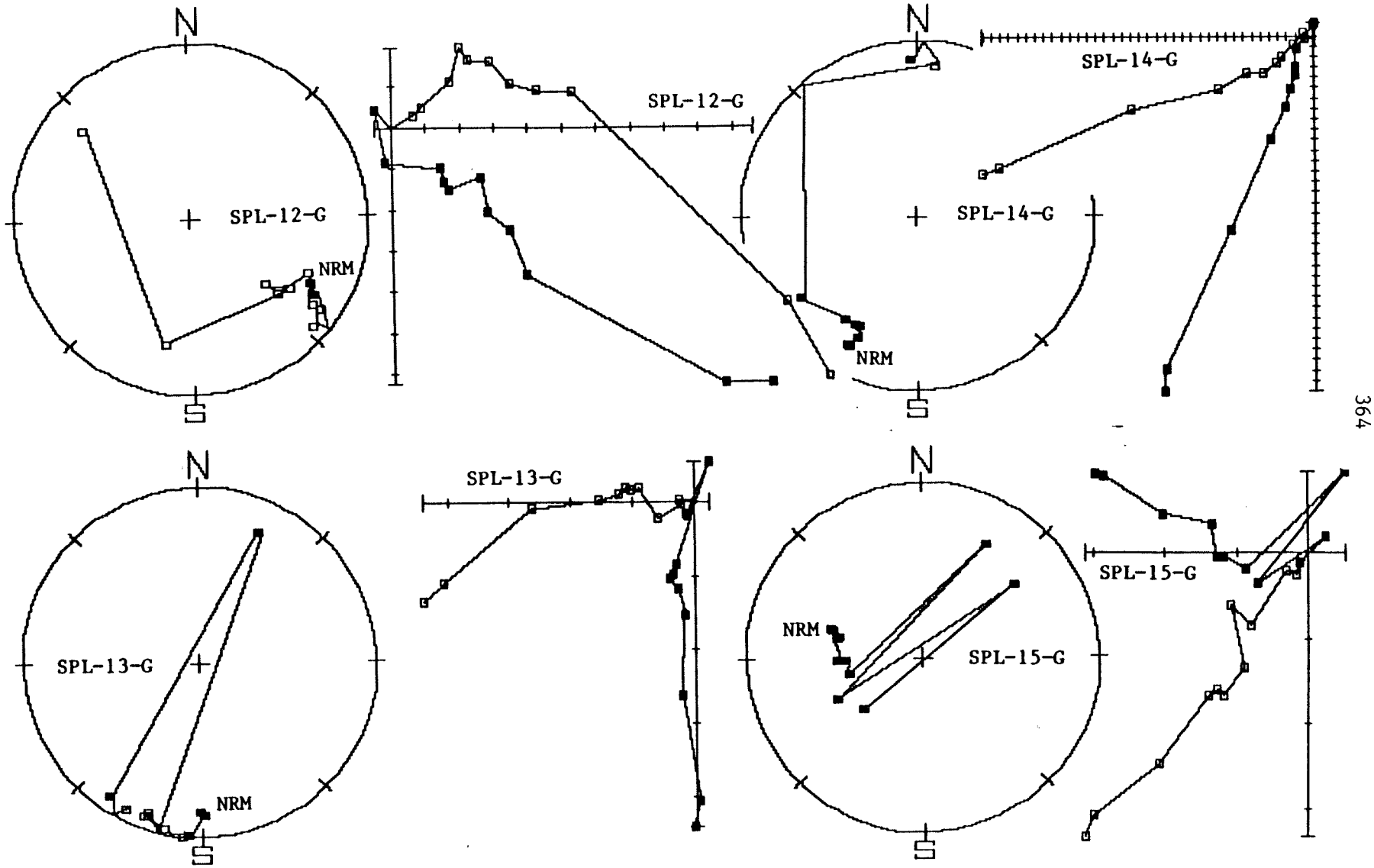
N
S
SPL-12-G
NRM
SPL-12-G
N
S
SPL-14-G
NRM
SPL-14-G
N
S
SPL-13-G
NRM
SPL-13-G
N
S
SPL-15-G
NRM
SPL-15-G

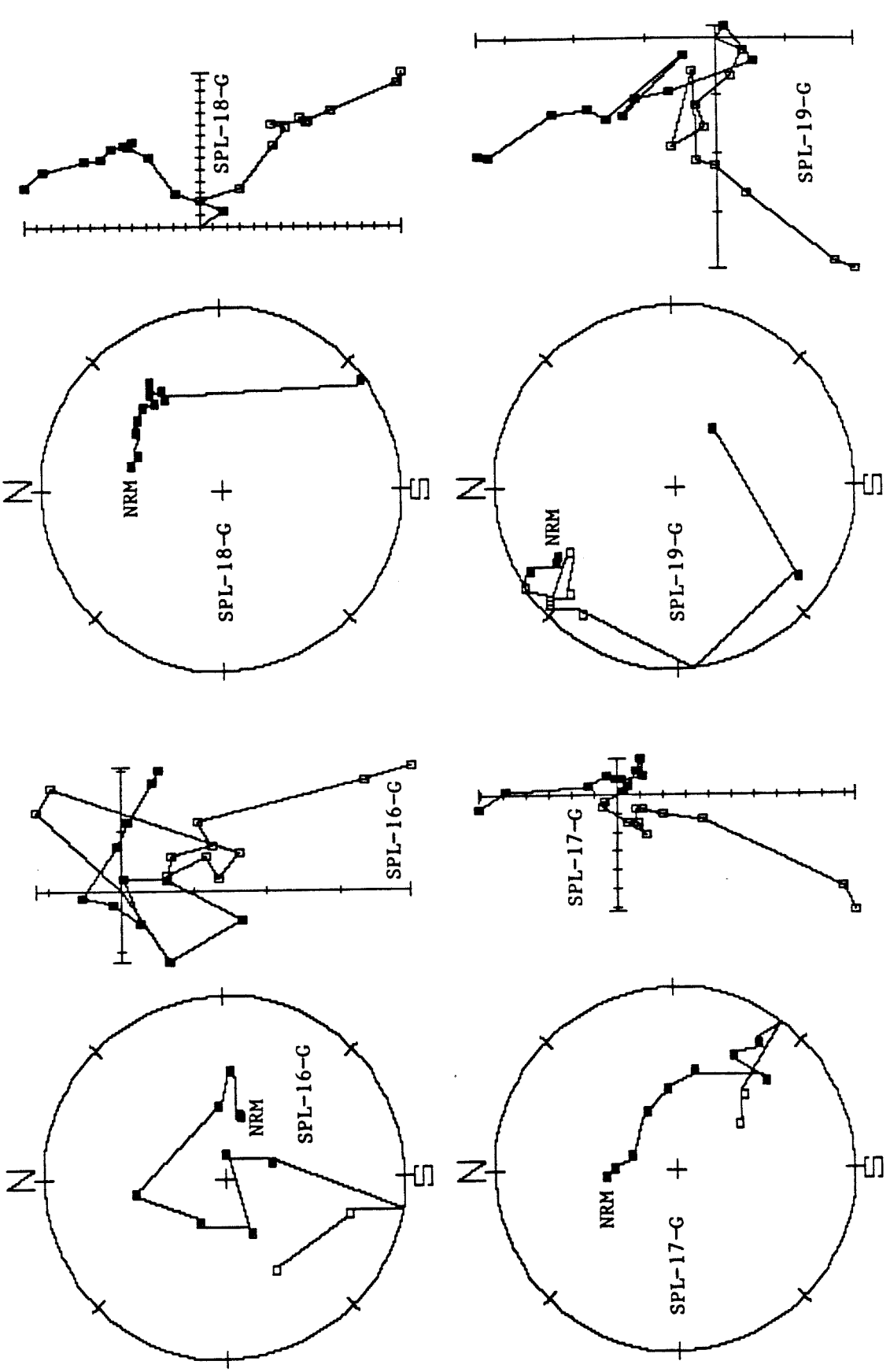
SPL-18-G
N
S
NRM
SPL-18-G
SPL-19-G
N
S
NRM
SPL-19-G
SPL-16-G
N
S
NRM
SPL-16-G
SPL-17-G
N
S
NRM
SPL-17-G

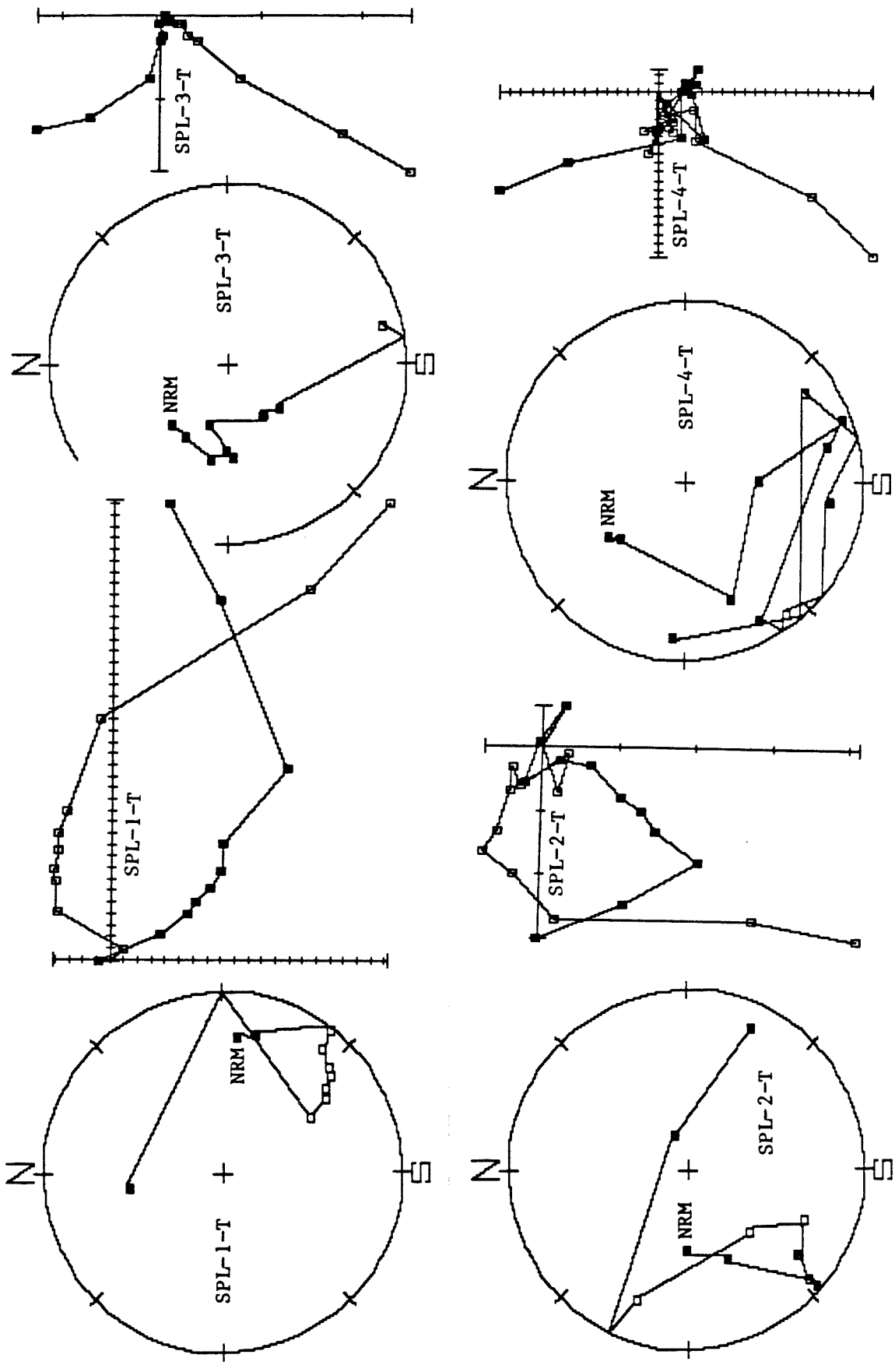
SPL-1-T
NRM
N
S
SPL-1-T
SPL-3-T
NRM
N
S
SPL-3-T
SPL-2-T
NRM
N
S
SPL-2-T
SPL-4-T
NRM
N
S
SPL-4-T

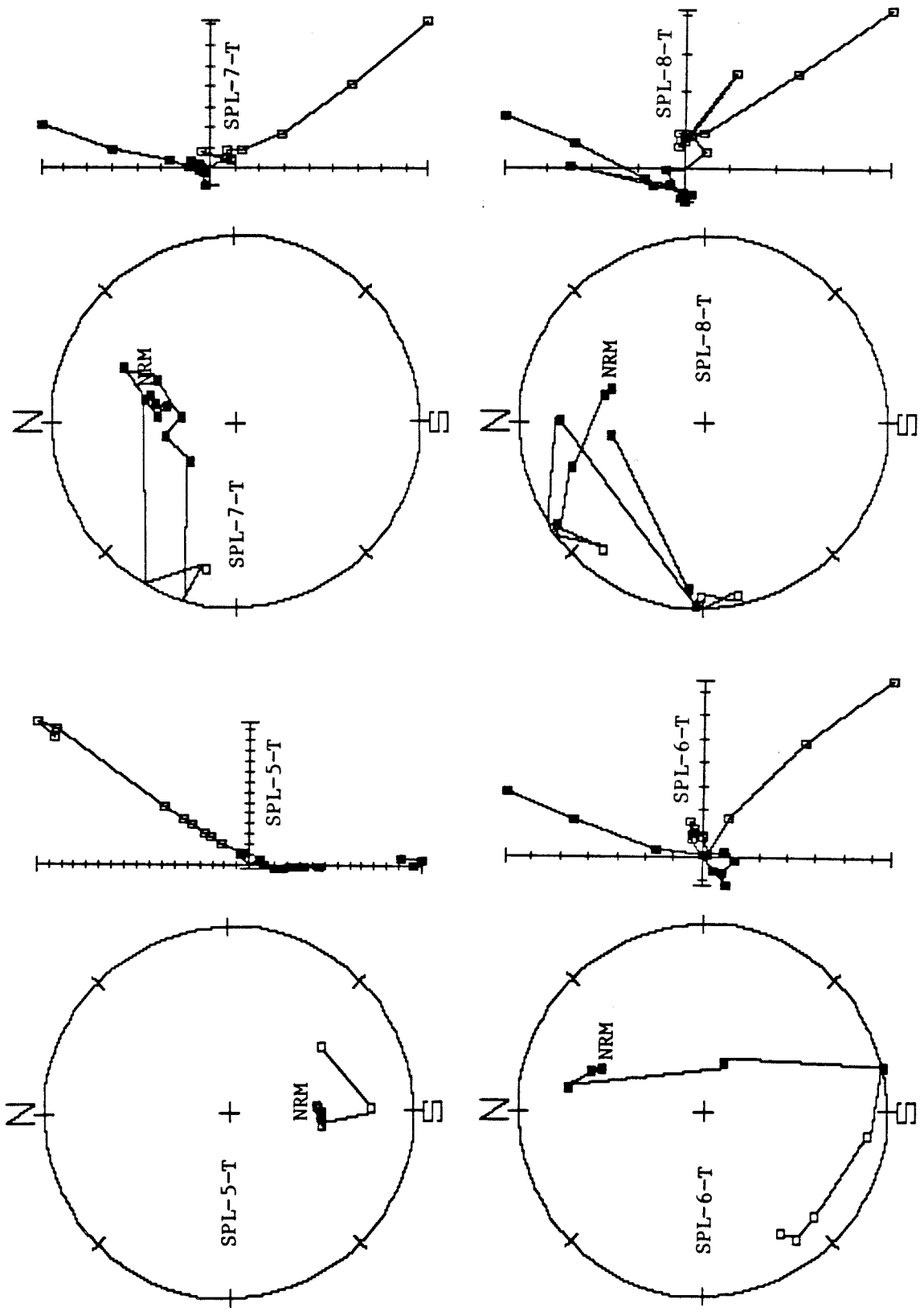
SPL-5-T
NRM
N
S
SPL-5-T
SPL-7-T
NRM
N
S
SPL-7-T
SPL-6-T
NRM
N
S
SPL-6-T
SPL-8-T
NRM
N
S
SPL-8-T

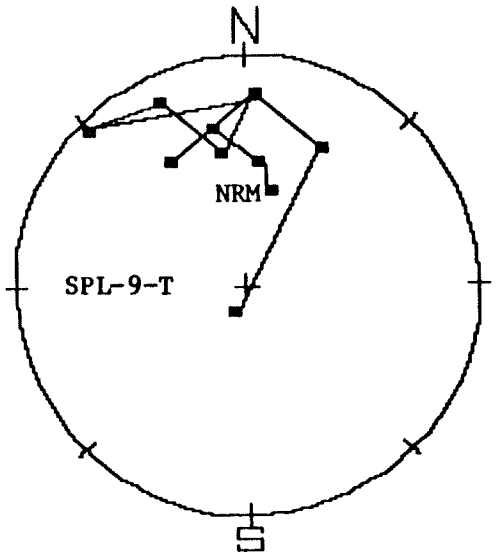
N
NRM
SPL-9-T
S

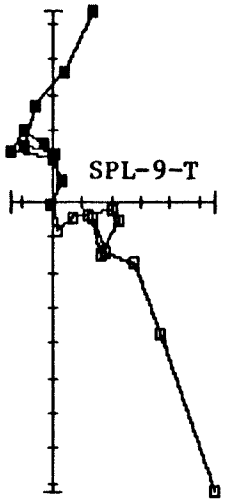
SPL-9-T

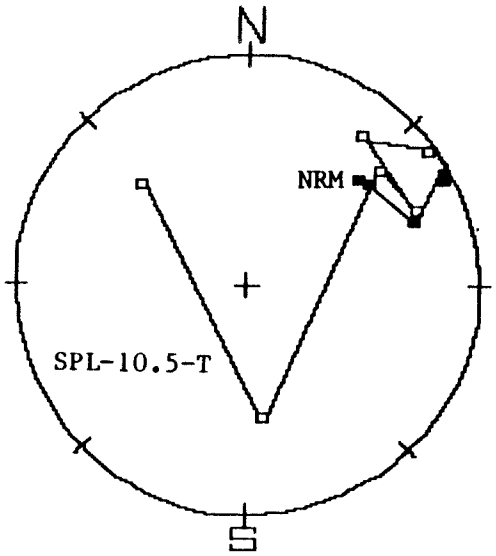
N
NRM
SPL-10.5-T
S

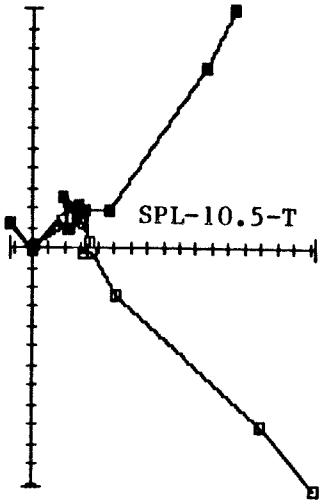
SPL-10.5-T

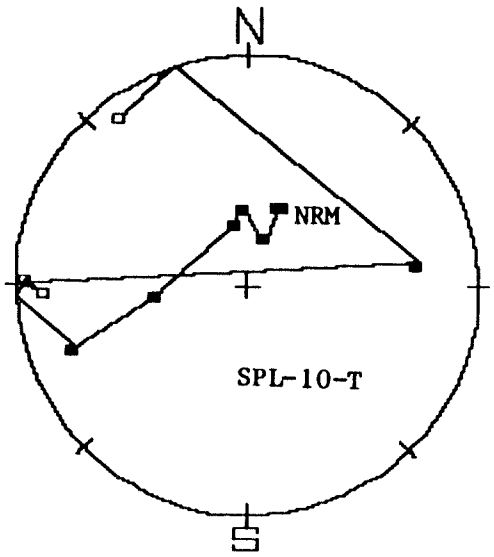
N
NRM
SPL-10-T
S

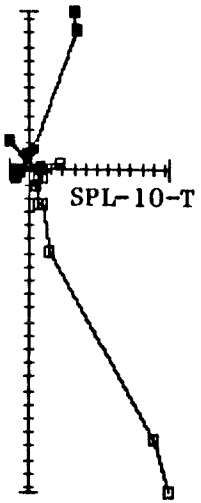
SPL-10-T

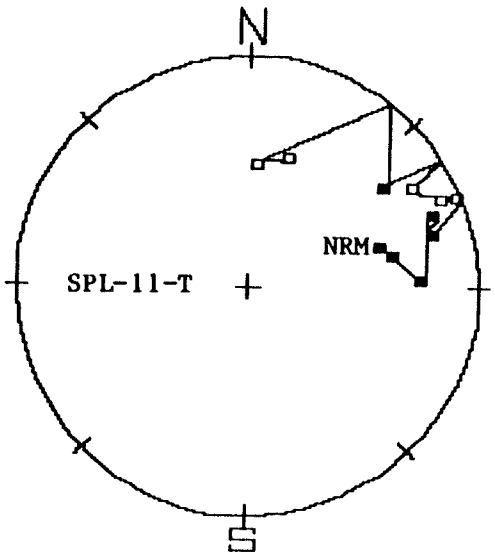
N
NRM
SPL-11-T
S

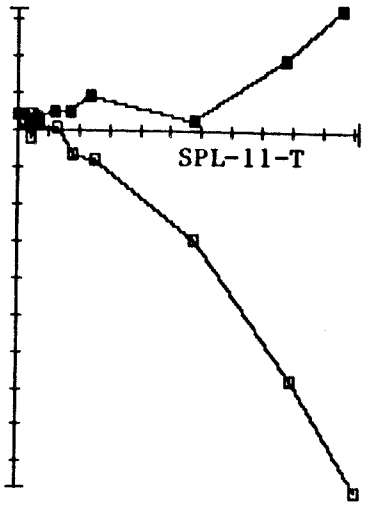
SPL-11-T

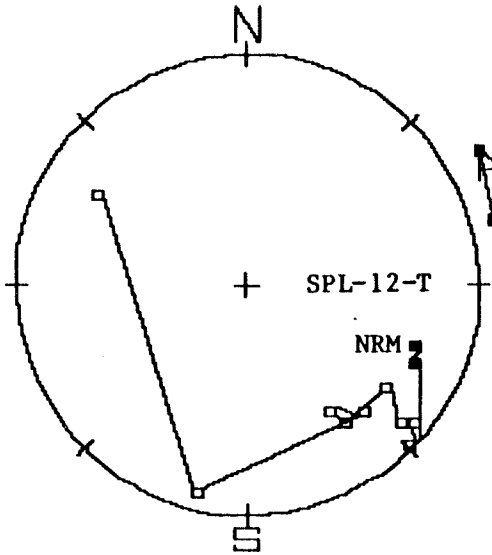
N
S
SPL-12-T
NRM

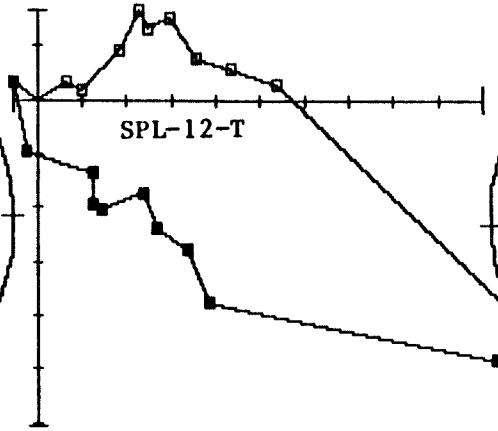
SPL-12-T

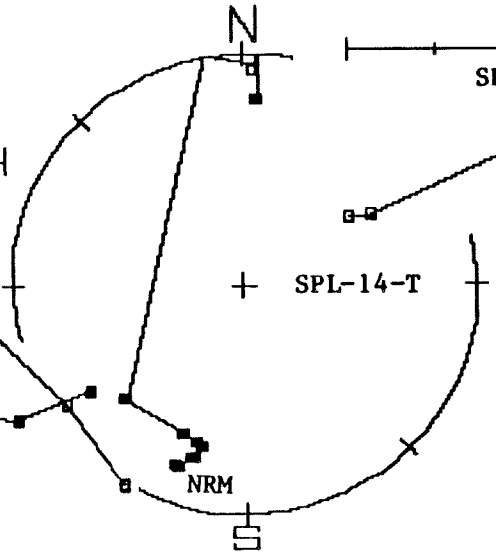
N
S
SPL-14-T
NRM

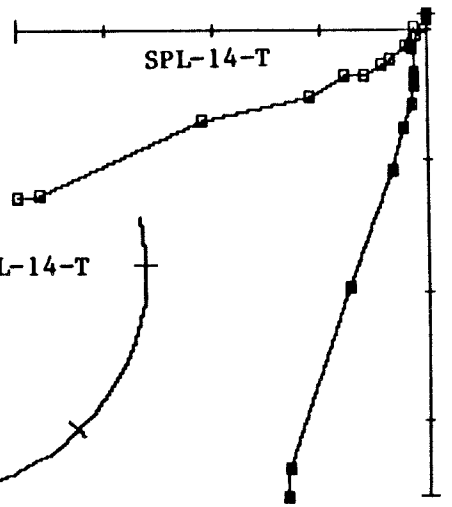
SPL-14-T

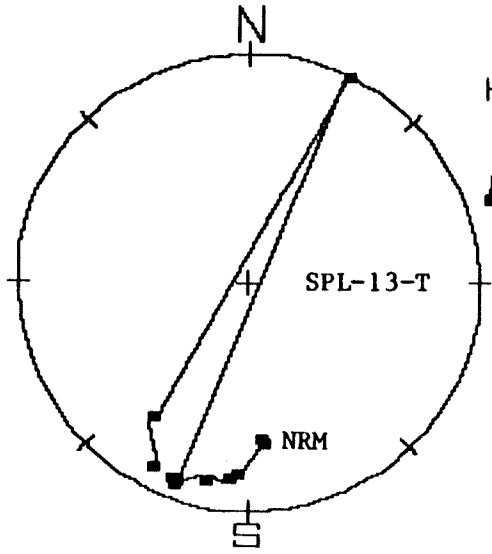
N
S
SPL-13-T
NRM

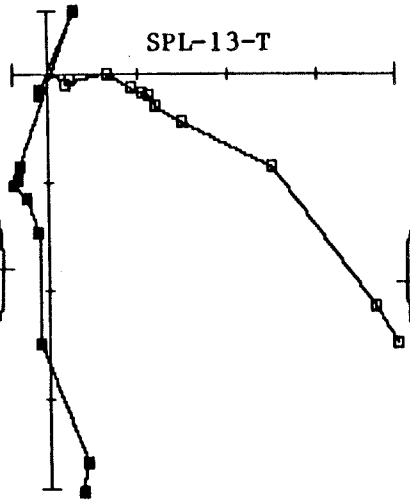
SPL-13-T

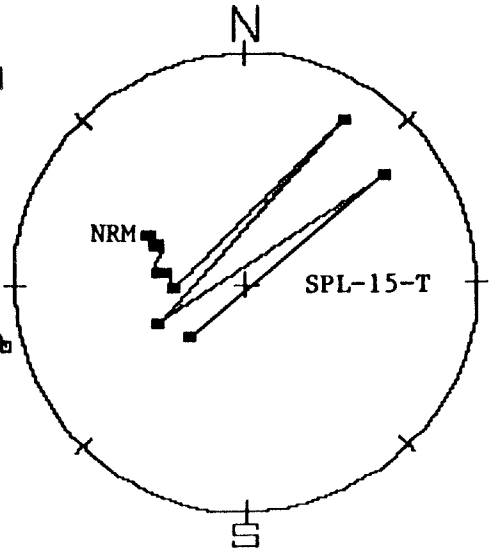
N
S
NRM
SPL-15-T

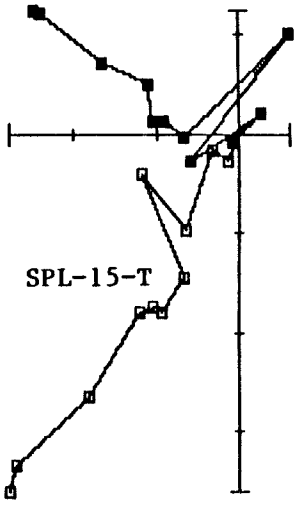
SPL-15-T

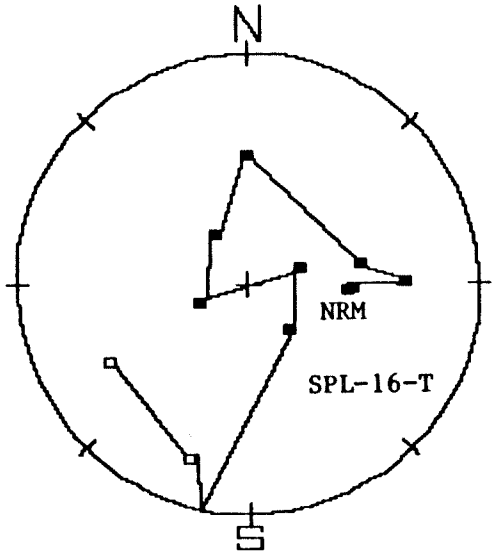
N
NRM
SPL-16-T
S

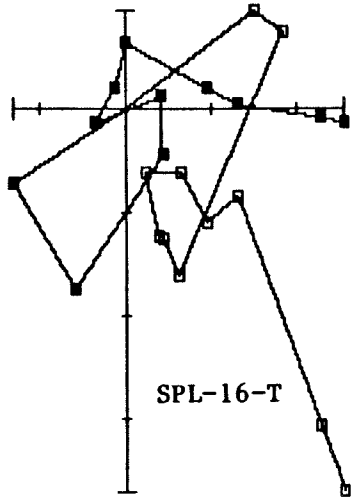
SPL-16-T

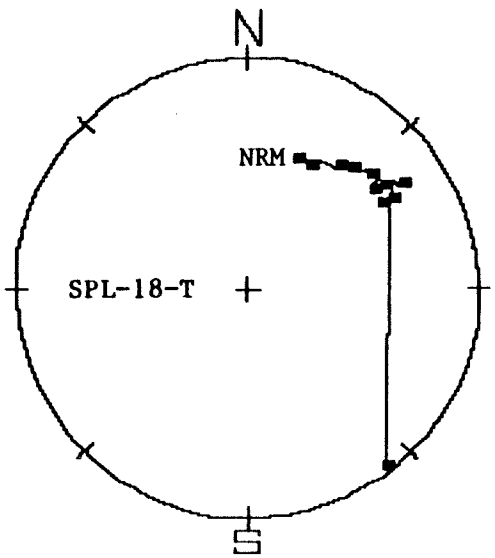
N
NRM
SPL-18-T
S

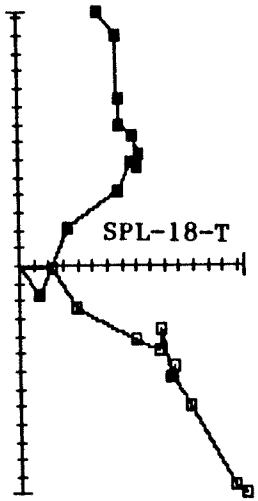
SPL-18-T

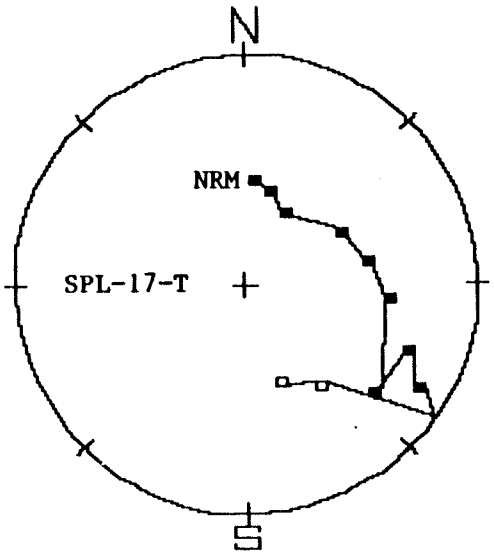
N
NRM
SPL-17-T
S

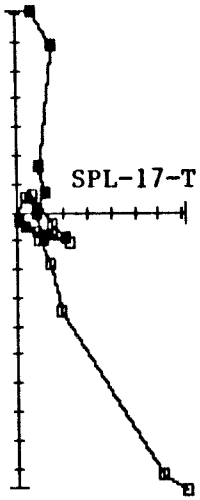
SPL-17-T

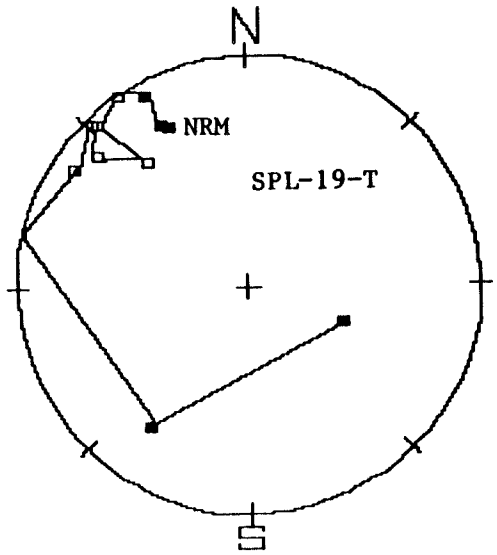
N
NRM
SPL-19-T
S

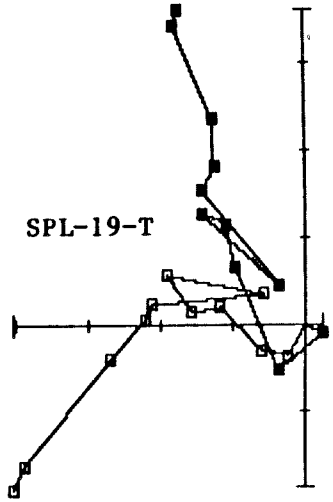
SPL-19-T

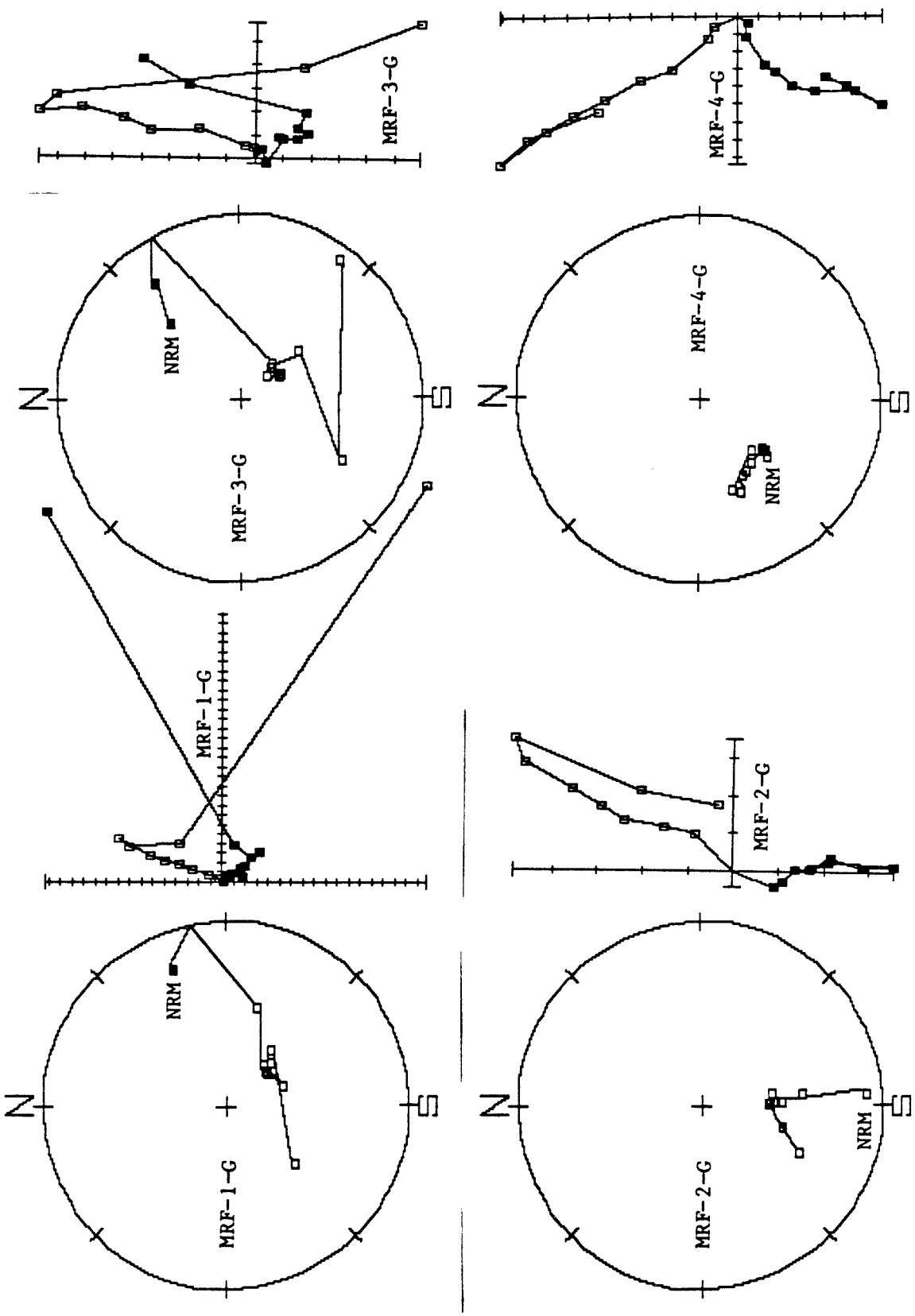
MRF-3-G
MRF-4-G
N
S
NRM
MRF-3-G
MRF-1-G
MRF-4-G
NRM
MRF-2-G
MRF-1-G
MRF-2-G
NRM

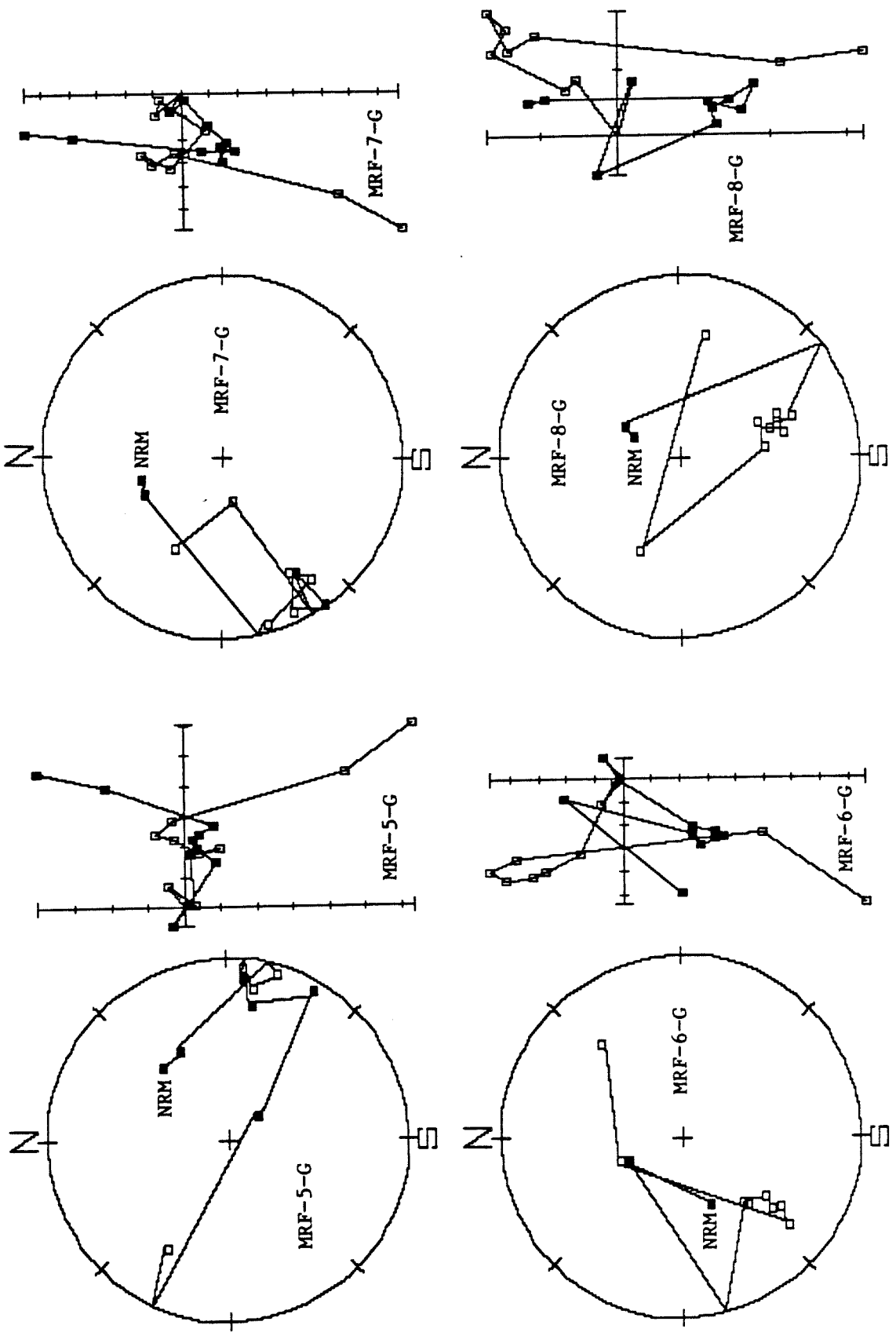
MRF-7-G
MRF-8-G
N
S
NRM
MRF-7-G
MRF-8-G
MRF-5-G
MRF-6-G

MRF-9-G
N
S
NRM
MRF-9-G
MRF-10-G
N
S
NRM
MRF-10-G

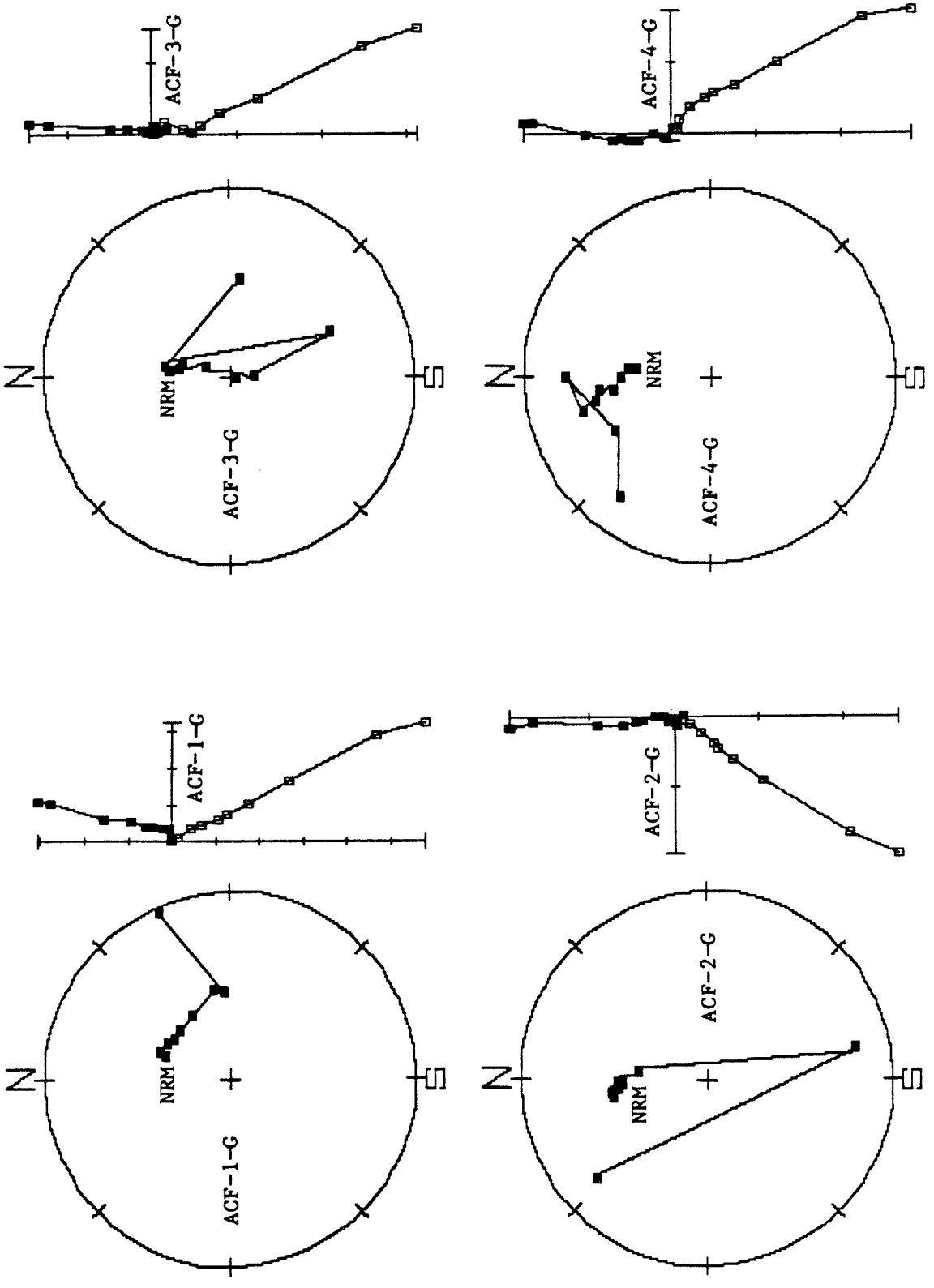
ACF-1-G
NRM
N
S
ACF-1-G
ACF-2-G
NRM
N
S
ACF-2-G
ACF-3-G
NRM
N
S
ACF-3-G
ACF-4-G
NRM
N
S
ACF-4-G

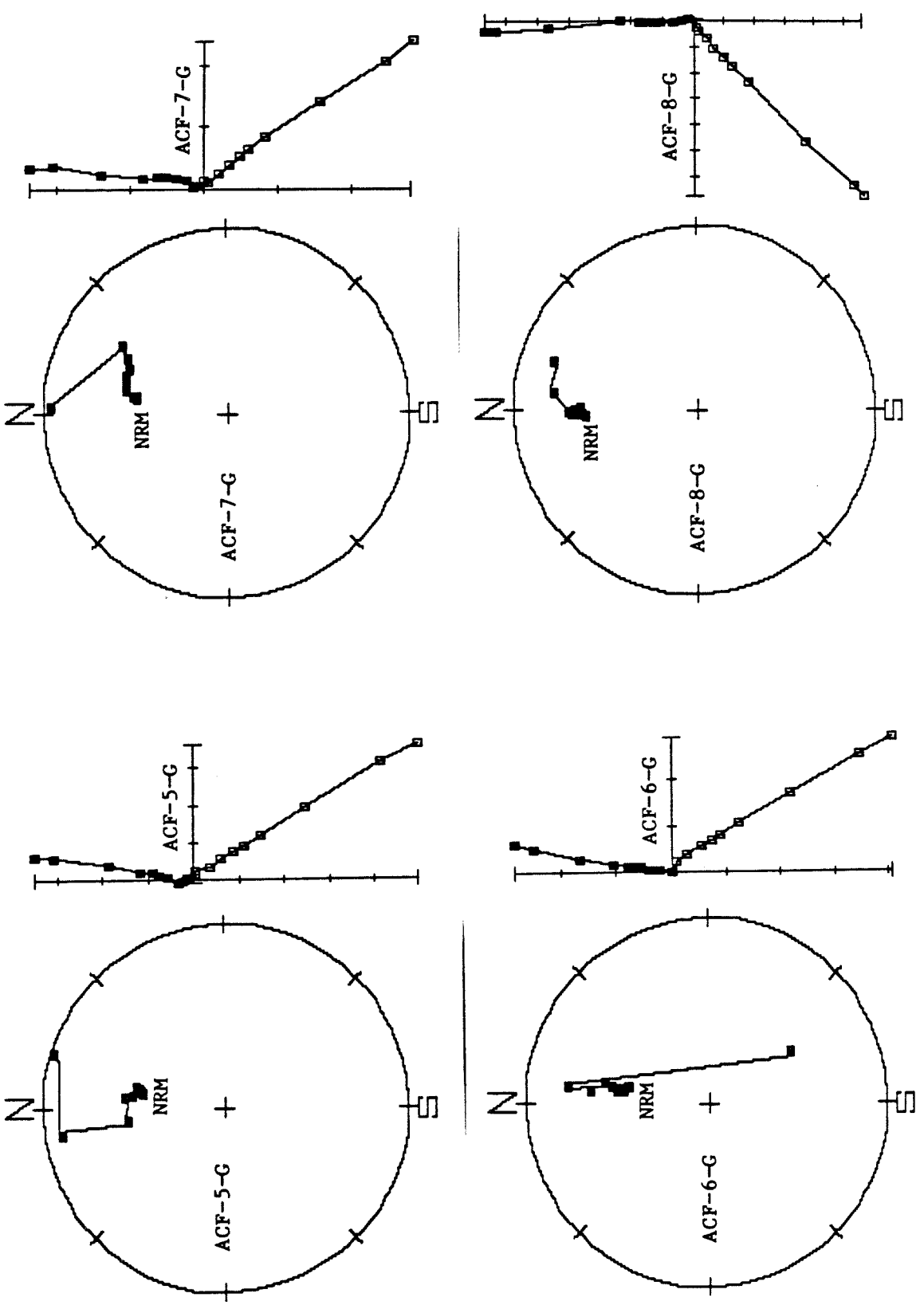
ACF-7-G
N
NRM
S
ACF-7-G
ACF-8-G
N
NRM
S
ACF-8-G
ACF-5-G
N
NRM
S
ACF-5-G
ACF-6-G
N
NRM
S
ACF-6-G

RSR-1-T
RSR-2-T
N
S
NRM
RSR-1-T
RSR-2-T
RSR-1-G
RSR-2-G
NRM
RSR-1-G
RSR-2-G

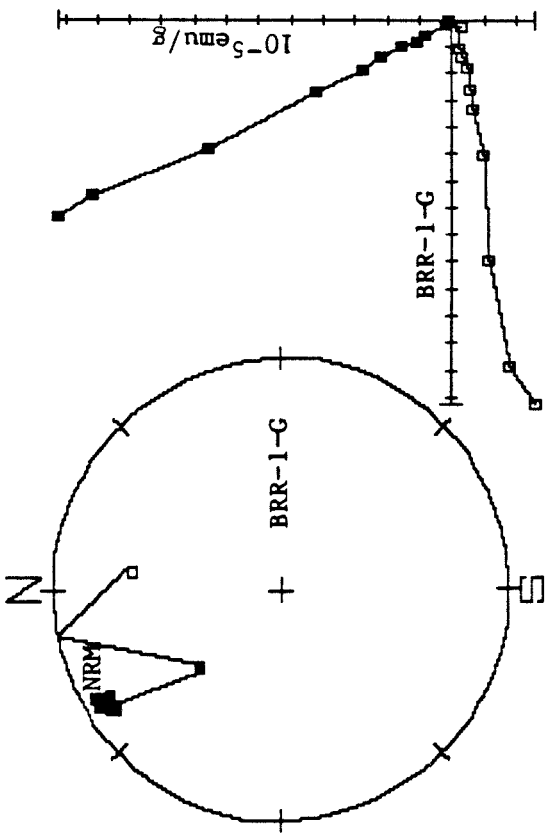
10^-5emu/g
BRR-1-G
BRR-1-G
N
S
NRM

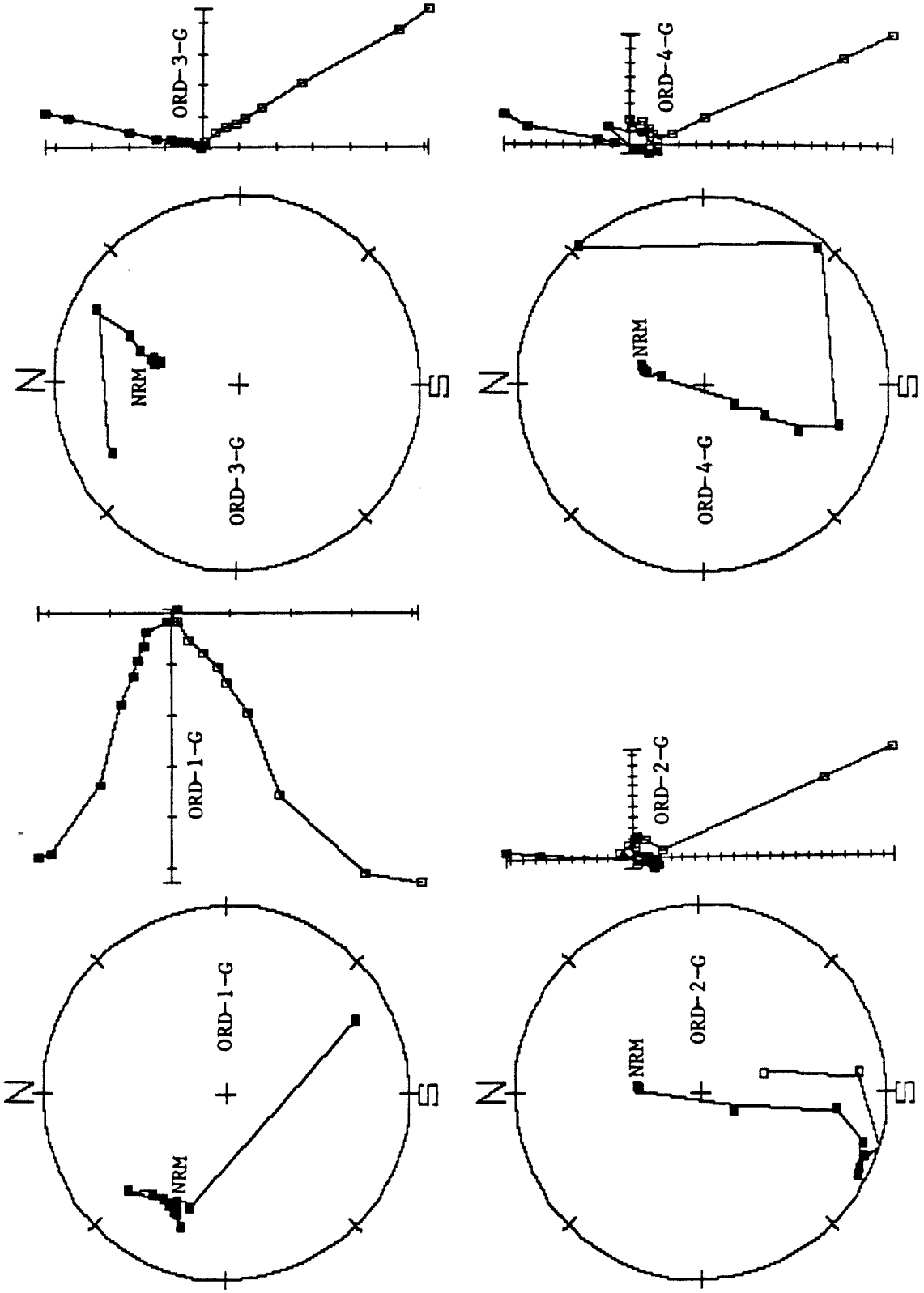
ORD-3-G
N
S
NRM
ORD-3-G
ORD-4-G
N
S
NRM
ORD-4-G
ORD-1-G
N
S
NRM
ORD-1-G
ORD-2-G
N
S
NRM
ORD-2-G

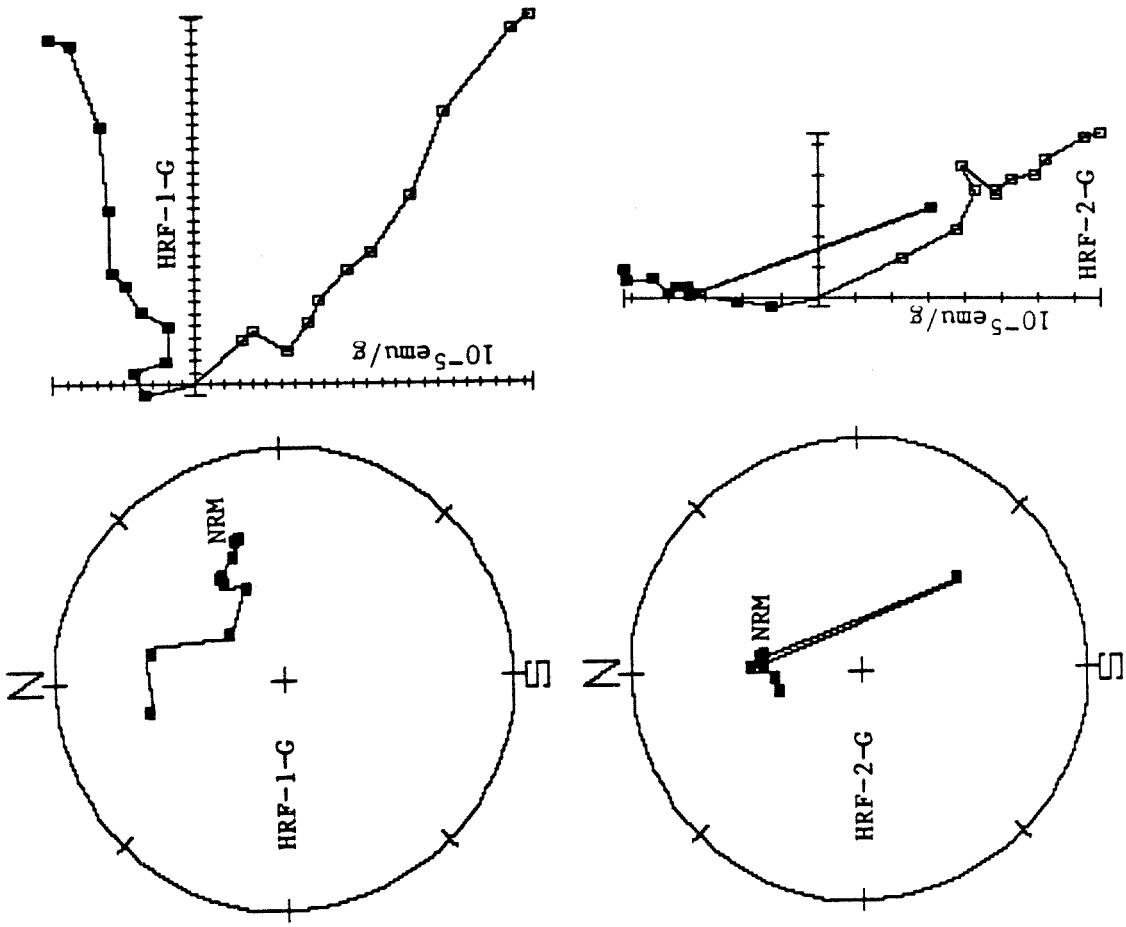
HRF-1-G
10⁻⁵emu/g
HRF-2-G
10⁻⁵emu/g
N
S
NRM
HRF-1-G
N
S
NRM
HRF-2-G

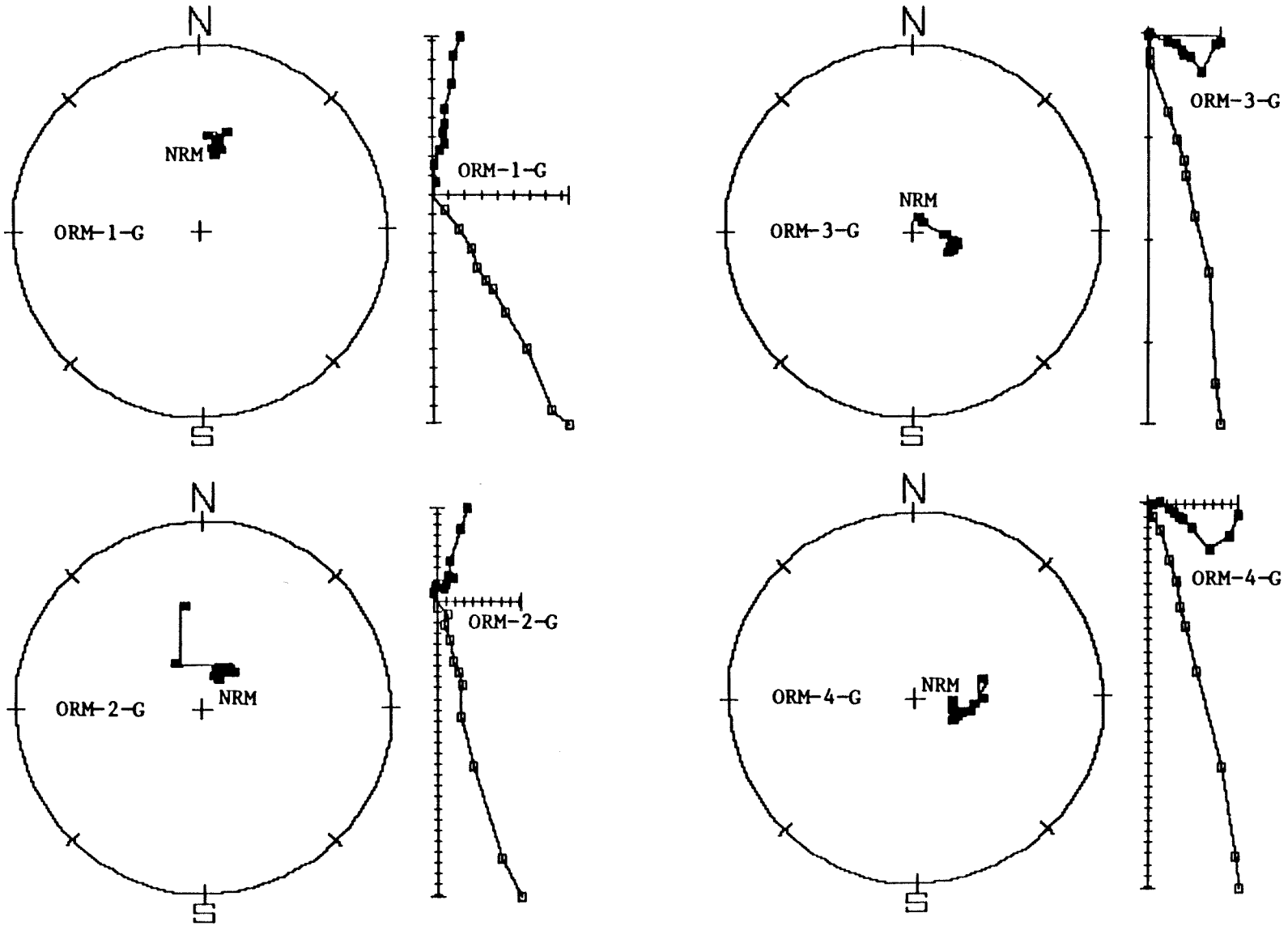
N
NRM
ORM-1-G
S
ORM-1-G
N
NRM
ORM-3-G
S
ORM-3-G
N
ORM-2-G
NRM
S
ORM-2-G
N
ORM-4-G
NRM
S
ORM-4-G

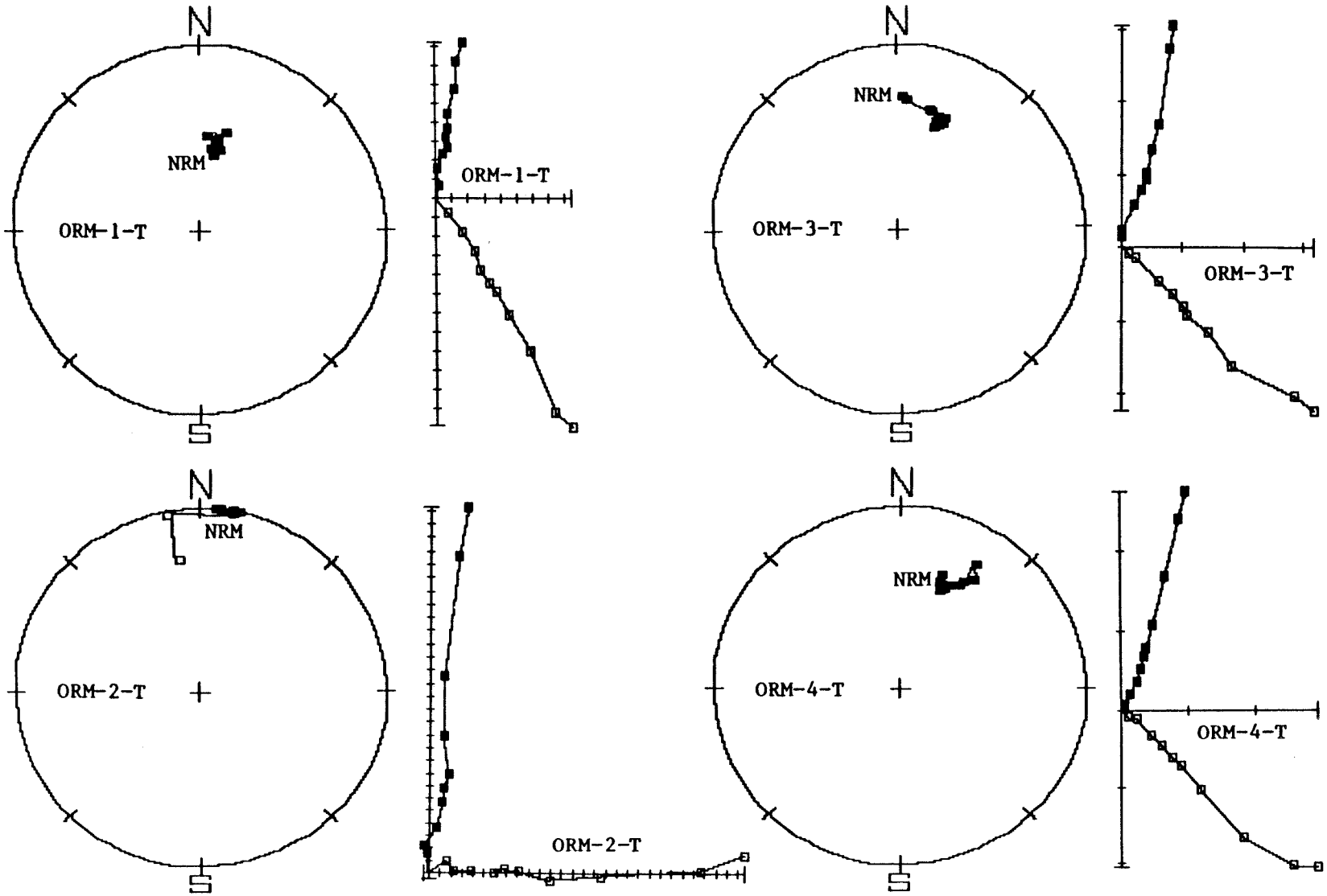
N
NRM
ORM-1-T
S
ORM-1-T
N
NRM
ORM-3-T
S
ORM-3-T
N
NRM
ORM-2-T
S
ORM-2-T
N
NRM
ORM-4-T
S
ORM-4-T

APPENDIX B

STRATIGRAPHIC AND GEOMORPHIC LOCALITIES

This appendix contains section, range and township locations and a brief description of stratigraphic and geomorphic features bearing a superscripted locality number in Chapters II and III. The numbers correspond to circled numbers with arrows indicating exact locations on Plates 1A and 1B.

Plate	Locality	Location	Brief Description of Feature
1A	1	NW1/4 of SW1/4 SEC 12 R5W T2N	hornblendite inclusions in qtz-monzonite in roadcut on HWY 138. Silverwood Lake.
1B	2	SE1/4 of NE1/4 SEC 33 R3W T4N	quartz-syenite sheet parallel to foliation, W of ridgecrest. Turtle Canyon, Ord Mtns.
1A	3	SE1/4 of NW1/4 SEC 8 R3W T3N	hornblende-diorite exposure, southwest side of SCE power-line road. Ord Mtns.
1B	4	NE1/4 of NE1/4 SEC 29 R2W T4N	hornblende-diorite exposure, cut for water main on section line. Milpas Rd area.
1B	5	SW1/4 of NE1/4 SEC 36 R2W T4N	hornblende-quartz-monzonite in natural exposure south of High Rd at Sky High Ranch.
1B	6	NW1/4 of NE1/4 SEC 9 R3W T3N	dolomitic marble exposure in foundation for SCE power-line tower. Ord Mtns.
1A	7	SW1/4 of SW1/4 SEC 4 R3W T3N	phyllite with interbedded marble & quartzite in streamcut canyon exposures. Ord Mtns.
1B	8	NW1/4 of NW1/4 SEC 34 R3W T4N	hornfelsic calc-silicate in natural exposure W of ridge-crest. Turtle Cyn, Ord Mtns.
1A	9	NE1/4 of NW1/4 SEC 9 R3W T3N	quartzite in natural exposure just below ridge-crest in phyllite. Ord Mtns.
1B	10	SE1/4 of NW1/4 SEC 33 R3W T4N	stromatolite *conophyta* collected in float derived from dolomitic marbles. Turtle Cyn, Ord Mtns.

Plate	Locality	Location	Brief Description of Feature
1A	11	NW1/4 of NW1/4 SEC 8 R3W T3N	coarse-grained, milky white quartzite exposed in roadcut for SCE power-line road. Ord Mtns.
1A	12	NE1/4 of NE1/4 SEC 8 R3W T3N	gray pelitic granofels exposed in roadcut of access road to SCE power-line tower. Ord Mtns.
1A	13	NW1/4 of NW1/4 SEC 8 R3W T3N	biotite-sillimanite gneiss in natural exposures just west of SCE powerline road. Ord Mtns.
1A	14	NE1/4 of NE1/4 SEC 9 R3W T3N	phyllonite with intense folding and boudinage in stream-cut canyon walls. Ord Mtns.
1A	15	NW1/4 of NW1/4 SEC 4 R4W T2N	hornblende-biotite granodiorite in quarry for Cedar Springs Dam rip-rap. Silverwood Lake.
1A	16	NE1/4 of NW1/4 SEC 15 R4W T2N	medium-grained biotite-quartz-monzonite in roadcut on Hwy 138. Miller Canyon.
1A	17	NE1/4 of NE1/4 SEC 10 R4W T2N	marble pendant with dikes, skarn and mineralization in USFS access road. Miller Canyon, Pilot Rock.
1A	18	NE1/4 of SW1/4 SEC 33 R4W T3N	epidote-filled fractures in migmatitic granodiorite in roadcut on USFS 2N33. Silverwood Lake.
1B	19	NW1/4 of SE1/4 SEC 31 R4W T4N	porphyritic biotite-quartz-monzonite of Rattlesnake Mountain Pluton in foundation of SCE tower. Bowen Ranch Road.
1A	20	SE1/4 of NW1/4 SEC 1 R5W T2N	cataclastic gneiss traceable to batholithic protolith in roadcut on USFS 3N40. Cleghorn Valley.
1B	21	SW1/4 of NE1/4 SEC 28 R2W T4N	"granulite" and "alaskite"(MacColl, 1964) in foundation of SCE power-line tower. Milpas area.
1A	22	SE1/4 of NE1/4 SEC 12 R6W T2N	San Francisquito(?) Formation exposed in cut for AT&SF railway line. Cajon Creek.
1A	23	SE1/4 of SE1/4 SEC 26 R6W T3N	Unit 1 of lower Crowder Formation exposed in roadcut for Hwy 138 Cajon Pass.

Plate	Locality	Location	Brief Description of Feature
1A	24	SW1/4 of NW1/4 SEC 25 R7W T3N	Unit 2 of lower Crowder Formation in natural streamcut exposure in Crowder Canyon. Cajon Pass.
1A	25	NW1/4 of NW1/4 SEC 25 R7W T3N	Unit 3 of lower Crowder Formation in natural streamcut exposure in Crowder Canyon. Cajon Pass.
1A	26	SE1/4 of SE1/4 SEC 23 R7W T3N	Unit 4 of lower Crowder Formation in cut for AT&SF railway line. Cajon Pass.
1A	27	NE1/4 of NE1/4 SEC 7 R4W T2N	lower(?) Crowder Formation on grus on granodiorite at intake tower. Silverwood Lake
1A	28	SW1/4 of SE1/4 SEC 33 R4W T3N	lower(?) Crowder Formation on migmatitic granodiorite on USFS 2N33. Silverwood Lake.
1A	29	SE1/4 of SE1/4 SEC 26 R6W T3N	mid- to upper Miocene fauna in Unit 1 of lower Crowder Fm. at CalTrans borrow site. Cajon Pass.
1A	30	NE1/4 of NE1/4 SEC 27 R4W T3N	volcanogenic siltstones and tuff in borrow site for earth dam on Las Flores Ranch. Summit Valley.
1A	31	NW1/4 of SW1/4 SEC 26 R4W T3N	fine-grained sandstone in natural exposures W of Hwy 173 on Las Flores Ranch. Summit Valley.
1A	32	NE1/4 of SW1/4 SEC 24 R4W T3N	swelling claystones in streamcut exposure N of Arrowhead Hwy at Hwy 173. Summit Valley.
1A	33	NE1/4 of SW1/4 SEC 27 R4W T3N	tuffs interfingered with arkose on abandoned haul road, Las Flores Ranch. Summit Valley.
1A	34	NE1/4 of NE1/4 SEC 27 R4W T3N	Collection site for tuff yielding fission-track age of 3.8 ± 0.4 my, Las Flores Ranch. Summit Valley.
1A	35	SE1/4 of SE1/4 SEC 23 R4W T3N	quartz-monzonite boulders in volcanogenic section, Mojave River Forks Campground. Summit Valley.
1B	36	SW1/4 of SW1/4 SEC 19 R1E T4N	western facies of Old Woman Sandstone in natural exposures south of Hwy 18. Lucerne Valley.

Plate	Locality	Location	Brief Description of Feature
1B	37	SW1/4 of SE1/4 SEC 30 R4W T4N	fine-grained sediments in natural and roadcut exposure under terrace gravel on Bowen Ranch Road.
1A	38	SE1/4 of SE1/4 SEC 18 R6W T3N	Harold Formation exposed in roadcut for SCE power-line road N of Hwy 138. Cajon Pass.
1A	39	NE1/4 of SE1/4 SEC 18 R6W T3N	gradational contact between Harold Fm. and Shoemaker Gravel off SCE power-line road. Cajon Pass.
1A	40	NE1/4 of SW1/4 SEC 20 R6W T3N	Shoemaker Gravel exposed in roadcut for SCE power-line road at Cajon Pass.
1A	41	SW1/4 of NW1/4 SEC 17 R6W T3N	Old Alluvium unconformably overlying Shoemaker Gravel in roadcut for gas pipeline road. Cajon Pass.
1A	42	NE1/4 of NE1/4 SEC 7 R3W T3N	Deep Creek facies of Ord River Gravel exposed in roadcut for SCE power-line road. Ord Mtns.
1B	43	NE1/4 of NW1/4 SEC 32 R3W T4N	Summit Valley facies of Ord River Gravel exposed in streamcut exposure. Apple Valley Highlands.
1B	44	NE1/4 of NW1/4 SEC 22 R3W T4N	Ocotillo Ridge deposits exposed in roadcut at intersection of Ocotillo and Pioneer Roads. Marianas Rancho.
1B	45	NE1/4 of SE1/4 SEC 21 R3W T4N	basalt and syenite clasts in Ocotillo Rodge deposits in natural exposure. Marianas Rancho.
1B	46	NE1/4 of SW1/4 SEC 16 R2W T4N	Milpas Ridge deposits exposed in cut for AT&SF railway line. Milpas area.
1B	47	SE1/4 of SW1/4 SEC 16 R2W T4N	rounded quartzite clasts in Milpas Ridge deposits, in natural gulley exposure. Milpas area.
1B	48	NW1/4 of SE1/4 SEC 16 R2W T4N	quartz-monzonite boulders in debris-flow deposits overlying Milpas Ridge deposits in cut for AT&SF railway line. Milpas area.

Plate	Locality	Location	Brief Description of Feature
1B	49	NW1/4 of NE1/4 SEC 36 R2W T4N	arkose in roadcut for spring access road at Sky High Ranch, S end of High Road. Fifteenmile Valley.
1B	50	SE1/4 of SW1/4 SEC 23 R2W T4N	arkose in roadcut for SCE power-line road at Grapevine Canyon. Fifteenmile Valley.
1A	51	SE1/4 of SW1/4 SEC 5 R4W T2N	rounded residual boulders in matrix of grus. 2N33 on Pilot Rock ridge.
1A	52	NE1/4 of NE1/4 SEC 7 R4W T2N	angular fragments of granodiorite in thick grus layer west of intake tower. Silverwood Lake
1A	53	SE1/4 of SW1/4 SEC 18 R4W T2N	fault-bounded wedge of Crowder Fm overlying relict erosion surface. W of Cedar Pines Park.
1B	54	NW1/4 of NW1/4 SEC 3 R3W T3N	surface of subdued relief with deep weathering profile. Ord Mountains.
1B	55	NW1/4 of SW1/4 SEC 32 R2W T4N	rounded lag gravel on ridge bounded by faults. Arrastre Canyon.
1A	56	SW1/4 of NW1/4 SEC 6 R4W T2N	remnants of rounded-cobble-bearing gravel in headless stream course. W of Silverwood Lake.
1A	57	NE1/4 of SE1/4 SEC 6 R4W T2N	remnants of rounded-cobble-bearing gravel on flat-topped ridges. W shore of Silverwood Lake.
1A	58	NW1/4 of NE1/4 SEC 29 R5W T3N	terrace gravel containing Pelona Schist clasts deposited on Crowder Fm. Deep soil. Summit Valley.
1A	59	NE1/4 of SW1/4 SEC 27 R4w T3N	Pelona-Schist-bearing terrace gravel on volcanogenic Crowder Fm. Las Flores Ranch.
1A	60	SE1/4 of SW1/4 SEC 14 R4W T3N	cut terrace level expressed in bluff of Mojave River. W of Deep Creek Dam.
1A	61	SE1/4 of SE1/4 SEC 13 R4W T3N	low terrace level expressed in gravel S of W dike of Deep Creek Dam.

Plate	Locality	Location	Brief Description of Feature
1A	62	NE1/4 of SW1/4 SEC 7 R3W T3N	angular fanglomerate interfingering with rounded-cobble-conglomerate. E of Deep Creek Rd.
1A	63	NE1/4 of NW1/4 SEC 7 R3W T3N	angular fan gravel overlying Pelona-bearing conglomerate in roadcut for SCE powerline road.
1B	64	SW1/4 of SE1/4 SEC 31 R3W T4N	two strath terraces cut in Pelona Schist bearing fill. N of Piedmont Rd at Deep Creek Rd.
1B	65	SW1/4 of SE1/4 SEC 31 R3W T4N	linear buttress unconformity resulting from fans over-running strath terrace riser. Piedmont Rd.
1A	66	NE1/4 of SW1/4 SEC 11 R4W T2N	deeply weathered alluvial fan deposits on quartz monzonite in streamcut exposure. Miller Creek.
1A	67	SE1/4 of NW/4 SEC 11 R4W T2N	terrace gravel on quartz monzonite in roadcut exposure on abandoned mine road. Pilot Rock ridge.
1A	68	NW1/4 of SW1/4 SEC 10 R4W T2N	terrace gravel on quartz monzonite at mouth of canyon in shape of fan graded to Qtl. Miller Cyn.
1A	69	SE1/4 of SE1/4 SEC 27 R4W T3N	fan-shaped pediment surface on Crowder Formation with a thin veneer of overlying alluvium.
1A	70	SW1/4 of SE1/4 SEC 7 R3W T3N	deeply dissected old alluvial fan deposits in streamcut exposures overlying Victorville Fan beds.
1B	71	SW1/4 of NW1/4	limestone fanglomerate exposed in streamcut cliff just E of Winchell Ranch.
1B	72	NW1/4 of NW1/4 SEC 33 R3W T4N	limestone and quartz monzonite cemented talus breccia in natural exposures. W flank of Ord Mtns.
1B	73	NE1/4 of NW1/4 SEC 33 R3W T4N	finger-shaped deposits of fanglomerate in Tortoise Canyon. W flank of Ord Mtns.
1B	75	SW1/4 of NE1/4 SEC 28 R3W T4n	steep buttress unconformity between old fanglomerate and basement with no shearing.

Plate	Locality	Location	Brief Description of Feature
1B	76	SW1/4 of NW1/4 SEC 26 R3W T4N	abruptly truncated surface of subdued relief atop the north flank of the Ord Mountains.
1B	77	SE1/4 of SW1/4 SEC 24 R3W T4N	subdued ridge-crests of incised erosion surface. S end of Valley Vista Road.
1B	78	SW1/4 of NE1/4 SEC 27 R3W T4N	flat concordant ridge-crests possibly remnants of an old pediment surface.
1B	79	NW1/4 of NE1/4 SEC 6 R1W T3N	remnant of older, higher alluvial fan deposit, Qt2.
1B	80	NW1/4 of SW1/4 SEC 5 R1W T3N	deep incision into older fan surface and deposit exposing underlying hornblende diorite.
1B	81	SE1/4 of SE1/4 SEC 26 R2W T4N	deeply incised fan head trench. Grapevine Canyon.
1B	82	SE1/4 of SE1/4 SEC 31 R1W T4N	oversteepened fan surface along White Mountain fault.
1B	83	SW1/4 of NW1/4 SEC 32 R1W T4N	incised younger Qt1 fan surface.
1A	84	SEC 2 R5W T2N	cross-cutting relationships in south-block-down faults.
1A	85	SEC 20 R5W T3N	Harold Formation overlying south-block-down fold.
1A	86	SEC 2 R5W T2N	south-block-down faults truncated by Cleghorn fault zone.
1A	87	SEC 7 R3W T2N	south-block-down fault cutting Tunnel Ridge lineament.
1A	88	SEC 12 R5W T2N	south-block-down fault cutting north-plunging monocline.
1A	89	SEC 12 R5W T2N	gentle drag fold developed next to south-block-down fault.
1A	90	NW1/4 of SW1/4 SEC 3 R5W T2N	undisturbed Crowder Formation next to south-block-down fault.
1A	91	SEC 24 R5W T3N	south-block-down folds in Crowder Formation.

Plate	Locality	Location	Brief Description of Feature
1A	92	SEC 12 R5W T2N	pure dip-slip motion on south-block-down fault offsetting plunging monocline.
1A	93	NW1/4 of NW1/4 SEC 6 R4W T2N	south-block-down faults offset by northeast splays.
1A	94	NW1/4 of NW1/4 SEC 2 R5W T2N	north-block-down faults truncating south-block-down faults.
1A	95	SEC 2 R5W T2N	bends and cusps in the trace of the Cleghorn fault.
1A	96	NW1/4 of NW1/4 SEC 2 R5W T2N	Notch fault cutting south-block-down fault.
1A	97	NW1/4 of NW1/4 SEC 2 R5W T2N	Notch fault cutting Crowder Formation.
1A	98	NW1/4 of NW1/4 SEC 2 R5W T2N	Notch fault overlain by Qt2 terrace deposit.
1A	99	SEC 1 & 2 R5W T2N	microcosm of fault evolution in western San Bernardino Mts.
1A	100	SW1/4 of NE1/4 SEC 9 R4W T2N	small north-trending fold in Crowder Formation.
1A	101	SEC 34 & 35 R5W T3N	folding expressed in late Miocene erosion surface.
1A	102	SEC 34 & 35 R4W T3N	drainages terminating at Grass Valley fault.
1A	103	SE1/4 of SE1/4 SEC 34 R4W T3N	broad valley terminating at Grass Valley fault.
1A	104	NE1/4 of NE1/4 SEC 34 R4W T3N	dissected fan-shaped pediment surface.
1A	105	NW1/4 of SW1/4 SEC 33 R4W T3N	structural ridge confining Silverwood Lake.
1A	106	SW1/4 of SW1/4 SEC 29 R4W T3N	vertical bedding and clay zone in Crowder Formation.
1A	107	SE1/4 of NW1/4 SEC 24 R4W T3N	vertical bedding in volcanogenic eastern facies of the Crowder Fm.
1A	108	SE1/4 of SW1/4 SEC 24 R4W T3N	fresh bedrock along Deep Creek fault zone.

Plate	Locality	Location	Brief Description of Feature
1A	109	NW1/4 of NE1/4 SEC 8 R3W T3N	scarp in Qf2.
1A	110	SE1/4 of SE1/4 SEC 13 R4W T3N	reverse fault exposed in east abutment of Mojave River Dam.
1A	111	NW1/4 of SE1/4 SEC 24 R4W T3N	basement rocks topographically over Crowder Formation.
1A	112	SEC 25 & 26 R4W T3N	base of late Miocene erosion surface displaced by faulting.
1A	113	NW1/4 of NW1/4 SEC 25 R4W T3N	Summit Valley fault zone displacing late Miocene surface.
1A	114	SE1/4 of SE1/4 SEC 5 R3W T3N	connecting structure between Deep Creek and Apple Valley Highlands fault zones.
1B	115	NE1/4 of SW1/4 SEC 28 R3W T4N	Apple Valley Highlands fault scarp in Qf2 fanglomerate.
1B	116	SE1/4 of SE1/4 SEC 21 R3W T4N	Qf2 fanglomerate topographically over Ord River Gravel.
1B	117	SE1/4 of SE1/4 SEC 21 R3W T4N	steep dips in Qf2 fanglomerate.
1B	118	SE1/4 of NE1/4 SEC 5 R3W T3N	undisturbed Qf1 fanglomerate across Apple Valley Highlands fault zone.
1B	119	SE1/4 of SE1/4 SEC 21 R3W T4N	splay off Apple Valley Highlands fault zone.
1A	120	SE1/4 of SE1/4 SEC 5 R3W T3N	brecciation of bedrock at south end of Apple Valley Highlands fault zone.
1A	121	SE1/4 of NE1/4 SEC 7 R3W T3N	folding in Ord River Gravel next to Powerline Road fault zone.
1A	122	NW1/4 of SE1/4 SEC 7 R3W T3N	undisturbed surface of Qf2 fanglomerate across Powerline Road fault zone.
1B	123	NW1/4 of SE1/4 SEC 28 R3W T4N	late Miocene erosion surface in bench west of Juniper Ranch fault zone.
1B	124	SW1/4 of SW1/4 SEC 33 R3W T4N	breccia associated with Juniper Ranch fault zone.

Plate	Locality	Location	Brief Description of Feature
1B	125	NW1/4 of SE1/4 SEC 28 R3W T4N	Qf2 fanglomerates in steep buttress unconformity against bedrock.
1B	126	SW1/4 of SW1/4 SEC 33 R3W T4N	Juniper Ranch fault defines eastern limit of Qf2.
1B	127	SEC 28 & 29 R3W T4N	linear contacts between Ord River Gravel and Qf2 fanglomerate.
1B	128	SE1/4 of SW1/4 SEC 28 R3W T4N	north-northeast trending lineament in Qf2 fanglomerate.
1B	129	SE1/4 of SE1/4 SEC 21 R3W T4N	junction of Apple Valley Highlands and Juniper Ranch fault zones.
1A	130	NW1/4 of NW1/4 SEC 9 R3W T3N	tight folding and boudinage in phylonite of Ord Mountains pendant
1A	131	SEC 9 R3W T3N	Powerline Canyon fault zone cutting biotite-quartz-monzonite. Fault overlain by Qf2.
1B	132	SEC 33 R3W T4N	northwest-trending faults cutting crystalline rocks of Ord Mountains pendant.
1B	133	NE1/4 of NE1/4 SEC 36 R3W T4N	half-meter-wide gouge zone on Bowen Ranch fault.
1B	134	NE1/4 of SW1/4 SEC 1 R3W T3N	Bowen Ranch fault cutting Ord River Gravel.
1B	135	SE1/4 of NW1/4 SEC 1 R3W T3N	undisturbed Holocene(?) terrace overlying Bowen Ranch fault.
1B	136	NW1/4 of NW1/4 SEC 30 R2W T4N	Ord River Gravel offset in east-block-down sense on Bowen Ranch fault.
1B	137	SEC 1 R3W T3N	margin of Rattlesnake Mountain pluton offset about 1/2km.
1B	138	SW1/4 of NW1/4 SEC 30 R2W T4N	possible left-lateral stream offsets on Bowen Ranch fault.
1B	139	NW1/4 of SW1/4 SEC 32 R2W T4N	late Miocene(?) lag gravel on ridge in Arrastre Canyon Narrows fault zone.

Plate	Locality	Location	Brief Description of Feature
1B	140	SEC 32 R2W T4N	coalescing drainages behind pressure ridge in Arrastre Canyon fault zone.
1B	141	SE1/4 of NW1/4 SEC 33 R2W T4N	Arrastre Canyon fault trace on flank of ridge.
1B	142	SW1/4 of SW1/4 SEC 27 R2W T4N	physiographic trough associated with gouge zone.
1B	143	SW1/4 of NE1/4 SEC 33 R2W T4N	broad zone of cataclasis in Arrastre Canyon fault zone.
1B	144	S1/2 of SEC 26 R2W T4N	Arrastre Canyon Narrows fault zone following White Mountain thrust system.
1B	145	NE1/4 of SE1/4 SEC 27 R2W T4N	northeast-trending splay of Arrastre Canyon fault zone.
1B	146	SE1/4 of SW1/4 SEC 31 R2W T4N	Ord River Gravel displaced by Arrastre Canyon fault zone.
1B	147	SE1/4 of NW1/4 SEC 33 R2W T4N	members of Lovelace Canyon fault system cut by Arrastre Canyon fault zone.
1B	148	SE1/4 of NW1/4 SEC 34 R2W T4N	meter-wide gouge zone on Lovelace Canyon fault.
1B	149	SEC 4 R2W T3N	Lovelace Canyon fault cutting east-northeast trending faults.
1B	150	SW1/4 of SE1/4 SEC 27 R2W T4N	Lovelace Canyon fault truncated by Arrastre Canyon fault zone.
1B	151	SE1/4 of NW1/4 SEC 3 R2W T3N	left-lateral separation on mafic body.
1B	152	NW1/4 of NW1/4 SEC 29 R2W T4N	east-northeast trending fault cutting Arrastre Canyon deposits.
1B	153	NE1/4 of NE1/4 SEC 36 R2W T4N	Sky Hi Ranch fault splays joining Arrastre Canyon fault zone.
1B	154	SEC 16 R2W T4N	Sky Hi Ranch fault becomes fold.
1B	155	SEC 4 R1W T3N	Sky Hi Ranch fault joins White Mountain thrust system.
1B	156	NW1/4 of NW1/4 SEC 9 R1W T3N	northwest-trending fault cutting White Mountain thrust zone.

Plate	Locality	Location	Brief Description of Feature
1B	157	SE1/4 of SE1/4 SEC 31 R1W T4N	shutter ridges on north side of Sky Hi Ranch fault.
1B	158	NE1/4 of NE1/4 SEC 6 R1W T3N	ponded alluvium behind shutter ridges on Sky Hi Ranch fault.
1B	159	NE1/4 of NE1/4 SEC 6 R1W T3N	capture of adjacent drainage due to fault movement.
1B	160	NW1/4 of SW1/4 SEC 31 R1W T4N	disturbed drainage at fault trace.
1B	161	NW1/4 of NW1/4 SEC 5 R1W T3N	vertical attitude on exposure of Sky Hi Ranch fault.
1B	162	NE1/4 of NE1/4 SEC 22 R2W T4N	possible folding of Qf2 surface.
1B	163	NE1/4 of SE1/4 SEC 31 R1W T4N	north-dipping thrust faults in Qf2.
1B	164	NE1/4 of NW1/4 SEC 6 R1W T3N	Qf2 overlying White Mtn. thrust.
1B	165	SW1/4 of SE1/4 SEC 30 R1W T4N	alluvial infilling reducing scarp height.
1B	166	SW1/4 of SE1/4 SEC 30 R1W T4N	undisturbed Qf1 overlying low-angle fault trace.
1B	168	SEC 26 R2W T4N	possible extension of White Mtn. thrust system to Lovelace Cyn.
1B	169	SEC 3 R1W T3N	thrust fault scarps in Dry Canyon fan.
1B	170	SE1/4 of NW1/4 SEC 6 R1W T3N	south-dipping thrust plane.
1B	171	NW1/4 of SW1/4 SEC 31 R1W T4N	north-dipping thrust plane.
1B	172	NE1/4 of NE1/4 SEC 36 R2W T4N	highly fractured cataclastic rock in lower plate of thrust.
1A	173	SEC 12 R5W T2N	north-plunging monocline.
1A	174	SEC 33 R5W T3N	antiformal ridge in erosion surface.
1A	175	SEC 10 & 11 R4W T2N	plunging monoclines in Crowder Formation south of Cleghorn fault.

Plate	Locality	Location	Brief Description of Feature
1A	176	NE1/4 of SE1/4 SEC 11 R4W T2N	north-plunging monocline cut by Cedar Springs fault.
1A	177	NE1/4 of NE1/4 SEC 19 R5W T3N	folds in Crowder Formation overlain by Harold Formation.
1B	178	SW1/4 of NW1/4 SEC 22 R3W T4N	Ocotillo Ridge fold turns south and joins Apple Valley Highlands fault zone.
1B	180	SE1/4 of SE1/4 SEC 16 R2W T4N	Ocotillo Ridge fold turns south-east and joins Sky Hi Ranch fault.
1B	181	NE1/4 of NE1/4 SEC 22 R2W T4N	possible folding in Qf2 on Ocotillo Ridge fold.
1A	182	NW1/4 of NW1/4 SEC 25 R4W T3N	Grass Valley warp expressed in late Miocene(?) erosion surface.